MOLECULAR BASIS OF Fcε RECEPTOR : IgE INTERACTIONS

A THESIS SUBMITTED FOR THE DEGREE OF
DOCTOR OF PHILOSOPHY

By

AVELINE JOAN RIGBY

THE AUSTIN RESEARCH INSTITUTE

AND

CENTRE FOR BIOPROCESSING AND FOOD TECHNOLOGY*
VICTORIA UNIVERSITY OF TECHNOLOGY

2001

To My Family

My parents who gave me a desire for knowledge.

Paul, Peter and Fiona
who encouraged, supported and believed in me.

My extended family who gave me time.

Thank you.

DECLARATION

The experimental work embodied in this thesis constitutes original work performed by myself, except in the individual instances cited in the text. Chapters 1, 2 and 3 were collaborative studies and published as such, in which the majority of research and experimentation was conceived and performed by me. This thesis conforms to the requirements of the Victoria University regulations in that it contains between 50,000 and 100,000 words exclusive of figures and tables.

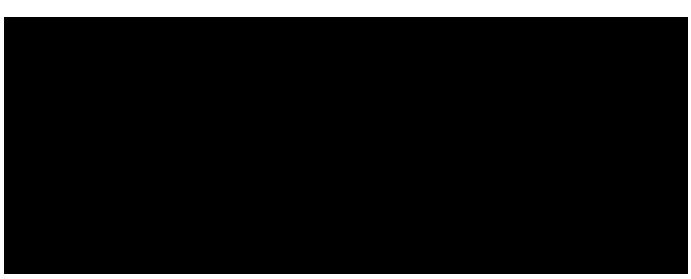

AVELINE J. RIGBY

The Austin Research Institute

and

Centre for Bioprocessing and Food Technology*
Victoria University of Technology

* Food Safety, Authenticity and Quality Unit as of 01.01.2001

TABLE OF CONTENTS

ACKNOWLEDGEMENTS

I would like to thank Ian McKenzie and Mark Hogarth for accepting me as a student at the Austin Research Institute, and Mark for his supervision and friendship. I would also like to thank Paul Chambers for agreeing to supervise me, his encouragement and words of wisdom were always of great benefit; Margaret Britz for providing the initial impetus for my enrolment; and the Victoria University for honouring me with the inaugural Return to Study Research Award.

At the ARI there are many people who have contributed to the production of this thesis, the senior researchers: Bruce Loveland, Xing Pei-Xiang, Geoff Pietersz, Sarah Russell, Mauro Sandrin, Mark Smith and Joe Trapani who all willingly gave of their time and knowledge, the individual members of all the labs especially the inhabitants of Siberia: Nadine Barnes, Tessa Bradford, Dimi Emmanouilidis, Sandra Esparon, Amanda Gavin, Suzanne Holt, Mark Hulett, Gary Jamieson, Beth McInnes, Karl Poetter, Maree Powell, Joe Spratt, Peck Szee Tan, Caroline Tan, Halina Trist, Bruce Wines and fleetingly, Lyn Dalgarno and Graham MacKay who have shared experience and advice, laughter and lunches. I also appreciate the contribution of all the support staff, particularly Leanne Bell, Jim Karkaloutsos for making the oligonucleotides and peptides used herein, the staff of the BRL, and also Janet Cameron and Susan Collins who have eased communications.

Specifically I need to thank Mark Hulett for his directions at the bench, Bruce Wines and Gary Jamieson for reading papers and chapters and their unfailing support and good humour, and Halina and Nadine for being themselves.

At Victoria University I would like to acknowledge the support and encouragement from staff, Paul Chambers, Bob Fairclough, Michelle Tostowless, Jack Antonas and Lily Stojanovska, Michael Barry, Ian Sullivan and also Sylvia Travaglia and Peter Thomson; and students Matthew Knight and Ann Wilson.

Above all I acknowledge the contribution of my family who have supported me continuously, who not only gave up the diningroom table, but my company and attendance at home, school and social functions; my parents-in-law who have done everything in their power to help; and last but not least, I thank my parents.

I acknowledge the specific contributions of others to this thesis:
The molecular modelling of FcεRI in Chapter 1 was performed by Dr Ross Brinkworth, and that in the following chapters was performed by Dr Vidana Epa.
Many of the peptide ELISA's in Chapter 2 were performed by Halina Trist who also provided purified FcεRI-α and γεγ.
Dr Mark Hulett produced the original εεγ and γεγ constructs and Dr Graham MacKay produced the original R15A and F17A constructs.
Nadine Barnes and Dr Maree Powell provided purified FcγRIIa.

INTRODUCTION TO THE THESIS.

Allergic diseases such as asthma and hay fever cause distress to numerous individuals throughout the world, sometimes with fatal consequences. Many associated costs - physical absences, psychological corollaries or medication - are borne by the community via health agencies or the government. The symptoms of these diseases, such as inflammation of the airways, are initially caused by the apposite allergen crosslinking at least two molecules of IgE bound to their high-affinity cell surface receptor FcεRI. This interaction initiates intracellular signalling starting a cascade of events resulting in cellular degranulation and the release of inflammatory mediators. Many present treatments for these conditions act at this stage to inhibit the activity of these chemical intermediaries, after inflammation has been initiated.

The interaction of IgE with FcεRI-α is an event common to all IgE based allergic responses, regardless of the allergen involved, and therefore presents itself as an ideal juncture for early intervention in the allergic response. Monoclonal antibodies with epitopes in the binding site of the receptor have been shown to block the binding of IgE, but can themselves precipitate the degranulation mechanism, or initiate an immune response with repeated application. This work seeks to define the relationship between the two extracellular domains of FcεRI-α to determine the contribution of domain one to the presentation of the receptor and the interaction with IgE. This information may lead to the location of sites for therapeutic intervention prior to and without itself causing the degranulation response.

This thesis specifically addresses the high-affinity receptor for IgE (α chain) - FcεRI-α, chimeric receptors of FcεRI-α and FcγRIIa, with FcεRI-α point mutants, and their interaction with IgE.

The objectives of this study were:

1. To produce anti-FcεRI-α monoclonal antibodies for epitope mapping studies to delineate structural features on the surface of the receptor and for use as reagents in the study.

2. To investigate the molecular basis for the interaction of FcεRI-α and IgE.

(a) To determine the role of domain one FcεRI-α in this interaction.

(b) To determine the relationship between domain one and domain two.

(c) To determine the effect of changes in the microenvironment on the FcεRI-α : IgE interaction.

FORMAT OF THE THESIS.

This thesis comprises six chapters. The first chapter reviews the literature on FcεRI and its ligand IgE, their genes, structure, and sites of interaction up until the time of publication.

Chapters two to five describe the experimental work undertaken in the course of the study and the results attained.

- Chapter 2 describes the production and characterisation of monoclonal antibodies to FcεRI-α.
- Chapter 3 details the contribution of domain one to the interaction of FcεRI-α and IgE. It also examines the structure relative to the function of the receptor.
- Chapter 4 examines the effects of different membrane anchors on FcεRI-α , and on its interaction with IgE. It also describes a novel assay for determining the interaction of FcεRI-α with IgE, when the IgE is immobilised.
- Chapter 5 focuses on the effects of pH and ionic strength on the interaction of FcεRI-α and IgE using a biosensor.

Chapter 6 summarises the results and relevance of the experimental chapters, and relates the findings to other studies, specifically the recently published solved structure of FcεRI-α interacting with IgE Fc.

Appendix I contains amino acid and nucleotide sequences of FcεRI-α, IgE, FcγRIIa, FcγRIII and Decay Accelerating Factor (DAF).

Appendix II contains formulae for the experimental calculations used in this thesis.

Appendix III contains recipes and methods not included in the chapters.

Figure 1.3B, Figure 2.5E and Figure 3.3 are in stereo. They can be viewed in three dimensions using a stereoscope or by using the 'magic eye' technique to converge the two images.

Chapter 1 has been published as:-
Rigby LJ, Hulett MD, Brinkworth RI, and PM Hogarth. The structural basis of the interaction of IgE and FcεRI. In: Hamawy MM, editor. IgE Receptor (FcεRI) Function in Mast Cells and Basophils. Molecular Biology Intelligence Unit. R.G.Landes Company, 1996:7-32.
This chapter retains the format required by the publishers.

Chapter 2 has been published as:-
Rigby LJ, Trist H, Epa VC, Snider J, Hulett MD and PM Hogarth. Monoclonal antibodies and synthetic peptides define the active site of FcεRI and a potential receptor antagonist. Allergy 2000, 55:609-619.
This chapter retains the format required by the journal Allergy.

Chapter 3 has been published as:-
Rigby LJ, Epa VC, Mackay GA, Hulett MD, Sutton BJ, Gould HJ, and PM Hogarth. Mutagenesis and homology modelling define the role of domain one in the high affinity Fc epsilon receptor, FcεRI. J Biol Chem 2000; 275(13):9664-9672.
This chapter retains the format required by the Journal of Biological Chemistry.

Chapters 3, 4, 5 and 6 have been formatted in the manner of the Journal of Biological Chemistry except for the references which are presented in the format used by Medline.

All experimental work contained in this thesis was performed at the Austin Research Institute between March 1992 and December 1999.

ABSTRACT TO THE THESIS

Allergies, including allergic asthma and rhinitis are caused by inappropriate immune and cell responses involving IgE and its receptor. This thesis describes work of fundamental importance in defining key features of the interaction of IgE with the ligand binding alpha chain of its primary receptor - FcεRI. Using a combination of technologies including molecular biology techniques, molecular modelling, monoclonal antibody-based epitope mapping, peptide chemistry and surface plasmon resonance, sites and amino acids within FcεRI that are critical for binding to ligand were identified. The first reliable molecular model of FcεRI was constructed and was used to define the receptor structure, monoclonal antibody epitopes and for the identification of potential sites for novel therapeutics.

Chimeric and mutant receptors were assayed for IgE binding following transfection into receptor negative cells and expression confirmed using monoclonal antibodies raised to recombinant soluble FcεRI-α and subsequently characterised by epitope mapping. Immobilised soluble IgE receptors were assayed using a biosensor to characterise ligand binding under varying pH and ionic strength, and a novel biosensor assay was developed to measure receptor:ligand interactions with IgE in the immobile phase. A region in the receptor was identified as a potential target for the design of a therapeutic agent that would specifically inhibit binding of IgE to its receptor. Such an agent would have an inhibitory effect on IgE-induced cell activation, including degranulation, and thereby abrogate the allergic response.

This work has been published and cited in international scientific and medical journals and text.

ABBREVIATIONS

α	alpha (alpha chain of FcεRI complex)
β	beta (beta chain of FcεRI complex)
γ	gamma (gamma chain of FcεRI complex)
γε	recombinant soluble chimeric FcR, D1 FcγRIIa, D2 FcεRI-α
δ	delta
ε	epsilon
εε	recombinant soluble FcεRI-α, D1 FcεRI-α, D2 FcεRI-α
ζ	zeta
μ	micro (mu)
μg	microgram
μl	microlitres

A	Absorbance
bp	Base pair(s)
BSA	Bovine serum albumin
C	Constant immunoglobulin domain
Cε	IgE heavy chain constant domain
cDNA	Complementary DNA
cpm	Counts per minute
COS-7	Monkey kidney fibroblast cell line
CT	Cytoplasmic tail
CR	Cytoplasmic region
D	Domain
D1γ	Domain 1 of hFcγRIIa
D2γ	Domain 2 of hFcγRIIa
D1ε	Domain 1 of hFcεRI-α chain
D2ε	Domain 2 of hFcεRI-α chain
DAF	Decay accelerating factor
DEAE	Diethylaminoethyl
DMEM	Dulbecco's modified Eagles medium
DNA	Deoxyribonucleic acid
EA	Erythrocytes sensitised with antibody
EC	Extracellular
EDC	*N* - ethyl - *N'*- (dimethylaminopropyl) carbodiimide
EDTA	Ethylenediaminetetra-acetic acid

ELISA	Enzyme-linked immunosorbent assay
Fab	Fragment antigen binding (of antibody)
FACS	Fluorescence activated cell sorter
Fc	Fragment crystallisable (of antibody)
FcR	Fc receptor(s)
FcαRI	FcR for IgA (class I)
FcδR	FcR for IgD
FcϵRI	FcR for IgE (class I - high affinity)
FcϵRII	FcR for IgE (class II - low affinity)
FcγRI	FcR for IgG (class I)
FcγRII	FcR for IgG (class II)
FcγRIIIa	FcR for IgG (class III) (Peptide anchor)
FcγRIIIb	FcR for IgG (class III) (GPI anchor)
FcμR	FcR for IgM
FCS	Fetal calf serum
FITC	Fluorescein isothiocyanate
GPI	Glycosyl phosphatidylinositol
GPI PL-C	Glycosyl phosphoinositol phospholipase C
GPI PL-D	Glycosyl phosphoinositol phospholipase D
h	Human
hr	Hour(s)
Ig	Immunoglobulin
i.p.	Intraperitoneal
K_A	Association affinity constant
kb	Kilobase(s)
K_D	Dissociation affinity constant
L or l	Litres
M	Molar
M^{-1}	Litres per Mole
mo	Mouse
mAb	Monoclonal antibody
mCi	Millicurie
2ME	2-Mercaptoethanol
mAb(s)	Monoclonal antibody (antibodies)
m fl	Mean fluorescence
mg	Milligram(s)
min	Minute(s)

ml	Millilitre(s)
mM	Millimolar
MP	Membrane proximal
mRNA	Messenger RNA
ng	Nanogram(s)
ND	Not determined
NHS	*N*-hydroxy succinimide
nM	Nanomolar
NP	4-hydroxy-nitrophenolacetyl
NP-Cap-OSu	3-nitro-4-hydroxyphenylacetic caproic acid, succinimide ester
NS	Normal Saline
OD	Optical density
O/N	Overnight
PAGE	Polyacrylamide gel electrophoresis
PBS	Phosphate buffered saline
PCR	Polymerase chain reaction
PIPLC	Phosphoinositol phospholipase C
pM	Picomolar
PMSF	Phenylmethylsulphonyl fluoride
r	Recombinant
Ref	Reference(s)
Req	Predicted equilibrium
RIA	Radioimmunoassay
RNA	Ribonucleic acid
RT	Room Temperature
RU	Response units
s	Soluble
SD	Standard deviation
sec	Second(s)
SOE	Splice overlap extension
SPR	Surface plasmon resonance
SRBC	Sheep red blood cell
TM	Transmembrane
TNBS	2,4,6-trinitrobenzene sulphonic acid
TNP	Trinitrophenol
Tris-HCl	Tris(hydroxymetyl)aminomethane hydrochloride

CHAPTER ONE:

Literature Review

Published: Rigby LJ, Hulett MD, Brinkworth RI, and PM Hogarth.
In: Hamawy MM, editor. IgE Receptor (FcεRI) Function in Mast Cells and Basophils. Molecular Biology Intelligence Unit. R.G.Landes Company, 1996:7-32.

INTRODUCTION

FcεRI is capable of inducing one of the most powerful and violent pharmacological responses known. Indeed the association of IgE with FcεRI, and subsequent aggregation is a most important interaction in the induction of human disease, and causes more chronic misery (in the West at least) than the engagement of any other immunological receptor. As approximately one in five people are afflicted with IgE dependent allergies - most notably allergic rhinitis or 'hay-fever' and asthma - there has been a large effort made by many groups in studying this receptor, its ligand and the consequences of its activation. Certainly, the impetus to study this receptor probably stems from its pathological role rather than its physiological one, which is still somewhat undefined, but with evidence pointing to an anti-parasite role.[1]

Yet despite the importance of the interaction of IgE and FcεRI, the widespread interest in this interaction (or its consequences) and its obvious importance to the pharmaceutical industry, we still do not know the structure of these molecules. At the time of writing there is still no published three dimensional structure of either IgE or its high affinity receptor, or the 'Holy Grail' of all in this field - a structure of FcεRI interacting with its ligand.[FOOTNOTE 1] None-the-less many groups have contributed to the substantial progress in defining the overall structure of IgE and FcεRI, the regions of these that influence their interaction, and how these structures may sit on the cell surface.

In this chapter we have attempted to bring together the work of many, on the structural aspects of FcεRI and IgE. We have drawn on models of IgE and FcεRI to compile, and present, the data of many groups in defining the nature of this interaction.

The FcR nomenclature throughout this review follows that proposed by the IUIS/WHO subcommittee on nomenclature for Fc receptors.[2]

[1] The structure of IgE Fc bound to FcεRI-α has recently been published.[125]

STRUCTURE OF FcεRI AND IgE

FcεRI

Biochemical and molecular structure

The FcεRI has been characterised in three different species, human, rat and mouse. Structurally, it has been defined as a tetrameric surface glycoprotein, comprising an alpha chain, a beta chain and a dimer of disulphide linked gamma chains. The alpha chain has been shown to bind IgE ($>10^{10}\ M^{-1}$), and to be homologous to the FcγR, whilst the beta and gamma chains are involved in cell signalling and surface expression. The characteristics of this receptor from mouse, rat and human are summarised in Table 1.1.

The earliest cell culture model used to demonstrate the interaction of IgE and FcεRI was that of the rat basophilic cell line RBL-2H3[3] which was used for the initial attempts to purify the receptor.[4,5,6] A single polypeptide chain with an apparent molecular weight of 50-60 kDa was initially purified (the α chain), the conditions too stringent to maintain the non-covalent association between the four subunits. This α chain was later found to be associated with other polypeptides, the β chain of 33 kDa,[7,8,9] and the two disulphide linked γ chains of 7-9 kDa each.[9,10] Purification of the intact complex required less stringent and protective phospholipid, or submicellular concentrations of detergent.[11,12]

Further characterisation of the receptor involved monoclonal antibodies (mAbs) raised against the FcεRI complex, and showed the FcεRI-α chain to be highly glycosylated and expressed on the exterior surface of the cell. The β subunit and the disulphide linked γ dimer were not glycosylated.[13,14] Human, rat and mouse cDNA has been cloned for each of the FcεRI subunits, their molecular structures determined (Table 1.1), and a stylised model of the topology of the FcεRI complex proposed (See Fig. 1.1).[15]

Table 1.1. Characteristics of FcεRI

CHARACTERISTIC	Human FcεRI	Mouse FcεRI	Rat FcεRI
Affinity for IgE (Ka)	$10^{10}M^{-1}$ (human)	$10^{10}M^{-1}$ (mouse)	$10^{10}M^{-1}$ (rat)
Specificity	human, mouse or rat lgE	mouse or rat lgE only	rat or mouse lgE only
Associated subunits	α, β, γ	α, β, γ	α, β, γ
Forms of receptor	αβγ2 (Mast cells) αγ2 (Langerhans cells)	αβγ2	αβγ2
Molecular weight (kDa)			
-apparent	45-65 α, 32 β, 7-9 γ	45-65 α, 32 β, 7-9 γ	45-65 α, 32 β, 7-9 γ
-protein backbone	26.4 α, 25.9 β, 7.8 γ	25.8 α, 25.9 β, 7.8 γ	25.2 α, 27 β, 7.8 γ
Chromosome	1q23 α, 11q13 β, 1q23 γ	1 α, 19 β, 1 γ	ND
Cell distribution	Mast cells Basophils Langerhans cells Eosinophils Monocytes (activated)	Mast cells Basophils	Mast cells Basophils

ND = Not determined.

Figure 1.1 Diagrammatic representation of FcεRI-α on the cell membrane and the bent and rotated IgE. The extracellular domains of FcεRI-α are indicated as D 1 and D2; the IgE heavy chain domains as Cε or V and the light chains are shaded (After Sutton and Gould).

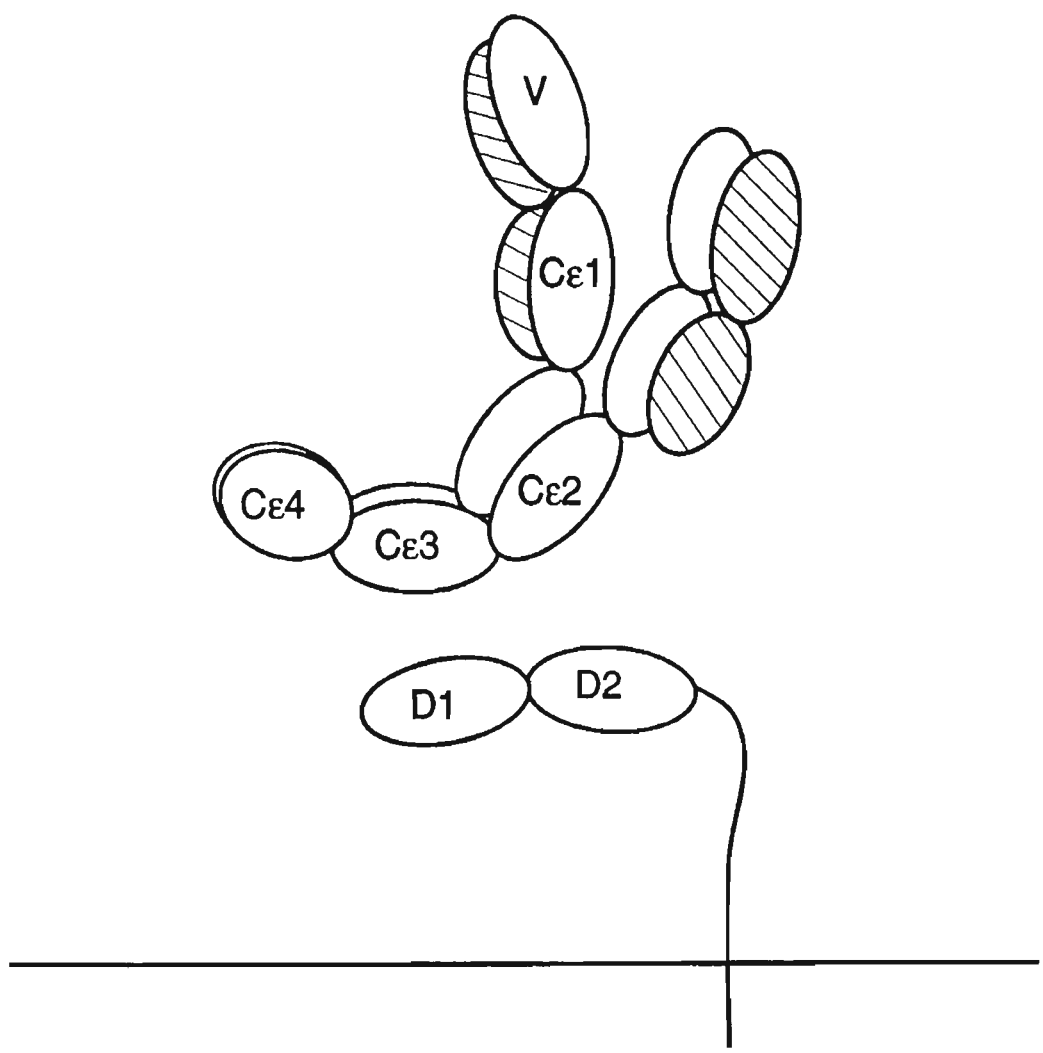
V
Cε1
Cε2
Cε3
Cε4
D1
D2

α Subunit

FcεRI-α subunit cDNAs have been cloned in the human, mouse and rat,[16-20] and a single transcript has been identified for human and mouse. In the rat one major full length clone has been identified, and three shorter clones comprising varying deletions from the full length FcεRI-α chain gene,[16,18,19] which probably arise from alternative splicing of the genomic DNA.[18,21] The FcεRI-α cDNA encodes a transmembrane glycoprotein comprising an extracellular region of two immunoglobulin(Ig)-like domains, (human 180, mouse 181, rat 181 amino acids), a 21 amino acid transmembrane region, and a cytoplasmic tail of 22-31 amino acids (human 31, mouse 25, rat 22).

A comparison of the amino acid sequences of the individual subunits of FcεRI of different species and also with other receptors is revealing.[FOOTNOTE 2] The sequence identity between the encoded FcεRI-α proteins of mouse and rat, compared to human is approximately 38%, displaying the least homology of the FcεRI subunits (α, β and γ) between species.[20] The FcεRI-α cytoplasmic domains are the least conserved between species (16%) but the FcεRI-α chain transmembrane region is highly conserved (62%), with the eight amino acid motif (LFAVDTGL) present in each species. This sequence is essential for interaction with the FcεRI-γ subunit,[22] and is also conserved in the transmembrane regions of mouse, rat, and human FcγRIII which like FcεRI-α require association with the FcεRI-γ chain for cell surface expression.[23] From the point of view of the interaction of the FcεRI-α subunit with Ig, a comparison with other FcR is interesting.

The FcεRI-α chains exhibit homology with all the FcγR but have the greatest identity with the FcγRIII subclass.[20,24] Comparisons of mouse FcεRI-α and FcγRIII demonstrate this relationship as they exhibit 33% amino acid identity over their entire sequence, with 35% and 48% identity in the extracellular and transmembrane regions, respectively. Of the 95 residues conserved in the mouse, rat and human extracellular region of the FcεRI-α chains, 61 are found in both mouse and human FcγRIII; which suggests that the 34 residues unique to FcεRI-α could be involved in IgE specific binding.[24] Indeed it

[2] The amino acid sequence of the human FcεRI-α chain used in this chapter is from Genbank, accession number X06948, and the numbering system is as shown in Appendix I.1.

is clear that all the leukocyte FcR that are Ig-superfamily members have a common evolutionary history. The rat, mouse and human FcεRI-α chain genes have been cloned and share a common structure of 5 exons; one each encoding the 5'UTR, leader sequence, and each of the two Ig-like domains, and a single exon for the transmembrane and cytoplasmic regions, and 3'UTR.[21,25,26] Indeed the human and mouse FcγRIII genes also exhibit a similar five exon gene structure, suggesting the FcεRI-α and FcγRIII genes arose by gene duplication from a common ancestor.[27,28] The human FcεRI-α chain gene has been mapped to chromosome 1q23 which also contains the low affinity FcγR genes (Table 1.1).[29]

β Subunit

cDNA clones of the FcεRI-β subunit have been isolated from the mouse,[20] rat[30] and human,[31] and encode proteins of 243, 235 and 244 amino acids, respectively, that are highly conserved exhibiting 91% amino acid homology and 69% identity. Two mRNA species have been observed in the mouse and rat (1.75 and 2.7 kb) arising from alternate polyadenylation, and two transcripts of human FcεRI-β have also been described, detected as a doublet around 3.9 kb.[31]

The rat FcεRI-β amino acid sequence, like the mouse and human, has four hydrophobic segments suggestive of transmembrane domains, and no leader peptide. Hydrophobicity plots and studies with monoclonal antibodies suggest that both the N and C termini are positioned in the cytoplasm. Rat FcεRI-β has two linear cytoplasmic domains of 46 and 62 residues[15] and the C-terminal cytoplasmic domain has been shown spectroscopically and by NMR to contain three α-helices possibly important in interaction with the membrane and/or other cytoplasmic domains.[32,33]

The human FcεRI-β gene has been isolated[32] and mapped to chromosome 11q13.[34] It appears to be a single copy gene of seven exons spanning 10kb. The 5'UTR and part of the N-terminal cytoplasmic domain comprise exon 1, the initial transmembrane region is encoded by exons 2 and 3, the second transmembrane region by exons 3 and 4, the third by exon 5, the fourth by exon 6, and the C-terminal cytoplasmic domain and 3'UTR by exon 7.[31] The mouse and rat FcεRI-β genes have not been isolated, but in the mouse it is believed to be a single gene linked to the *Ly-1* locus which maps to chromosome 19 (Table 1.1).[35,36]

γ Subunit

The FcεRI-γ subunit is expressed as a disulphide bonded dimer; with the disulphide bond formed between the cysteine residues located at the N-terminus of the transmembrane region.[22] cDNA clones have been isolated in the rat,[15] mouse,[20] and human[37] and encode highly related proteins that have 86% amino acid identity (Table 1.1).[37]

The FcεRI-γ subunit is an integral membrane protein with an extracellular region of five amino acids, a transmembrane region of 21 amino acids (as does FcεRI-α), and a cytoplasmic region of 36 amino acids.[37] It belongs to a small family of molecules which also contains the ζ and η chains of the TCR complex which are usually homodimeric, but can form heterodimers.[38] Studies using circular dichroism and Fourier-transform infrared spectroscopy (FRET) of the 62 amino acid rat γ subunit[39] agree with the proposed hydropathicity plot based structure of a five amino acid extracellular domain, an α helix in the transmembrane region and a 36 amino acid cytoplasmic tail.[15] FcεRI-γ has also been shown to associate with rat and mouse FcγRIII, human FcγRIIIa and FcγRII,[40,41] human FcγRI[42-44] mouse FcγRI (A. Gavin, personal communication) and human FcαRI.[45] In addition FcεRI-γ also associates with the TCR/CD3 complex of human and murine T cells.[38,46,47] The human gene has been mapped to chromosome 1q23[29] and that of the mouse to chromosome 1 along with gene encoding the closely related TCR ζ protein.[36] These regions also contain the respective FcεRI-α and FcγR low affinity loci which could indicate some coordinate regulation of these genes.

Expression of the FcεRI-αβ$(\gamma)_2$ complex on the cell surface.

Cloning of FcεRI-α, β and γ cDNA has been crucial for our understanding of the receptor structure and its expression. Early experimentation on rat FcεRI cDNA indicated that the FcεRI-α subunit expression could not be detected on the surface of COS-7 cells by transfection of FcεRI-α cDNA alone,[16,18] and this is also true for human[17,18] and mouse[20] FcεRI-α. Rat and mouse FcεRI-α chains are not efficiently expressed without co-transfection of the β and γ subunits, however, surface expression can be increased if the β and γ cDNAs of a different species are co-transfected. Optimal expression requires all three subunits to be of the same species. In these species the β subunit has a greater effect on expression than the γ subunit.[20] Surprisingly, the requirements for expression of the human FcεRI-α

subunit are different from those of rodent FcεRI-α in that the β chain is not required for cell surface expression. The γ subunit is required and can be of human, rat or mouse origin,[20,37,48] and co-transfection of FcεRI-α and γ subunits with either rat or human β subunit cDNA does not increase expression.

Indeed only 20% of receptors show the FcεRI-αβ(γ)2 phenotype under these conditions, the remaining 80% have been shown to express as FcεRI-α(γ)2.[31] It has been postulated that human FcεRI could exist *in vivo* in the FcεRI-α(γ)2 form[20,31] without the FcεRI-β subunit, and the existence of this complex has recently been confirmed on human Langerhans cells,[49] where it is capable of signal transduction resulting in calcium mobilisation and FcεRI internalisation. It has been suggested that the FcεRI-β subunit may be involved in unknown mechanisms related to activation or release of preformed cellular granules found in mast cells, which do not occur in Langerhans cells.[49] The lack of a β subunit in Langerhans cells may not therefore be surprising. However, it cannot be ruled out that Langerhans cells may possess a novel β-like subunit.

Mutagenesis of FcεRI-α, β and γ subunits have identified some of the structural requirements for assembly and expression of the FcεRI complex. In transfection studies using COS-7 cells, expression of the rat FcεRI complex has been shown to be unaffected by removal of any single FcεRI-α, β or γ subunit cytoplasmic domain, indeed, the removal of all the FcεRI-α, β and γ cytoplasmic domains reduces but does not eliminate expression - although it does affect aggregation.[50] Conversely, mutations in the rat FcεRI complex transmembrane regions resulted in either reduced or eliminated expression. These results suggest that the transmembrane regions are critical for rat receptor expression and a model encompassing this has been suggested.[22] Unlike the rat, co-transfection of human FcεRI-α with a truncated rat FcεRI-γ has been shown to ablate expression, indicating that in the human the cytoplasmic domain of FcεRI-γ is necessary for assembly and/or expression; strengthening suggestions that the rat and human receptors assemble in a different manner.

Human FcγRIIIa has been shown to associate with FcεRI-γ and TCR/CD3-ζ subunits.[51] These related homodimer subunits are highly homologous as are the transmembrane regions of the FcεRI-α chains: thus ζ could be expected to be able to

associate with FcεRI-α and substitute for the γ dimer. In the *Xenopus* oocyte expression system rat FcεRI fails to express when FcεRI-α and β chain RNA are injected, although fully functional expression occurs when FcεRI-α, β and γ RNA are co-injected. The receptor function and recognition by monclonal antibodies (mAbs) can also be restored by co-injecting human CD3-ζ RNA with the rat FcεRI-α and β RNA. However, this would not be expected to occur *in vivo*, as CD3-ζ does not occur naturally with FcεRI-α.[52]

Mutation experiments on FcεRI-α have shown that it can be expressed without the FcεRI-γ subunit by fusing the extracellular domains of FcεRI-α to the transmembrane region and cytoplasmic domain of another receptor molecule, for instance p55 IL-2R,[53] FcγRIIa,[54] FcεRI-γ (MH Kershaw personal communication). These chimeric receptors all express on the cell surface and can bind IgE with an affinity comparable to wild type. It has also been shown that glycosylation of a soluble form of FcεRI-α, is necessary for the proper folding of FcεRI in the endoplasmic recticulum, and also its secretion.[55]

IgE

Biochemical and Molecular Structure

Like all immunoglobulins, IgE consists of two disulphide bonded heavy chains, and two light chains bound to the heavy chains. The ε heavy chain is composed of approximately 550 amino acids that make up a variable region and four constant domains (Cε), unlike IgG, IgD and IgA which have three. The amino acid sequence of the IgE Fc portion (Cε2, Cε3, Cε4) is shown in Appendix 2. It appears that Cε3 and Cε4 are equivalent domains to the IgG constant domains Cγ2 and Cγ3 which make up the classic IgG-Fc region. The second constant domain Cε2 which is presumed to have the structure of a typical immunoglobulin constant domain, appears to take the place of the hinge region that occurs in IgG, IgD or IgA immunoglobulins.

The heavy chains are attached to each other by two interchain disulphide bonds and their location is unusual in that they occur in distinct regions being either end of a domain.

These disulphide bonds occur at Cys241[FOOTNOTE 3] (between Cϵ1 and Cϵ2) and Cys328 (between Cϵ2 and Cϵ3) which interact with Cys 241 and Cys328 respectively on the other heavy chain[56] to form parallel disulphide bonds as suggested by Dorrington and Bennich[57] and confirmed experimentally by Helm *et al.*,[56] not the diagonal disulphide bonding that was proposed by Padlan and Davies.[58] It should be noted that the region surrounding the Cys328 is important in binding to FcϵRI and in maintaining the conformation of human IgE.[56,59] In rat IgE it is the intrachain disulphide bonds that confer structural stability to the molecule.[60]

Considerable effort has been made to define the structure of IgE; as yet no authentic structure is available but a large body of data has been generated that provides some insight into the probable overall configuration of IgE (Fig. 1.1). Furthermore, with the development of molecular modelling based on authentic homologous structures, several models of IgE have been developed which are supported by experimentally derived data (see below).

It was originally suggested that IgE was a planar molecule,[56,58,61,62] with an extended section between Cϵ2 and Cϵ3, that could provide segmental flexibility to this region. The present concensus is that in solution IgE is a compact, fairly rigid and bent Ig (Fig. 1.1),[57,63-66] and FRET measurements indicate that the antigen combining sites lie approximately 7.1 nM from the C-terminus(Cϵ4) rather than the 17.1 nM expected for a planar Y-shaped molecule like IgG. Furthermore the apparent compact and rigid nature of IgE is clearly different from IgG1 which is much more flexible (probably because of the hinge) and able to adopt multiple conformations.[67] These studies have been used to refine the model of IgE[56] and indicate that fitting the experimental data to the model requires bending at the junction of Cϵ2/Cϵ3 and/or Cϵ3/Cϵ4, but most likely at Cϵ2/Cϵ3.[68] This also requires a change in the relative orientation of the Cϵ3 domains by rotating these $\pm 10°$ asymmetrically, and also the rotation of Cϵ2 by 40-50°.[68] Thus it appears likely that rodent and human IgE is bent in a U-shape, in agreement with the previous experimental data[64,67,69] and recent hydrodynamic studies.[70]

[3] The amino acid sequence of IgE used in this chapter is from Genbank, accession number L00022. The numbering system is based on that of Bennich[57], and is shown in Appendix I.2.

Despite the fact that IgE is more rigid than other Igs there is some considerable segmental flexibility; this is mostly manifest in the Fab arms where rotation and wagging take place.[69] The asymmetric nature of IgE probably explains the observed 1:1 stoichiometry of IgE:FcεRI interaction, and has several functional implications.[63,64,67,69-73] First, the FcεRI binding site on the concave surface of IgE may be obscured as Cε2 and/or Cε4 are in closer proximity to it, this then allows only the convex surface to bind to FcεRI. Second, the rotation at Cε2/Cε3 may also assist in 'spacing' the antigen combining sites of the Fab arms away from the FcεRI binding site, thereby minimising any steric hinderance by antigen of IgE/ FcεRI binding. Third, one binding site ensures no receptor aggregation (and therefore activation) in the absence of antigen.

TOPOLOGY OF FcεRI AND IgE COMPLEXES ON THE CELL SURFACE

At present it is believed that the extracellular region of FcεRI lies along the cell membrane rather than being a rigid upright structure. Unlike other related FcR e.g. FcγRII and FcγRIII, the membrane proximal region has additional sequence which is likely to provide a rigid extended stalk that may be required to space the two Ig-like domains 'away' from the membrane.[74]

The bent IgE molecule retains its bent conformation when bound to FcεRI (Fig. 1.1). FRET measurements indicate that when bound to the receptor, the C terminus sits approximately 53Å (5.3 nM) off the membrane with the antigen combining site 69Å (6.9 nM) distant.[64] Overall the antigen combining sites sit >10 nM from the cell surface[75] the disulphide bonds of Cε2 are located approximately 4.5 nM from the surface, level with the Cε2/Cε3 junction. FRET measurements also indicate that, in solution, the antigen combining sites lie approximately 7.1 nM from the C-terminus (Cε4) rather than the 17.1 nM expected for a planar Y-shaped molecule like IgG. Moreover the apparent compact and rigid nature of IgE is clearly different from IgG1 which is much more flexible (probably because of the hinge) and able to adopt multiple conformations.[67]

As a consequence of binding to FcεRI, IgE becomes more rigid.[67] However, the magnitude of this change appears to be relatively small.[67,76] Nonetheless it is clear that relative to the segmental motion of FcεRI in solution, movement is reduced but still occurs when the receptor is bound. This is especially relevant to the Fab arms where most of the segmental flexibility is thought to occur.[69,76]

The measured loss of flexibility is likely to occur at the site of interaction of IgE with FcεRI rather than a generalised alteration of conformation throughout the IgE molecule.[64,67,76] Thus it seems that the bent IgE molecule, with Fab arms that wag and rotate, binds via its convex surface to FcεRI. At this point a transition from a 'low to high affinity state' may occur[77] when, as a consequence of binding, the structure becomes somewhat more rigid but the Fab arms and their antigen combining sites are orientated away from the cell surface and continue to rotate and move.

Even though most of the studies of the topology of the IgE:FcεRI interaction have been performed in rodent systems, given the similar 'bent' conformation of human IgE[68] it is likely that the same events occur in the interaction of human IgE with human FcεRI.

MOLECULAR BASIS FOR FcεRI:IgE INTERACTIONS

Regions of FcεRI That Influence Binding to IgE.

Recent studies by ourselves and others have made significant advances into defining the IgE binding site of FcεRI-α -aspects well reviewed [78-82] (Table 1.2, Fig.1.2, 1.3). The FcεRI-α subunit is the IgE binding chain of the FcεRI-$\alpha\beta\gamma_2$ tetrameric receptor complex, as it is capable of binding IgE with high affinity in the absence of associated FcεRI-β or γ subunits. This has been directly demonstrated through the construction of chimeric receptors comprising the extracellular region of the FcεRI-α chain linked to either the transmembrane and cytoplasmic tails of the p55 subunit of the IL-2 receptor,[53] or the transmembrane and cytoplasmic tail of human FcγRII,[54] which retain high affinity IgE binding.[53,54] Soluble human FcεRI-α, consisting of only the extracellular region, has also

been shown to bind IgE with an affinity that is comparable to that of the wild-type cell-surface receptor, providing further evidence that the FcεRI-α subunit is sufficient for high affinity IgE binding.[83]

The second extracellular domain of the hFcεRI-α chain has been identified as the principal IgE interactive domain (Fig. 1.2, 1.3, Table 1.2). This was first suggested in a study which demonstrated that FcεRI-α mAbs capable of blocking IgE binding to FcεRI-α recognised epitopes in domain 2, whereas mAbs unable to block binding recognised epitopes mapping to domain 1 (Table 1.2).[84] However, these data did not exclude the possibility that the blocking of IgE binding by the domain 2 mAbs was a result of steric hindrance from a site distant to the actual binding site, or due to a conformational change induced in the binding site.

Direct evidence for the role of domain 2 as the binding domain has come from studies utilising chimeric receptors in which extracellular domains of human FcεRI-α were exchanged with human FcγRIIa,[54,85] rat FcεRI-α or human FcγRIII (Table 1.2).[86] These studies also showed that domain 1 plays a crucial role in the high affinity binding of IgE although, with the exception of rat IgE, direct participation in binding was not demonstrated. In our study, we generated chimeric receptors by exchanging the extracellular domains between human FcεRI-α and human FcγRIIa.[54,85] The chimeric receptor comprising domain 1 of human FcγRIIa and domain 2 of the human FcεRI-α chain bound IgE (although with low affinity), whereas a chimera containing domain 1 of the human FcεRI-α chain and domain 2 of human FcγRIIa exhibited no IgE binding (Table 1.2). Similar studies using interspecies chimeras of rat and human FcεRI-α chains, or human FcγRIIIA with the human FcεRI-α chain, have also demonstrated that domain 2 of the human FcεRI-α chain directs the binding of IgE. In these studies, the substitution of domain 2 of human FcεRI-α with domain 2 of human FcγRIII or rat FcεRI-α (neither of which bind human IgE) was found to result in the loss of human IgE binding, whereas the substitution of domain 1 of human FcεRI-α with domain 1 of human FcγRIII or rat FcεRI, maintained human IgE binding.[73,86] The major difference in our studies and those of Mallamaci [86] was that our substitution of domain 1 with human FcγRII resulted in an apparent decrease of high affinity binding, whereas the use

Table 1.2. IgE binding of chimeric FcεRI-α receptors and epitope mapping of anti-FcεRI-α mAb

Chimera[a]		Ig Binding			Inhibitory mAb Binding	
Domain 1	Domain 2	hIgE	rIgE	mIgE	anti-hFcεRI-α	anti-rFcεRI-α
H1	H2	+	+	+	+	-
R1	R2	-	+	+	-	+
II1	II2	+[b]	-	-	-	-
III1	III2	-	-	-	-	-
II1	H2	-[c]	nt	+[c]	+	-
H1	II2	-	nt	-	-	-
III1	H2	+	+	nt	+	-
H1	III2	-	-	nt	-	-
H1	R2	-	-	nt	-	-
R1	H2	+	+	nt	+	+[d]

a. H = human FcεRI-α domain 1 or 2; R = rat FeεRI-α domain 1 or 2
II = human FcγRIIa domain 1 or 2; III = human FcγRIII domain 1 or 2

b. In a single report mouse FcγRIIa has been shown to bind mouse IgE with low affinity,[120] however human FcγRII does not bind human or rodent IgE.

c. Low affinity binding $<10^7 M^{-1}$

d. Binds two inhibitory mAb

of human FcγRIII or rat FcεRI-α as described by Mallamaci *et al.*[86] had no effect on high affinity binding (Table 1.2).

Clearly domain 1 of human FcγRIII and rat FcεRI-α must be better able to substitute for human FcεRI-α domain 1 than human FcγRII domain 1 to maintain correct receptor conformation. This is perhaps not surprising as both human FcγRIII and rat FcεRI-α domain 1 exhibit significantly higher amino acid identity to human FcεRI-α domain 1 than human FcγRIIa. Indeed, the finding that domain 2 of human FcεRI-α when expressed as a single domain in either a filamentous phage display system[73,87] or in a transient COS cell system[86] exhibited only weak or no IgE binding, respectively, clearly indicates that domain 1 of human FcεRI-α plays an important role to ensure correct receptor interaction with IgE.

Of interest is the observation that rat IgE appears to interact with rat FcεRI differently than does human IgE with human FcεRI.[86] A chimera containing domain 1 of human FcεRI-α and domain 2 of rat FcεRI-α did not bind rat IgE; however, a chimera containing domain 1 of rat FcεRI-α and domain 2 of human FcεRI-α bound rat IgE with higher affinity than wild-type human FcεRI-α (Table 1.2). This finding, together with the observation that rat FcεRI-α chain mAb that inhibit rat IgE binding recognise epitopes localised in domain 1, suggest that domain 1 plays a crucial role in the interaction of rat IgE with rat FcεRI-α. These data suggest that the focus of the interaction of human and rat IgE with their respective receptors is different, which may not be surprising given that human and rat FcεRI-α share only 38% amino acid sequence identity. Thus it is possible that distinct IgE binding sites do exist in human and rat FcεRI-α, with domain 2 of human FcεRI-α containing a binding site for human IgE and domain 1 of rat FcεRI-α a binding site for rat IgE. It is interesting to note that rat IgE was found to bind to a chimera comprising domain 1 of human FcγRIII and domain 2 of human FcεRI-α, suggesting that human FcεRI-α interacts with rat IgE principally though domain 2, in contrast to rat FcεRI-α which appears to bind rat IgE through domain 1. Another possible explanation or the apparent difference in the binding of rat and human IgE to FcεRI-α is that certain domains are not able to substitute fully for others in the context of specific chimeric receptors to ensure conservation of correct receptor structure. Therefore, whilst it is

Figure 1.2 IgE binding regions of human FcεRI-α.

Regions of the extracellular domains of human FcεRl-α which influence the binding of (A) human, (B) mouse and (C) rat IgE are shaded, and flanking residues numbered. See text for details.

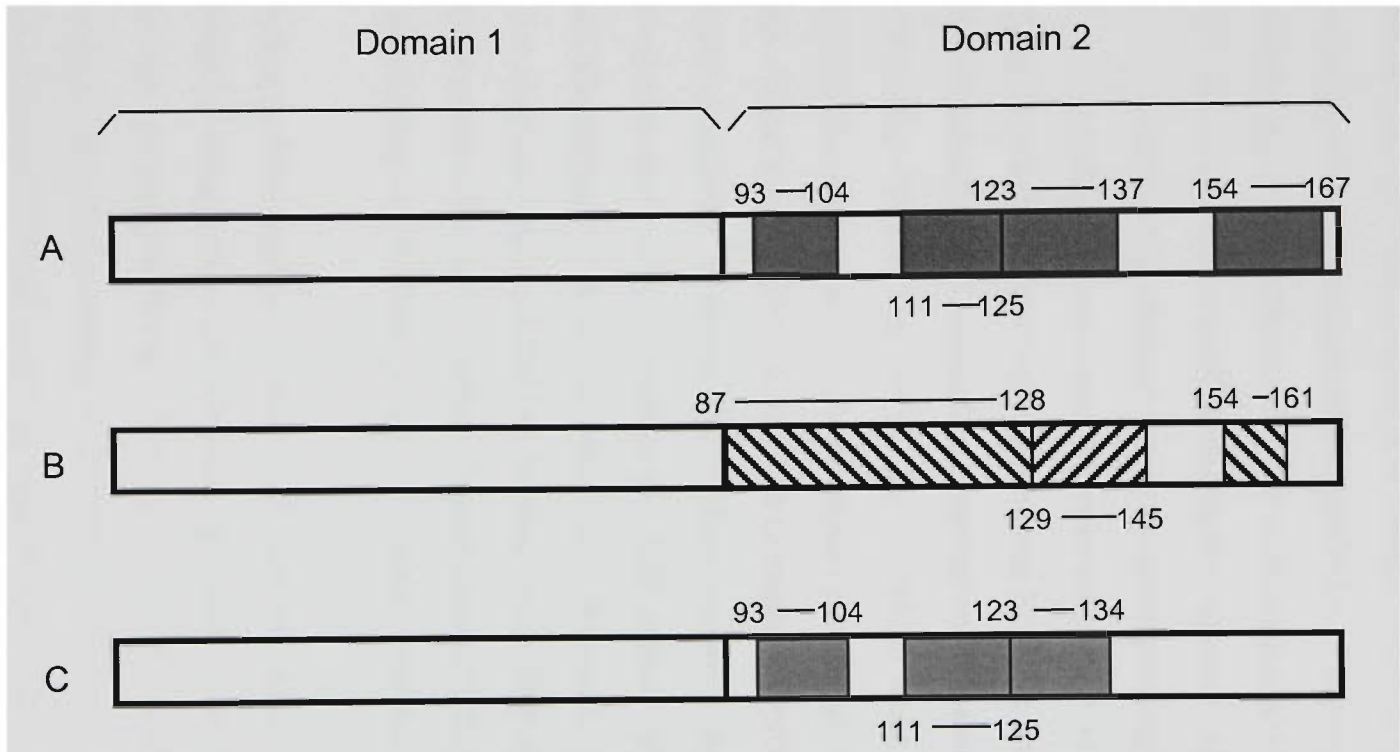
Domain 1
Domain 2
A
93 104
123 137
154 167
111 125
B
87 128
154 161
129 145
C
93 104
123 134
111 125

17a

apparent from the chimeric receptor studies that specific domains interact with IgE the precise role of other regions or domains still remains unclear; for example, domain 2 of rat FcεRI-α.

The IgE binding regions within domain 2 of human FcεRI-α have been mapped further to subregions using homologous scanning mutagenesis. Two separate studies have both identified multiple regions of domain 2 as crucial in the interaction with IgE (Fig.1.2, 1.3).[54,86] We used human FcγRIIa as a scaffold to display regions of human FcεRI-α by replacing segments of human FcγRIIa domain 2 with the corresponding regions of human FcεRI-α domain 2.[54] Using this 'gain of function' approach (i.e., FcγR binding IgE) we have identified at least three independent regions of human FcεRI-α domain 2 capable of *directly* binding IgE. The human FcεRI-α domain 2 regions encompassed residues Trp 87 to Lys 128, Tyr 129 to Asp 145 and Lys 154 to Glu 161 which when inserted into into human FcγRIIa were each independently found to *impart* mouse IgE binding to human FcγRIIa (Fig. 1.2A). These human FcεRI-α/FcγRIIa chimeric receptors bound IgE only in the form of immune complexes, implying that all three regions (together with domain 1 as discussed above) contribute to the formation of a high affinity IgE binding site. A similar approach utilising human FcεRI-α/ human FcγRIII chimeras, employing a loss of function strategy, has also identified multiple IgE binding sites of human FcεRI-α domain 2.[86] This approach involved the insertion of homologous regions of human FcγRIIIa into human FcεRI-α, and the *loss* of IgE binding function was determined.

The substitution of three regions of human FcεRI-α with the equivalent regions of human FcγRIII resulted in the complete loss of human IgE binding; Ser 93 to Phe 104, Arg 111 to Glu 125 and Asp 123 to Ser 137 (Fig. 1.2B). These regions correlate with two of the three IgE binding regions defined in our study, as both the Ser 93 to Phe 104 and Arg 111 to Glu 125 regions identified by Mallimaci *et al.*[86] are situated in our Trp 87 to Lys 128 region, and the Asp 123 to Ser 137 region of Mallimaci *et al.*[86] overlaps our Tyr 129 to Asp 145 region. Substitution of a fourth region of hFcεRIα (Lys 154 to Ile 167) resulted in a partial loss of IgE binding and corresponds with the third of the direct IgE binding regions defined in our study, i.e., Lys 154 to Glu 161. As the readout for the Mallimaci experiments was loss of IgE binding, these data can also be interpreted as the replacement of these

Figure 1.3 Postulated alpha carbon backbone of the extracellular domains of human FcεRI-α. (A) Domains 1 and 2 are shown, the β-strands of Domain 2 are labelled with black letters. Consensus regions known to be involved in the interaction with IgE as defined in chimeric receptor studies are shown in red, loops between β-strands in this region are labelled in green. (B) Stereo view of FcεRI-α model labelled in (A).

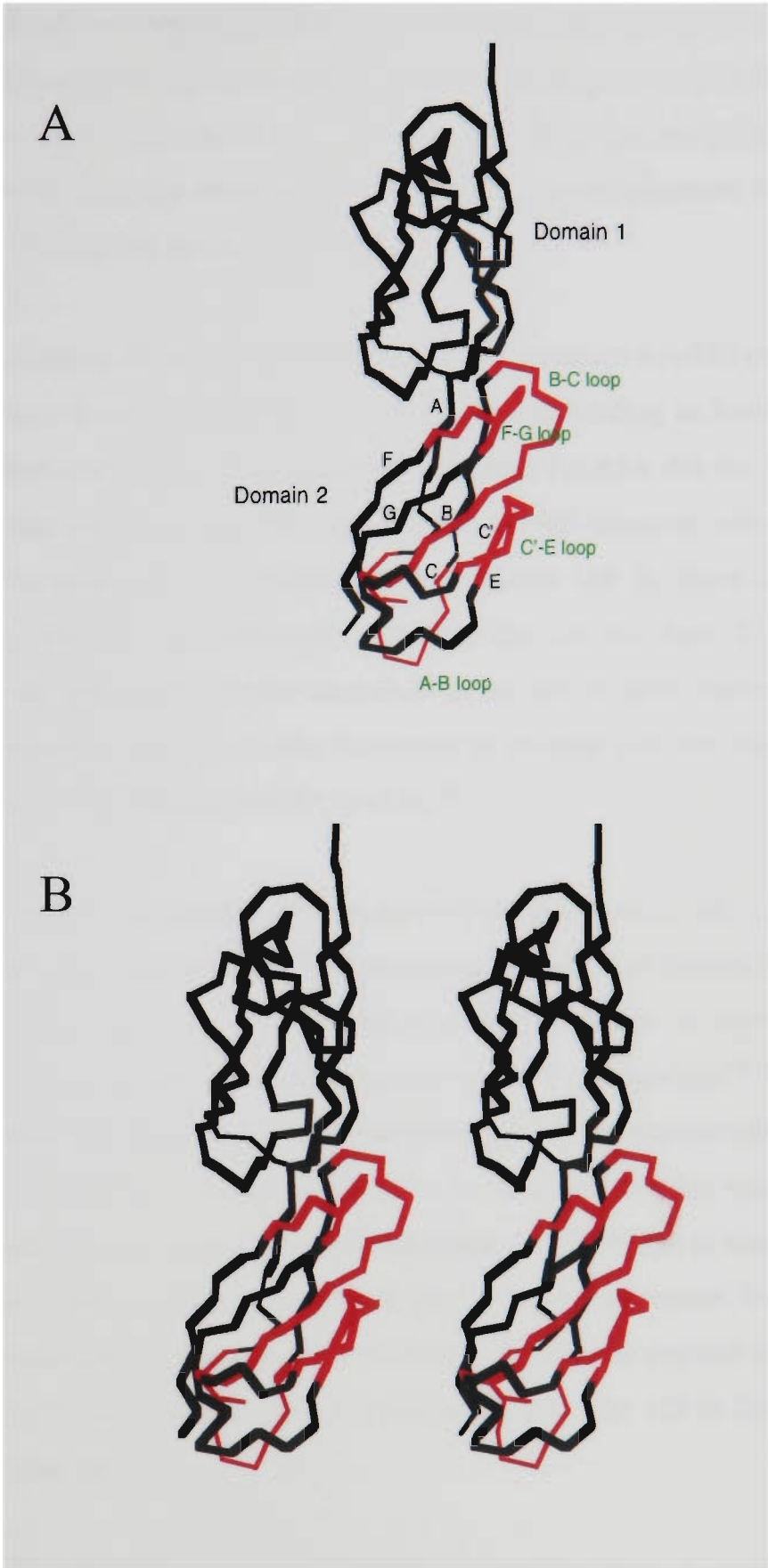
A
Domain 1
B-C loop
A
F-G loop
F
Domain 2
G
B
C'
C'-E loop
C
E
A-B loop
B

regions of FcεRI-α simply resulting in a conformational change in the receptor, thus altering IgE binding to a distant binding site. With the exception of the Lys 154 to Ile 167 substitution, none of the domain 2 chimeric receptors were recognised by any of the inhibitory mAb, thus the possibility of an alteration in conformation being responsible for loss of IgE binding cannot be excluded.

The binding of rat IgE to the human FcεRI-α/human FcγRIII chimeras was also examined, and found to exhibit the same pattern of binding as human IgE with the exception that residues Lys 154 to Ile 167 of human FcεRI-α did not influence rat IgE binding in this system. These data suggest that rat IgE interacts with human FcεRI-α differently to human IgE. However, rat and human IgE do share common binding regions, i.e., Ser 93 to Phe 104 and Arg 111 to Glu 125 and Asp 123 to Ser 137 (Fig. 1.2C). The rat IgE binding region contained in the last of these regions can be further located to residues Asp 123 to His 134 based on overlap with the His 134 to Glu 163 region identified as not required for binding.[86]

Whilst the role of domain 2 has been well characterised, the role of domain 1 is still unclear. The substitution of two regions in domain 1 of human FcεRI-α, namely residues 35-46 and 80-92, were found to result in a loss of human IgE binding, suggesting these regions may also play a role in human IgE binding.[86] However, both of these chimeras, although expressed on the cell surface, were not recognised by any of the FcεRI-α mAb tested, thus they are likely to be incorrectly folded making conclusions about the role of these regions in IgE binding difficult. Therefore in summary, the results of these two studies clearly demonstrate that domain 2 of human FcεRI-α is an IgE interactive domain of human FcεRI, and identify at least four regions contributing to the binding of IgE, Ser 93 to Phe 104, Arg 111 to Glu 125, Tyr 129 to Ile 137,[FOOTNOTE 4] and Lys 154 to Glu 161 .

In the absence of a genuine 3-dimensional structure, a number of molecular models of human FcεRI-α have been proposed.[80,85,88] We have generated a model of

[4] Overlapping region of the 123-137 region identified by Mallimaci *et al.*,[86] and the 129-145 region identified by Hulett *et al.*[54]

human FcεRI-α domain 2 based on the structure of domain 2 of CD4.[85] The model is a truncated C2-SET domain comprising seven β-strands forming two antiparallel β-sheets, linked by a disulphide bridge between strands B and F (Fig.1.3). Similar models have also been proposed based on CD2 domain 2,[80,89] or antibody domains.[88] The latter group has proposed two models which differ in the orientation of the two extracellular domains relative to one another. One model has the two domains positioned end-to-end allowing only longitudinal interaction between the domains, with the second proposing a bent conformation promoting more lateral interaction between the two domains. Based on all of these models, the identified IgE binding regions of human FcεRI domain 2 are situated predominantly in loop regions juxtaposed at the interface with domain 1, specifically the F-G, C'-E and B-C loops, with contributions also from the B and C strands (Fig. 1.3).

The localisation of the domain 2 IgE interactive sites to this region of domain 2, together with the finding that domain 1 also plays a key role, suggests it is this interdomain interface between domains 1 and 2 that comprises the IgE binding site of human FcεRI-α. In support of this model, the mAb 15A5 which recognises an epitope encompassed by residues 100-115 of human FcεRI-α (corresponding to the B-C loop and B strand), can completely block the binding of IgE to FcεRI, suggesting the multiple IgE binding sites are indeed juxtaposed.[84]

It is becoming apparent that, based on the studies described herein for FcεRI-α and those described elsewhere for the FcγR, i.e., FcγRI,[90] FcγRII[91,92] and FcγRIII,[93] there are a number of structural similarities in the molecular basis of how these receptors interact with their respective ligands. The two Ig-like domain structure of the extracellular regions of the leukocyte FcRs clearly represents a conserved binding motif of this receptor family.[90] The second extracellular domain of all these receptors is responsible for the direct binding of Ig, with the first domain playing a crucial role in maintaining optimal binding.[54,73,86,93] The mapping of the Ig binding regions in domain 2 of human FcεRI and human FcγRII has indicated that the interaction of these receptors with their Ig ligands involves similar regions. Three homologous regions of both human FcεRI-α and human FcγRIIa domain 2 play crucial roles in the binding of IgE and IgG respectively.[54,86,92]

Based on model domain structures, the Ig binding regions of both receptors are located in similar regions of domain 2 juxtaposed at the domain 1 interface, namely the B-C, C'-E and F-G loops (Fig. 1.3).[80,85,88,92] The influence of domain 1 on the Ig binding by domain 2 in both human FcγRII and human FcεRI, is consistent with the location of the binding regions of these receptors in close proximity with domain 1, i.e., the interface of domains 1 and 2. Thus, the finding that these loop regions are involved in the binding of Ig by two functionally distinct FcRs, in conjunction with the conserved nature of the two domain extracellular binding 'unit' of the leukocyte FcRs, strongly suggests that this region will also comprise the key interactive site of all members of this family. Based on this observation, it can be postulated that the structurally conserved 'Ig folds' of the second extracellular domains of the leukocyte FcRs are providing the 'scaffolding' to display 'variable' loop regions which contain determinants directing the specificity of these receptors for their Ig ligands.

Since submission of this review, the crystal structures of FcγRIIa [121], FcγRIIb[122] and FcεRI-α[123,124] have all been solved. Prior to publication of the structure of FcγRIIa, Maxwell and Powell kindly made the co-ordinates available to enable a structure of FcεRI to be modelled after the closely related receptor FcγRIIa. The crystal structure of FcγRIIa displays the two extracellular Ig-like domains "bent" to form an angle of 52° between domains 1 and 2. This was the most acute angle determined in Ig-like molecules to date, and it is interesting in that the FcR are the only molecules of this group (with two Ig-like domains) that contain the major binding region in the second domain of the molecule. This feature, along with the twist in the domains that causes the A strands of both domains to lie close to the interdomain interface, permits the display and projection of the binding site away from the cell surface and to solvent. It is probable that interactions within the interdomain interface, including molecules of water, maintain this acute interdomain angle, and presentation of the ligand binding site. The acute interdomain angle is maintained in FcεRI although neither the precise angle, nor the presence of water molecules has been reported. FcεRI and FcγRIIa display a 40% amino acid identity, and greater homology, thus it is probable that FcεRI would have a similar structure to that of FcγRIIa. Indeed, comparison of the FcεRI homology model and published information regarding the solved FcεRI structure[123] confirms the similarity.

The solved x-ray structure of FcεRI-α[123] strongly resembles that of FcγRIIa, and therefore that of the FcεRI-α homology model. Indeed, the FcεRI-α homology model and the x-ray structure of FcεRI-α show compelling concurrence in comparisons of structure and molecular interactions.

Regions of IgE That Influence Binding to FcεRI.

Intense interest in how IgE binds to FcεRI has involved many groups over a considerable time. These data are summarised in Figure 1.4 and in the model structures of Figure 1.5. In these the essential binding regions are indicated. In the model (Fig. 1.5) the relationships of different regions of IgE, shown by different investigators to influence binding to FcεRI, are presented. It is noteworthy that despite obvious differences in the extent of the mutations of IgE, there are clearly overlapping regions that influence binding; these are shown in stereo in Figure 1.5E.

Early studies using papain digestion of IgE to produce Fc fragments capable of blocking IgE binding to mast cell FcεRI, localised binding to Cε2, Cε3 and Cε4 (Fig. 1.4). However, attempts to further localise this IgE binding region by continued fragmentation of IgE were unsucessful, indeed Fab'2 fragments or isolated Cε2 failed to block IgE binding. Thus these experiments suggested that the tertiary and quaternary structure of IgE-Fc was important for receptor binding.[60,94,95] A separate study observed that the junction region of rat Cε2/Cε3 was partially protected from tryptic digestion when cell bound, and proposed this region as the FcεRI binding site.[96] Circular dichroism with thermal inactivation of human myeloma IgE indicated that Cε3 and Cε4 were likely to be implicated in binding, but not Cε2.[57]

Synthetic peptides have been used in separate approaches to identify the FcεRI binding site of IgE. These include use as competitive inhibitors of IgE binding to FcεRI and in epitope mapping studies using monoclonal anti-peptide antibodies or anti-IgE antibodies. An early study reported that a synthetic pentapeptide of amino acids residues

Figure 1.4 Compilation of data from a number of studies which identify regions of IgE influencing binding to FcεRI. Sources of the data are from indicated references. (After Beavil)

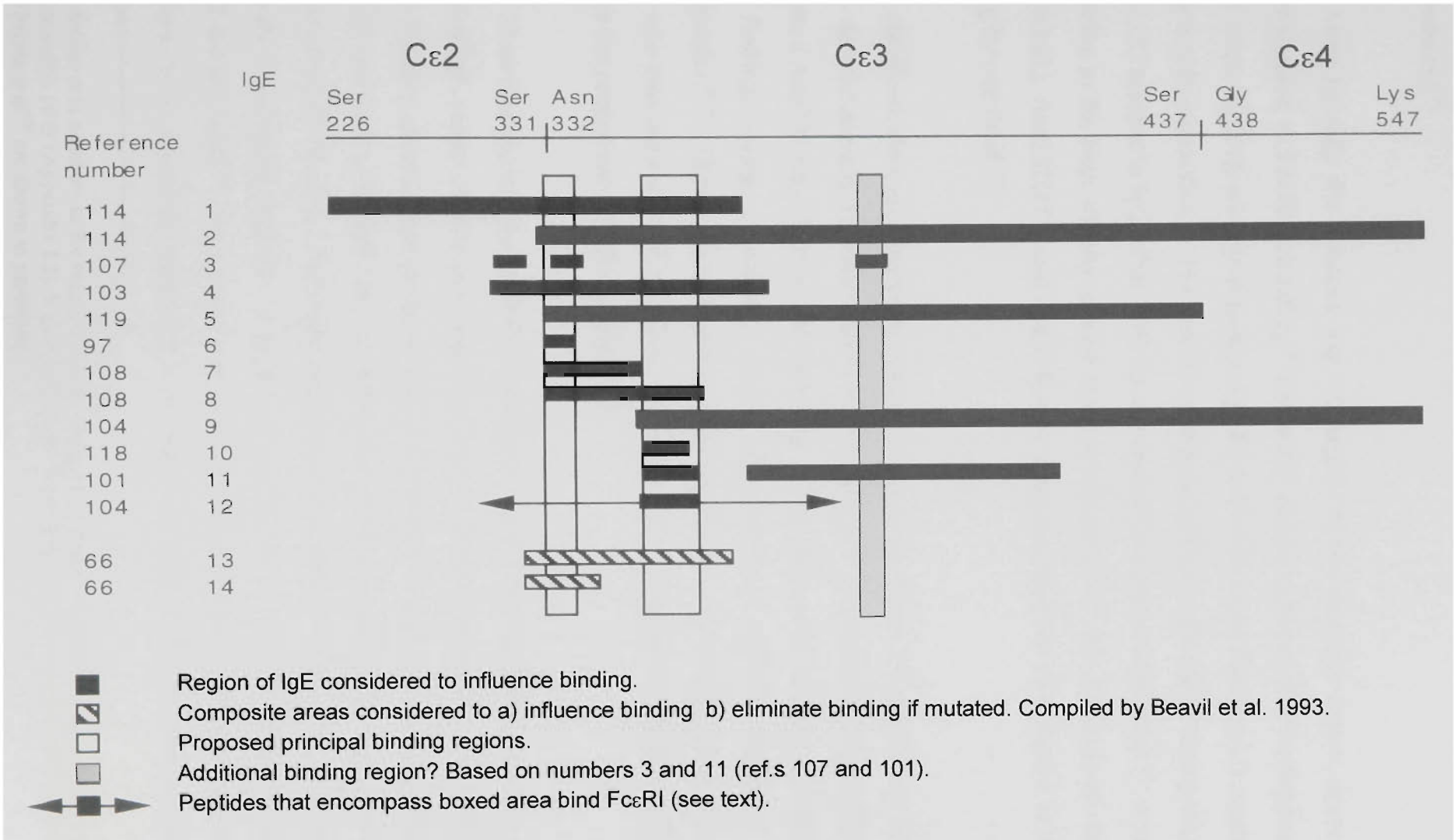
IgE
Cε2
Cε3
Cε4
Ser 226
Ser 331
Asn 332
Ser 437
Gly 438
Lys 547
Reference number
114 1
114 2
107 3
103 4
119 5
97 6
108 7
108 8
104 9
118 10
101 11
104 12
66 13
66 14
Region of IgE considered to influence binding.
Composite areas considered to a) influence binding b) eliminate binding if mutated. Compiled by Beavil et al. 1993.
Proposed principal binding regions.
Additional binding region? Based on numbers 3 and 11 (ref.s 107 and 101).
Peptides that encompass boxed area bind FcεRI (see text).

Asp330 - Gly 335 (320-324)[FOOTNOTE 5] in the human Cε2/Cε3 junction region was able to partially inhibit the Prausnitz-Küstner reaction,[97] although the experiment was unable to be reproduced.[98]

More recently the residues Asp330-Arg334 in this junction region, again have been implicated in FcεRI-α binding,[80] and it has been suggested that mutagenesis of Pro333 alters binding affinity of human IgE-Fc to FcεRI-α and thus could impart high affinity to this interaction.[66] The Pro333 residue is located in the equivalent position to the Leu 235 residue in IgG1 that, with its associated residues Leu234-Gly237, is crucial for binding to the high affinity gamma receptor (FcγRI).[99,100] Mutagenesis of residues Asp330(361), Asn332(363) and Arg334(365) to alanine has also been shown to reduce binding by one third.[101]

An *E.coli*-derived peptide of amino acid residues Gln301-Lys376 was the first *E.coli*- derived peptide demonstrated to bind FcεRI-α,[102] and it encompasses this often implicated Asp330-Gly335 residue block (Fig. 1.5A). However, attempts to reproduce these findings using a similar, active, *E.coli*-derived IgE-Fc fragment were unsuccessful.[81,103] The explanation for this discrepancy may be in the experience of Liu *et al*[95] who also used active *E.coli*-derived fragments, but suggest that incorrect folding reduces the proportion of active molecules.

Notwithstanding the potential problems in the native folding of the *E.coli* produced IgE, recent studies have shown that *E.coli*-derived, Glutathione-S-transferase (GST) ε heavy chain fusion proteins, containing approximately 120 amino acids from Cε2,Cε3 and Cε4 will inhibit human IgE binding to FcεRI-α if they *encompass* a Cε3 sequence Pro343-Ser 353. This sequence of Cε3 is positioned in the loop that joins the β-strands A and B,although the 18 amino acid sequence Leu340-Thr357 fused directly to GST did not bind.[104] Thus, large fragments need the Pro343-Ser353 sequence to bind, but there is a structural requirement enabling binding to occur that is provided

[5] Amino acid numbers in the sequence of IgE used in this chapter are based on those of Dorrington and Bennich 1978 (Appendix I.2). It should be noted that residue numbers used by Hamburger[97] and Presta *et al*[101] are shown in parenthesis.

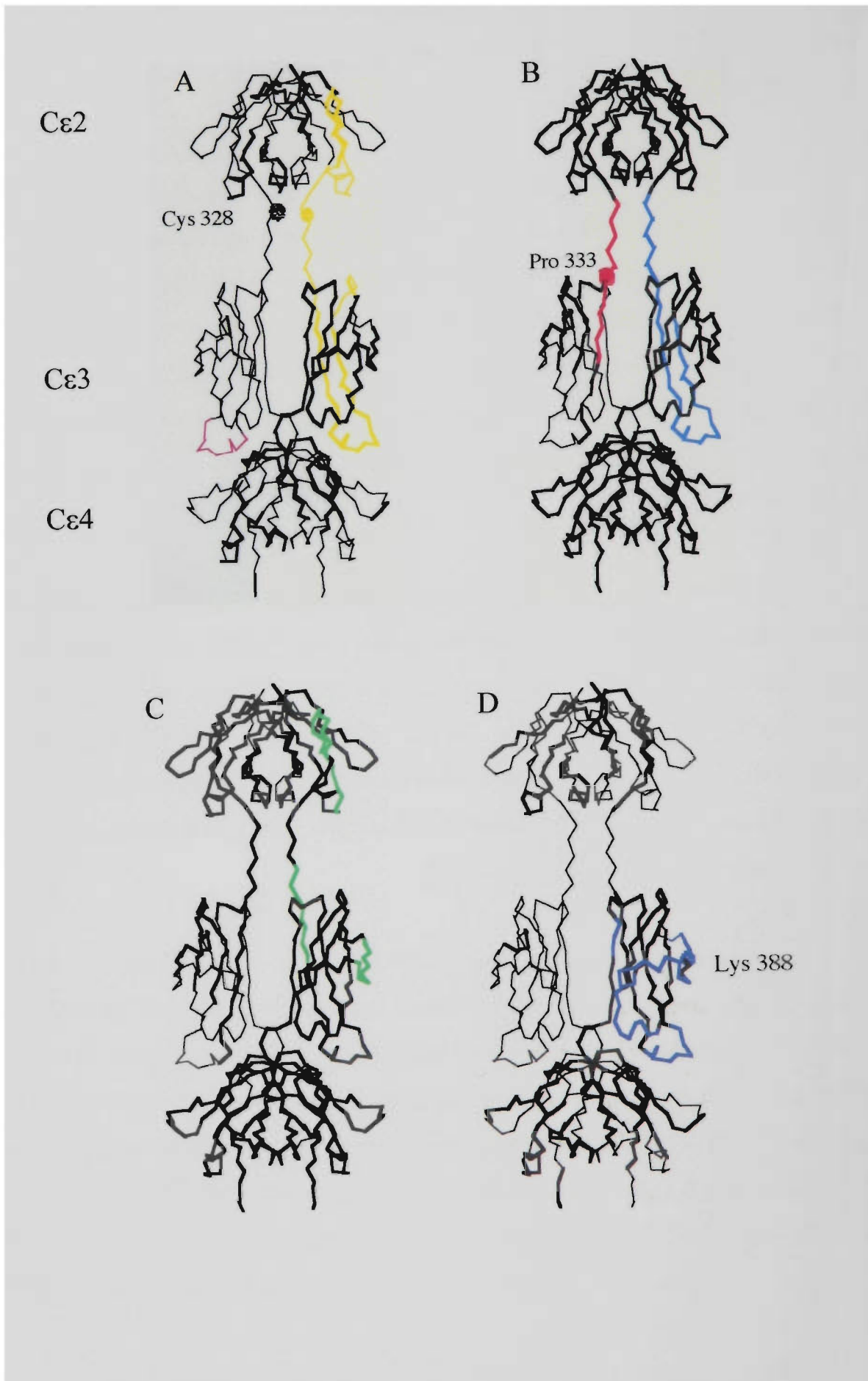
A
B
Cε2
Cys 328
Pro 333
Cε3
Cε4
C
D
Lys 388

E

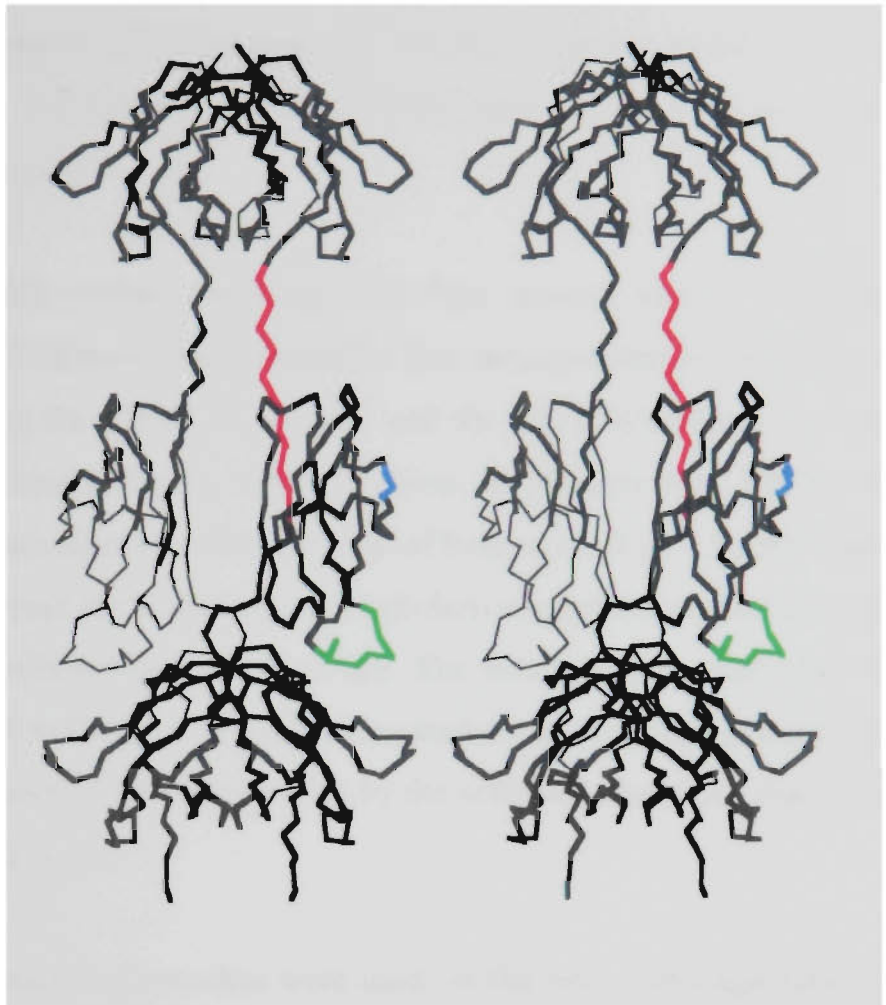

Figure 1. 5 Alpha carbon backbone models of IgE-Fc showing regions identified by different investigators to influence binding to FcεRI-α.

For the sake of clarity the models are based on a planar structure (Padlan and Helm, PDB Identifier 2IgE) not bent, and are designed merely to indicate the extent and location of various residues involved in the IgE:FcεRI interaction. Data from (A) Helm[104], yellow indicates the region equivalent to the original peptide that blocked binding; magenta, the region that large peptides need to encompass in order to block binding. Data from (B) Beavil[66], blue, indicates the region of residues necessary for binding; red, regions in which mutations destroy binding. Data from (C) Takemoto[107] and (D) Presta[101] indicating regions involved in receptor binding. (E) Stereo view of regions in Cε3 common to more than one of the studies above.

by other amino acids in Cε2,Cε3 and Cε4.[56,59,60] It is interesting to note that in experiments using eukaryotic expression of truncated IgE fragments fused to p55 (the IL-2 receptor signal peptide) the smallest functional fragment produced was composed of residues Ala 329-Lys 547, deletions from either the N or C termini rendered the fragments inactive.[103]

A recent review compiling data from several studies[43,102,105,106] using *E.coli* fragments and chimeric IgE antibodies, has indicated that residues Cys 328-Val 361 (encompassing the Cε2/Cε3 junction and the AB loop) appear to be sufficient for binding/inhibition activity, while deletions in residues Cys 328-Tyr 339 destroys activity,[66] which agrees with the findings of Helm *et al.* (Fig. 1.5A,B). Epitope mapping using monoclonal antibodies to IgE or IgE-derived peptides is an alternative approach to define the FcεRI-α binding site on IgE. The action of such antibodies that block the binding of IgE to FcεRI-α have also been studied, and while introducing the problem of steric hinderance of receptor binding by the antibody, also show that Cε3 contains the major binding site(s).

Two related approaches were used, in the first, Fab fragments of mouse anti-human IgE monoclonal antibodies - the epitopes of which were localised to residues Ser 306-Gln 313, Thr 311-Thr 320 of Cε2, Ser 331-Ala 338 or Val 382-Lys 391 of Cε3 - could inhibit IgE binding to FcεRI-α, though not completely. However, some combinations of these were more potent which implies that either multiple contact sites (defined by these epitopes) are involved in binding, or that these epitopes are close to, but not part of, the binding region (Fig.1.5C).[107] However, the location of these epitopes correlate with FcεRI-α binding sites in IgE defined by use of recombinant IgE proteins. Thus the Thr 311-Ala 338 encompasses the Cε2/Cε3 junction region, and residues Val 382-Lys 391 coincide with the β-strand D where Presta[101](Fig. 1.5D) also found that exchanging Lys 388-Arg 393 for the equivalent section of IgG could remove binding, or, changing Lys 388(423) to Pro, but not Ala could obliterate binding. The Thr 311-Ala 338 region is within the Gln 301-Lys 376 critical binding region of Helm,[61,102] and Ser 331-Ala 338 overlaps the Cys 328-Val 361 segment of Beavil,[66] but not the Pro 343-Ser 353 segment recently defined.[104] More recent work[108] has confirmed that human Cε3 is the

main binding site for human FcεRI-α, and has proposed that Cε2 is required for conformation and stability; also that FcεRI-α binding is probably not restricted to any one site on IgE.

It is not surprising that these data, accumulated in various expression systems,with different assay methods, differ in their conclusions. The Cε2/Cε3 junction region has been implicated many times, as has the Cε3 AB loop; other regions showing binding interaction are those on the Cε3 EF loop and CD loop[101] facing the same Cε2/Cε3 cleft as the Cε3 AB loop, also the Cε3 FG loop which impinges into the spatial area of the Asp 330-Gly 335 (Cε2/Cε3) junction site. The sensitivity of IgE binding to mutation of the Cε3 D strand implies the segment may impart structural stability to Cε3.[101] These site directed mutagenesis experiments, have led Presta[101] to propose that the exposed face of the human Cε3 domain binds human FcεRI-α by electrostatic interaction. However, the radical amino acid replacements that were employed in this study, could have, by their size or charge difference, caused major structural alterations.[104]

Rat and mouse IgE have been shown to bind rodent FcεRI-α[3] with a stoichiometry of 1:1[109] and also to human FcεRI-α[110] with lower affinity but the same stoichiometry. However, human IgE does not bind to rodent FcεRI-α.[104,110] The differences in specificity have been exploited to localise binding sites by building chimeric immunoglobulins from rodent or human IgE with IgG. Human IgG1/ mouse IgE chimeras have shown that both Cε2 and Cε3 are necessary for rodent (mouse) IgE to bind rodent (rat) FcεRI,[111] but human IgE/ mouse IgE chimeras suggest that only Cε3 is necessary.[106] This could imply that γ at C2 obstructs binding, and human or mouse Cε2 is required for conformational stability.[106] Only Cε3 and Cε4 are required for high affinity binding in human IgE,[106] although Cε2 has been implicated,[107] rodent (mouse) Cε4 is not required for binding rodent (rat) FcεRI.[111,112] Further human IgE/mouse IgE chimeras of Cε3 have shown that exchanges to mouse at residues Ser 300-Phe 346 in the Cε2/Cε3 junction region of human IgE, cannot impart the ability to bind rodent FcεRI-α, nor can this exchange with mouse Cε2 replacing human Cε2;[108] although both chimeras bind human FcεRI-α.

In human IgE the Cε2/Cε3 junction region and the Cε3 AB loop have been implicated

in high affinity binding. In rodent FcεRI binding, the AB loop exchanged for rat in a human IgE/rat IgE chimera, does not confer rodent FcεRI-α binding to the human IgE, and the chimera continues to bind human FcεRI-α.[104] Chimeras containing both these regions (Ser 300-Ile 356) as rodent, with either mouse or human Cε2, do not bind rodent FcεRI-α, but retain the ability to bind human FcεRI-α. An additional Cε3 chimera containing more Cε3-derived sequence (Thr 357-Val 399) did not bind rat FcεRI-α and had reduced binding to human FcεRI-α; confirming the need for a complete rodent Cε3 for rodent FcεRI binding.[106,108,112,113] Cε4 is not required for binding, but is important in conformation.[113]

The binding region of IgE would appear to involve several sites, with the major sites in the Cε2/Cε3 junction region[80] and the Cε3 AB loop (residues Pro 343-Ser 353).[114] The former region has homology with the region of IgG1 that imparts high affinity binding to FcγRI and is conserved in human and rodent IgE. The latter region projects into the cleft between Cε3 and Cε4, which has homology to a site on rat IgG1 that contains many histidine residues, and has been shown by crystallography to bind the side of the neonatal rat receptor FcRn at the junction of domain 1 and domain 2.[115] However, this IgG receptor is unrelated to FcεRI-α or any other Fc receptor, thus the significance of this interaction is difficult to assess.

In summary, human IgE can bind human FcεRI, but not rodent FcεRI; and the main regions of binding appear to be at the Cε2/Cε3 junction and the Cε3 AB loop with perhaps, the D β-strand and/or a face of Cε2 fronting the Cε2/Cε3 cleft assisting. The Cε2 and Cε4 domains have been implicated more for their donation to structure than high affinity binding. The rodent IgE molecule appears to be more sensitive than human IgE, and requires the Cε3 domain to be intact and totally rodent in order to bind to rodent FcεRI, but is capable of binding human FcεRI with Cε3 in intact rodent or chimeric form. As with the human, the major function of the Cε2 and Cε4 domains appears to involve supplying a stable supporting structure. Noting the small but significant differences between human and rodent FcεRI binding regions on their IgE, it is interesting to return to the suggestion that *domain 1* of rodent FcεRI-α is important in *rat IgE* binding, whereas human FcεRI-α *domain 2* is the principal binding region for both human and rat IgE.[86]

CONCLUDING REMARKS

How does the IgE:FcεRI interaction take place?

We have come a long way in attempting to define the molecular basis of the IgE:FcεRI interaction but the details of how IgE and FcεRI react is, at present, a difficult question to answer with certainty. The prodigious effort in attempting to define how this interaction takes place has improved our knowledge of the likely portions of IgE and FcεRI that govern the interaction. Structure:function studies, especially those of the last decade, have provided us with a better understanding of key regions of IgE and FcεRI that influence their interaction. Together with biophysical experiments, these have given us a general picture of a bent IgE with several areas of its convex face interacting with a receptor whose two domains also contain multiple regions that enable it to interact with its ligand.

There are still many issues to be resolved, and none more sought after than the elucidation of the precise interatomic associations that collectively define this high affinity interaction. It is almost certain that such information will come from solving the structure of FcεRI:IgE co-crystals. Such information has been elusive, but as protein expression systems and crystallisation technologies improve, the day will come when such information will become available to us - even if only through the patent literature! At present, however, we can develop plausible hypotheses on how this interaction takes place.

It has been suggested that when bound, IgE lies along the receptor on its two fold axis of symmetry, [66,80,116] but it has not been determined whether the binding site(s) are all on one, or on both IgE heavy chains. Indeed there is ample evidence that the latter may be the case: (1) the IgE:FcεRI stoichiometry is 1:1; (2) the Cε2/Cε3 junction of IgE is protected from trypsinisation when bound;[96] (3) this protection is bilaterally symmetrical[96] and that IgE monomer does not bind;[117] (4) whole IgE will not bind if its critical interchain (human, intrachain-rat) disulphide bonds are not intact;[60] and (5) it has been suggested that Cε2 is rotated.[68] This could occur if the Cε2 (a) chain was rotated to align with protruding portions of the Cε3 (b) chain. It is also possible that the IgE molecule could bind at an angle across the domain 1/domain 2 junction of the receptor, (and not along the long axis

of the receptor) with different segments of Cϵ2/Cϵ3 interacting with the receptor; - do the Cϵ2/Cϵ3 junction and the Cϵ3 AB loop interact with different segments of FcϵRI?

Thus, the challenge of the moment is to refine the models on the basis of solid data, and accept or reject these as maybe. At the end of the day resolution of co-crystal structures will be informative, and in combination with the already assembled data will provide the impetus for the development of effective strategies for the treatment of IgE induced inflammation.

REFERENCES

1. Gounni AS, Lamkhioued B, Ochiai K et al. High-affinity IgE receptor on eosinophils is involved in defence against parasites. Nature 1994; 367:183-186.
2. Conrad D, Cooper M, Fridman WH et al. IUIS/WHO Subcommittee on nomenclature of Fc receptors. Nomenclature of Fc receptors. Bulletin of the World Health Organisation. 1994; 72(5):809.
3. Kulczycki Jnr A, Metzger H. The interaction of IgE with rat basophilic leukemia cells. II. Quantitative aspects of the binding reaction. J Exp Med 1974; 140:1676-1695.
4. Conrad DH, Froese A. Characterization of the target cell receptor for IgE. II. Polyacrylamide gel analysis of the surface IgE receptor from normal rat mast cells and from rat basophilic leukemia cells. J Immunol 1976; 116:319-326.
5. Kulczycki A Jnr, McNearney TA, Parker CW. The rat basophilic leukemia cell for IgE. I. Characterization as a glycoprotein. J Immunol 1976; 117:661-665.
6. Kanellopolous J, Rossi G, Metzger H. Preparative isolation of the cell receptor for immunoglobulin E. J Biol Chem 1979; 254(16):7691-7697.
7. Holowka D, Hartmann H, Kanellopolous J et al. Association of the receptor for immunoglobulin E with an endogenous polypeptide on rat basophilic leukemia cells. J Recept Res 1980; 1:41-68.
8. Holowka D, Metzger H. Further characterization of the β-component of the receptor for immunoglobulin E. Mol Immunol 1982; 19(2):219-227.
9. Perez-Montfort, R Kinet J-P, Metzger H. A previously unrecognised subunit of the receptor for immunoglobulin E. Biochemistry 1983; 22:5722-5728.
10. Alcaraz G, Kinet J-P, Kumar N et al. Phase separation of the receptor for immunoglobulin E and its subunits in Triton X-114. J Biol Chem 1984; 259(23):14922-14927.
11. Rivnay B, Wank SA, Poy G et al. Phospholipids stabilize the interaction between the alpha and beta subunits of the solubilized receptor for immunoglobulin E. Biochemistry 1982; 21:6922-6927.
12. Kinet J-P, Alcaraz G, Leonard A et al. Dissociation of the receptor for immunoglobulin E in mild detergents. Biochemistry 1985; 24:4117-4124.

13. Metzger H, Kinet J-P, Perez-Montfort R et al. A tetrameric model for the structure of the mast cell receptor for immunoglobulin E. Prog Immunol 1983; 5:493-501.

14. Metzger H, Alcaraz G, Hohman R et al. The receptor with high affinity for immunoglobulin E. Ann Rev Immunol 1986; 4:419-470.

15. Blank U, Ra C, Miller L et al. Complete structure and expression in transfected cells of high affinity IgE receptor. Nature 1989; 337:187-189.

16. Kinet J-P, Metzger H, Hakimi J et al. A cDNA presumptively coding for the α subunit of the receptor with high affinity for immunoglobulin E. Biochemistry 1987; 26:4605-4610.

17. Kochan J, Pettine LF, Hakimi J et al. Isolation of the gene coding for the α subunit of the human high affinity IgE receptor. Nuc Acid Research 1988; 16:3584.

18. Shimizu A, Tepler I, Benfey PN et al. Human and rat mast cell high-affinity immunoglobulin E receptor: characterization of putative α chain gene products. Proc Natl Acad Sci USA 1988; 85:1907-1911.

19. Liu F-T, Albrandt K, Robertson MW. cDNA heterogeniety suggests structural variants related to the high-affinity IgE receptor. Proc Natl Acad Sci USA 1988; 85:5639-5643.

20. Ra C, Jouvin M-HE, Kinet J-P. Complete structure of the mouse mast cell receptor for IgE (FcεRI) and surface expression of chimeric receptors (rat-mouse-human) on transfected cells. J Biol Chem 1989b; 264(26):15323-15327.

21. Tepler I, Shimizu A, Leder P. The gene for the rat mast cell high affinity IgE receptor α chain. Structure and alternative mRNA splicing patterns. J Biol Chem 1989; 264(10):5912-5915.

22. Varin-Blank N, Metzger H. Surface expression of mutated subunits of the high affinity mast cell receptor for IgE. J Biol Chem 1990; 265(26):15685-15694.

23. Farber DL, Sears DW. Rat CD16 is defined by a family of class III Fcγ receptors requiring co-expression of heteroprotein subunits. J Immunol 1991; 146(12):4352-4361.

24. Ravetch JV, Kinet J-P. Fc Receptors. Annu Rev Immunol 1991; 9:457-492.

25. Ye Z-S, Kinet J-P, Paul WE. Structure of the gene for the α-chain of the mouse high affinity receptor for IgE (FcεRI). J Immunol 1992; 149(3):897-900.

26. Pang J, Taylor GR, Munroe DG et al. Characterization of the gene for the human

high affinity IgE receptor (FcεRI) α-chain. J Immunol 1993; 151:6166-6174.

27. Ravetch JV, Perussia B. Alternative membrane forms of FcγRIII (CD16) on human NK cells and neutrophils. Cell-type specific expression of two genes which differ in single nucleotide substitutions. J Exp Med 1989; 170:481-491.

28. Qui WQ, De Bruin D, Brownstein BH et al. Organization of the human and mouse low-affinity FcγR genes: duplication and recombination. Science 1990; 248:732-735.

29. Le Conait M, Kinet J-P, Berger R. The human genes for the α and γ subunits of the mast cell receptor for immunoglobulin E are located on human chromosome band 1q23. Immunogenetics 1990; 32:183-186.

30. Kinet J-P, Blank U, Ra C et al. Isolation and characterization of cDNAs coding for the β subunit of the high-affinity receptor for immunoglobulin E. Proc Natl Acad Sci USA 1988; 85:6483-6487.

31. Küster H, Zhang L, Brini AT et al. The gene and cDNA for the human high affinity immunoglobulin E receptor β chain and expression of the complete human receptor. J Biol Chem 1992; 267(18):12782-12787.

32. Zloh M, Anderson G, Clark-Lewis I et al. N.m.r. studies of the cytoplasmic C-terminal β-subunit domain of the high-affinity IgE receptor. Biochem Soc Trans 1994a; 22:1027-1029.

33. Zloh M, Anderson G, Clark-Lewis I et al. Spectroscopic and conformational studies of the C-terminal cytoplasmic beta subunit 46-peptide of the high affinity IgE receptor. Biochem Soc Trans 1994b; 22:450S.

34. Sandford AJ, Shirakawa T, Moffat MF et al. Localisation of atopy and β subunit of high-affinity IgE receptor (FcεRI) on chromosome 11q. Lancet 1993; 341:332-334.

35. Hogarth PM, Houlden BA, Latham SE et al. Ly-12.1, a lymphocyte specific alloantigen encoded by a gene linked to Ly-1. Immunogenetics 1988; 27:383-387.

36. Huppi K, Siwarski D, Mock BA et al. Gene mapping of the three subunits of the high affinity FcR for IgE to mouse chromosomes 1 and 19. J Immunol 1989; 143:3787-3791.

37. Küster H, Thompson H, Kinet J-P. Characterization and expression of the gene for the human Fc receptor γ subunit: Definition of a new gene family. J Biol Chem

1990; 265(11):6448-6452.

38. Orloff DG, Ra C, Frank SJ et al. Family of disulphide-linked dimers containing the ζ and η chains of the T-cell receptor and the γ chain of Fc receptors. Nature 1990; 347:189-191.

39. Anderson GJ, Haris PI, Chapman D et al. Synthesis and spectroscopy of membrane receptor proteins. The γ subunit of the IgE receptor. Eur J Biochem 1992; 207:51-54.

40. Masuda M, Roos D. Association of all three types of FcγR (CD64, CD32, CD16)with a γ chain homodimer in cultured human monocytes. J Immunol 1993; 151:7188-7195

41. Ra C, Jouvin M-H, Blank U et al. A macrophage Fcγ receptor and the mast cell receptor for immunglobulin E share an identical subunit. Nature 1989a; 341:752-754.

42. Ernst LK, Duchemin AM, Anderson CL. Association of the high affinity receptor for IgG (FcγRI) with the γ subunit of the IgE receptor. Proc Natl Acad Sci USA 1993; 90:6023-6027.

43. Geha RS, Helm BA, Gould H. Inhibition of the Prausnitz-Küstner reaction by an immunoglobulin ϵ-chain fragment synthesised in *E.coli.* Nature 1985; 315:577-578.

44. Scholl PR, Geha RS. Physical association between the high-affinity IgG receptor (FcγRI) and the γ subunit of the high-affinity IgE receptor. Proc Natl Acad Sci USA 1993; 90:8847-8850.

45. Morton HC, Van den Herikoudijk IE, Vossebeld P et al. Functional association between the human myeloid immunoglobulin A Fc receptor (CD89) and FcR gamma chain - molecular basis for CD89/FcR gamma chain association. J Biol Chem 1995; 270(50):29781-29787.

46. Viver E, Rochet N, Kochan J et al. Structural similarity between Fc receptors and T cell receptors. Expression of the γ-subunit of FcϵRI in human T cells, natural killer cells and thymocytes. J Immunol 1991; 147(12):4263-4270.

47. Qian D, Sperling AI, Lancki DW et al. The γ chain of the high-affinity receptor for IgE is a major functional subunit of the T-cell antigen receptor complex in γδ T lymphocytes. Proc Natl Acad Sci USA 1993; 90:11875-11879.

48. Miller L, Blank U, Metzger H et al. Expression of high-affinity binding of human immunoglobulin E by transfected cells. Science 1989; 244:334-337.

49. Jürgens M, Wollenberg A, Hanau D et al. Activation of human epidermal Langerhans cells by engagement of the high affinity receptor for IgE, FcεRI. J Immunol 1995; 155: 5184-5189.

50. Mao S-Y, Varin-Blank N, Edidin M et al. Immobilization and internalization of mutated IgE receptors in transfected cells. J Immunol 1991; 146(3):958-966.

51. Anderson P, Caligiuri M, O'Brien C et al. Fcγ receptor type III (CD16) is included in the ζ NK receptor complex expressed by human natural killer cells. Proc Natl Acad Sci USA 1990; 87:2274-2278.

52. Howard FD, Rodewald H-R, Kinet J-P et al. CD3ζ subunit can substitute for the γ subunit of Fcε receptor type I in assembly and functional expression of the high-affinity IgE receptor: evidence for interreceptor complementation. Proc Natl Acad Sci USA 1990; 87:7015-7019.

53. Hakimi J C, Seals C, Kondas JA et al. The α subunit of the human IgE receptor (FcεRI) is sufficient for high affinity IgE binding. J Biol Chem 1990; 265(36):22079-22081.

54. Hulett MD, McKenzie IFC, Hogarth PM. Chimeric Fc receptors identify immunoglobulin-binding regions in human FcγRII and FcεRI. Eur J Immunol 1993; 23:640-645.

55. Letourneur O, Sechi S, Willette-Brown J et al. Glycosylation of human truncated FcεRI α chain is necessary for efficient folding in the endoplasmic recticulum. J Biol Chem 1995; 270(14):8249-8256.

56. Helm BA, Ling Y, Teale C et al. The nature and importance of the inter-ε chain disulphide bonds in human IgE. Eur J Immunol 1991; 21:1543-1548.

57. Dorrington KJ, Bennich HH. Structure-function relationship in human immunoglobulin E. Imunol Rev 1978; 41:3-25.

58. Padlan EA, Davies DR. A model of the Fc of immunoglobulin E. Mol Immunol 1986; 23(10):1063-1075.

59. Takatsu K, Ishizaka T, Ishizaka K. Biologic significance of disulphide bonds in human IgE molecules. J Immunol 1975; 114:1838-1845.

60. Rousseaux-Prevost R, Rousseaux J, Bazin H et al. Differential reduction of the

inter-chain disulphide bonds of rat immunoglobulin E: relation to biological activity. Mol Immunol 1984; 21:233-241.

61. Helm BA, Marsh P, Vercelli D et al. The mast cell binding site on human immunoglobulin E. Nature 1988; 331:180-183.

62. Padlan EA, Helm BA. A modeling study of the α-subunit of human high-affinity receptor for immunoglobulin-E. Receptor 1992; 2:129-144.

63. Holowka D, Wensel T, Baird B. A nanosecond fluorescence depolarization study on the segmental flexibility of receptor-bound immunoglobulin E. Biochemistry 1990; 29:4607-4612.

64. Zheng Y, Shopes B, Holowka D et al. Conformations of IgE bound to its receptor FcεRI and in solution. Biochemistry 1991; 30(38):9125-9132.

65. Davis KG, Glennie M, Harding SE et al. Biochem Soc Trans 1990; 18:935-936.

66. Beavil AJ, Beavil RL, Chan CMW et al. Structural basis of the IgE-FcεRI interaction. Biochem Soc Trans 1993; 21(4): 968-972.

67. Zheng Y, Shopes B, Holowka D et al. Dynamic conformations compared for IgE and IgG1 in solution and bound to receptors. Biochemistry 1992; 31(33):7446-7456.

68. Beavil AJ, Young RJ, Sutton BJ et al. Bent domain structure of recombinant human IgE-Fc in solution by X-ray and neutron scattering in conjunction with an automated curve fitting procedure. Biochemistry 1995; 34:14449-14461.

69. Holowka D, Conrad DH, Baird B. Structural mapping of membrane-bound immunoglobulin E-receptor complexes: Use of monoclonal anti-IgE antibodies to probe the conformation of receptor-bound IgE. Biochemistry 1985; 24:6260-6267.

70. Keown M, Ghirlando R, Young RJ et al. Hydrodynamic studies of a complex between the Fc fragment of human IgE and a soluble fragment of the FcεRI α chain. Proc Natl Acad Sci 1995; 92:1841-1854.

71. Kanellopolous J, Liu TY, Poy G et al. Composition and subunit structure of the cell receptor for immunoglobulin E. J Biol Chem 1980; 255(19):9060-9066.

72. Ra C, Kuromitsu S, Hirose T et al. Soluble human high-affinity receptor for IgE abrogates the IgE-mediated allergic reaction. International Immunology 1993; 5(1):47-54.

73. Robertson MW. Phage and Escherichia coli expression of the human high affinity

immunoglobulin E receptor α-subunit ectodomain. J Biol Chem 1993; 268(17):12736-12743.

74. Kershaw MH, Darcy PK, Hulett MD et al. Redirected cytotoxic effector function: requirements of chimeric single chain high affinity IgE receptors. J Biol Chem 1996; 271(35):21214-21220.

75. Baird B, Holowka D. Structural mapping of Fc receptor bound immunoglobulin E: proximity to the membrane surface of the antibody combining site and another site in the Fab segments. Biochemistry 1985; 24:6252-6259.

76. Slattery J, Holowka D, Baird B. Segmental flexibility of receptor-bound immunoglobulin E. Biochemistry 1985; 24:7810-7820.

77. Ortega E, Licht A, Biener Y et al. A glycolipid-specific monoclonal antibody modulates Fcε receptor stimulation of mast cells. Molec Immunol 1990; 27(12):1269-1277.

78. Metzger H. Molecular aspects of receptors and binding factors for IgE. Adv Immunol 1988; 43:277-312.

79. Burton DR, Woof JM. Human antibody effector function. Adv Immunol 1992; 51:1-84.

80. Sutton BJ, Gould HJ. The human IgE network. Nature 1993; 366:421-428.

81. Kochan JP, Mallamaci M, Gilfillan A et al. Characterization of the human IgE Fc - FcεRIα interaction. In: M.Z.Atassi (ed). Immunobiology of Proteins and Peptides VII. NY: Plenum Press 1994; 31-38.

82. Hulett MD, Hogarth PM. Molecular basis of Fc receptor function. Adv Immunol 1994; 57:1-127.

83. Blank U, Ra C, Kinet J-P. Characterization of truncated α chain products from human, rat and mouse high affinity receptor for immunoglobulin E. J Biol Chem 1991; 266(4):2639-2646.

84. Riske F, Hakimi J, Mallamaci M et al. High affinity human IgE receptor (FcεRI). Analysis of functional domains of the α-subunit with monoclonal antibodies. J Biol Chem 1991; 266(17):11245-11251.

85. Hogarth PM, Hulett MD, Ierino FL et al. Identification of the immunoglobulin binding regions (IBR) of FcγRII and FcεRI. Immunological Reviews 1992; 125:21-35.

86. Mallamaci MA, Chizzonite R, Griffin M et al. Identification of sites on the human FcεRIα subunit which are involved in binding human and rat IgE. J Biol Chem 1993; 268(29):22076-22083.

87. Scarselli E, Esposito G, Traboni C. Receptor Phage. Display of functional domains of the human high affinity IgE receptor on the M13 phage surface. FEBS Let 1993; 329:223-226.

88. Padlan EA, Helm BA . Modelling study of IgE/receptor interactions. Biochem Soc Trans 1993; 21(4):963-967.

89. McDonell JM, Beavil AJ, Mackay et al. Structure based design and characterisation of peptides that inhibit IgE binding to its high affinity receptor. Nature Struct Biol 1996; 3(5):419-426.

90. Hulett MD, Osman N, McKenzie IFC et al. Chimeric Fc receptors identify functional domains of the murine FcγRI high affinity receptor for IgG. J Immunol 1991; 147:1863-1868.

91. Hulett MD, Witort E, Brinkworth R I et al. Identification of the IgG binding site of the low affinity receptor for IgG FcγRII: enhancement and ablation of binding site directed mutagenesis. J Biol Chem 1994; 269:15287:15293.

92. Hulett MD, Witort E, Brinkworth R I et al. Multiple regions of human FcγRII (CD32) contribute to the binding of IgG. J Biol Chem 1995; 270(36):21188-21194.

93. Hibbs ML, Tolvanen M, Carpen O. Membrane-proximal Ig-like domain of FcγRIII (CD16) contains residues critical for ligand binding. J Immunol 1994; 152:4466-4474.

94. Ishizaka T, Ishizaka K. Biology of immunoglobulin E. Prog Allergy 1975; 19:60-121.

95. Liu F-T, Albrandt K, Bry CG et al. Expression of a biologically active fragment of human IgE ϵ chain in *Escherichia coli.* Proc Natl Acad Sci USA 1984; 81:5369-5373.

96. Perez-Montfort R, Metzger H. Proteolysis of soluble IgE-receptor complexes: Localization of sites on IgE which interact with the Fc receptor. Mol Immunol 1982; 19:1113-1125.

97. Hamburger R. Peptide inhibition of the Prausnitz-Küstner reaction. Science 1975; 189:389-390.

98. Bennich H, Ragnarsson U, Johansson SGO et al. Failure of the putative IgE pentapeptide to compete with IgE for receptors on basophils and mast cells. Int Archs Allergy appl Immun 1977; 53:459-468.

99. Duncan AR, Woof JM, Partridge LJ et al. Localization of the binding site for the human high-affinity Fc receptor on IgG. Nature 1988; 332:563-564.

100. Canfield SM, Morrison SL. The binding affinity of human IgG for its high affinity Fc receptor is determined by multiple amino acids in the CH2 domain and is modulated by the hinge region. J Exp Med 1991; 173:1483-1491.

101. Presta L, Shields R, O'Connell L et al. The binding site on human immunoglobulin E for its high affinity receptor. J Biol Chem 1994; 269(42):26368-26373.

102. Helm BA, Kebo D, Vercelli D et al. Blocking of passive sensitization of human mast cells and basophil granulocytes with IgE antibodies by a recombinant human ϵ-chain fragment of 76 amino acids. Proc Natl Acad Sci USA 1989; 86:9465-9469.

103. Basu M, Hakimi J, Dharm E et al. Purification and characterization of human recombinant IgE-Fc fragments that bind to the human high affinity IgE receptor. J Biol Chem 1993; 268(18): 13118-13127.

104. Helm BA, Sayers I, Higginbottom A et al. Identification of the high-affinity receptor binding region in immunoglobulin E. J Biol Chem 1996; 271:7494-7500.

105. Stanworth DR, Humphrey JH, Bennich H et al. Inhibition of Prausnitz-Küstner reaction by proteolytic- cleavage fragments of a human myeloma protein of immunoglobulin class E. Lancet 1968; 11:17-18.

106. Nissim A, Jouvin M-H, Eshhar Z. Mapping of the high affinity Fcϵ receptor binding site to the third constant region domain of IgE. EMBO J 1991; 10:101-107.

107. Takemoto H, Nishimura S, Kosada Y et al. Anti-human IgE monoclonal antibodies recognizing epitopes related to the binding sites of high and low affinity IgE receptors. Microbiol Immunol 1994; 38(1):63-71.

108. Nissim A, Schwartzbaum S, Siraganian R et al. Fine specificity of the IgE interaction with the low and high affinity Fc receptor. J Immunol 1993; 150(4):1365-1374.

109. Baniyash M, Eshhar Z, Rivnay B. Relationships between epitopes on IgE

recognized by defined monoclonal antibodies and by the Fcϵ receptor on basophils. J Immunol 1986; 136: 588-593.

110. Conrad DH, Wingard JR, Ishizaka T. The interaction of human and rodent IgE with the human basophil IgE receptor. J Immunol 1983; 130(1):327-333.

111. Weetall M, Shopes B, Holowka D et al. Mapping the site of interaction between murine IgE and its high affinity receptor with chimeric Ig. J Immunol 1990; 145(11):3849-3854.

112. Keegan AD, Fratazzi C, Shopes B et al. Characterisation of new rat anti-mouse IgE monoclonals and their use along with chimeric IgE to further define the site that interacts with FcϵRII and FcϵRI. Molec Immunol 1991; 28: 1149-1154.

113. Schwarzbaum S, Nissim A, Alkalay I et al. Mapping of murine IgE epitopes involved in IgE-Fcϵ receptor interactions. Eur J Immunol 1989; 19:1015-1023.

114. Helm BA. Is there a link between the nature of agents that trigger mast cells and the induction of immunoglobulin (Ig)E synthesis? In: M.Z.Atassi (ed). Immunobiology of Proteins and Peptides VII. NY: Plenum Press 1994; 1-10.

115. Burmeister WP, Huber AH, Bjorkman PJ. Crystal structure of the complex of rat neonatal Fc receptor with Fc. Nature 1994; 372:379-383.

116. Burt DS, Hastings GZ, Healy J et al. Analysis of the interaction between rat immunoglobulin E and rat mast cells using anti-peptide antibodies. Mol Immunol 1987; 24(4):379-389.

117. Coleman JW, Helm BA, Stanworth DR et al. Inhibition of mast cell sensitization *in vitro* by a human immunoglobulin ϵ-chain fragment synthesized in Escherichia coli. Eur J Immunol 1985; 15:966-969.

118. Nio N, Seguro K, Ariyoshi Y et al. Inhibition of histamine release by synthetic human IgE peptide fragments: Structure-activity studies. In: Yanaihara N, ed. Peptide Chemistry 1989. Osaka: Protein Res Found, 1990:204-208.

119. Nissim A, Eshhar Z. The human mast cell receptor binding site maps to the third constant domain of immunoglobulin E. Molec Immunol 1992; 29(9):1065-1072.

120. Takizawa F, Adamczewski M, Kinet J-P. Identification of the low affinity receptor for immunoglobulin E on mouse mast cells and macrphages as FcγRII and FcγRIII. J Exp Med 1992: 176:469-475.

121. Maxwell KF, Powell MS, Hulett MD, Barton PA, McKenzie IFC, Garrett TPJ,

Hogarth PM. Crystal structure of the human leukocyte Fc receptor, Fc gamma RIIa. Nat Struct Biol 1999; 6(5):437-42.

122. Sondermann P, Huber R, Jacob U. Crystal structure of the soluble form of the human Fcgamma-receptor IIb: a new member of the immunoglobulin superfamily at 1.7 A resolution. EMBO J 1999;18(5),1095-1103.

123. Garman SC, Kinet J-P, Jardetzky TS. Crystal structure of the human high-affinity IgE receptor. Cell 1998;95:951-961.

124. Garman SC, Kinet JP, Jardetzky TS. The crystal structure of the human high-affinity IgE receptor (Fc epsilon RI alpha). Annu Rev Immunol 1999;17:973-6.

125. Garman SC, Wurzburg BA, Tarchevskaya SS, Kinet JP and Jardetzky TS. Structure of the Fc fragment of human IgE bound to its high-affinity IgE receptor FcεRIα. Nature 2000;406:259-266.

CHAPTER TWO:

Monoclonal antibodies and synthetic peptides define the active site of FcεRI and a potential receptor antagonist.

Published: Rigby LJ, Trist H, Epa VC, Snider J, Hulett MD and PM Hogarth. Allergy 2000, 55:609-619.

Abstract

Defining the structure of the human high affinity receptor for IgE, FcεRI, is crucial to the understanding of the receptor:ligand interaction, and to the development of drugs preventing IgE dependent allergic diseases. To this end a series of four anti-FcεRI monoclonal antibodies, including three new antibodies, mAbs 47, 54, and 3B4, were used in conjunction with synthetic FcεRI peptides to define functional regions of the Fc IgE binding site and identify an antagonist of IgE binding. The spatial orientation of the epitopes detected by these antibodies and their relationship to the IgE binding region of FcεRI was defined using a homology model based on the closely related FcγRIIa. Using recombinant soluble FcεRI-α as well as FcεRI-α expressed on the cell surface, a series of direct and competitive binding experiments indicated that the mAbs detected non-overlapping epitopes. One antibody (15-1), previously thought to be located close to the IgE binding site, was precisely mapped to a single loop within the IgE binding site using both mutagenesis, and overlapping synthetic peptides encompassing the entire extracellular domain. A synthetic peptide εRI-11 containing the amino acids 101-120 and the mAb 15-1 epitope inhibited IgE binding and may form the basis for the development of a useful receptor based therapeutic.

Introduction

IgE dependent allergic diseases including atopic asthma, allergic rhinitis and atopic dermatitis, are major health problems of epidemic proportions (1). The binding of serum IgE to its high affinity cell surface receptor FcεRI, with cross-linking by allergen, is responsible for initiating the inflammatory events associated with these conditions.

Human FcεRI is a tetrameric cell surface complex which is detected on mast cells and basophils (2), eosinophils (3) platelets and megakaryocytes (4) and a trimeric complex on Langerhans cells (5, 6) and activated monocytes (7). The receptor comprises an alpha chain, a beta chain (but not in monocytes or Langerhans cells), and a dimer of disulphide linked gamma chains which are crucial for receptor expression; with the ligand binding regions found in the extracellular domains of the alpha chain - FcεRI-α (8, 9). The cytoplasmic tail and transmembrane region of FcεRI-α have both been shown to exert no effect on binding (10), and the extracellular membrane proximal region, has been demonstrated to be important in the presentation of the two extracellular domains to enable binding to occur (11, 12, 13). The second extracellular Ig-like domain has been shown to be the principal ligand binding domain (14,15,16,17), as in other related Fc receptors, and contains a number of regions which contribute to the binding of IgE (18,19). The recently solved crystal structure of the closely related molecule FcγRIIa (20), which has been used to build a homology model of FcεRI-α (21), and based on this model the IgE binding region comprises the F-G, B-C and C'-E loops which are juxtaposed on the surface of the molecule exposed to solvent. This model structure is supported by the x-ray crystallographic structure of FcεRI (22).

This study reports the production and characterization of three new anti-FcεRI-α monoclonal antibodies (mAb) and the use of these, together with a previously defined antibody, as well as synthetic peptides, to define the IgE binding site of FcεRI-α. A homology model of FcεRI-α is used to provide a structural basis for interpreting the mAb epitope analysis and IgE binding site data.

Material and Methods

Production of recombinant soluble human FcεRI-α

Soluble recombinant human FcεRI (hFcεRI) was produced in yeast (*Pichia pastoris*). cDNA encoding the two extracellular domains of FcεRI-α (residues 1-173) was generated by PCR from rFcεRI-α cDNA (14) using the oligonucleotides,

HT11 - 5'-AGCGTG GAATTC GTCCCTCAGAAACC-3' (sense primer)

HT12 - 5'-GTACTT GAATTC CTAAGCTTTTATTACAG-3' (antisense primer).

HT12 adds a termination codon (TAG) after codon 173 and a following EcoRI site. The product was digested with EcoRI and ligated into the unique EcoRI site in pPIC9 (*P. pastoris* expression vector, Invitrogen). The cDNA was transformed into *P. pastoris,* with selection and expression as described by the manufacturer (Invitrogen).

Purification of recombinant soluble FcεRI (rsFcεRI)

Five litres of buffered minimal media with glycerol was innoculated with a *P. pastoris* clone producing rsFcεRI. The supernatant was filtered, precipitated with 66% saturated ammonium sulphate, resuspended in, and dialysed (x2, overnight) against 10 mM sodium dihydrogen orthophosphate pH 5.8 and loaded onto a Q-Sepharose column (Pharmacia). The column was eluted with 40% then 100% 200mM sodium dihydrogen orthophosphate pH 5.8, rsFcεRI fractions were identified by ELISA, pooled, dialysed against 10 mM Tris pH 7.5 and passed over an affinity column consisting of the anti-FcεRI mAb 3B4 immobilised onto CNBr- Sepharose 4B (Pharmacia). FcεRI was then eluted with 0.1 M sodium acetate/0.5 M sodium chloride pH 4.7, and immediately neutralised with saturated Tris pH 10.0. Fractions containing FcεRI were pooled, and the concentration was determined at Abs 280 nm and a molar extinction coefficient of $E^{1mg/ml} = 2.5$ (23).

Production of monoclonal anti-FcεRI antibodies

8-10 week old BALB/c mice were immunised by four weekly i.p. injections of 10 μg affinity purified rsFcεRI that was produced in *Pichia pastoris* with Freunds complete adjuvant. Three days after the last immunisation spleen cells were fused to P3-NS1-Ag4-1 cells (24). Hybridoma supernatants were screened by ELISA on rsFcεRI (see below), and detected using anti-mouse Ig-HRP (Amersham), and OPD (Sigma). Positive cell lines were cloned by

limiting dilution, and ascites was produced in BALB/c mice. Two antibodies were produced, mAb 47 and mAb 54 from cell lines X52-47-5.4 and X52-54.1 respectively. Anti-FcεRI monoclonal antibody 3B4 was produced after immunisation of BALB/c mice with a Chinese hamster ovary fibroblast cell line expressing a membrane bound form of FcεRI (25). Fusion of spleen cells from these mice with P3-NS1-Ag4-1 cells produced a monoclonal cell line mAb 3B4 secreting an IgG1 antibody (26).
Murine anti-human FcεRI monoclonal antibody 15-1 was the generous gift of J-P Kinet (Beth Israel Hospital, Boston), murine anti-human FcγRI (IgG1) monoclonal antibody 32.2 (27), murine anti-mouse FcγRI (IgG1) monoclonal antibody X54-5/7.1 was provided by Dr Peck Szee Tan, (Austin Research Institute, Australia.), murine anti-human FcγRIIa monoclonal antibody 8.26 was made in this laboratory (28) murine anti-human IgE (IgG1) monoclonal antibody HB121 was obtained from the ATCC.

Ligand Capture ELISA for detection of rsFcεRI

Recombinant soluble FcεRI was detected in a ligand based 'capture-tag' assay. 'High Bind' EIA/RIA plates (Costar 3690) were coated with the anti-human IgE mAb HB121 (54 nM, 50 µl/well) in PBS overnight at 25°C, and washed 7x in water. The plates were then blocked (60 min, 22°C) with PBS containing 1.5%BSA, 150 µl per well, coated with human IgE (myeloma serum, 1/30000 dilution in PBS/BSA, 50 µl/well, 60 min 22°C), and samples containing rsFcεRI were added (50 µl per well), incubated for 60 min at 25°C then washed. Bound rsFcεRI was detected using HRP conjugated 3B4, a non-blocking anti-FcεRI mAb (6.8 nM, 50 µl/well) and incubated (60 min, 22°C). The plates were washed 7 times with water between each incubation step. Colour development was with *o*-phenylenediamine (OPD) Sigma Biosciences, St Louis, MO), and stopped after 15 min with 25 µl 4M sulphuric acid. The optical density was determined by the absorbence at 490 nm. Competition for the IgE binding site on FcεRI between mAbs and hIgE was determined by the ligand capture ELISA (above). FcεRI mAbs (30 µl) were serially diluted from 1.4 µM and incubated with FcεRI (280 nM, 30 µl, 60 min. 22°C), prior to addition to the captured human IgE on the plate (20 µl, 60 min, 22°C). The plates were washed and IgE bound FcεRI was detected using mAb 3B4-HRP or mAb 47-HRP.

ELISA detection of anti-FcεRI monoclonal antibodies

The binding of mAbs to FcεRI was determined by ELISA. Plates were coated with 140 nM rsFcεRI and incubated overnight at 22^{0}C, then plates were blocked (150 µl/well, 60 min, 22^{0}C) with PBS containing 1.5%BSA, and washed. mAb either purified or in culture supernatant were serially diluted in PBS containing 1.5% BSA in the plate, and incubated 60 min 22^{0}C, the plates were washed and incubated for a further 60 min with a 1/2000 dilution of sheep anti-mouse IgG HRP linked whole antibody (Amersham), before colour development with OPD as above. The mAbs were also assayed in plates coated with 250 nM rsFcγRIIa, to determine the specificity of mAbs for FcεRI. This ELISA method was also used to determine whether the mAbs compete for epitopes on FcεRI. Detection of FcεRI after incubation with mAbs was with mAb 3B4-HRP or mAb 47-HRP.

Epitope mapping of mAbs.

An ELISA based inhibition assay using FcεRI peptides (see below) and FcεRI mAb was used to define epitopes detected by the mAbs. Antibodies at a concentration predetermined to give submaximal binding (mAb 47, 9.5 nM; mAb 54, 0.5 nM; mAb 15-1, 1 nM; mAb 3B4, 5 nM), were incubated with a range of peptide concentrations (initially 2500 to 20 µg/ml) and incubated for 60 min at 22^{0}C. The mAb/peptide mixtures (50 µl) were then added to the ELISA based assay for direct detection of mAb as described above; note that the quantity of rsFcεRI used to coat the plates was optimised to give the greatest signal to noise ratio, and sensitivity for binding of each anti-FcεRI antibody (mAb 47, 75 nM; mAb 54, 1 nM; mAb 15-1, 18.5 nM; mAb 3B4, 0.7 nM). EIA plates were coated with rsFcεRI and incubated with mAbs as above. Detection of the antibodies was by mAb 47-HRP or mAb 3B4-HRP, and colour development with OPD.

Definition of IgE binding site and mAb epitopes by FcεRI peptides:

Production of FcεRI peptides. A series of 20mer peptides overlapping by 10 amino acids comprising the entire two extracellular domains of FcεRI were generated by a Synergy Personal Peptide Synthesizer (Applied Biosystems) (Table 2.1). Purity and sequence of the peptides was confirmed by electrospray mass spectroscopy. The peptides were dissolved in water, diluted in PBS, and used to coat EIA plates (Costar) at 20 µg/ml, or incubated with mAb in an inhibition ELISA.

Table 2.1. A series of 20mer peptides overlapping by 10 amino acids were generated of the two extracellular domains of FcεRI-α.

εRI-1	V	P	Q	K	P	K	V	S	L	N	P	P	W	N	R	I	F	K	G	E
εRI-2	P	P	W	N	R	I	F	K	G	E	N	V	T	L	T	C	N	G	N	N
εRI-3*	N	V	T	L	T	C	N	G	N	N	F	F	E	V	S	S	T	K	W	F
a		V	T	L	T	C	N	G	N	N	F	F	E	V	S					
b				L	T	C	N	G	N	N	F	F	E	V	S	S				
c				L	T	C	N	G	N	N	F	F	E	V	S	S	T	K		
εRI-4	F	F	E	V	S	S	T	K	W	F	H	N	G	S	L	S	E	E	T	N
εRI-5	H	N	G	S	L	S	E	E	T	N	S	S	L	N	I	V	N	A	K	F
εRI-6	S	S	L	N	I	V	N	A	K	F	E	D	S	G	E	Y	K	C	Q	H
εRI-7	E	D	S	G	E	Y	K	C	Q	H	Q	Q	V	N	E	S	E	P	V	Y
εRI-8	Q	Q	V	N	E	S	E	P	V	Y	L	E	V	F	S	D	W	L	L	L
εRI-9†						D	W	L	L	L	Q	A	S	A	E	V				
εRI-10	Q	A	S	A	E	V	V	M	E	G	Q	P	L	F	L	R	C	H	G	W
εRI-11	Q	P	L	F	L	R	C	H	G	W	R	N	W	D	V	Y	K	V	I	Y
εRI-12	R	N	W	D	V	Y	K	V	I	Y	Y	K	D	G	E	A	L	K	Y	W
εRI-12a‡	R	N	W	D	V	Y	K													
εRI-12b				D	V	Y	K	V	I	Y	Y	K	D							
εRI-13	Y	K	D	G	E	A	L	K	Y	W	Y	E	N	H	N	I	S	I	T	N
εRI-14	Y	E	N	H	N	I	S	I	T	N	A	T	V	E	D	S	G	T	Y	Y
εRI-15	A	T	V	E	D	S	G	T	Y	Y	C	T	G	K	V	W	Q	L	D	Y
εRI-16	C	T	G	K	V	W	Q	L	D	Y	E	S	E	P	L	N	I	T	V	I
εRI-16s				K	V	W	Q	L	D	Y	E	S	E	P	L	N				
εRI-16ss				K	V	W	Q	L	D	Y	E	S	E							
εRI-17†	E	S	E	P	L	N	I	T	V	I	Q	V	P	S	M	G	S	S	S	

* Generation of peptide εRI-3 produced a mixture of three shorter peptides with approximately equal concentration.

† Peptides εRI-9 and εRI-17 could only be synthesised as the 12mer and 19mer shown.

‡ Peptides εRI-12a and 12b were generated to determine the epitope of mAb 15-1.

** Peptides εRI-16s and 16ss were synthesised to determine the epitope of mAb 47.

Determination of IgE binding site(s) using FcεRI-α peptides.

The ligand capture ELISA (above) was used to determine competition by FcεRI-α peptides for IgE binding to FcεRI-α. Serial dilutions of the 20mer FcεRI peptides at an initial concentration of 2.5 mg/ml, were added to a 96 well plate containing the immobilised IgE and incubated overnight at 4^0C. Then rsFcεRI (10 nM, 20 µl) was added and incubated (60 min, 22^0C). The plates were washed and IgE bound FcεRI was detected using mAb 3B4-HRP at 50 µl per well (60 min, 22^0C). The plates were washed 7x with water after each incubation, and HRP activity was measured as described previously.

Construction of FcεRI chimeric receptors

Chimeric receptors were produced whereby specific loops, strands or regions of FcγRIIa D1 were replaced with the equivalent portion of FcεRI (21) using splice overlap extension - polymerase chain reaction (SOE-PCR), previously described in detail (14, 29). Briefly these were constructed using a 'template' chimera (γεγ) comprising domain one of FcγRIIa fused to domain two of FcεRI-α, but with the membrane proximal region, transmembrane region and cytoplasmic tail of FcγRIIa permitting expression of the FcεRI receptor in the absence of its gamma subunit (14).

The chimeric receptors used herein were generated using the following oligonucleotides; portions containing sequence complementary to FcεRI-α cDNA are underlined and italicised (ε), and FcγRII are in plain text (γ). The region of hybridisation to the Fc receptor DNA is stated in parentheses after the oligonucleotide sequence. LR3 5'-*CGT CTC TTC TGA CAG GCT* GCC ATT GTG GAA CCA C-3' (ε222-205, γ234-219), LR 4 5'-*G TCA GAA GAG ACG AAT TCA* CCC AGC TAC AGG TTC-3' (ε210-228, γ259-273), LR 9 5'-*C AAT ATT CAA ACT TGA ATT CGT CTC TTC TG*-3 (ε 241-222), LR 10 5'-*G AAT TCA AGT TTG AAT ATT G*-3' (ε222-241), LR 20 5'-*GAC TTC AAA GAA ATT GTT CCC ATT* GCA TGT CAG AGT CAC-3' (ε177-154, γ183-169), LR 21 5'-*G AAC AAT TTC TTT GAA GTC AGT* TCC ATT CAG TGG TTC C-3' (ε159-180, γ211-226), EG 32 5'-*AAA TTT GGC ATT CAC AAT ATT CAA* GCT GGG CTG CGT GTG G-3' (ε255-232, γ264-249), EG 33 5'-*AAT ATT GTG AAT GCC AAA TTT GAA* GAC AGC GGG GAG TAC AC-3' (ε235-258, γ289-305).

The BC loop ϵ chimera comprising the BC loop of FcϵRI, aminoacid residues (aa) 29-37, with the sequence NGNNFFEVS; was produced by SOE-PCR with the first reaction using the template cDNA of γϵγ and the sense (s) oligonucleotide LR 20 paired with the nonsense (ns) oligonucleotide EG 5 (ref. 14). In a second separate reaction the nonsense (ns) oligonucleotide LR 21, and the template-γϵγ, paired with the sense oligonucleotide NR1 (ref. 14). The products of these reactions were purified, mixed, and the SOE-PCR reaction completed using the oligonucleotide primers NR1 and EG5. The SOE-PCR reaction used the oligonucleotides NR1 and EG5 for each of the chimeras. All the chimeras were produced in a similar fashion with variations in the oligonucleotides and the templates as follows. The C' strand ϵ chimera, comprising the C' strand of FcϵRI (aa44-51, SLSEETNS), was produced using the oligonucleotides (s) LR 3, and (ns) EG5 and the template -γϵγ in the first reaction and (ns) LR4 with (s) NR1, and the template γϵγ in the second reaction. The C'E region ϵ chimera, comprising the region from the C' strand to and including the E strand of FcϵRI (aa44-58, SLSEETNSSLNIVNA), was produced using, reaction one, the oligonucleotides (s) LR 9 and EG5 with the E strand ϵ chimera (described below) as the template; and reaction two, oligonucleotides (ns) LR 10 with NR1 and the C'strand ϵ chimera as a template. The C'EF region chimera, comprising the region from the C' strand, the EF loop of FcϵRI (aa44-61, SLSEETNSSLNIVNAKFE), was produced as the C'E chimera above, but in reaction one, the oligonucleotides (s) LR 9 and EG5 were used with the EF loop ϵ chimera (see below) as the template replacing the E strand chimera. The E strand ϵ chimera, comprising the E strand of FcϵRI (aa53-58, LNIVNA) was a mutant arising from the production of the EF ϵ chimera. The EF loop ϵ chimera, comprising the E strand and EF loop of FcϵRI (aa53-61, LNIVNAKFE) was produced using the oligonucleotides, reaction one, (s) EG 32 with EG5 and γϵγ, as template; and reaction two, (ns) EG 33 with NR1 and the template γϵγ.

cDNA constructs were ligated into the vector pCR™3 using the "Eukaryotic TA Cloning™ Kit" (Invitrogen Corp. San Diego CA) and transformed into competent *E.coli* Top10 F' bacterial cells for DNA production according to the manufacturer's instructions. cDNA was purified by centrifugation in a CsCl gradient and the constructs sequenced in total using the ABI Dye Terminator reaction kit with the automatic ABI Prism 377 DNA sequencer (Perkin Elmer).

COS-7 cells were maintained and transiently transfected with chimeric cDNA using Lipofectamine (Life Technologies Inc) according to the method described elsewhere (21).

Radioligand Binding Assay

COS-7 cells were transfected with cDNA of chimeric or template receptors, or irrelevant cDNA. 10 μg of mAb 3B4 in 50 μl PBS pH 7.4 was radiolabelled by the chloramine T (Merck, Darmstadt, FRG) method (14). The radioligand binding assay used ^{125}I mAb 3B4, serially diluted (50 μl, 27-0.2 nM) and 50 μl COS-7 cells resuspended at $5x10^6$/ml, as in the method described elsewhere (14).

Modelling of the epitopes detected by anti-FcεRI antibodies

As the co-ordinates of the recently solved crystal structure of FcεRI (22) were unavailable, a homology model (21) based on the x-ray crystal structure of the closely related and highly homologous Fc receptor FcγRIIa (20) was used to display the epitopes of the anti-human FcεRI monoclonal antibodies utilised here.

Figure 2.1 Monoclonal antibodies display specific binding to FcεRI.

MAbs were serially diluted in an ELISA, using plates coated with either rsFcεRI or rsFcγRII. Results are expressed in colourimetric units at Abs 490 nm, and clearly show mAb binding to FcεRI, but not to the closely related protein FcγRII.

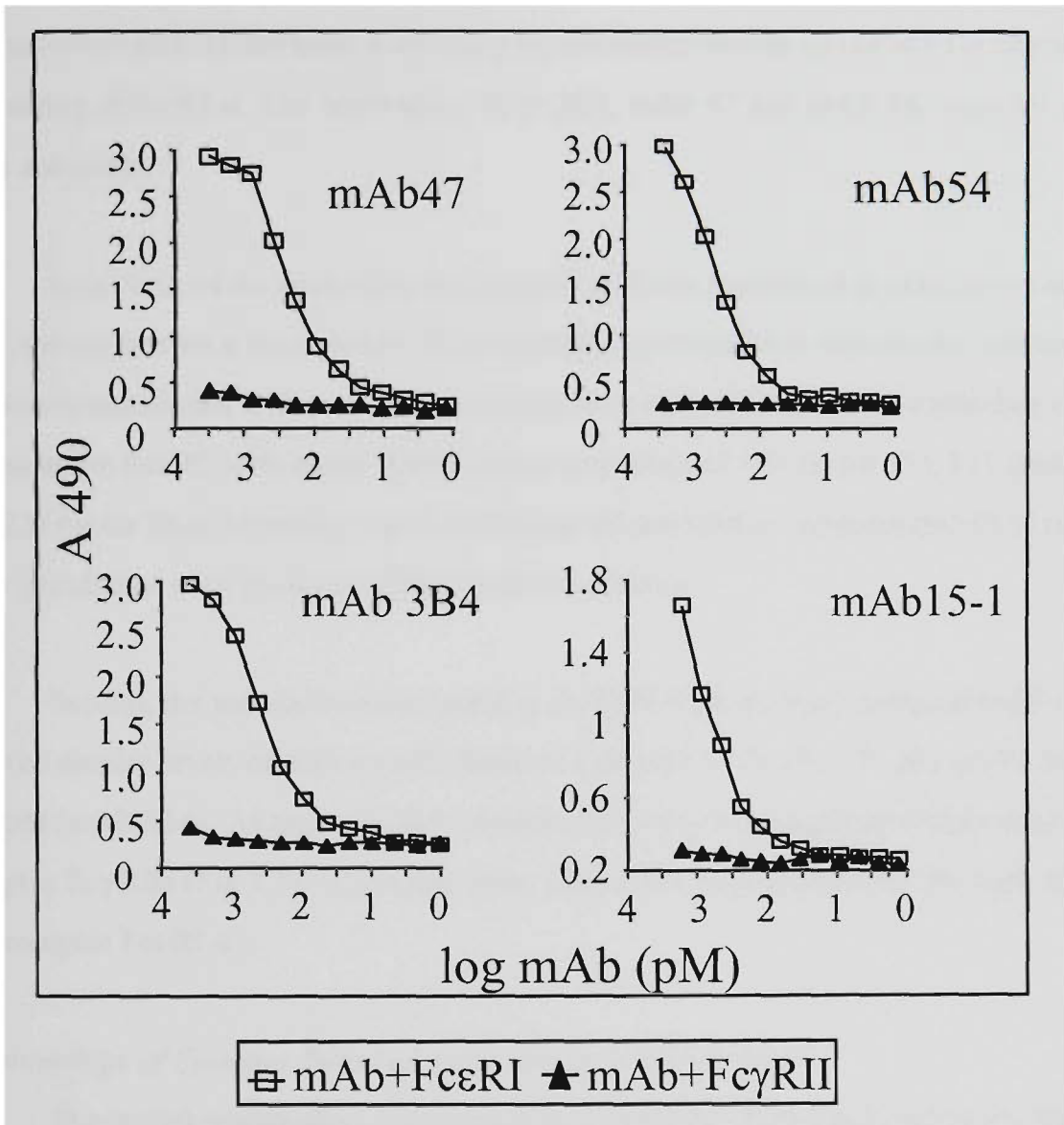
mAb47
mAb54
mAb 3B4
mAb15-1
A 490
log mAb (pM)
mAb+FcεRI
mAb+FcγRII

Results

Production, Characterisation and Specificity of Monoclonal Antibodies

Three monoclonal anti-human (h)FcεRI antibodies were produced after immunisation of BALB/c mice with either recombinant soluble (rs) hFcεRI or fibroblasts expressing rhFcεRI-α. The antibodies, mAb 3B4, mAb 47 and mAb 54, were all of the IgG1 subclass.

Specificity of the antibodies for human FcεRI was confirmed in two distinct assays. First, the antibodies were tested by flow cytometry with indirect immunofluorescence on COS cells transfected with a membrane bound form of FcεRI. All three antibodies clearly bound to the FcεRI, with mean fluorescence intensities of 139 (mAb 47), 131 (mAb 54) and 239 (mAb 3B4). However, these antibodies did not bind to untransfected COS cells or cells transfected with irrelevant DNA (data not shown).

Second, the antibodies were tested in an ELISA based assay using rsFcεRI-α, and showed similar levels of activity with titres of 170 pM (mAb 47), 170 pM (mAb 54) and 204 pM (mAb 3B4). As expected, there was no detectable binding to the highly related IgG receptor FcγRIIa (Fig 2.1). Therefore these antibodies were specific for the high affinity IgE receptor FcεRI-α.

Relationships of Epitopes Detected by Competition Experiments

The spatial relationship of the epitopes detected by the monoclonal antibodies was determined by ELISA in competition experiments where purified, unlabelled antibodies were used as competitive inhibitors of the binding of (HRP) labelled monoclonal antibody (see Material and Methods) i.e. mAb 47-HRP or mAb 3B4-HRP (Fig 2.2). MAb 54 and mAb 3B4 displayed some inhibition of mAb 47-HRP binding, but only at high concentrations. MAb 15-1, a neutralising antibody previously indicated to detect an epitope in the second domain of FcεRI (4,6), failed to inhibit the binding of mAb 47-HRP and complete inhibition of mAb 47-HRP was only obtained by competition with unlabelled mAb 47. MAb 54 and mAb 15-1 failed to inhibit mAb 3B4-HRP binding, and mAb 47 appeared to show some weak inhibition of mAb 3B4-HRP binding at very high

Figure 2.2 Relationship of epitopes defined by competitive binding experiments. Serial dilutions of purified monoclonal antibodies were tested for inhibition of binding of HRP conjugated (a) mAb 3B4 or (b) mAb 47. Antibodies used were FcεRI mAbs 47, 54, 3B4, 15-1 and negative control mAb HB121.

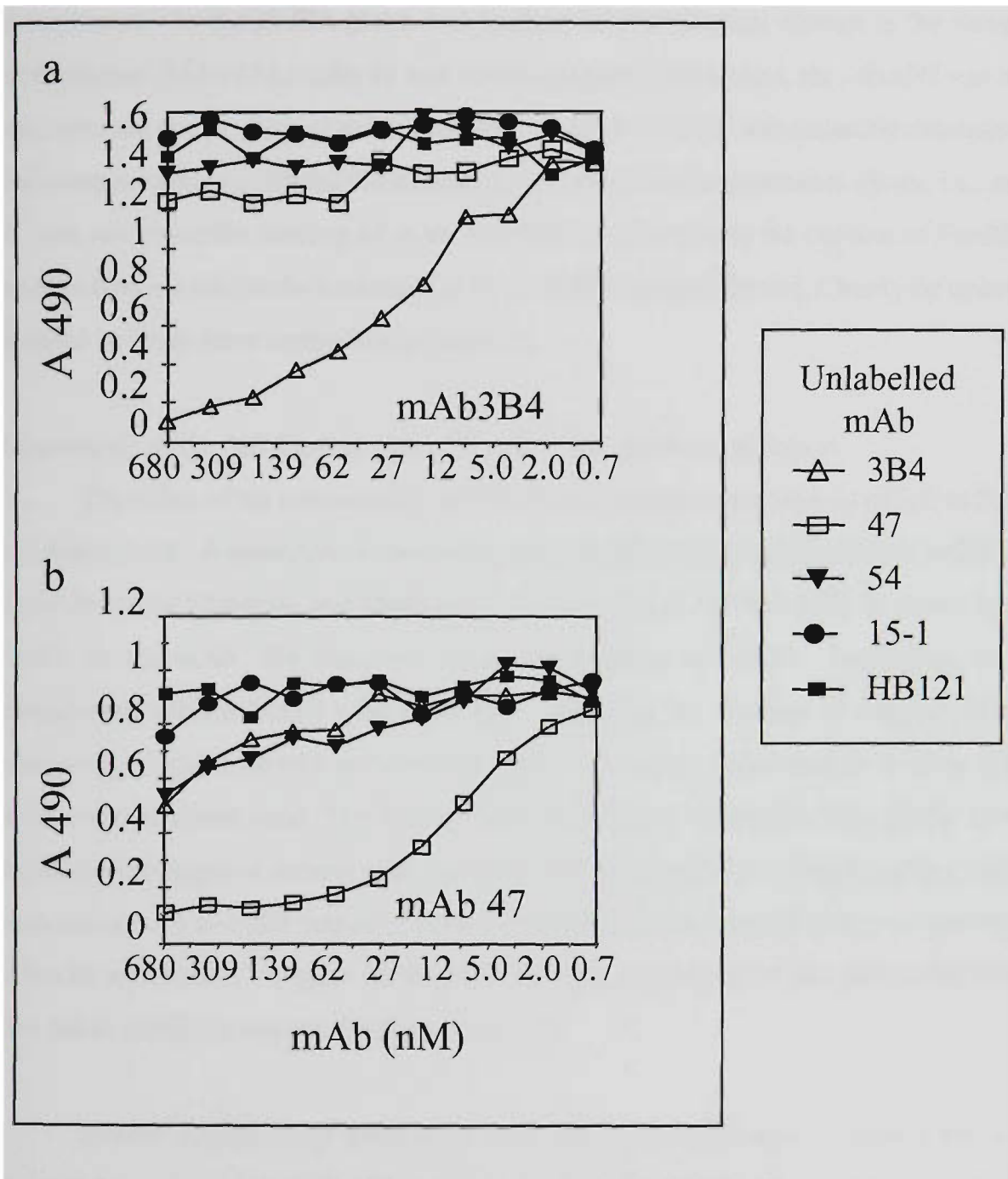
a
A 490
1.6
1.4
1.2
1
0.8
0.6
0.4
0.2
0
mAb3B4
680 309 139 62 27 12 5.0 2.0 0.7
b
A 490
1.2
1
0.8
0.6
0.4
0.2
0
mAb 47
680 309 139 62 27 12 5.0 2.0 0.7
mAb (nM)
Unlabelled mAb
3B4
47
54
15-1
HB121

concentrations (2.7 nM). Thus the epitope detected by mAb 3B4 is distinct from that detected by mAb 47 or mAb 54 or mAb 15-1 (summarised in Table 2.2).

A capture:tag ELISA was established to eliminate the possibility that attachment of the receptor to the ELISA plates was leading to an artifactual change in the receptor conformation. MAb 47 or mAb 54 was coated onto an ELISA plate, the rsFcεRI was then captured, and the binding of mAb 3B4-HRP or mAb 47-HRP subsequently determined. These experiments confirmed the results of the competition experiments above, i.e., mAb 47 does not block the binding of mAb 3B4-HRP, and similarly the capture of FcεRI by mAb 54 does not inhibit the binding of mAb 47-HRP (data not shown). Clearly the epitopes detected by these three antibodies are distinct.

Relationship of the IgE Binding Site of FcεRI to the Antibody Epitopes

The effect of the monoclonal anti-FcεRI antibodies on the binding of IgE to FcεRI was determined. A quantitative assay measuring the binding of soluble FcεRI to IgE was established (see Materials and Methods), initially using mAb 3B4-HRP to detect bound FcεRI, as the mAb 3B4 does not block IgE binding to FcεRI. Incubation of the recombinant soluble FcεRI with mAb 15-1 inhibited the binding of receptor to IgE, however pre-incubation with mAb 54 and mAb 47 failed to inhibit receptor binding to IgE at the concentrations used. The level of binding of these antibodies was similar to that shown for the negative control class matched antibody, mAb 32.2. (Fig 2.3a) In a similar assay using mAb 47-HRP instead of mAb 3B4-HRP to detect bound FcεRI, pre-incubation of FcεRI with mAb 15-1 again inhibited the binding of receptor to IgE, and mAbs 54 and 3B4 failed to inhibit receptor binding (Fig 2.3b).

Similar results were obtained in cell binding experiments where COS cells expressed membrane bound FcεRI-α. MAb 15-1 inhibited IgE binding, whereas mAb 3B4, mAb 47 and mAb 54 failed to inhibit the binding of IgE (data not shown).

Table 2.2. Amino acid sequence alignment of FcεRI-α and FcγRIIa and chimeras encompassing the regions of exchange from FcγRIIa to domain 1 FcεRI.

		*Binding of mAbs	
		54	3B4
	30 40 50 60		
†BC loop	‡NGNNFFEVS	+	-
BCC	NGNNFFEVSSTK(WFHNG)	+	-
C'EF region	(WFHNG)SLSEETNSSLNIVNAKFE(DSGEY)	-	+
C'E region	(WFHNG)SLSEETNSSLNIVN	-	-
C'strand	(WFHNG)SLSEETNS	-	-
E strand	SLNIVN	-	-
EF loop	LNIVNAKFE(DSGEY)	-	-
FcεRI	NGNNFFEVSSTK(WFHNG)SLSEETNSSLNIVNAKFE(DSGEY)	+	+
FcγRII	*QGARSPESDSIQ*(WFHNG)*NLIPTHTQPSYRFKANNN*(DSGEY)	-	-

* MAbs 54 and 3B4 have epitopes in domain one of FcεRI. The ability of mAbs 54 and 3B4 to bind the chimeric receptors is indicated here. (+) indicates antibody detection of the epitope, and (-) the absence of antibody binding.

† The name of the chimera indicates the approximate region of FcεRI domain 1 introduced into domain 1 of FcγRIIa in each case.

‡ The amino acid sequences of exchange to FcεRI in each of the chimeras. The sequences in plain text are from FcεRI, and those in italics are from FcγRIIa. The two series of amino acids shown in parentheses are common to both receptors,

Figure 2.3 15-1 is the only mAb that blocks IgE binding.

The effect of anti-receptor antibodies on the binding of IgE to FcεRI was determined in a capture:tag ELISA. Soluble FcεRI was preincubated with serial dilutions of the unlabelled mAb, including the negative control mAb 32.2, and then captured by IgE. FcεRI bound to IgE was then identified by using either of two mAbs that detect different epitopes; (a) mAb 3B4 conjugated to HRP, (b) mAb 47-HRP.

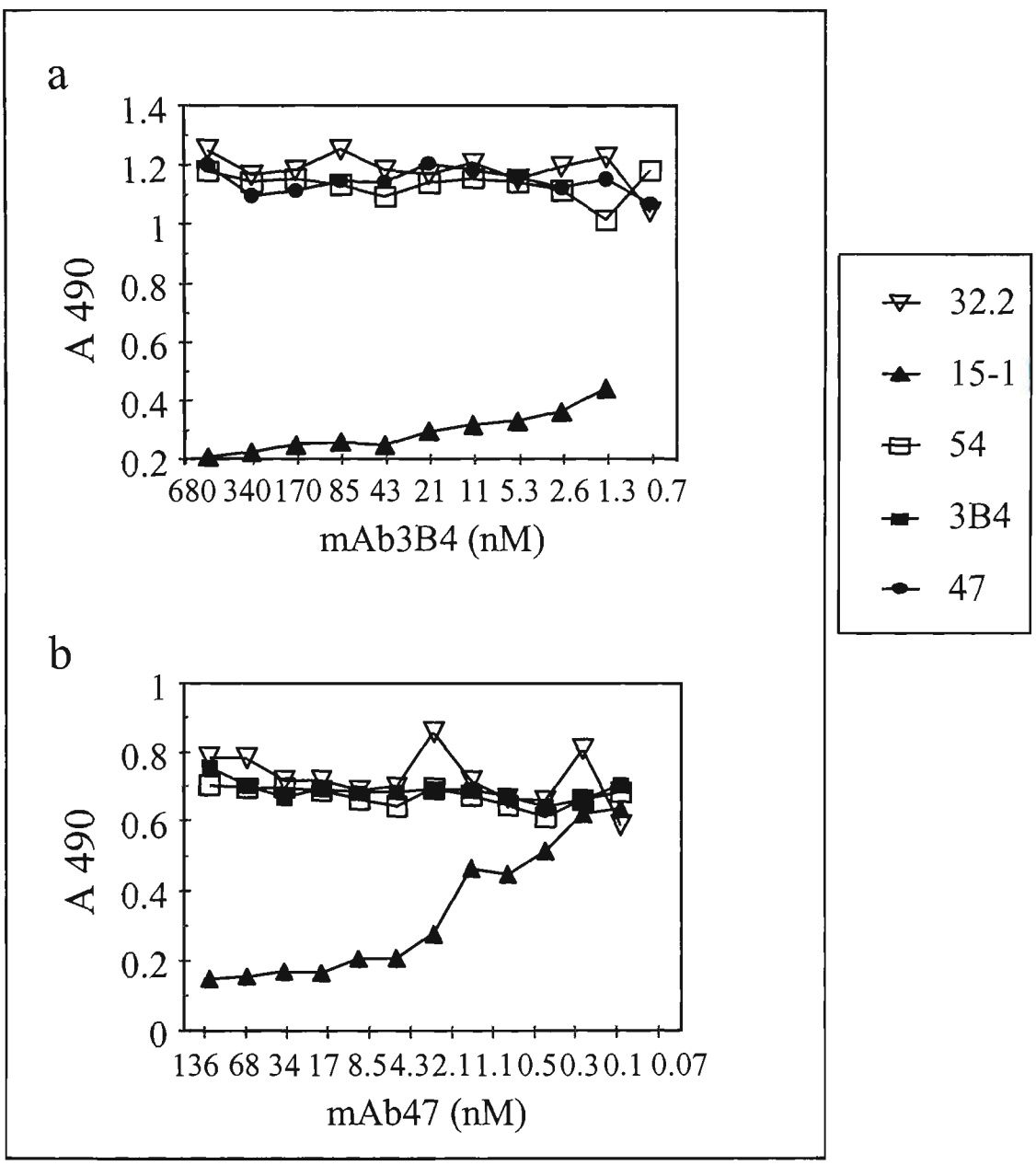
a
1.4
1.2
1
0.8
0.6
0.4
0.2
A 490
680 340 170 85 43 21 11 5.3 2.6 1.3 0.7
mAb3B4 (nM)
b
1
0.8
0.6
0.4
0.2
0
A 490
136 68 34 17 8.5 4.3 2.1 1.1 0.5 0.3 0.1 0.07
mAb47 (nM)
32.2
15-1
54
3B4
47

Use of peptides to define mAb epitopes

A series of overlapping synthetic peptides was produced that encompassed the entire extracellular region of FcεRI-α (Table 2.1) These 20 mer peptides overlapped each other by 10 amino acids and were used to define the epitopes detected by the monoclonal antibodies in an inhibition assay. Peptides in solution were tested for inhibition of mAb binding to rsFcεRI-α and the epitopes detected by mAbs 47, 54 and 15-1 were defined. However the epitope detected by the 3B4 antibody could not be identified (Fig 2.4). The binding of mAb 47 to FcεRI was inhibited by peptides εRI-16 and εRI-16s, with approximately 58% and 35% inhibition observed respectively at 5 μg/ml. These peptides both contain the sequence KVWQLDYESEPLN (residues 154-166). However, peptide εRI-16ss (KVWQLDYESE), which did not inhibit the binding of mAb 47 to FcεRI, has a further truncation of three amino acids (PLN) relative to εRI-16s. Thus the epitope detected by mAb 47 lies in, or is dependent on, the 'PLN' sequence, which in native FcεRI is located in the G strand of the second domain (Fig 2.5).

The binding of mAb 54 to FcεRI was inhibited by the overlapping peptides εRI-3 (55% at 39 ng/ml) and εRI-4 (49% at 2.4 ng/ml). Thus the FFEVSSTKWF (residues 31-40) sequence shared between these two peptides contains the epitope for mAb 54. Mass spectroscopy of peptide εRI-3 showed that it did not contain the full length peptide expected, but was composed of three smaller peptides of approximately equal concentration (Table 2.1). The longest of these peptides restricts the overlapping region of peptides εRI-3 and εRI-4 and epitope of mAb 54 to the sequence FFEVSSTK. This sequence is located in the first domain and covers part of the BC loop into the C strand. To further define this epitope mAb 54 was tested on cos cells expressing either of two chimeric receptors containing the FcεRI aminoacid sequences of the domain one BCC region or BC loop of FcεRI-α, NGNNFFEVSSTK and NGNNFFEVS respectively (Table 2.3). MAb 54 was able to bind both chimeras, and this taken together with the peptide binding data, indicates that the region common to both chimeras and peptide was the sequence FFEVS. Thus, the epitope of mAb 54 was located within the FFEVS sequence, and is displayed on the model of FcεRI-α (Fig 2.5).

Figure 2.4 Peptide inhibition of mAbs binding to FcεRI.

Overlapping 20mer peptides were serially diluted and incubated with a constant concentration of monoclonal antibody. The mixture was then transferred into ELISA plates coated with rsFcεRI, and inhibition of colour development (by anti-mouse Ig-HRP) was determined. Full colour development was ascertained by a direct reaction of mAb at the same concentration, with FcεRI. Results are expressed as percent inhibition of mAb/FcεRI binding at the concentration closest to the IC50 of the major inhibitory peptide. That is mAb 47 - 5 μg/ml, mAb 54 - 2.4 ng/ml and mAb 15-1 - 1.25 mg/ml.

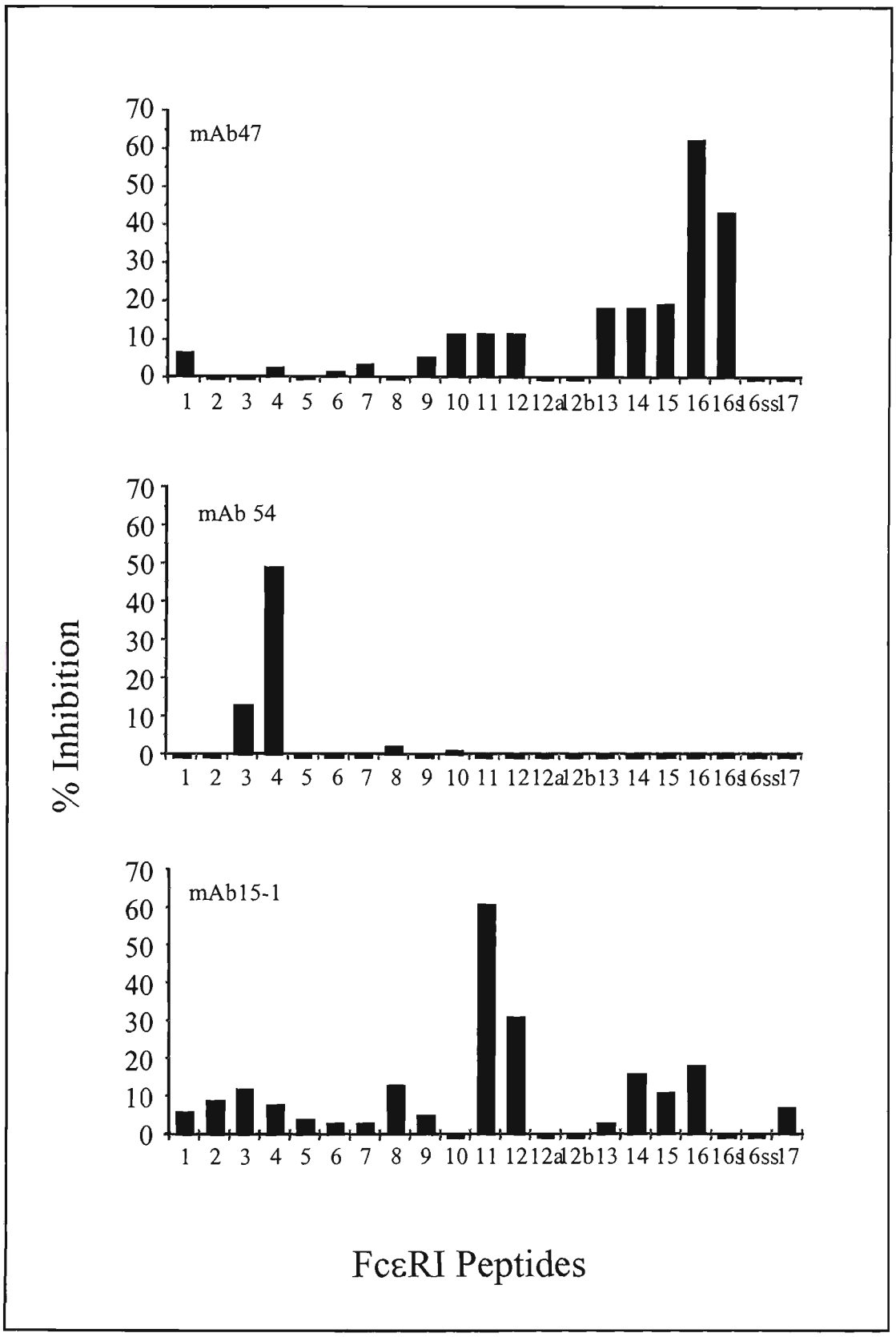
mAb47
mAb 54
mAb15-1
70
60
50
40
30
20
10
0
1 2 3 4 5 6 7 8 9 10 11 12 12a 12b 13 14 15 16 16s 16ss 17
% Inhibition
FcεRI Peptides

Figure 2.5 Anti-FcεRI monoclonal antibody epitopes are displayed on a homology model of FcεRI.

The individual mAb epitopes have been displayed as 'stick' amino acids with a translucent spacefill 'Connolly' surface, and labelled in blue. The β-strands of each domain (A, A',B, C, C', E, F, G) are shown, as are the amino (n) and carboxy (c) termini.

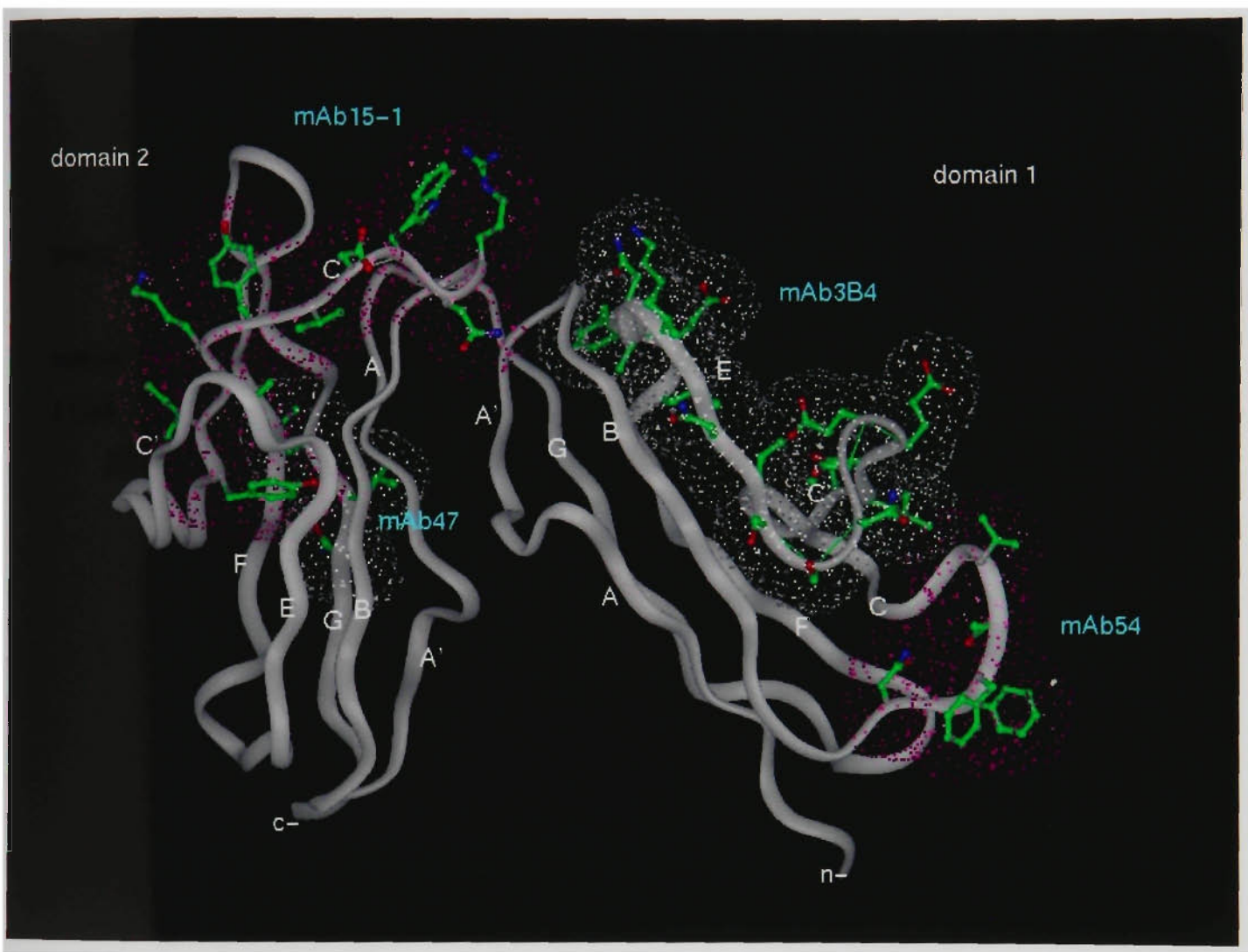
mAb15-1
domain 2
domain 1
mAb3B4
mAb47
mAb54
C
C'
A
A'
B
G
E
F
c-
n-

Table 2.3. Summary of monoclonal antibody characteristics

Cell Line (mAb)	Ig Class	Epitope Detected Residue No's. Sequence	3D Location		MAb Inhibition of IgE/FcR Binding	Western Blot Reduced	Western Blot Non-reduced	Peptide Inhibition of mAb/FcR Binding	K_D(M)[a]
3B4 (3B4)	IgG1	aa 44-61 SLSEETNSSLNIVNAKFE	C'EF region	D1	NO	NO	YES	-	$2x10^{-9}$
X52-47-5.4 (47)	IgG1	aa 164-166 PLN	G' strand	D2	NO	YES	YES	16,16s	$6x10^{-8}$
X52-54.1 (54)	IgG1	aa 31-35 FFEVS	BC loop	D1	NO	YES	YES	3,4	$<1x10^{-7}$
15-1 (15-1)	IgG1	aa 111-120 RNWDVYKVIY	BC loop	D2	YES	YES[b]	YES	11,12	$\geq 1x10^{-10}$

a. For intact antibody
b. Letourner et al. 1995

The overlapping peptides ϵRI-11 and ϵRI-12 inhibit the binding of mAb 15-1 to FcϵRI by 65% and 52% respectively at 1.25 mg/ml). The sequence common to these peptides is RNWDVYKVIY (residues 111-120) which places the likely binding site of mAb 15-1 in the BC loop of domain 2. Two shorter peptides ϵRI-12a (RNWDV) and ϵRI-12b (DVYKVIYYKD) were synthesised to further define the epitope within this area of overlap, however, these failed to inhibit the binding of mAb 15-1. It is possible that the epitope detected by mAb 15-1 is dependent on constraints dictated by the conformation of the amino acids both comprising and surrounding the epitope, and their arrangement in the shorter peptides was unable to match these requirements. The finding that the mAb 15-1 epitope was located in the sequence RNWDVYKVIY was surprising as recent mutation studies have implied that the epitope involves tryptophan 156 (30). However peptides ϵRI-15 and ϵRI-16 which contain tryptophan 156 display little specific inhibition of mAb 15-1 binding rsFcϵRI, implying that this region contributes only marginally to the mAb 15-1 epitope. This is an important distinction as the BC loop not the FG loop may have the more important role in interaction with IgE (see below).

There was no specific inhibition of mAb 3B4 binding FcϵRI by any FcϵRI peptide. Thus epitope mapping was performed by determining its ability to bind a series of FcϵRI / FcγRIIa chimeric receptors.

Determination of mAb3B4 epitope using chimeric receptors

A series of chimeric receptors had previously been constructed based on a chimeric receptor consisting of domain 1 of FcγRIIa and domain 2 of FcϵRI-α (14). Specific loops, strands or regions of the FcγRII domain one were replaced with the equivalent portion of FcϵRI to generate seven chimeric receptors which were transiently expressed in COS-7 fibroblasts (21), and incubated with ^{125}I labelled mAb 3B4 in an equilibrium binding assay (Fig 2. 6). MAb3B4 bound only the FcϵRI chimera which contained the FcϵRI domain one C'EF region derived sequence SLSEETNSSLNIVNAKFE comprising residues 44-61 (Table 2.2). Four additional chimeras were tested to further define the epitope in domain one of FcϵRI, these contained shorter segments of the C'EF sequence such as SLSEETNSSLNIVN (C'E), SLSEETNS (C'), SLNIVN (E) or LNIVNAKFE (EF), and also overlapped each other. No mAb 3B4 binding was detected to these shorter segments of the

C'EF region. These results would indicate that mAb 3B4 recognises a conformational epitope in the C' strand to the EF loop region of FcεRI domain 1 (Fig 2.5).

Synthetic peptide antagonist and defining the IgE binding site

The epitope mapping studies indicated that the mAb epitopes in domain 1 are not 'close' to the IgE binding site. This is consistent with chimeric receptor studies showing that the IgE binding site is located in domain 2 (14, 15). The mAb 47 epitope (PLN) is located within domain 2 although distal to the mAb 15-1 epitope, and mAb 47 inhibited neither IgE binding nor mAb 15-1 binding, which is consistent with the peptide mapping studies. However, the mAb 15-1 epitope was located in the sequence RNWDVYKVIY which is positioned at the surface of domain two in the exposed BC loop. This loop and adjacent areas have been implicated in IgE binding (14, 15). Thus peptide εRI-11 and all overlapping peptides were tested for their capacity to inhibit IgE binding to FcεRI and only peptide εRI-11, containing the mAb 15-1 epitope significantly (61% at 750 μg/ml) inhibited IgE binding to FcεRI (Fig 2.7). Marginal inhibition by peptides εRI-10 and εRI-12 which flank and overlap peptide εRI-11 was also observed. Peptide εRI-11 encompasses the B strand and BC loop region of FcεRI domain two, an area that has previously been implicated as part of the IgE binding region of FcεRI-α (14, 15).

Figure 2.6 The epitope for mAb 3B4 is located in the C'EF region of FcεRI domain one.

COS-7 cells were transiently transfected with cDNA encoding chimeric membrane bound Fcε receptors and identified by the approximate region of exchange. mAb 3B4 was radiolabelled and utilised in an equilibrium binding assay with the chimeric receptors. Results are presented as ^{125}I- mAb 3B4 bound to transfected cells, and indicate that mAb 3B4 binds FcεRI and the C'EF region, but not to shorter segments thereof.

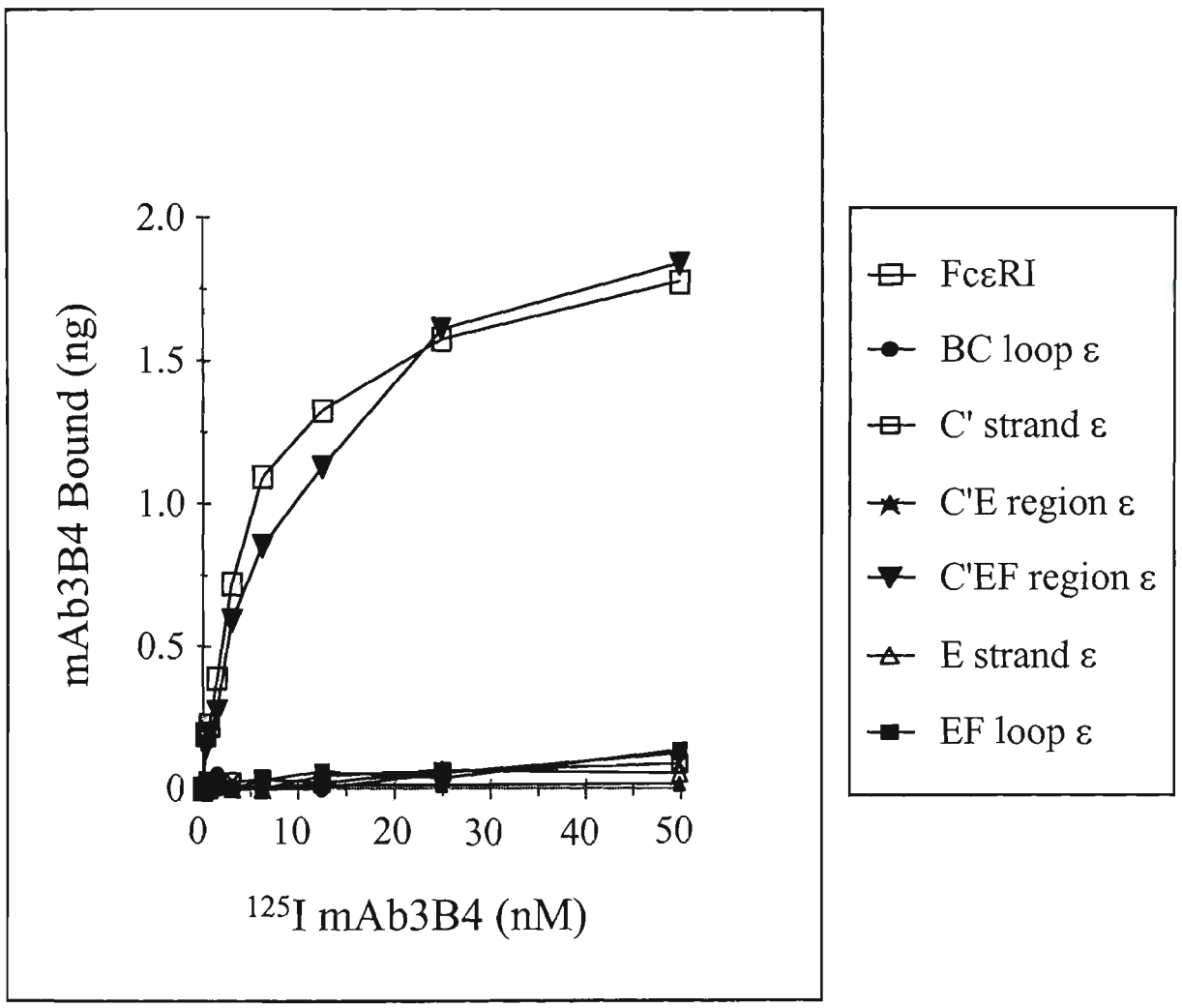
mAb3B4 Bound (ng)
2.0
1.5
1.0
0.5
0
0
10
20
30
40
50
125I mAb3B4 (nM)
FcεRI
BC loop ε
C' strand ε
C'E region ε
C'EF region ε
E strand ε
EF loop ε

Figure 2.7 Peptide inhibition of IgE binding to FcεRI.

Overlapping 20mer peptides were serially diluted and incubated with captured hIgE overnight. rsFcεRI at 350 ng/ml was added to the peptides in the plate, incubated, and binding detected with 3B4-HRP. Results are expressed as percent inhibition of total IgE/FcεRI binding at 750 μg/ml, the concentration closest to 50% inhibition by peptide εRI-11.

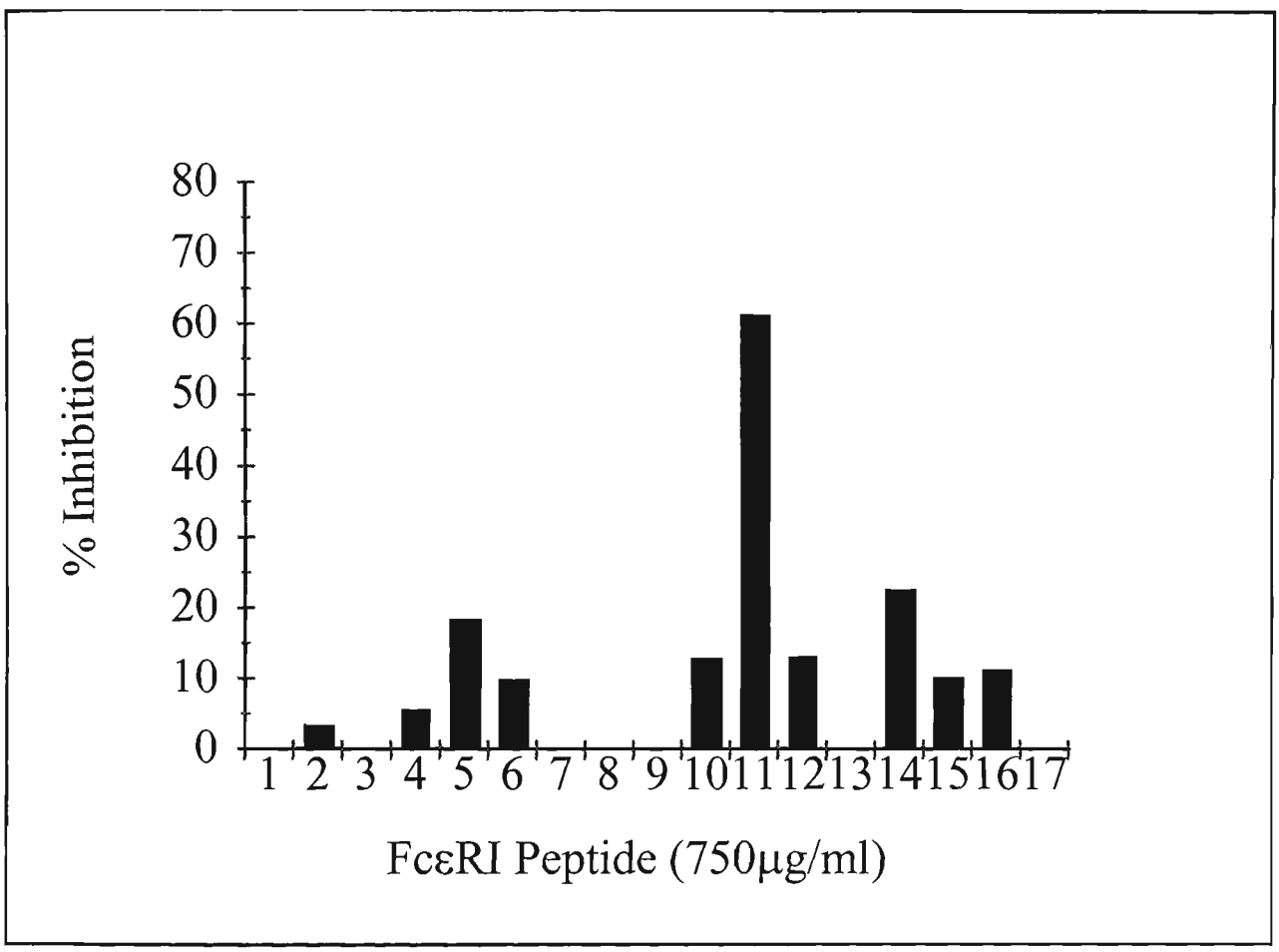
% Inhibition
80
70
60
50
40
30
20
10
0
1 2 3 4 5 6 7 8 9 10 11 12 13 14 15 16 17
FcεRI Peptide (750μg/ml)

Discussion

The detected anti-FcεRI monoclonal antibody epitopes are displayed on the homology model of the extracellular domains of FcεRI-α (Fig 2.5). This model was based on the x-ray crystallographic structure of the closely related molecule FcγRIIa (20). The spatial relationships of the epitopes and the IgE binding site described in this model are consistent with the experimental data using the monoclonal antibodies and IgE as follows.

Relationship to the IgE binding site. The mAb 15-1 blocks IgE binding to FcεRI (6), and in contrast to previous indirect studies we have directly identified the mAb 15-1 epitope to be in the BC loop of domain 2 and not in the FG loop as previously thought (30). The mAb 15-1 epitope as determined by peptide inhibition (peptides εRI-11 and εRI-12) covers the BC loop of domain 2, and in addition, the binding of IgE to FcεRI was primarily inhibited by peptide εRI-11. This implies that the two sites are close to each other, within a ten amino acid region covering the BC loop. The apparent affinity of mAb 15-1 ($\sim 10^{-10}$ M) is similar to that of IgE (2×10^{-9} M), also with a very slow dissociation rate (unpublished data), and as its epitope is closely associated with the IgE binding site, this high affinity contributes to its efficient ability to block IgE binding. Comprehensive mutagenesis and chimeric receptor studies have clearly defined the IgE binding region as including the BC, C'E and FG loops of domain two, all of which are in close proximity (14, 18). Whilst our studies clearly define the 15-1 epitope in the BC loop, a recent study (30) in which tryptophan 156 (FG loop of FcεRI domain two) was mutated to alanine caused ablation of mAb 15-1 binding, but not of IgE binding. Also, a mutation of valine 155 to leucine was seen to affect the 15-1 epitope and IgE binding. However it is clear from the model that both Trp156 and Val155 impinge on the BC loop (Fig 2.8), where there are hydrophobic interactions with Trp113 and Val115. Trp113 and Val115 form part of the mAb 15-1 epitope as determined by peptide inhibition. The Trp156Ala or Val155Leu mutations would disrupt the conformation of the BC loop and directly affect the structure of the mAb 15-1 epitope.

The epitope of mAb 47 is dependent upon the 'PLN' sequence at the start of the G strand of domain two, prior to the transmembrane portion of the receptor. This is distinct

Figure 2.8 Homology model of FcεRI with an expanded view of the region encompassing the mAb 15-1 epitope and IgE binding site.

The amino acids of the BC loop (W110, R111, N112, W113, D114, V115, Y116, K117, V118, I119, Y120) are displayed in ball and stick format and labelled, as are the amino acids W87, W156 and V155. Nitrogen atoms are shown in *blue*, and oxygen atoms in *red*. The β-strands (A, B, C, C', E, F, G) of domain two are also shown.

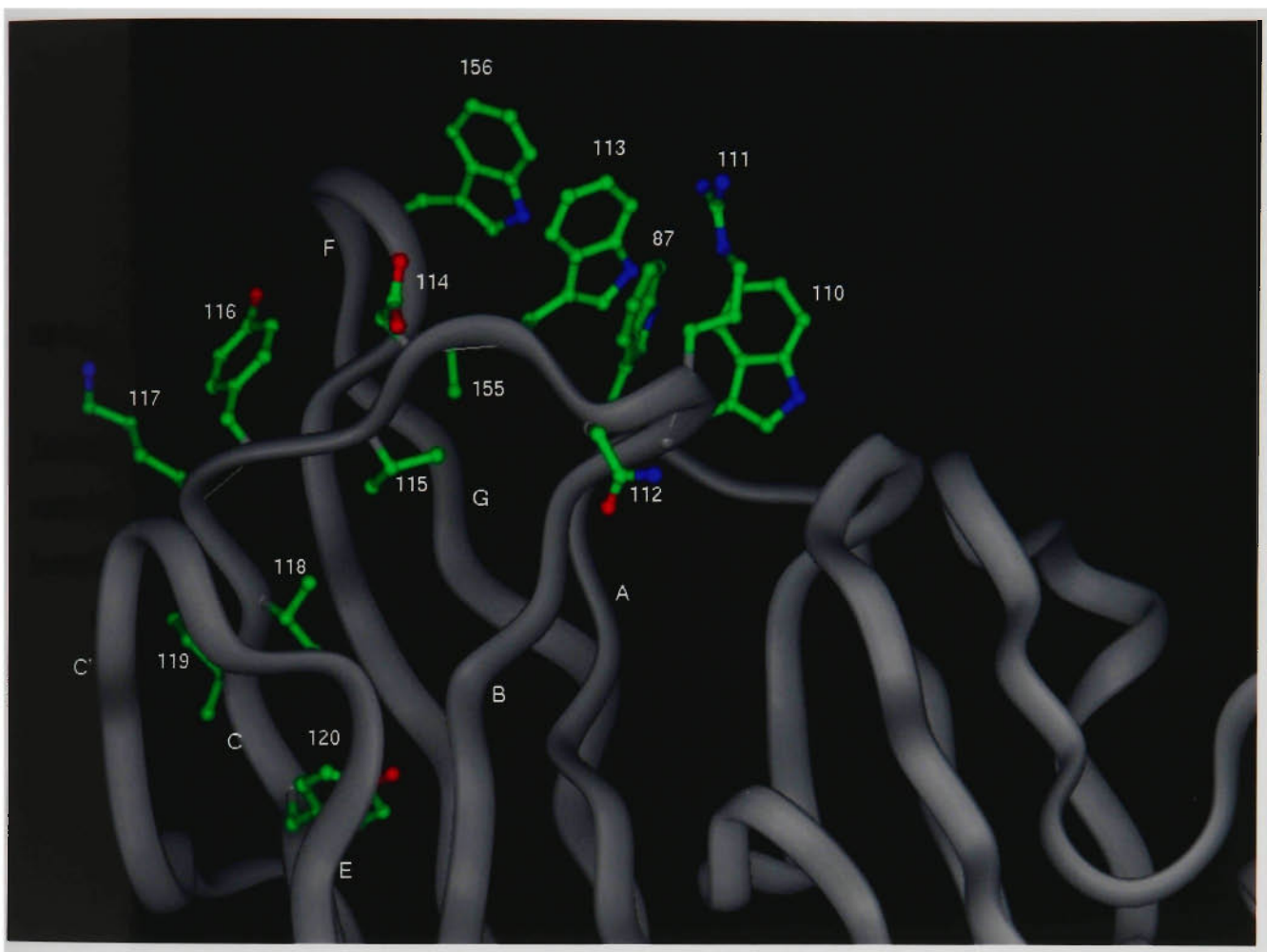
156
113
111
87
F
114
110
116
155
117
115
G
112
118
A
C'
119
B
C
120
E

from the IgE binding site which is exposed on the surface of two and, as would be expected, this antibody does not affect the binding of IgE to FcεRI. The ability of this antibody to bind an epitope in domain two separate from the IgE binding site suggests it may be useful in the determination of structural integrity in mutant and chimeric receptors, especially those unable to bind ligand.

MAb 3B4 recognises an epitope in the region comprising the C' strand through to the end of the E/F loop of domain one, and it appears to be dependent on receptor conformation. Although this region is on the superior surface of domain one (Fig 2.5), it is distant from the IgE binding site in domain two, and as expected, the antibody does not block ligand binding.

The epitope of mAb 54 (FFEVS) is located in the c-terminal part of the BC loop in domain one; the most distal portion of domain one relative to the IgE binding site in domain two. There is no competition between IgE and mAb 54 when binding the receptor, and the considerable distance between the two sites is consistent with this observation.

Interaction between the monoclonal antibody epitopes. As mentioned above, the mAb 47 epitope is dependent on the PLN sequence in the G strand of domain two. MAb 47 neither inhibited, nor was inhibited by the binding of mAbs 54, 3B4 or 15-1, and there was no competition for epitopes between the antibodies. The epitopes have been mapped onto the homology model of FcεRI , and the spatial separation of all four mAb epitopes is apparent (Fig 2.5).

MAb15-1 is the only mAb that blocks IgE binding, and it does not block or compete for the epitopes of mAbs 47, 54 or 3B4. MAb 15-1 has been mapped to an epitope in the BC loop of domain two on the superior surface of the receptor near and superior to the domain one/domain two interface. The IgE binding site has also been shown to involve the BC loop (14).

The mAb 3B4 epitope was unable to be defined by peptide inhibition of antibody binding, and the epitope was unable to be refined to a region of less than 18 amino acids

by binding to chimeric receptors. This strongly suggests that the mAb 3B4 recognises an epitope that is conformational and not linear, and indeed, chemical reduction of FcεRI in a western blot (Table 2.3) destroys the mAb 3B4 epitope. There is no competition between the anti-FcεRI domain one mAbs 54 and 3B4 when binding receptor, which suggests that the epitope of mAb 3B4 is nearer to the E strand of FcεRI domain one, than to the C' strand. The homology model (Fig 2.5) suggests that competition between the two antibodies would be expected if the mAb 3B4 binding site were near the C' strand, as the domain one BC loop and the domain one C'E loop are close to each other, and although there are no direct interactions between the loops, steric effects would be likely.

Identification of an Antagonistic FcεRI Derived Peptide. The major inhibition of IgE binding to FcεRI was by peptide εRI-11, which covers the B strand with the BC loop region of domain two. This region is also close to the C'E and FG loops of domain two, and peptides of both areas showed slight inhibition of IgE binding. It is noteworthy that all three loops have been implicated as part of the ligand binding region (14). This data implies that the B strand - BC loop of FcεRI domain two may contain the primary IgE binding region, as a peptide of this region has a greater inhibitory effect on IgE binding than that of any other segment of the FcεRI. This is consistant with previous studies where linear peptides failed to inhibit IgE binding. These peptides would have contained either the B strand and only part of the BC loop, or the BC loop C and C'strands (see ref.31, peptides 125-140 and 134-158, described therein). Indeed, peptide εRI-12 in our study, which is identical to that used by Riske *et al.* (1991), was shown in both studies to demonstrate relatively little or no inhibition. In addition, linear peptides of the C-C'-F-G region of FcεRI domain two (32) also displayed no significant inhibition of IgE binding at 1 mM concentrations, although inhibition was achieved by a similar circular peptide (32). Thus, the peptide εRI-11 is a uniquely inhibitory peptide.

In conclusion, the epitope binding properties of the monoclonal antibodies have been shown to be consistent with mutagenesis data and the homology model of FcεRI-α, and, together with the use of synthetic peptides or mimetics, may form the basis of a rational approach for the design of new therapeutic compounds. As with the possible use of all protein derived therapeutics, there is potential to induce immune responses to the native

protein; and this can only be realistically determined in the appropriate clinical trials. Certainly anti-FcεRI auto-antibodies have been implicated in the pathogenesis of chronic urticaria, and are even present in other autoimmune diseases (34,35,36); although it has recently been suggested that these may be a response to tetanus toxoid immunisation (37). Also, no genetic polymorphism of the region comprising the εRI-11 peptide has been defined, reducing the likelihood of immunogenicity and, therefore, adverse immune based reactions. Finally, such receptor based antagonists may offer better therapeutic potential than anti-FcεRI antibodies that block IgE and are likely to be anaphylactogenic (4,38).

References

1. Gaskell D. Allergy, an epidemic of our time. Chem Br 1996;5:6-8.
2. Metzger H, Kinet J-P, Perez-Montfort R, Rivnay B, Wank SA. A tetrameric model for the structure of the mast cell receptor for immunoglobulin E. Prog Immunol 1983;5:493-501.
3. Gounni AS, Lamkhioued B, Ochiai K, Tanaka Y, Delaporte E, Capron A, Kinet J-P, Capron M. High-affinity IgE receptor on eosinophils is involved in defence against parasites. Nature 1994;367:183-186.
4. Joseph M, Gounni AS, Kusnierz JP, Vorng H, Sarfati M, Kinet JP, Tonnel AB, Capron A, Capron M. Expression and functions of the high affinity IgE receptor on human platelets and megakaryocyte precursors. Eur J Immunol 1997;27(9):2212-2218.
5. Bieber T, de la Selle H, Woolomberg A, Hakimi J, Chizzonite R, Ring J, Hanau D, de la Selle C. Human epithelial Langerhans cells express the high affinity receptor for immunoglobulin E (FcεRI). J Exp Med 1992;175:1285-1291.
6. Wang B, Rieger A, Kilgus O, Ochiai K, Maurer D, Födinger D, Kinet J-P, Stingl G. Epidermal Langerhans cells from normal human skin bind monomeric IgE via FcεRI. J Exp Med 1992;175:1353-1358.
7. Maurer D, Fiebiger E, Reininger B, Wolff-Winiski B, Jouvin M-H, Kilgus O, Kinet J-P, Stingl G. Expression of functional high affinity IgE receptors (FcεRI) on monocytes of atopic individuals. J Exp Med 1994;179:745-750.
8. Blank U, Ra C, Miller L, White K, Metzger H, Kinet J-P. Complete structure and expression in transfected cells of high affinity IgE receptor. Nature 1989;337:187-189.
9. Hakimi JC, Seals JA, Kondas L, Pettine L, Danho W, Kochan J. The α subunit of the human IgE receptor (FcεRI) is sufficient for high affinity IgE binding. J Biol Chem 1990;265:22079-22081.
10. Varin-Blank N, Metzger H. Surface expression of mutated subunits of the high affinity mast cell receptor for IgE. J Biol Chem 1990; 265:15685-15694.
11. Blank U, Ra C, Kinet J-P. Characterization of truncated α chain products from human, rat and mouse high affinity receptor for immunoglobulin E. J Biol Chem

1991;266(4):2639-2646.

12. Kershaw MH, Darcy PK, Hulett MD, Hogarth PM, Trapani JA, Smyth MJ. Redirected cytotoxic effector function. Requirements for expression of chimeric single chain high affinity Immunoglobulin E receptors. J Biol Chem 1996;271(35):21214-21220.
13. Suzuki K, Hirose T, Matsuda H, Hasegawa S, Okumura K, Ra C. The Fc receptor γ subunit is essential for IgE binding activity of cell-surface expressed chimeric receptor molecules constructed from human high-affinity IgE receptor (FcεRI) α and FcRγ subunits. Mol Immunol 1998; 35:259-270.
14. Hulett MD, McKenzie IFC, PM Hogarth. Chimeric Fc receptors identify immunoglobulin-binding regions in human FcγRII and FcεRI. Eur J Immunol 1993;23:640-645.
15. Mallamaci MA, Chizzonite R, Griffin M, Nettleton M, Hakimi J, Tsien W-H, Kochan JP. Identification of sites on the human FcεRI α subunit which are involved in binding human and rat IgE. J Biol Chem 1993; 268(29):22076-22083.
16. Robertson MW. Phage and Escherichia coli expression of the human high affinity immunoglobulin E receptor α-subunit ectodomain. J Biol Chem 1993;268(17):12736-12743.
17. Scarselli E, Esposito G, Traboni C. Receptor Phage. Display of functional domains of the human high affinity IgE receptor on the M13 phage surface. FEBS Let 1993;329:223-226.
18. Hulett MD, Brinkworth RI, McKenzie IFC, Hogarth PM. Fine structural analysis of interaction of FcεRI with IgE. J Biol Chem 1999;274(19):13345-13352.
19 Rigby LJ, Hulett MD, Brinkworth RI, and Hogarth, P.M. The structural basis of the interaction of IgE and FcεRI. In: Hamawy MM, editor. IgE Receptor (FcεRI) Function in Mast Cells and Basophils. Molecular Biology Intelligence Unit. R.G.Landes Company, 1996:7-32.
20. Maxwell KF, Powell MS, Hulett MD, Barton PA, McKenzie IFC, Garrett TPJ, Hogarth PM. The crystal structure of the human leukocyte Fcreceptor, FcγRIIa. Nat Struct Biol 1999;6(5):437-442.
21. Rigby LJ, Epa VC, Mackay GA, Hulett MD, Sutton BJ, Gould HJ, Hogarth PM. Mutagenesis and homology modelling define the role of domain one in the high

affinity Fc epsilon receptor, FcεRI. J Biol Chem 2000; 275(13):9664-9672.

22. Garman SC, Kinet J-P, Jardetsky TS. Crystal Structure of the Human High-Affinity IgE Receptor. Cell 1998;95:951-961.
23. Gill SC, von Hippel PH. Calculation of protein extinction coefficients from aminoacid sequence data. Analytical Biochem 1989;182:319-326.
24. Hogarth PM, Potter TA, Cornell FN, McLaughlin R, McKenzie IFC. Monoclonal antibodies to murine cell surface antigens. I. Lyt 1.1. J Immunol 1980;125:1618-1624.
25. Gavin A, Snider J, Hulett MD, McKenzie IFC, Hogarth PM. Expression of recombinant soluble FcεRI:Function and tissue distribution studies. Immunology 1995;86:392-398.
26. Snider J. University of Melbourne PhD Thesis 1994
27. Anderson CL, Guyre PM, Whitin JC, Ryan DH, Looney RJ, Fanger MW. Monoclonal antibodies to Fc receptors for IgG on human mononuclear phagocytes. Antibody characterisation and induction of superoxide production in a monocyte cell line. J Biol Chem 1986; 261:12856-12864.
28. Ierino LF, Hulett MD, McKenzie IFC, Hogarth PM. Mapping epitopes of human FcγRII (Cdw32) with monoclonal antibodies and recombinant receptors. J Immunol 1993;150:1794-1803.
29. Hogarth PM, Ierino FL, Hulett MD. Characterisation of FcR Ig-Binding Sites and Epitope Mapping. Immunomethods 1994;4:17-24.
30. Nechansky A, Aschauer H, and Kricek F. The membrane-proximal part of FcεRIα contributes to human IgE and antibody binding - Implications for a general structural motif in Fc receptors. FEBS 1998;441:225-230.
31. Riske F, Hakimi J, Mallamaci M, Griffin M, Pilson B, Tobkes N, Lin P, Danho W, Kochan J, Chizzonite R. High affinity human IgE receptor (FcεRI). Analysis of functional domains of the α-subunit with monoclonal antibodies. J Biol Chem 1991;266(17):11245-11251.
32. McDonnell JM, Beavil AJ, Mackay GA, Jameson BA, Korngold R, Gould HJ, SuttonBJ. Structure based design and characterisation of peptides that inhibit IgE binding to its high affinity receptor. Nat Struct Biol 1996;3(5):419-426.
33. Letourner O, Sechi S, Willette-Brown J, Robertson MW, Kinet J-P. Glycosylation of

human truncated FcεRI α chain is necessary for efficient folding in the endoplasmic recticulum. J Biol Chem 1995;270:8249-8256.

34. Fiebiger E, Hammerschmid F, Stingl G, Maurer D. Anti-FcepsilonRIalpha autoantibodies in autoimmune-mediated disorders. Identification of a structure-function relationship. J Clin Invest 1998;101(1):243-51.
35. Tong LJ, Balakrishnan G, Kochan JP, Kinet JP, Kaplan AP. Assessment of autoimmunity in patients with chronic urticaria. J Allergy Clin Immunol 1997;99(4):461-5.
36. Hide M, Francis DM, Grattan CE, Hakimi J, Kochan JP, Greaves MW. Autoantibodies against the high-affinity IgE receptor as a cause of histamine release in chronic urticaria. N Engl J Med 1993;328(22):1599-604.
37. Horn MP, Gerster T, Ochensberger B, Derer T, Kricek F, Jouvin M-H, Kinet J-P, Tschernig T, Vogel M, Stadler BM, Miescher SM. Human anti-FcepsilonRIalpha autoantibodies isolated from healthy donors cross-react with tetanus toxoid. Eur J Immunol 1999;29(4):1139-1148.
38. Baniyash M, Alkalay I, Eshhar Z. Monoclonal antibodies specific to the alpha-subunit of the mast cell's Fc epsilon R block IgE binding and trigger histamine release. J Immunol 1987;138(9):2999-3004.

CHAPTER THREE:

Domain One of the High Affinity Fc epsilon Receptor, FcεRI, Regulates Binding to IgE through its interface with Domain Two.

Published: Rigby LJ, Epa VC, Mackay GA, Hulett MD, Sutton BJ, Gould HJ and PM Hogarth J Biol Chem 2000; 275:9664-9672.

SUMMARY

The high affinity receptor for IgE, FcεRI, binds IgE through the second Ig-like domain of the alpha subunit. The role of the first Ig-like domain is not well understood, but it is required for optimal binding of IgE to FcεRI; either through a minor contact interaction or in a supporting structural capacity. The results reported here demonstrate that domain one of FcεRI plays a major structural role supporting the presentation of the ligand binding site, by interactions generated within the interdomain interface. Analysis of a series of chimeric receptors and point mutants indicated that specific residues within the A' strand of domain one are crucial to the maintenance of the interdomain interface, and IgE binding. Mutation of the Arg 15 and Phe 17 residues caused loss in ligand binding, and utilising a homology model of FcεRI-α based on the solved structure of FcγRIIa, it appears likely that this decrease is brought about by collapse of the interface and consequently the IgE binding site. In addition discrepancies in results of previous studies using chimeric IgE receptors comprising FcεRI-α with either FcγRIIa or FcγRIIIA can be explained by the presence or absence of Arg 15 and its influence on the IgE binding site. The data presented here suggests that the second domain of FcεRI-α is the only domain involved in direct contact with the IgE ligand, and that domain one has a structural function of great importance in maintaining the validity of the domain interface and through it, the ligand binding site.

INTRODUCTION

The high affinity IgE receptor, FcεRI, is a tetrameric complex composed of an IgE binding alpha subunit associated with a tetraspan beta subunit and homo-dimeric gamma subunits, and is a key player in IgE dependent effector mechanisms. The alpha subunit, FcεRI-α, is the ligand binding chain and is composed of two Ig-like domains. The role of the second domain has been clearly defined as containing the IgE binding region. However, the role of the first domain is not clear in FcεRI nor indeed in any Fc receptor. Analyses to date have variously indicated that domain one is necessary for optimal binding (1,2,3), that it has a possible role in direct interaction with IgE (4,5), and that it provides a supportive role in maintaining receptor integrity (1,2). The structural reasons for this are not apparent. FcεRI, however, is related to FcγRIIa and the recent description of the three dimensional structure of FcγRIIa (6), FcγRIIb (7) and FcεRI-α (8) may provide a basis for the understanding of the roles of the individual domains in FcεRI and other Fc receptors.

In the crystal structure of FcγRIIa the extracellular domains are "bent" to form an acute angle (52°) between domains 1 and 2. In this orientation, the IgG binding site of domain 2 points away from the cell in such a manner as to be accessible to ligand, and domain 1 is angled away from the binding site and down toward the cell membrane. The acute angle is dictated by interactions within the interdomain interface, and the structural studies indicate that domain 1 is likely to support domain 2 providing an architectural role in the positioning of the binding site. As FcεRI and FcγRIIa show 40% amino acid identity, and considerably higher amino acid homology, it is probable that FcεRI has a similar structure to that of FcγRIIa, confirmed by the recent publication of the solved FcεRI structure (8).

In the study described herein we have utilized a model of FcεRI-α (see Figure 3.1) based on the solved crystal structure of FcγRIIa (6), and undertaken a mutagenesis study of domain 1 to define its role in the interaction with IgE. The solved x-ray structure of FcεRI-α (8) strongly resembles that of FcγRIIa, and therefore that of the FcεRI-α homology model. Indeed, the FcεRI-α homology model and the x-ray structure of FcεRI-α, as described by Garman (8), show compelling concurrence in comparisons of

structure and molecular interactions. Here, data from the chimeric Fc receptors and alanine mutants have been used together with molecular modelling to propose a functional structure of FcεRI-α.

Figure 3.1 Homology model of the extracellular region of FcεRI-α, based on the solved crystal structure of FcγRIIa.

The β strands of each domain are labelled, as are the carboxyl (c) and amino (n) termini. The IgE binding region is indicated in *pink*, and the A' strand of domain one in *green*.

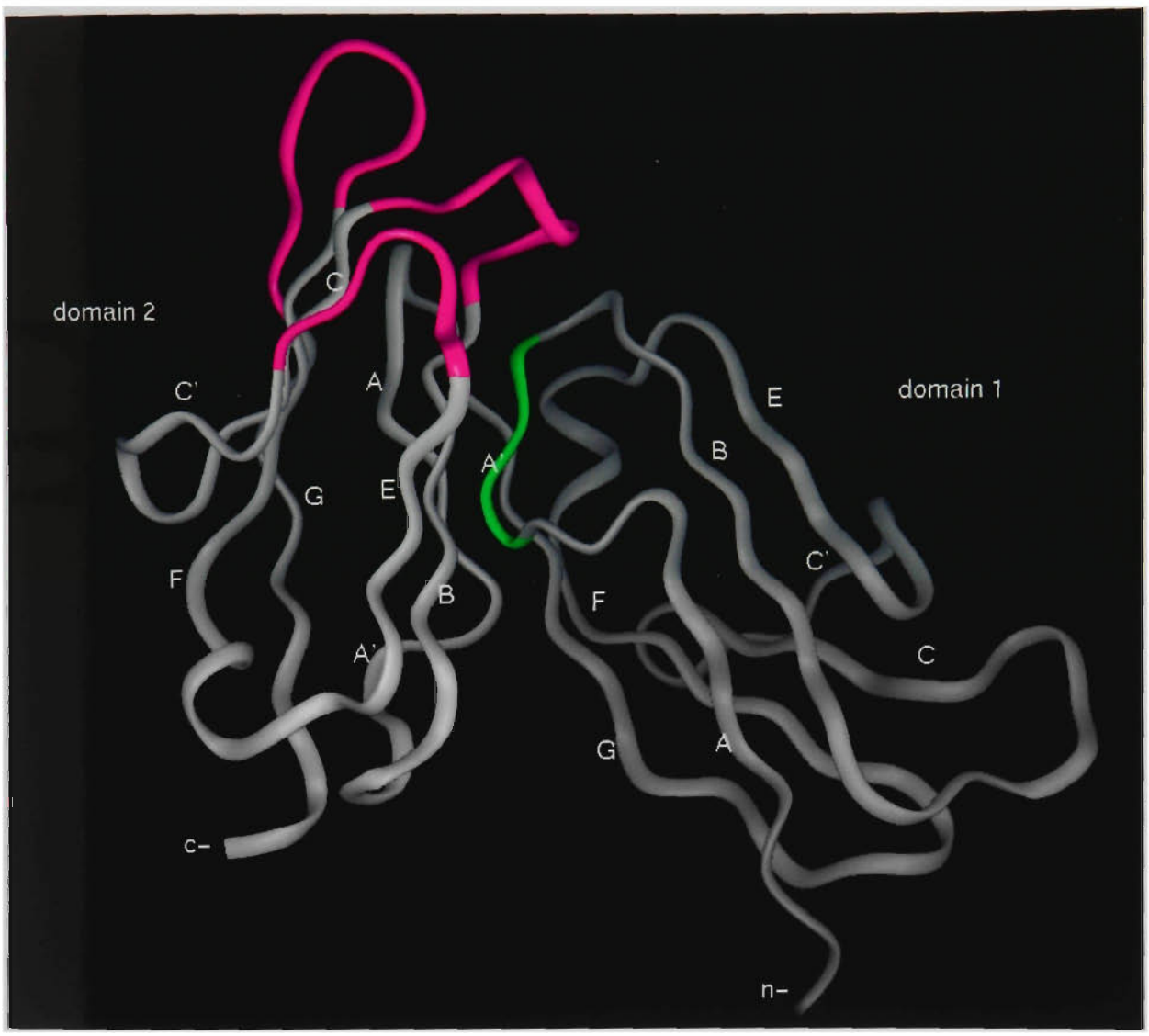
domain 2
C
C'
A
A'
G
E'
F
B
A'
E
B
domain 1
C'
F
C
G
A
c-
n-

EXPERIMENTAL PROCEDURES

Production and nomenclature of FcεRI-α chimeric cDNA receptor constructs— Two previously produced chimeric cDNA receptor constructs (1) were used as templates in the construction of this series of FcRs. The amino acid sequences of the chimeras and chimera nomenclature are displayed in Table 3.I. The first template was designated **εεγ** and comprised domain one (D1) and domain two (D2) of FcεRI-α linked with the transmembrane region and cytoplasmic membrane anchor of FcγRIIa. The second chimeric template was based on a simple domain exchange, and comprised D1 of FcγRIIa and D2 of FcεRI-α, also with the transmembrane region and cytoplasmic sequence of FcγRIIa, and was designated **γεγ**. Chimeric receptors were generated using the template receptor γεγ or εεγ. Specific loops, strands or regions of the FcγRIIa D1 were replaced with the equivalent portion of FcεRI (or *vice versa*) to produce a series of chimeric receptors using splice overlap extension - polymerase chain reaction (SOE-PCR) using the method previously reported (9). A further template receptor was constructed with a glycosyl-phosphatidylinositol (GPI) membrane anchor of FcγRIIIB replacing the FcγRIIa cytoplasmic tail of the γεγ construct. This chimera was designated γεRIII, and was generated by SOE-PCR. Substitution into domain one of the γεRIII template receptor of the A strand of FcεRI D1 produced the γ(Aε)εRIII chimera. The FcεRI D1 A' strand point mutants, R15A and F17A, were made using SOE-PCR, and incorporated into εεγ. The FcεRI D1 A' strand point mutants N14A and R15L were constructed using the Quikchange™ Site-Directed Mutagenesis Kit (Stratagene). cDNA was purified by centrifugation in a CsCl gradient (10) and the mutations verified by nucleotide sequencing.

Production and purification of IgE— Human IgE (hIgE) (ATCC clone TIB196) was affinity purified over an anti-human IgE affinity column (ATCC clone HB121 purified supernatant, coupled to cyanogen bromide-activated Sepharose beads (Pharmacia, Uppsala, Sweden). Bound IgE was eluted in 1 ml fractions with 0.5 M sodium citrate/0.5 M NaCl (pH 2.7) into tubes containing 50 µl 1 M Tris (pH 9.0), buffer exchanged to phosphate buffered saline (7.6 mM Na_2HPO_4/ 3.25 mM NaH_2PO_4/ 145 mM NaCl, pH 7.4) on a Sephadex G-25 PD-10 column (Pharmacia), and concentrated in a centrifugal concentrator (Macrosep, Filtron, Life Technologies).

Table 3.I

Aminoacid Sequences of FcγRIIa, FcεRIα, hFcγRIIIa and Chimeric Clones

a) 'Wild-type' receptor sequences with identity indicated between hFcγRIIa and hFcεRI-α, hFcγRIIIa and hFcεRI-α in domain 1 only.

Strands: A, A′, B, C, C′, E, F, G

DOMAIN 1	1 · 10 · 20 · 30 · 40 · 50 · 60 · 70 · 80
hFcγRIIa	APPKAVLKLEPPWINVLQEDSVTLTCQGARSPESDSIQWFHNGNLIPTHTQPSYRFK-ANNNDSGEYTCQTGQTSLSDPVHLTVLSE
hFcεRI	VPQKPKVSLNPPWNRIFKGENVTLTCNGNNFFEVSSTKWFHNGSLSEET-NSSLNIVNAKFEDSGEYKCQHQQVNESEPVYLEVFSD
hFcγRIIIa	DLPKAVVFLEPQWYRVLEKDSVTLKCQGAYSPEDNSTQWFHNESLISSQ-ASSYFKDAATVDDSGEYRCQTNLSTLSDPVQLEVHIG

Strands: A, A′, B, C, C′, E, F, G

DOMAIN 2	90 · 100 · 110 · 120 · 130 · 140 · 150 · 160 · 169
hFcγRIIa	WLVLQTPHLEFQEGETIMLRCHSWKDKPLVKVTFFQNGKSQKFSHLDPTFSIPQANHSHSGDYHCTGNIGYTLFSSKPVTITV
hFcεRI	WLLLQASAEVVMEGQPLFLRCHGWRNWDVYKVIYYKDGEALKYWYENHNISITNATVEDSGTYYCTGKVWQLDYESEPLNITV

b) Domain 1 aminoacid sequences of chimeric clones

Strands: A, A′, B, C, C′, E, F, G

CLONE	1 · 10 · 20 · 30 · 40 · 50 · 60 · 70 · 80
hFcγRIIa	APPKAVLKLEPPWINVLQEDSVTLTCQGARSPESDSIQWFHNGNLIPTHTQPSYRFK-ANNNDSGEYTCQTGQTSLSDPVHLTVLSE
γεγ	APPKAVLKLEPPWINVLQEDSVTLTCQGARSPESDSIQWFHNGNLIPTHTQPSYRFK-ANNNDSGEYTCQTGQTSLSDPVHLTVLSE
γ(Aε)εRIII[a]	**VPQKPKVSLN**PPWINVLQEDSVTLTCQGARSPESDSIQWFHNGNLIPTHTQPSYRFK-ANNNDSGEYTCQTGQTSLSDPVHLTVLSE
γ(A'Bε)εγ	APPKAVLKLEPPW**NRIFKGEN**VTLTCQGARSPESDSIQWFHNGNLIPTHTQPSYRFK-ANNNDSGEYTCQTGQTSLSDPVHLTVLSE
γ(AA'Bε)εγ	**VPQKPKVSLNPPWNRIFKGEN**VTLTCQGARSPESDSIQWFHNGNLIPTHTQPSYRFK-ANNNDSGEYTCQTGQTSLSDPVHLTVLSE
γ(ABCε)εγ	**VPQKPKVSLNPPWNRIFKGENVTLTCNGNNFFEVSS**IQWFHNGNLIPTHTQPSYRFK-ANNNDSGEYTCQTGQTSLSDPVHLTVLSE
γ(ABCC'ε)εγ	**VPQKPKVSLNPPWNRIFKGENVTLTCNGNNFFEVSSTK**WFHNGNLIPTHTQPSYRFK-ANNNDSGEYTCQTGQTSLSDPVHLTVLSE
γ(Gε)εγ	APPKAVLKLEPPWINVLQEDSVTLTCQGARSPESDSIQWFHNGNLIPTHTQPSYRFK-ANNNDSGEYTCQTGQTSL**SEPVYLEVFSD**
ε(A'Bγ)εγ	**VPQKPKVSLNPPW**MNVLQEDS**VTLTCNGNNFFEVSSTKWFHNGSLSEET-NSSLNIVNAKFEDSGEYKCQHQQVNESEPVYLEVFSD**
εεγ	**VPQKPKVSLNPPWNRIFKGENVTLTCNGNNFFEVSSTKWFHNGSLSEET-NSSLNIVNAKFEDSGEYKCQHQQVNESEPVYLEVFSD**
hFcεRI	**VPQKPKVSLNPPWNRIFKGENVTLTCNGNNFFEVSSTKWFHNGSLSEET-NSSLNIVNAKFEDSGEYKCQHQQVNESEPVYLEVFSD**

c) Aminoacid sequences of membrane proximal (MP), transmembrane (TM), and membrane anchor (MA) regions of chimeric constructs with FcγRII or FcγRIIIb membrane anchor.

Clone	D2 ε (159)	MP γ	TM γ	MA γ
εεγ	DYESEPLNITV	QVPSMGSSS	PMGIIVAVVIATAVAAIVAAVVALIYC	RKKRISANSTDPVKAAQFEPPGRQMIAIRKR MA γ continued -QLEETNNDYETADGGYMTLNPRAPTDDDKNIYLTLPPNDHVNSNNend

Clone	D2 ε (159)	MP γ	TM γRIII	MA γRIII
εεRIII	DYESEPLNITV	QVPSMGSSI	SSFSPPGYQVSFCLVMVLLFAVDTGLY	FSVKTNIend

a. Mutant clone nomenclature: the initial character (γ or ε) designates the receptor of D1 origin - FcεRI, FcγRIIa -, the portion in parentheses indicates the region exchanged (e.g. A'B loop) and its receptor of origin.

Possible sites for N-linked glycosylation have been underlined.

Detection of IgE activity by ELISA— High bind EIA/RIA plates (Costar 3690) were coated with 8 μg/ml of anti-human IgE mAb HB121 in PBS overnight. The plates were blocked prior to the addition of serially diluted monoclonal IgE in PBS containing 1.5%BSA (50 μl/well, 60 min). rsFcεRI (11) was then added (50 μl per well, 60 min). Bound rsFcεRI was detected using HRP conjugated 3B4, a non-blocking anti-human FcεRI mAb (1 μg/ml, 50 μl/well, 60 min). The assay was carried out at 20°C, and the plates were washed 7 times with water between each incubation step. Colour development was with *o*-phenylenediamine OPD (Sigma Biosciences, St Louis, MO), and stopped after 15 min with 25 μl 4 M sulphuric acid. The optical density was measured at 490 nm.

Transfection of mammalian cells with cDNA— COS-7 cells were maintained (1) in Dulbecco's modified Eagles medium (DMEM) (Gibco BRL, Life Technologies Inc., Gaithersburg, MD). For transient transfection Lipofectamine (Life Technologies Inc) reagent was used, with plasmid DNA of interest, according to the manufacturer's instructions.

Immune Complex Binding— The binding of IgE or IgG immune complexes to cells transfected with chimeric or mutant cDNA was determined by erythrocyte-antibody (EA) rosetting, which was assayed and scored according to the method previously reported (1). Briefly, mouse anti-TNP IgE or IgG (moIgE or moIgG) was incubated with TNP coated sheep red blood cells to form complexed IgE or IgG. These antibody sensitised erythrocytes were mixed with transfected cells, and the binding of these complexes to cells was determined microscopically (1). The utilisation of avidity in this way permits the determination of low affinity binding.

Measurement of IgE/ FcεRI by Equilibrium Binding— Equilibrium binding was determined by the method previously reported (1). IgE was radioiodinated using IODO-GEN (Pierce) according to the manufacturer's instructions. The ^{125}I disintegrations per min were determined separately for the cell pellets (bound IgE) and the supernatant (free IgE) in a WALLAC 1470 WIZARD™ automatic gamma counter. Non-linear regression analysis was performed by plotting IgE free versus IgE bound in the program "Curve

Expert", using the formula for single site binding, $y = (a*x)/(b+x)$; where y=IgE bound, and x=free IgE. The equilibrium binding dissociation constant (K_D) was obtained from three experiments with a correlation coefficient of >0.99 (Table 3.II). The maximum binding (Bmax) of IgE was also determined and used to estimate receptor expression.

Detection of membrane-bound FcεRI by monoclonal antibodies using Flow Cytometry— COS-7 cells were transiently transfected with rFcεRI cDNA as above. Approximately 40 hrs post transfection the COS-7 cells were incubated with saturating amounts of antibody, on ice, for 45 min; the cells were washed, resuspended in a 1/100 dilution of anti-mouse Ig $(Fab')_2$-FITC (Silenus) and incubated for 30 min on ice. The cells were washed and resuspended in PBS containing 0.5% BSA, 0.1% Glucose, 3 μg/ml propidium iodide and analysed in a FACScalibur (Becton Dickinson). All washes and dilutions were in PBS containing 0.5% BSA, 0.1% Glucose. Analysis was conducted on live (propidium iodide negative) cells.

Monoclonal antibodies— Anti-human FcεRI-α monoclonal antibodies from hybridoma cell lines X52-47-5.4 (mAb 47), X52-54.1 (mAb 54), and 3B4 (mAb 3B4), all mouse IgG1, were used to determine FcεR expression. These antibodies recognise separate epitopes :- MAb 47 recognises an epitope in the G strand D2, mAb 54 - an epitope in the BC loop of D1, and mAb 3B4 - an epitope in the C'EF region of D1. Anti-human FcεRI-α mouse monoclonal antibody 15-1 was generously supplied by J-P Kinet. Anti-mouse FcγRI (IgG1) monoclonal allo-antibody from the hybridoma cell line X54-5/7.1 was kindly provided by Peck Szee Tan for use as an isotype control antibody. The anti-TNP mouse monoclonal antibodies were moIgE anti-TNP (ATCC clone TIB142) and moIgG1 anti-TNP (A3), the latter was the gift of Dr A Lopez (Institute of Medical and Veterinary Science, Adelaide, Australia).

Modelling of FcεRI, chimerae and mutants— The extracellular regions of the α-chain of the human Fc epsilon receptor type I (FcεRI-α) and the human Fc gamma Receptor type II a (FcγRIIa) show a sequence identity of about 40% for 172 residues (This consists of a sequence identity of about 45% for the first domain and about 36% for the second domain). FcγRIIa is the protein most homologous to FcεRI for which the

3-dimensional structure is known (6). With the significant sequence identity, even higher sequence similarity, and the conservation of several important amino acid residues between the two proteins (see the sequence alignment given in Table 3.I), clearly FcγRIIa is the most appropriate 3-dimensional structural template to use in modelling FcεRI, more suitable than the structures of CD2 or CD4 which have been used in the past to construct models of FcεRI (12,13). The recently solved crystal structure of FcεRI (8) confirmed the similarity of the two structures, including the C2 sub type of the Ig-like domains and the acute angle between the two domains. However, the cartesian coordinates of the crystal structure of FcεRI were not available, and therefore we made use of the homology model of FcεRI built in this work.

FcεRI-α model— Modeler (14) as implemented in the InsightII_Homology software package (Insight II (97.0), MSI, San Diego) was used to build 3-dimensional models of FcεRI-α using a number of different initial sequence alignments and two structural templates of FcγRIIa. One of the structural templates was the 3-dimensional coordinates of FcγRIIa where for the residues that had alternative side-chain conformations (residue numbers 10, 21, 33, 57, 60, 61, 65, and 89) the conformations labelled 'A' were selected, while in the other template the conformations labelled 'B' were selected. In each Modeler run, five structural models of FcεRI-α were generated. The following parameter values or options were used: 'library_schedule' of 1, 'max_var_iterations' of 300, 'md_level' of 'refine1', 'repeat_optimization' of 3, and 'max_molpdf' of 106. The best model from these runs had the sequence alignment given in Table I, and used the structural template of FcγRIIa where residues 10, 21, 33, 57, 60, 61, 65, and 89 had side-chains in the 'A' conformation. The criteria for judging the 'best' model included the lowest value of the Modeler objective function (or - 1.0xln (Molecular probability density function = Mpdf)), 'well-behaved' ProsaII (15) residue energy plot for the model (for example, negative residue energy scores throughout the sequence), and 'well-behaved' Profiles-3D (16) local 3D-1D compatibility score plot (for example, positive plot scores throughout the sequence).

Next, Modeler was used to generate 20 different structural models of FcεRI-α using the sequence alignment and template selected above, and using the parameter

values and options listed above. From these, the model with the lowest - ln (Mpdf) value was then further improved (as measured by ProsaII, Profiles-3D, and Procheck (17) by being selected as the template to generate structural models of the FcεRI-α sequence in the next cycle of Modeler runs. At the end of four such cycles, the 'best' 3-dimensional model of the FcεRI-α structure (ie the model with the lowest value of the Modeler objective function) was selected as the final structural model of the FcεRI-α monomer. Secondary structure prediction performed on FcεRI-α sequence confirmed the validity of the alignment given in Table I and showed the pattern of β strands is the same in both FcεRI-α and FcγRIIa. The secondary structure prediction methods used were PHD (18) and PREDATOR (19). The model is displayed in Figure 3.1.

Mutant and chimeric receptors— The R15A and the F17A point mutants of FcεRI-α were modelled from the above FcεRI-α model by mutating the R15 and F17 residues to alanines with InsightII_Homology module (MSI, San Diego), adding hydrogens to the two models, and energy minimizing the structures, keeping all heavy atoms fixed except for the A15 and A17 residues, respectively. The program Discover v. 2.98 (MSI, San Digeo) was used for the energy minimization with the CFF91 force field and a distance-dependent dielectric constant of 1.0xr, and the minimization was done with the conjugate gradients method until the maximum energy gradient was less than 0.01 kcal/Å.

Three chimera structures of FcεRI that were experimentally constructed, and the binding to IgE investigated, were modelled based on the structural template of FcγRIIa. The sequences of these three chimera, labelled γεγ, γ(A'Bε)εγ, and ε(A'Bγ)εγ, respectively, are shown in Table 3.I. The same sequence alignment as shown in Table 3.I, and the same Modeller parameter values and options as were used to generate the model of FcεRI-α (as described earlier) were used to construct these chimera models. Again, out of 20 models generated for each chimera, the model with the lowest Modeller objective function was selected, and the model structure validated with ProsaII, Profiles-3D, AND Procheck.

Finally the electrostatic potential was calculated and mapped onto the molecular

surface (see Figure 3.2) of the constructed FcεRI-α model using the program GRASP (20). The 'PARSE3' (21) charge set was used in computing the electrostatic potential. It can be seen that one 'face' of FcεRI-α has a considerably more negative electrostatic potential than the other face.

The co-ordinates of the FcεRI-α model are available on request.

Note added in proof.

The comparison of the model of FcεRI-α with the crystal structure (accession number: 1F2Q), for the alpha carbon atoms of residues 4-31 and 36-172, produces a root mean square deviation of 2.5 Angstroms. The residues 32-35 excluded comprise the highly variable C' region.

Figure 3.2 FcεRI-α homology model with electrostatic potential displayed.
The electrostatic potential of FcεRI-α model was calculated and mapped onto the molecular surface, with *red* indicating a negative, and *blue* indicating a positive electrostatic potential. It can be seen that the 'face' of FcεRI-α comprising the C/F/G strands of domain 1 and domain 2 (2a) has a considerably more negative electrostatic potential than the 'face' comprising the A/B/E strands of domain 1 and domain 2 (2b).

A

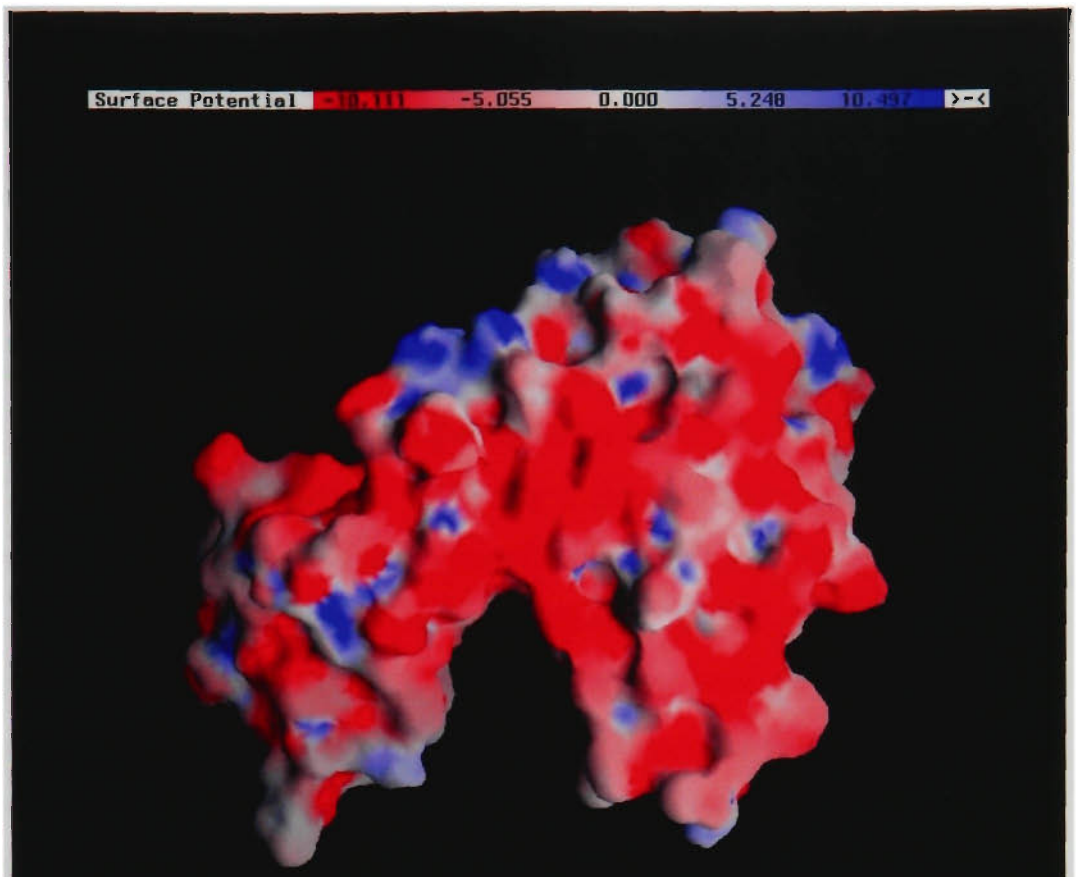
Surface Potential
-10.111
-5.055
0.000
5.248
10.497

B

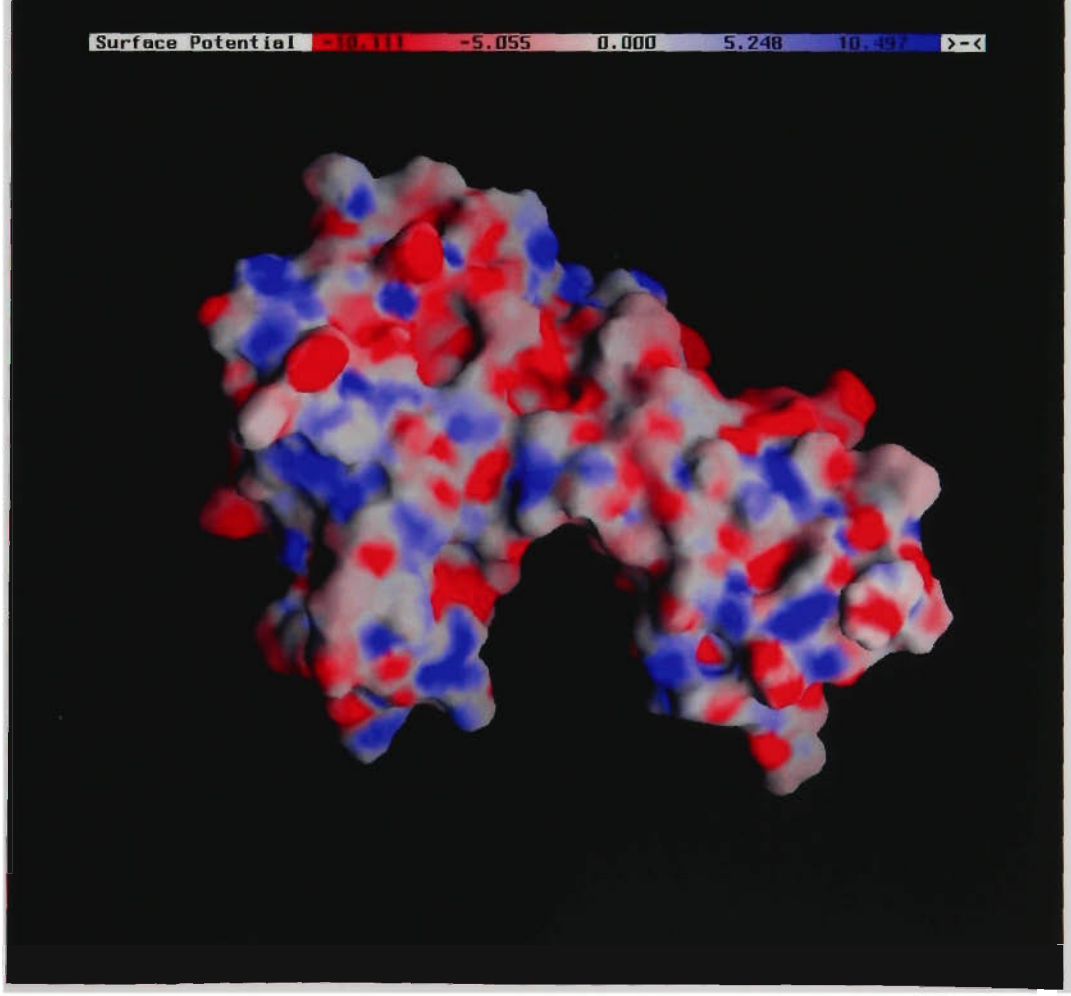
Surface Potential
-10.111
-5.055
0.000
5.248
10.497

RESULTS AND DISCUSSION

Analysis of chimeric receptors to establish the role of D1 FcεRI-α in IgE binding— Examination of the FcεRI-α homology model (shown in Figure 3.1 and fully described below) and the model of the γεγ chimera indicates that the two major regions of domain one (D1) that impinge on the D1/D2 interface are, first, the A strand, A' strand and A'B loop, and second, the G strand. Utilizing a chimeric FcR (γεγ) comprising FcγRIIa domain one (D1) and FcεRI domain two (D2) (IgE binding domain), those segments that form part of the D1/D2 interface of D1 FcγRIIa cDNA were replaced with the equivalent portion of FcεRI cDNA (Table 3.I). The receptors were assayed to determine which segments conferred a gain of function. Four chimeric receptors were constructed that encompassed the A' strand A'B loop region, namely, γ(ABCε)εγ, γ(ABCC'ε)εγ, γ(AA'Bε)εγ and γ(A'Bε)εγ. Analysis of the transfected receptors by EA-rosetting (1) indicated, surprisingly, that none of these chimeric receptors bound complexed moIgE as IgE coated erythrocytes; as expected, none bound moIgG.

To determine whether the receptors were expressed on the cell surface, the chimeras were tested by flow cytometry, using a panel of four anti-FcεRI-α monoclonal antibodies (mAbs) that recognised separate non-overlapping epitopes, two (mAb 3B4, mAb 54) in D1 and two (mAb 47, mAb 15-1) in D2 (11). Two of the four chimeras tested, γ(ABCε)εγ and γ(ABCC'ε)εγ, were not detected on the cell surface, and thus were assumed not to be expressed. However, the γ(AA'Bε)εγ and γ(A'Bε)εγ chimeras were detected on the cell surface by mAb, and were then tested for their ability to bind monomeric human IgE (hIgE) in an equilibrium binding assay (Table 3.II). Both chimeras failed to bind monomeric hIgE, which is consistent with their failure to bind moIgE complexes (Table 3.II). Thus, despite the fact that these interface sequences were derived from FcεRI, the chimeras were not able to bind IgE.

The γ(AA'Bε)εγ (FcεRI residues 1-21) and γ(A'Bε)εγ (FcεRI residues 14-21) chimeras differ only by the inclusion or absence of the FcεRI A strand of D1 (FcεRI residues 1-10), and although these chimeras were detected on the cell surface by mAb 47 (which maps to an epitope in D2 near the transmembrane region), they were not detected

Table 3.II.

Binding and expression of chimeric and mutant receptors of the A strand - A'B loop or G strand regions of D1.

	moIgE EA-rosetting[a] (Avidity)	Relative expression detected by IgE[b]	Relative expression detected by mAb[c]	K_D (M)[d]	Relative Affinity[e]
ϵϵγ	3+	1	1	$2.1x10^{-9}$[f] ± 7.2e-10	1
γϵγ	3+	0.5	1	$4.0x10^{-9}$[f] ± 8.0e-10	0.6
γ(AA'Bϵ)ϵγ	-	-	0.3	-	-
γ(A'Bϵ)ϵγ	-	-	0.2	-	-
γ(Aϵ)ϵRIII	3+	0.3	0.5	$2.9x10^{-9}$ ± 4.9e-10	0.7
ϵ(A'Bγ)ϵγ	-	-	0.6	-	-
F17A	1+	0.15	0.2	$4.1x10^{-8}$ ± 3.0e-08	0.05
R15A	-	-	0.2	$<1x10^{-6}$	<0.01
R15L	-	-	0.2	-	-
N14A	1+	0.2[g]	0.2	ND[h]	-
γ(Gϵ)ϵγ	3+	0.4	0.3	$3.3x10^{-9}$ ± 9.5e-10	0.65

a. Binding of immune complexes. MoIgE-EA rosetted cells were scored on a scale of + to 3+, with 3+ indicating the highest number of EA associated with a cell.

b. The average expression of a receptor determined by the maximum binding of IgE in equilibrium binding assays, and compared to that of ϵϵγ where ϵϵγ=1.

c. Average cell surface expression of the chimera as detected by anti-FcϵRI mAb 47 in flow cytometry, and compared with expression of ϵϵγ where ϵϵγ=1.

d. The equilibrium binding dissociation constant (average taken from three experiments) with the standard deviation indicated.

e. Relative affinity of chimeric receptors determined by K_D (ϵϵγ=1), all other chimeras had a lower apparent affinity.

f. Statistical significance of difference between the K_D of ϵϵγ and γϵγ was determined by Student's t-test to be p=0.01

g. Expression of N14A relative to ϵϵγ was determined by IgE binding and detected by flow cytometry.

h. Not Determined

by mAb 15-1, an antibody previously reported to detect an epitope in D2 within the IgE binding site (22). Thus, although the receptors were expressed, they were incapable of binding monomeric hIgE or moIgE complexes, implying significant disruption to the IgE binding site. This disruption is most probably caused by the segment that is common to both receptor chimeras, that of the A' strand, A'B loop (FcεRI residues 14-21), rather than the A strand which is present only in the γ(AA'Bε)εγ chimera. In the structure of FcγRIIa and the model of FcεRI, the cis Pro 11 at the start of the A' strand, is essential for maintaining the conformation of this part of the interdomain interface. This would imply that the A strand segment up until the cis Pro has little impact on the inter-domain interface and was probably not involved in the disruption to IgE binding, as would be expected from the structure. This was confirmed by testing a chimera with only the A strand segment from the N terminus to the cis Pro 11 from FcεRI in D1 FcγRIIa, namely γ(Aε)εRIII. This A strand chimera bound hIgE with an affinity approaching that of εεγ (Table 3.II), and is discussed below.

Evidently the loss of IgE binding function was related to the alteration of sequences in the interdomain interface, which implies a major role in IgE binding by domain 1. Furthermore, even though these sequences are derived from the same receptor as the IgE binding second domain, they do not provide the correct interactions unless in the context of an autologous first domain. Thus, it may be expected that IgE binding is dependent upon the A' strand - A'B loop segment. In order to confirm that this change of function was directly related to the A' strand - A'B segment and its impact on the D1/D2 interface, an additional chimera was created. This new chimera was constructed using FcεRI-α (εεγ) as the template, (rather than γεγ) in which the A'B strands and loop of FcγRIIa D1 were inserted into the corresponding position in FcεRI. This ε(A'Bγ)εγ chimera was expressed on the cell surface as measured by mAb 47, but mAb 15-1 again failed to detect its epitope in the IgE binding site (Table 3.II, 3.III). Moreover, the chimera did not bind monomeric hIgE or complexed moIgE confirming that the inter-domain interface has an essential role in the interaction of receptor with IgE.

Table 3.III

Expression and integrity of chimeric and mutant receptors of the A strand - A'B loop region of D1.

	mAb47 (D2)	mAb15-1(D2)	mAb54(D1)	mAb3B4(D1)
ϵϵγ	4	4	4	4
γϵγ	4	4	-	-
γ(AA'Bϵ)ϵγ	4	-	-	-
γ(A'Bϵ)ϵγ	4	-	-	-
γ(Aϵ)ϵRIII	4	4	-	-
ϵ(A'Bγ)ϵγ	4	-	4	ND[b]
F17A	4	-	2	1
R15A	4	-	3	2
R15L	4	-	3	2
N14A	4	4	4	ND

a. Receptor expression was determined by flow cytometry using mAbs. Expression was scored on a scale of 1-4 with maximum expression (4) determined after subtraction of background values (FITC labelled Fab'$_2$ sheep anti-mouse Ig). 3 = 60-80% of maximum, 2 = 40-60% of maximum and 1 = less than 40% of maximum.

b. Not Determined

Figure 3.3 Homology model of the FcεRI-α domain 1/domain 2 interface.
Stereo view of the FcεRI-α domain 1/domain 2 interface, with the protein backbone depicted in a *green* wire format and amino acids involved in transdomain interactions displayed in ball and stick form and labelled. Nitrogen atoms are displayed in *blue*, and oxygen atoms in *red*.

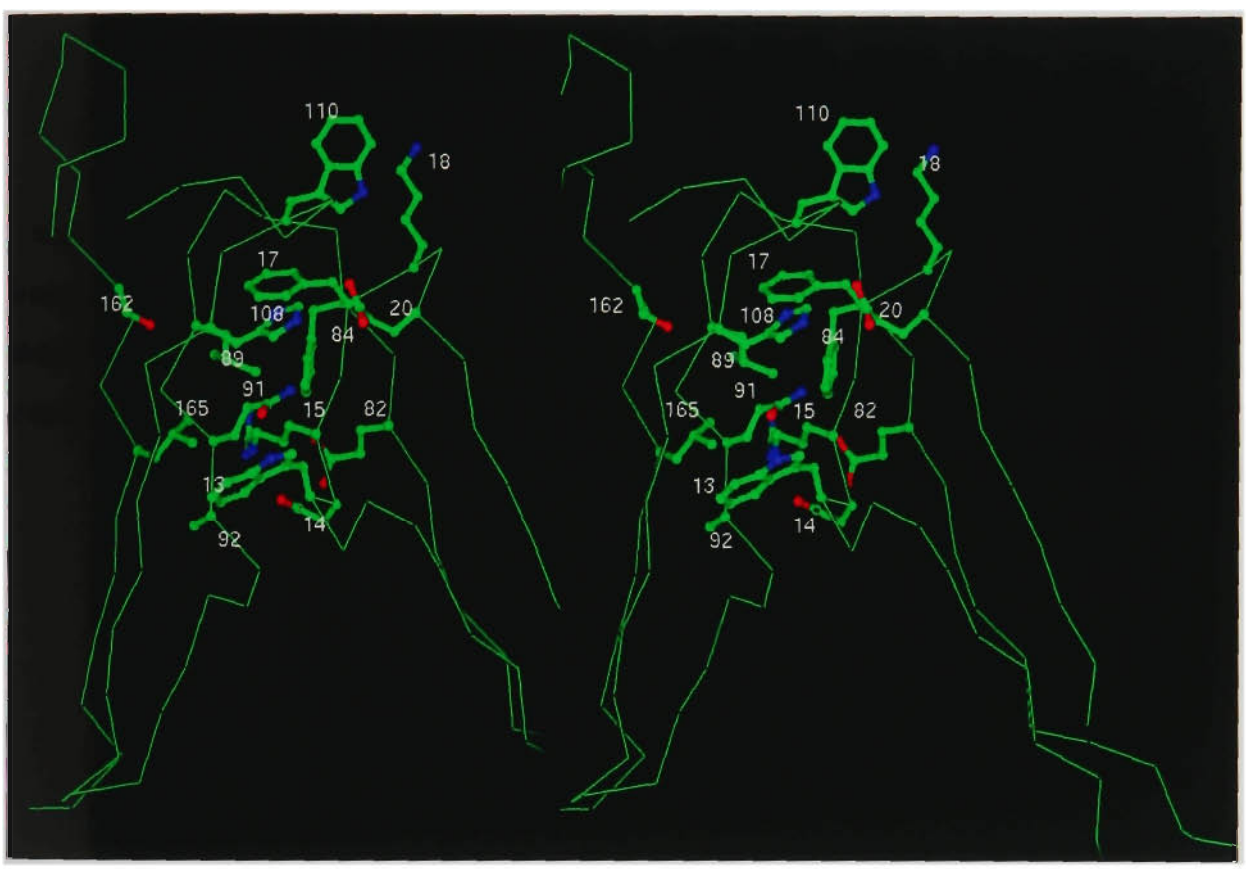
110
18
17
162
108
20
84
89
91
165
15
82
13
14
92
110
18
17
162
108
20
84
89
91
165
15
82
13
14
92

The inability of the ϵ(A'Bγ)ϵγ chimera to bind IgE is not an effect of distortion of D1, as a separate monoclonal antibody (mAb 54) which binds within the BC strand region of FcϵRI D1, also binds to this chimera. Thus, on the basis that the D2 mAb 47 and D1 mAb 54 bind the receptor, and the loss of the mAb 15-1 epitope, the effect of the ϵ(A'Bγ)ϵγ mutation on IgE binding is related directly to an impact of the D1/D2 interface on the IgE binding site.

Identification of crucial residues within the D1 interface of FcϵRI-α—To define further the role of the inter-domain interface, two residues of the A' strand FcϵRI, Arg 15 and Phe 17, that have substantial interactions within the interface, were mutated to alanine (R15A and F17A). In addition, Asn 14, with backbone-backbone interactions across the interface was mutated, also to alanine. Both the R15A and F17A mutants were recognised by mAb 47, and also by two mAbs with epitopes in FcϵRI D1, mAb 54 and mAb 3B4 (Table 3.III), and neither R15A nor F17A were detected by mAb 15-1 the hIgE binding site specific antibody 15-1. Both point mutants displayed a dramatic reduction in IgE binding, implying these mutants had altered IgE binding characteristics. The R15A mutant failed to bind monomeric mouse (data not shown) or hIgE, or moIgE complexes (Table 3.II). However the second point mutant, F17A, was able to bind moIgE complexes, but showed a substantial reduction in affinity when binding monomeric hIgE (Table 3.II).

The alanine mutants were modelled and compared with the homology model of FcϵRI to determine the possible effects of mutation. In the FcϵRI model, Arg 15 extends outward toward solvent whereas in the FcγRII crystal structure (FcγRII, Asn 15) it is constrained within the interface and oriented more toward D2. Asn 15 also forms an H-bond with the Leu 90 backbone carbonyl in the FcγRII crystal structure. No such H-bond is formed in the FcϵRI model with the distance between Leu 90:c and Arg 15:cγ being 4.75Å. Arg 15 participates in hydrophobic (van der Waals) contacts with Leu 89, Phe 84 and Leu 165 (Figures 3.3 and 3.4) in both the X-ray structure (8) as well as the model, but the interactions with Leu165 are lost while those with Phe 84 are severely reduced in the R15A mutant model structure. Furthermore, in the FcϵRI model, the Glu 82 carboxylate is parallel to the guanidinium of Arg 15, and the Arg 15:cζ and Glu 82:cδ are 4.2Å apart. If Arg 15 and Glu 82 exist in ionised forms in FcϵRI, this would lead to substantial loss of

Figure 3.4 Two dimensional depiction of the domain 1/domain 2 interface displaying distances of interactions between amino acids.

The core amino acids Asn 14, Arg 15, Ile 16 and Phe 17 are shown in *blue*, amino acids hydrogen bonded with the core amino acids are shown in *brown* with the bond length shown in *green*, and other amino acids involved in hydrophobic interactions with the core amino acids are labelled in *black* with a *red* ray. All hydrophobic interactions are displayed in *red* with the atom/s involved in contact/s shown in *black* with a *red* ray.

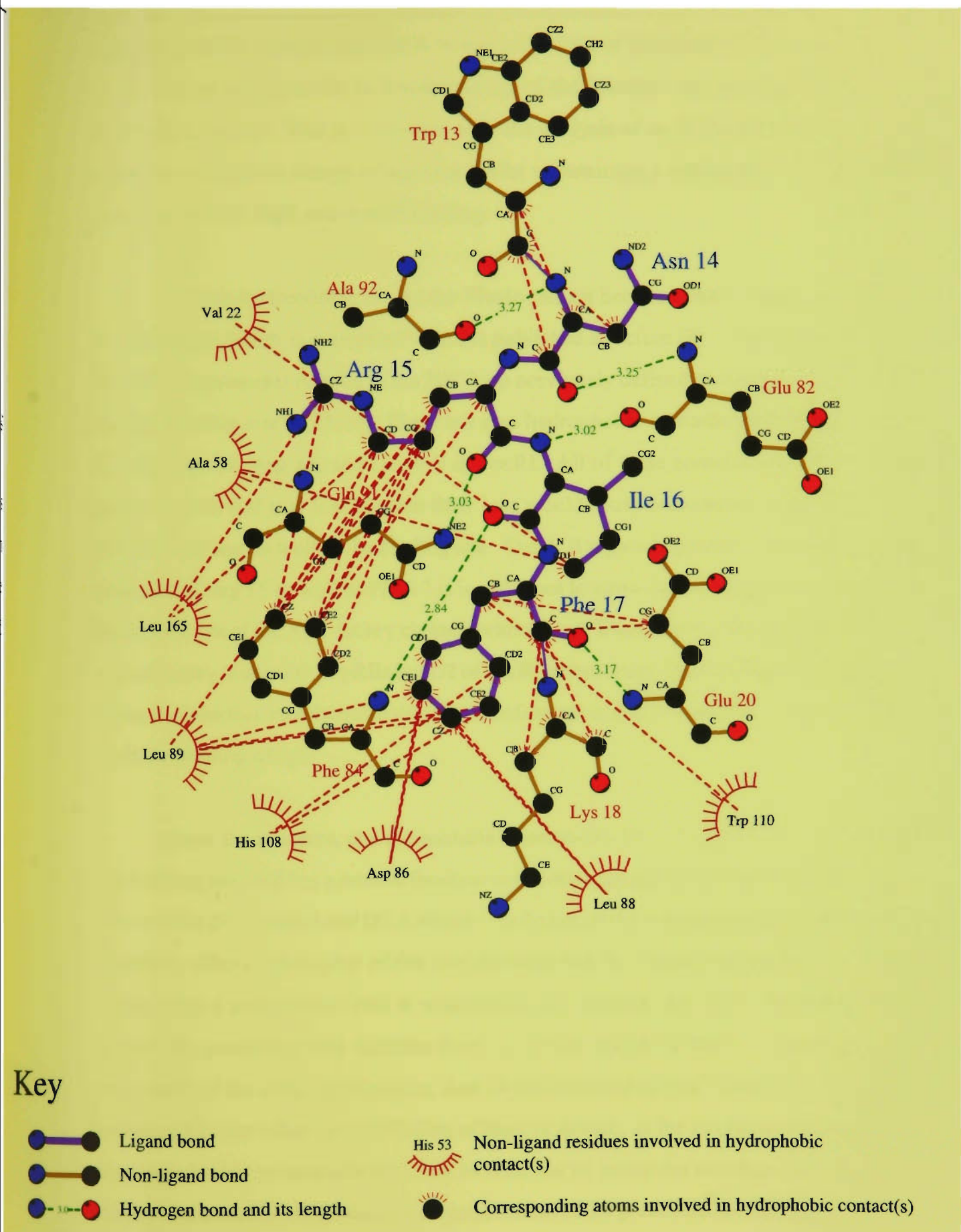
Trp 13
Asn 14
Ala 92
Val 22
Arg 15
Glu 82
Ala 58
Gln 9
Ile 16
Leu 165
Phe 17
Glu 20
Leu 89
Phe 84
Lys 18
Trp 110
His 108
Asp 86
Leu 88
3.27
3.25
3.02
3.03
2.84
3.17
Key
Ligand bond
Non-ligand bond
Hydrogen bond and its length
His 53
Non-ligand residues involved in hydrophobic contact(s)
Corresponding atoms involved in hydrophobic contact(s)

coulombic stabilisation in the R15A mutant. The loss of fundamental interactions in the R15A mutant would result in destabilisation of the interface and consequently the IgE binding site above. This is consistant with the analysis of an R15L point mutant which removes the positive charge of arginine whilst maintaining a similar size, and displays a total loss of both hIgE and moIgE binding.

There is hydrophobic or van der Waals contact between Phe 17 and Trp 110 in the FcεRI model, which is consistent with the published structure (8). This is significant as Trp 110 is a principal residue in the B/C loop previously defined as a major contributor to the IgE binding site (1,25,26). There are also hydrophobic contacts between Phe 17 and Leu 88, Leu 89, Asp 86, and His 108 in FcεRI. All of these contacts are lacking in the F17A mutant, and it is feasible that their loss would cause considerable distortion of the D1/D2 interface, as well as the binding site. The A'B region is sensitive to change, and the presence of Arg 15 as well as Phe 17 is insufficient to allow IgE binding. This is indicated by the analysis of the γ(A'Bε)εγ chimera where the A'B sequence of FcεRI (NRIFKGEN) placed in γεγ, that is D1 FcγRIIa but D2 of FcεRI, surprisingly failed to bind IgE (Table 3.I). Thus, the interface clearly maintains a series of complex interactions that work collectively to allow binding of IgE.

From the structure, and the contacts listed above, Phe 17 appears to lie beneath the IgE binding site, and has a critical function in maintaining organisation of the linker region between the D1 G strand and D2 A strand. The linker, at the membrane distal portion of the interface, effects the display of the two domains and the ligand binding region. Arg 15, which plays a more crucial role in maintaining IgE binding, lies closer to the membrane. To test the possibility that distance from the linker may be a factor in determining the magnitude of the effect of mutation, Asn 14 was mutated to Ala (Table 3.II). The N14A mutation has less effect on the binding of hIgE or moIgE, as the FcεRI model suggests by the single backbone interaction of Asn 14 with Ala 92 across the interface. The analysis of these point mutants would imply that maintenance of the presentation of the ligand binding site in FcεRI is dependent upon the structure of the D1/D2 interface which lies below the binding site, and that Arg 15 and Phe 17 are critical residues in this interaction.

Is Arg 15 a contact residue involved in IgE binding?— The loss of binding by the ϵ(A'Bγ)ϵγ chimera and the R15A and R15L point mutants, could also suggest a possible hIgE contact role for the Arg 15 residue. However it is more probable that Arg 15 is not a contact residue because firstly, it is distant from the ligand binding region which is exposed to solvent on the superficial surface of the receptor (Figure 3.1). Secondly, peptide inhibition (11) and mutagenesis analysis (23) have separately placed the mAb 15-1 epitope close to the IgE binding site, and mutations within, or expressed within, the D1/D2 interface have caused loss of binding of both IgE and mAb 15-1 independently (23). This would confirm that the D1/D2 interface is structurally important in the presentation of the IgE binding site, and mutations within the interface are sufficient to destroy the structure of this region. Thus, the exchange to alanine causes distortion of the receptor, and not necessarily removal of a critical binding residue. Thirdly, the complete first domain of FcγRIIa can be substituted for the first domain of FcϵRI (which replaces Arg 15 with Asn) while maintaining IgE binding, although with a twofold loss of apparent affinity.

Substitution of the complete first domain of FcγRIIIA for the first domain of FcϵRI maintains the Arg 15 residue, and this chimera retains the ability to bind both human and mouse IgE with an equivalent affinity to that of the 'wild-type' receptor (4). The presence of the entire FcγRIIa D1 may stabilise the interface region in the γϵγ chimera, and compensate to some extent for the loss of the Arg 15 residue.

The presence or absence of this critical Arg 15 residue may also resolve previously unexplained discrepancies between studies using FcγRIIIA D1/FcϵRI D2 and FcγRIIa D1/FcϵRI D2 chimeras.

A recently reported S162A mutant in FcϵRI D2 (23) causes destruction of IgE binding. Ser 162 is highly conserved within Fc receptors, and in the FcϵRI homology model Ser 162 interacts with Leu 89 of the D2 A strand, which in turn interacts with Arg 15 of the D1 A' strand (Figures 3.3 and 3.4). The Arg 15 residue has been shown above to be of importance in maintaining the D1/D2 interface, and thus it is possible that the ablation of ligand binding is caused by changes in this linkage. The ability of a point mutation distant from the IgE binding site to effect sufficient distortion of the receptor to destroy IgE

binding, further defines the importance and sensitivity of the D1/D2 interface structure in relation to IgE binding.

The A and G strands of D1 FcεRI play a critical supportive role in the maintenance of the D1/D2 interface— Chimeras containing either the A strand (γ(Aε)εRIII) or G strand (γ(Gε)εγ) alone of D1 FcεRI-α in the γεγ template chimera, were expressed, bound moIgE with an avidity similar to that of εεγ, and showed a small but reproducible increase in affinity for hIgE compared with γεγ (Table 3.II). Thus, although the high affinity of the 'wild-type' εεγ receptor was not totally restored by these chimeras, the increase in affinity would suggest a foundation role in the presentation of the IgE binding site.

In the case of the A strand, this role is most likely to be the structural support of the interface. The N-terminus of the A strand, and indeed the epsilon receptor, is probably located close to the cell membrane. The A strand interacts with other residues within D1 via hydrogen bonds, both in backbone interactions with the B strand and Asn 74 of the FG loop. Conformation of the A strand would assist the display of the A' strand in the interface so that crucial residues, such as Arg 15 and Phe 17, are appropriately presented.

The G strand of domain 1 abuts domain 2 directly via the G strand - A strand linker, and across the D1/D2 interface; it is also involved in interactions with the A' strand within D1. The G strand of D1 is highly conserved between FcεRI and FcγRIIa, with few differences between the interactions of the conserved amino acids. It is therefore surprising that introducing the G strand of FcεRI into the γεγ chimera is reflected in alterations to IgE binding. The residues in the G strand that are not conserved between FcεRI and FcγRIIa, may contribute specifically to IgE binding affinity. Glu 82 and Phe 84 interact with D1 A' strand residues Asn 14, Ile 16 and Arg 15, and Asp 86 with Phe 17; these latter two interactions are with residues shown above to be critical in maintaining the D1/D2 interface. It is therefore probable that interactions of the A and G strands as well as the A' strand of D1 effect a role in maintaining the interface between D1 and D2, and therefore, an indirect affect on IgE binding.

In both the FcεRI model and FcγRIIa structure, Trp 87 at the D1/D2 junction interacts with Trp110, which is contained within the BC loop of D2, a crucial IgE binding region (1,26). Residues adjacent to Trp 110, (Arg 106 and His 108), also interact with amino acids of the D1/D2 interface, the A' strand of D1 and the A strand D2, thus maintaining links between the interface and the IgE binding region. The conservation of these residues within the FcR probably contributes to the ability to substitute the D1 of FcγRIIa or FcγRIII, for the D1 of FcεRI, and retain IgE binding.

The homology model of FcεRI— A homology model of FcεRI (Figure 3.1), based on the recently solved structure of FcγRIIa (6) was employed to determine the structural basis of alterations in IgE binding by the FcεRI-α chimeras. The two structures are, therefore, very similar with some small variation at the point of sequence disparity in the region of the C'E loop of D1 (Table 3.I). The pattern of β strands is the same in both FcγRIIa and the FcεRI-α homology model, (as stated in Experimental Procedures), however the arrangement of the loops appears to depend more on the positioning of amino acids such as proline in FcγRIIa, whereas in FcεRI-α there are supplementary interactions between amino acids to preserve the loop structure. In this model of FcεRI-α, one face of the molecular surface, largely comprising the juxtaposed C/F/G strands of each domain has an overwhelmingly negative electrostatic potential (Figure 3.2), unlike the opposite face of the molecule. This marked disparity in the electrostatic potential between the two faces is not observed in the case of the FcγRIIa molecule (results not shown), and may be of biological significance. The negative surface of FcεRI-α would tend to sit away from the cell membrane, and as a consequence maintain the binding sites in a membrane distal position, on the 'upper' surface of the molecule. This supports the cell surface data (detailed in 12, 24, 25) asserting that the domains are aligned with the membrane along the long axis as shown in Figure 3.1, and do not project vertically from the membrane. The γεγ chimera (see Material and Methods) was also modelled and, as expected, was shown to have a similar structure to FcγRIIa, and the FcεRI-α homology model.

The FcεRI-α homology model has the features described for the x-ray crystallographic structure of Garman and co-workers (8). First, all the N-linked glycosylation sites, including the three described in the crystal structure, are solvent

exposed. Second, the interchain hydrogen bonds correlate well with those disclosed in Figure 1D of the published FcεRI structure. Third, the two domains are bent relative to each other and the model has an interdomain angle of 52^0 which is similar to that depicted by Garman *et al.* (8). Fourth, the IgE binding loops of domain 2 defined by Hulett *et al.* (1,26) are in close proximity, distal to the membrane and exposed to solvent.

By utilising the FcεRI-α homology model and the models of the chimeras and mutants, the authenticity of the interactions within the D1/D2 interface and the effects of the mutations on IgE binding could be defined with greater precision and fidelity. In conclusion, this data suggests that the second domain of FcεRI-α is the only domain involved in direct contact with the IgE ligand, and that domain one has a structural function of great importance in maintaining the validity of the domain interface and through it, the ligand binding site.

REFERENCES

1 Hulett, M.D., McKenzie, I.F.C., and Hogarth, P.M. (1993) *Eur. J. Immunol.* **23**, 640-645.

2 Robertson, M.W. (1993) *J. Biol. Chem.* **268**(17), 12736-12743.

3 Scarselli, E., Esposito, G., and Traboni, C. (1993) *FEBS Let.* **329**, 223-226.

4 Mallamaci, M.A., Chizzonite, R., Griffin, M., Nettleton, M., Hakimi, J., Tsien W-H. and Kochan, J.P. (1993) *J. Biol. Chem.* **268**(29), 22076-22083.

5 Cook, J.P., Henry, A.J., McDonnell, J.M., Owens, R.J., Sutton, B.J., and Gould, H.J. (1997) *Biochemistry* **36**(50), 15579-15588.

6 Maxwell K.F., Powell M.S., Hulett M.D., Barton P.A., McKenzie I.F.C., Garrett T.P.J., and Hogarth P.M. (1999) *Nat. Struct. Biol.* **6**(5), 437-442.

7 Sondermann, P., Huber, R., and Jacob U. (1999) *EMBO J.* **18**(5),1095-1103.

8 Garman, S.C., Kinet, J.-P., and Jardetzky, T.S., (1998) *Cell* **95**, 951-961

9 Hogarth, P.M., Ierino, F.L., and Hulett, M.D. (1994) *Immunomethods* **4**, 17-24.

10 Sambrook, J., Fritsch, E.F., and Maniatis, T. (1989) *Molecular Cloning: A Laboratory Manual*, 2nd Ed., Cold Spring Harbor Laboratory, Cold Spring Harbor, NY.

11 Rigby LJ, Trist H, Epa VC, Snider J, Hulett MD and PM Hogarth. (2000) *Allergy* **55**, 609-619.

12 Sutton, B.J., and Gould, H.J. (1993) *Nature* **366**, 421-428.

13 Hogarth, P.M., Hulett, M.D., Ierino, F.L., Tate, B., Powell, M.S., and Brinkworth, R.I., (1992) *Immunol. Rev.* **125**, 21-35.

14 Sali, A., and Blundell, T.L., (1993) *J. Mol. Biol.* **234**, 779-815.

15 Sippl, M. (1993) *Proteins* 17, 355-362.

16 Bowie, J.U., Luthy, R., and Eisenberg, D. (1991) *Science* **253**, 164-170.

17 Laskowski, R.A., MacArthur, M.W., Moss, D.S., and Thornton, J.M. (1993) *J. Appl. Cryst.* **26**, 283-291.

18 Rost, B., Sander, C., and Schneider, R. (1994) *CABIOS* **10**, 266-275.

19 Frishman, D., and Argos, P. (1997) *Proteins* **27**, 329-335.

20 Nicholls, A., Sharp, K.A., and Honig, B. (1991) *Proteins: Struct. Funct. Gent.* **11**,281-296.

21 Sitkoff, D., Sharp, K.A., and Honig, B. (1994) *J. Phys. Chem.* **98**,1978-1988.

22 Wang, B., Rieger, A., Kilgus, O., Ochiai, K., Maurer, D., Födinger, D., Kinet, J.-P., and Stingl, G. (1992) *J. Exp. Med.* **175**,1353-1358.

23 Nechansky, A., Aschauer, H., and Kricek, F. (1998) *FEBS letters*. **441**,225-230.

24 Beavil, A.J., Beavil, R.L., Chan, C.M.W., Cook, J.P.D., Gould, H.J., Henry, A.J., Owens, R.J., Shi, J., Sutton, B.J., and Young, R.J. (1993) *Biochem. Soc. Trans.* **21**(4),968-972.

25 Rigby, A.J., Hulett, M.D., Brinkworth, R.I., and Hogarth, P.M. (1996) *IgE Receptor (FcεRI) Function in Mast Cells and Basophils*. R.G.Landes Company. (Molecular Biology Intelligence Unit) 7-32.

26 Hulett, M.D., Brinkworth, R.I., McKenzie, I.F.C., and Hogarth, P.M. (1999) *J. Biol. Chem.* **274**(19),13345-13352.

CHAPTER FOUR:

The membrane anchor of chimeric FcεRI modifies cell surface expression and ligand binding.

SUMMARY

The importance of the nature of the membrane anchorage of FcεRI in ligand binding was investigated using chimeric FcεRI receptors. Previous investigations (reviewed in Chapter 4), involving the binding of ligand to chimeric FcεRI receptors, were conducted utilising the cytoplasmic anchors of related molecules (FcγRIIa or the p55 subunit of IL-2) in combination with the ectodomains of FcεRI-α to enable cell surface expression and negate the necessity for cotransfection of the FcεRI γ chain which is an absolute requirement for expression of the α chain. In this chapter, the FcγRIIa cytoplasmic anchor of a series of chimeric receptors were replaced with the glycosyl phosphatidylinositol (GPI) membrane anchor of FcγRIIIb, and, in one case, that of the complement regulating protein - decay-accelerating factor (DAF). The chimeric constructs were transiently transfected into COS-7 cells, and cell surface expression of chimeric receptors was determined by EA-rosetting and flow cytometry. The GPI chimeras were also assayed for their apparent affinity for IgE by equilibrium binding, both when attached to the cell surface and in a soluble form released from the cell surface following treatment with PIPLC.

In the studies I describe here, a novel method for the determination of ligand binding was developed using surface plasmon resonance (SPR). It has not previously been possible to test FcεRI-α or FcεRI chimeric receptors by SPR with the IgE ligand immobilised on the SPR chip as the IgE is inactived when immobilised by the approaches used to date. It was determined that (i), each of the GPI-anchored proteins displayed a higher level of cell surface expression than its polypeptide anchored counterpart (ii), that the GPI anchored receptors could be released from the cell surface by the action of phosphoinositol phospholipase C (PIPLC); and (iii), that the soluble εεRIII receptor (comprising the extracellular domains of FcεRI-α and GPI anchor of FcgRIIIb) released from the cell following treatment could be detected by SPR when binding IgE. However, insufficient quantities and unknown concentrations of soluble receptor rendered the system unable to produce association and dissociation kinetics data for the PIPLC released chimeras; however, refinement and quantitation of the receptor concentration of active PIPLC released GPI anchored receptors, provided a simple and rapid method to determine association and dissociation kinetics of FcR and other cell membrane receptors.

INTRODUCTION

This chapter follows the format of Chapter 3 and that of the Journal of Biological Chemistry, additional information on materials, recipes and methods will be given in Appendix III.

FcεRI, the high affinity receptor for IgE, comprises a ligand binding alpha chain of two Ig-like domains, a beta chain involved in the amplification of cell signalling, and two gamma subunits presented at the cell surface as a disulphide bonded homodimer; the presence of the gamma subunits are crucial for the cell surface expression of the receptor. Although the second (membrane proximal) Ig-like domain contains the IgE binding site, the first domain is required for high affinity binding (Chapter 3 and reviewed in Chapter 1 and references therein). Results from analyses of other receptors, such as FcγRI and FcγRIII (1, 2, 3), suggest that the membrane spanning region can influence the binding affinity, thus, in the study described here, the nature of the anchorage of FcεRI-α in the membrane, via either a polypeptide or lipid (GPI) membrane anchor was investigated.

The discovery of a variation in ligand binding between paired chimeras with either a polypeptide or lipid membrane anchor, led to testing the extracellular domains for their ability to bind ligand when in a soluble form. However, no system was available for testing small volumes of soluble FcεRI in a ligand binding assay to enable a comparison of the association and dissociation kinetics of the receptors. The cell surface expressed GPI anchored receptors were tested for their ability to be released from the membrane with phosphoinositol phospholipase C (see below).

Suface plasmon resonance (SPR) has become an important tool in the determination of interrelationships and affinities of protein:protein interactions, as it is rapid, sensitive and quantitative. One application of SPR has been its use in the determination of interactions between receptors and their ligands (references 4-8). Either purified ligand or receptor protein is immobilised to the surface of an SPR chip, the receptor/ligand counterpart is then passed, in fluid phase, over the immobilised protein and the interaction recorded. The fluid phase in the procedure, in this case protein, is not required to be purified.

SPR has been used previously to determine FcεRI : IgE interactions with purified receptor coupled to the SPR chip. However when ligand was coupled to the chip and receptor delivered in the fluid phase, no interaction occurred. Several researchers have found that IgE becomes inactivated when coupled directly to an SPR chip (B. Sutton, Randall Institute, London, personal communication; M. Powell and H. Trist, A.R.I., Melbourne, Australia, personal communications).

The work presented here is a *novel* method for the determination of FcεRI : IgE interactions by SPR, which is able to investigate the FcεRI : IgE interactions with the IgE immobilised. This method uses a high affinity antigen : antibody interaction, not chemical coupling, to orient the IgE. The 4-hydroxy-nitrophenolacetyl (NP) hapten is coupled to the SPR chip, and, utilising the high affinity of IgE anti-NP for the NP hapten, the IgE anti-NP becomes immobilised on the SPR chip; it is oriented with the Fab portion toward the chip, and the Fc region, containing the receptor binding site, presented into the receptor flowpath.

Review of the glycosyl-phospatidylinositol (GPI) membrane anchor.

The lipid modification of proteins has been noted since the early eighties, with the reported attachment of the protein, alkaline phosphatase, to the membrane via phosphatidylinositol in 1980 (9) and that of FcγRIII recognised in 1988 (10, 11, 12).

The glycosyl-phosphatidylinositol moiety is formed and stored attached to the internal surface of the endoplasmic reticulum until required for the post-translational modification of the target protein. A modification signal is necessary in the target protein and this is usually an amino acid with a small aliphatic group (e.g.serine) known as a signal amino acid, located toward the c-terminus of the protein, followed by a short length of hydrophilic amino acids, and then a region of hydrophobic amino acids. There are exceptions to this, for example, the modification signal amino acid of DAF is contained within the extracellular region of the protein (13).

The hydrophobic region on the carboxyl side of the signal amino acid is believed to play a transitory role in anchoring the protein to the membrane of the endoplasmic

reticulum until a rapid GPI modification occurs in a transamidase reaction. The attachment of the GPI anchor occurs at the signal amino acid, and this then becomes the c-terminal amino acid of the mature protein. The removed peptide sequence is broken down.

At a molecular level, the point of the GPI anchor attachment is a covalent bond between the signal/terminal amino acid and an ethanolamine molecule. The ethanolamine is connected to a phosphate residue that is then attached to three mannose molecules in series. A glucosamine connects the final carbohydrate to an inositol, and the anchor terminates with a second phosphate group and two lipid molecules. The latter anchor the molecule into the phospholipid bilayer of the membrane. The GPI-anchored protein is then transported to the membrane (Figure 4.1). The protein molecule can be released from its anchor, and therefore the membrane, by the activity of GPI specific enzymes. Phosphoinositol phospholipase C (PI PL-C) is a bacterial product capable of catalysing cleavage of the GPI anchor between the phosphate group and the lipids (Figure 4.1).

Analysis of binding in cell-free systems allows rapid and accurate assessment of receptor : Ig interaction. Therefore, creating receptors with GPI anchors, for rapid expression, production of soluble receptors, and identification of their binding characteristics, would be a significant advance on present, conventional systems.

This chapter will address, (i), the effect of the membrane anchor on ligand binding, (ii), the development of an orientation dependent binding assay, and (iii), the evaluation of a rapid expression/recovery system for analysis of receptor/ligand interaction by surface plasmon resonance.

Figure 4.1 Diagrammatic representation of the structure of the glycosyl phosphatidyl inositol (GPI) membrane anchor.

The ethanolamine of the GPI anchor proximal to the protein is attached to the protein at the signal amino acid. The arrows between the phosphatidylinositol phosphate group and the lipid membrane anchor indicate the region where the enzyme phosphatidylinositol phospholipase C (PIPL-C) is active. Activity of PIPL-C causes a break in the chemical bonding between the lipid membrane anchor and the phosphatidylinositol moiety, and causes release of the protein from the cell membrane as shown.

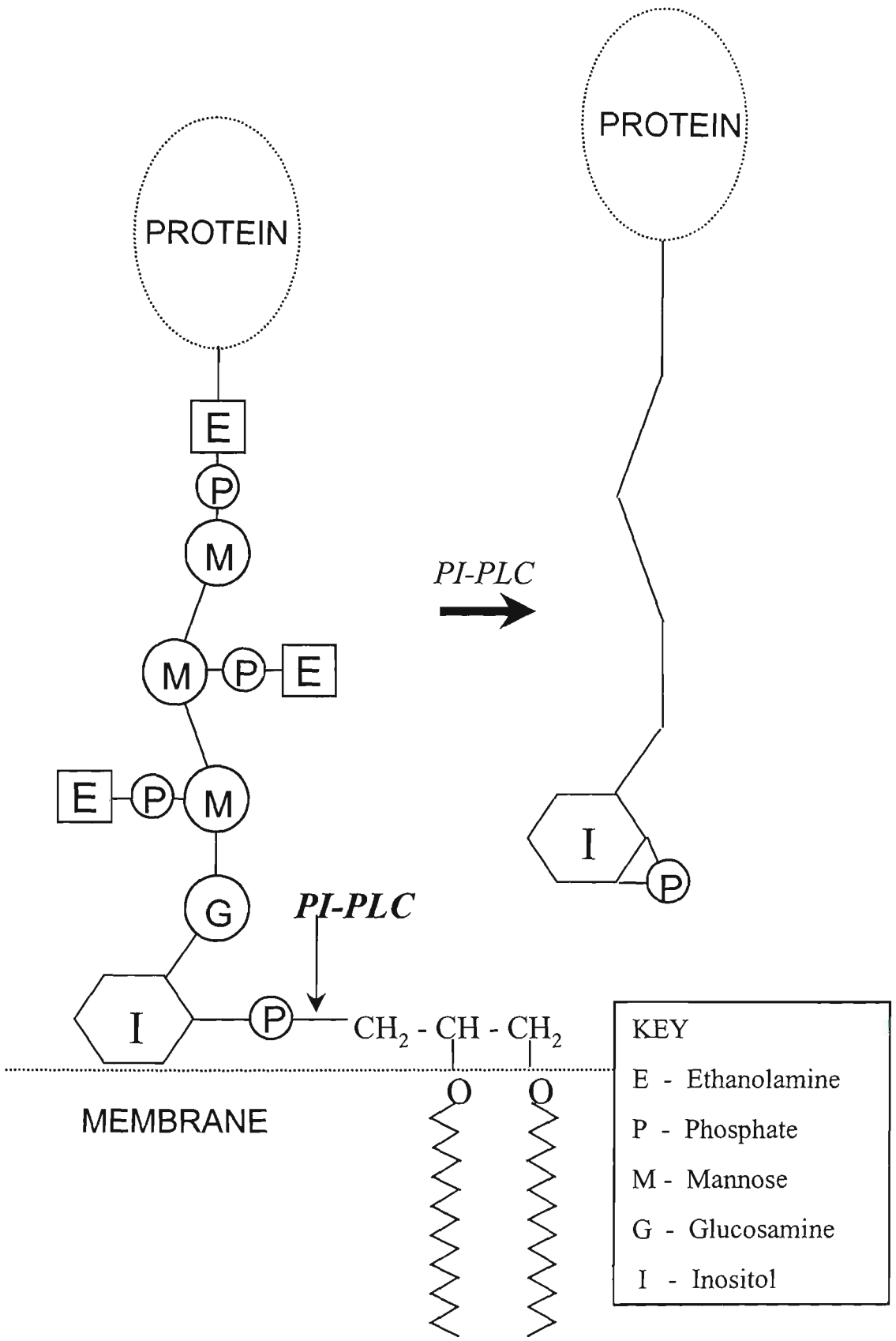
PROTEIN
PROTEIN
E
P
M
M
P
E
E
P
M
G
I
P
CH2 - CH - CH2
O
O
MEMBRANE
PI-PLC
PI-PLC
I
P
KEY
E - Ethanolamine
P - Phosphate
M - Mannose
G - Glucosamine
I - Inositol

EXPERIMENTAL PROCEDURES

Production of FcεRI-α chimeric cDNA receptor constructs with transmembrane peptide anchors— Two previously produced chimeric cDNA receptor constructs (14) were used in the experiments described. The first, designated **εεγ,** comprised D1 and D2 of FcεRI-α linked with the transmembrane region and cytoplasmic membrane anchor of FcγRIIa. Design of the second chimeric receptor was based on a simple domain exchange, and comprised D1 of FcγRIIa and D2 FcεRI-α, also with the transmembrane region and cytoplasmic membrane anchor of FcγRIIa, and was designated **γεγ**. All constructs were produced using splice overlap extension - polymerase chain reaction (SOE-PCR) per the method previously reported by Hogarth *et al.* (15, and Chapter 3).

Production of FcεRI-α chimeric cDNA carrying a codon for the amino acid attachment point for glycosyl phosphatidyl inositol membrane anchors— Template receptors were constructed such that they would carry a glycosyl phosphatidyl inositol (GPI) membrane anchor site to replace the cytoplasmic membrane anchor of the original constructs (Figure 4.2). The initial GPI anchored receptor construct (εεRIII) was used as a template and comprised FcεRI D1 and D2, with the FcγRIIa membrane proximal region of the parental receptor (εεγ), and the GPI anchor of FcγRIIIB replacing the cytoplasmic tail of FcγRIIa; this chimera was designated εεRIII. εεRIII was generated using splice overlap extension - polymerase chain reaction (SOE-PCR), using the oligonucleotide primers as shown in Table 4.I.

The construction of FcεRI with a GPI anchor derived from FcγRIIIb involved several steps. FcγRIIIa cDNA was available but FcγRIIIb cDNA was not. However, FcγRIIIa and b differ in this region by a single amino acid (Phe 182 in FcγRIIIa and Ser 182 in FcγRIIIb) that determines peptide or GPI membrane anchorage (16, 17), and by the position of the stop codon (position 235 in FcγRIIIa and 214 in FcgRIIIb) (see Appendix 1.4). Thus, FcγRIIIa was used as a template, and these variations were incorporated into the splice overlap oligonucleotides (Table 4.1). Thus, the initial reaction, to amplify the extracellular FcεRI domains from the εεγ cDNA, used a 5' primer that carried an *Eco*RI restriction enzyme site (EG6). The 3' antisense oligonucleotide primer for this reaction

Figure 4.2 Diagrams indicating the protein and glycosyl phosphatidylinositol membrane anchorage of the chimeric FcεRI receptors.

a. Depicts the position of the glycoprotein FcεRI receptors on the cell surface with either a cytoplasmic peptide anchor or the glycosyl phosphatidyl inositol (GPI) membrane anchor.

b. Shows an enlargement of the membrane proximal region of the protein indicating the possible position of the signal amino acid which initiates attachment of the GPI membrane anchor.

a

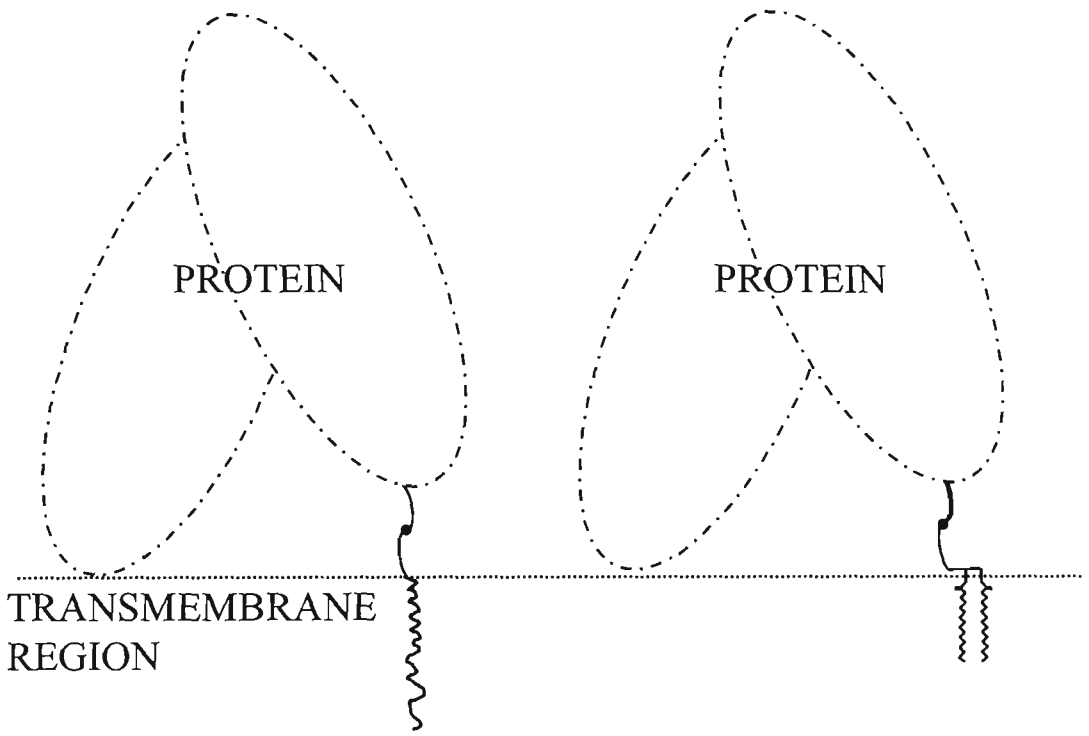
PROTEIN
PROTEIN
TRANSMEMBRANE
REGION

b

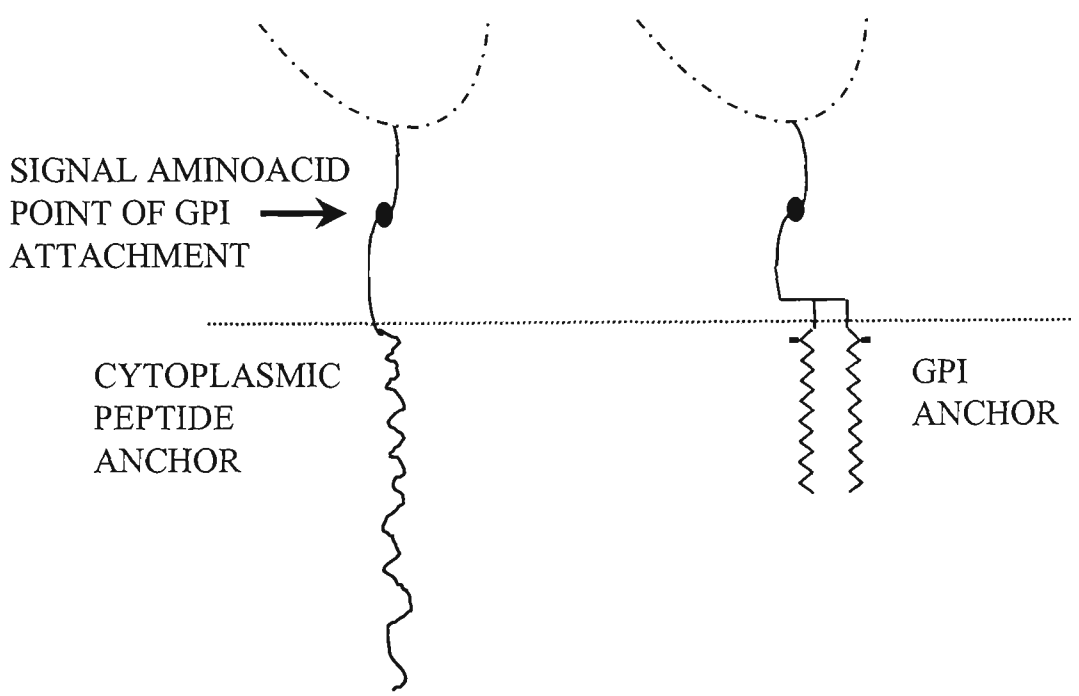
SIGNAL AMINOACID
POINT OF GPI
ATTACHMENT
CYTOPLASMIC
PEPTIDE
ANCHOR
GPI
ANCHOR

Table 4.1. SEQUENCES OF OLIGONUCLEOTIDES USED TO CONSTRUCT CHIMERIC FcR cDNAs.

Mutant	Name[a] of oligo. and template		Sequence of oligonucleotide 5'-3' [b]	cDNA Nucleotide Position[c]
γRIII D1,εD2	GE 02	γRIII	G CAG CCA *GCC GAT ATG GAC TTC TAG*[c]	ε265-271, γIII 247-264.
	GE 03	εεRIII	*CAT ATC GGC* TGG CTG CTC CTT CAG G	γIII 256-264, ε265-280.
εD2, γRII TM,	LR 24	εεγ/γεγ	*G AGA GAA TGA TGA GAT* **TGAAGA** GCC CAT GCT GGG CAC TTG	γIII 610-598, γ639-613.
γRIII GPI	**LR 25**	FcγRIIIB	**TCTTCA** *ACT TCA TCA TTC TCT CCA CCT G*	γ621-639, γIII 598-616.
εD2, DAF GPI	LR 30	εεγ	GT TCC ATG AAA ATG CTT TAC AGT AAT GGT GAG GG	DAF 1028-1012, γ510-494.
	LR 31	DAF	CC CTC ACC ATT ACT GTA AAG CAT TTT CAT GAA AC	γ494-510, DAF 1012-1028.
ϵRI D1	**EG 6**		TTT**GAATTC** AGC ACA GTA AGC ACC	ε 5' untranslated
γRII D1	**NR 1**		TAC**GAATTC** CA ACT, ATG GAG ACC CAA ATG TCT C	γ-5 -19.
γRIII D1	**EG 01**		TTT**GAATTC** GTC CAC TCC AGT GTG G	γIII 5' untranslated
γRII CR	EG 5		TTT**GTCGAC** CAC ATG GCA TAA C	γ 3' untranslated
γRIII GPI	LR26		GCAA**GTCGAC** TCA *AAT GTT TGT CTT CAC AGA G*	γIII 702-684.
DAF GPI	LR 32		CTTCTTA **GTCGAC** CTTTGG CTA AGT CAG CAA GCC	DAF 1146-1126

a Oligonucleotide names in bold type and underlined are for sense/forward primers, those not underlined are anti-sense/reverse primers.

b Portions of oligonucleotides containing sequence complementary to cDNA of :- FcεRIα are underlined (ε), FcγRIIa are not underlined (γ), FcγRIII are italicised (γIII) and DAF are double underlined. Restriction enzyme sites are shown in bold type and labelled.

c Nucleotide positions refer to nucleotide sequences of appropriate cDNAs.

D = domain. TM = Transmembrane. CR = Cytoplasmic region. GPI = Glycosyl phosphatidyl inositol membrane anchor.

(LR25) also coded for part of the FcγRIIa membrane-proximal region. A second reaction to amplify the FcγRIIIb membrane-proximal and GPI attachment regions, incorporated Ser 182 in the sense oligonucleotide primer (LR24), and the antisense primer (LR 26) encoded the stop codon of FcγRIIIb and incorporated a *SalI* restriction site. PCR products were purified by electrophoresis in agarose gels, and resuspended at an approximate concentration of 25 ng/μl. A third PCR reaction using the 5' oligonucleotide from the first reaction, and the 3' oligonucleotide from the second reaction spliced the two fragments of DNA together forming a full length chimeric cDNA containing the FcεRI-α with the membrane-proximal region and GPI signal peptide of FcγRIIIb; this receptor was designated εεRIII. The same template receptor (εεγ) was used to construct a second GPI anchored receptor, with FcεRI D1 and D2 and the transmembrane region and GPI anchor of Decay Accelerating Factor (DAF), generously provided by Dr Bruce Loveland (A.R.I., Melbourne, Australia); this receptor was designated εεDAF. The εεDAF construct was produced in a similar manner to εεRIII with oligonucleotides as stated in Table 4.I.

The RIIIεRIII chimera was also generated by SOE-PCR using FcγRIII and εεRIII as templates, with oligonucleotides GE03 and GE02 (Table 4.I) designed to enable a direct domain one exchange. Each of the PCRs were performed on 50 ng of cDNA, with 200 ng of each oligonucleotide primer, in a buffered solution 10 mMTris-Cl pH 8.3, 50 mM KCl, 1.5 mM $MgCl_2$ with 2.5 units Taq Polymerase (Becton Dickson) for 25 cycles of amplification.

Other chimeric constructs were generated with the GPI anchor of FcγRIIIa. This was performed by cutting the template GPI anchored construct εεRIII, with the restriction enzymes *Hind*III (in the vector multiple cloning site, N-terminus of construct) and *Stu*I (in D2 FcεRI), with the addition of Arctic Shrimp Alkaline Phosphatase. The cut εεRIII+vector cDNA was purified by electrophoresis in an agarose gel. The chimeric receptors γεγ and γ(Gε)εγ were also cut with *Hind*III and *Stu*I to release the complete chimeric D1 cDNA which was purified away from the vector by electrophoresis in an agarose gel. The two sections of the chimeric cDNA construct were ligated together (NEB Ligase and Ligation buffer) and transformed into competent *E.coli* Top 10 F' bacteria.

cDNA was purified by centrifugation in a CsCl gradient (18) or using a Wizard DNA Purification System (Promega, Madison, WI) and the constructs sequenced in total using the ABI Dye Terminator reaction kit with the automatic ABI Prism 377 DNA sequencer (Perkin Elmer).

Transfection of mammalian cells

(i) Transfection of mammalian cells for EA-rosetting— Cells of a simian renal fibroblast cell line (COS-7) were maintained (37^{0}C, 10% CO_2) in Dulbecco's modified Eagles medium (DMEM) (Gibco BRL, Life Technologies Inc., Gaithersburg, MD) with 2 mM Glutamine, 100 U/ml penicillin, 100 µg/ml streptomycin (Commonwealth Serum Laboratories, Australia), and 10% heat-inactivated foetal calf serum (CSL).

COS-7 cells were seeded in 6 well (5 cm^2) plates (Costar), and were transfected the following day at 30% confluence. For transient transfection Lipofectamine (Life Technologies Inc) reagent (9 µl) and cDNA (2 µg) were combined according to the manufacturer's instructions in 1ml serum free DMEM (CSL Biosciences) containing 2 mM glutamine (CSL), and incubated with the cell monolayer (37^{0}C, 10% CO_2) overnight. The medium was replaced after 18 hours with DMEM containing 2 mM glutamine, 100 U/ml penicillin, 100 mg/ml streptomycin and 10% heat inactivated foetal calf serum, and the cells tested for expression 36-48 hrs later.

(ii) Transfection of mammalian cells for equilibrium binding assay— COS-7 cells were seeded in 100 mm diameter tissue culture dishes (Corning 25020), and transfected the following day at 40-50% confluence. Lipofectamine (Life Technologies Inc) reagent 9 µg/ml and cDNA 2 µg/ml were combined as above in 4 ml serum-free DMEM, incubated (37^{0}C, 10% CO_2) overnight, and the medium replaced after 18 hours.

(iii) Transfection of mammalian cells for flow cytometry— COS-7 cells, maintained as above, were seeded with 10^6 cells/ml in 75 mm^2 (250 ml) tissue culture flasks (Falcon) and transfected the following day at 40% confluence. Transient transfection utilised Lipofectamine (as above) or DEAE dextran. Briefly, DEAE dextran (Pharmacia, Sweden), Chloraquine diphosphate (Sigma C-6628) and 5 µg/ml cDNA in 5 ml serum free DMEM plus 2 mM Glutamine, 100 U/ml penicillin, 100 mg/ml streptomycin. The solution was

incubated on the cells at 37°C for 3-4 hours, and removed prior to the addition of 10% DMSO for 1 min. The flasks were washed twice in DMEM alone and the cells maintained in DMEM plus 2 mM Glutamine, 100 U/ml penicillin, 100 mg/ml streptomycin and 10% heat-inactivated FCS.

Immune Complex Binding— The binding of immune complexes to cells transfected with chimeric or mutant cDNAs was determined by erythrocyte-antibody (EA) rosetting. Sheep red blood cells (srbc) in Alsever's solution were washed four times in isotonic saline, and sensitised (20 min, 22°C) with phosphate buffered saline (pH 7.2) containing 0.05 M 2,4,6-trinitrobenzene-sulphonic acid (TNBS) (Fluka Chemika, Switzerland). TNBS sensitised srbc were washed three times in PBS containing 0.5% BSA, resuspended to approximately $1x10^8$ per ml in PBS containing 0.5% BSA plus 1/3000 dilution mouse monoclonal IgE anti-DNP ascites (19), and incubated (1 hr, 22°C). The erythrocyte-antibody complex (EA) was washed x3 in PBS containing 0.5% BSA, and 2 ml $2x10^8$ per ml EAs were added into each 5 cm^2 well of transfected COS-7 cells (10 min, 37°C). Gentle centrifugation of the plates (700 G, 3 min) was followed by incubation (30 min, 4°C) prior to careful removal of excess EAs. The transfected COS cells were then examined microscopically for EA rosette formation (i.e. the attachment of EA-IgE to the transiently transfected membrane bound FcεRI). Alternatively EA were prepared with IgG1 anti-TNP (20). The IgG1 anti-TNP hybridoma cell line (A3) was the kind gift of Dr A. Lopez (Institute of Medical and Veterinary Science, Adelaide, Australia).

Radiolabelling of IgE— IgE was radioiodinated using IODO-GEN® (Pierce). 5 µg of IODO-GEN® in 50 µl chloroform was dried in a 1.5 ml Eppendorf tube under nitrogen, sealed and stored desiccated at 4°C. The IODO-GEN coated tube was rinsed in PBS (0.1 M Phosphate buffered saline pH 7.2) before use. 20 µg of protein in PBS was added to the tube with 100-200 µCi $Na^{125}I$ (Amersham, England). The tube was incubated for two minutes at 20°C with intermittent agitation, before the contents were transferred to a PD-10 Sephadex G-25 column (Pharmacia, Uppsala, Sweden) to stop the reaction and separate the radiolabelled protein from free $Na^{125}I$. 500 µl aliquots were collected, and aliquots containing iodinated protein were pooled.

Measurement of IgE/FcεRI Interactions by Equilibrium Binding— COS-7 cells, were transiently transfected with cDNA of chimeric or template receptors, or irrelevant cDNA (mock). Cells were harvested 42-48 hrs after transfection, washed twice in PBS/0.5%BSA, and resuspended at $5x10^5$/ml in L15-0.5%BSA for the assay. ^{125}I IgE ligand was serially diluted in L15-0.5%BSA 50 µl per well, and incubated with 50 µl aliquots of cells (2 hr 4^0C). Post incubation, cells plus ligand were spun through 200 ml phthalate oils (40% bis (2-ethylhexyl) phthalate : 60% dibutyl phthalate) (Fluka Chemika, Switzerland), and the ^{125}I counts/min determined separately for the cell pellets (bound IgE) and the supernatant (free IgE) in a WALLAC 1470 WIZARD™ automatic gamma counter. Scatchard analysis was performed by plotting IgE bound / IgE free, over IgE bound, and determining the line of best fit by linear regression (y = a+bx). Non-linear regression analysis was performed using the program "Curve Expert", based on the formula for single site binding, y = (a*x)/(b+x); where y=IgE bound, and x=free IgE. The equilibrium binding dissociation constant (K_D) values obtained from three experiments had correlation coefficients of >0.99. The maximum binding (Bmax) of IgE was also determined and used to estimate the level of receptor surface expression.

Enzyme hydrolysis of chimeric receptors by PI-PLC— COS-7 cells maintained and transiently transfected as above were harvested 3 days post transfection. 10^7 cells were washed and resuspended in 10 mM Hepes, 150 mM NaCl, 3.4 mM EDTA pH 7.4 containing $8x10^{-3}$ U/ml phosphatidylinositol phospholipase C (PI-PLC) (Boehringer Mannheim Biochemica, Germany). A sample of cells was removed prior to the addition of the PI-PLC and analysed by flow cytometry for receptor expression.

Detection of membrane-bound FcεRI by monoclonal antibodies using Flow Cytometry— 25 µl volumes of saturating amounts of antibody either purified from ascites fluid, using a Protein G - HiTrap column (Pharmacia, Uppsala, Sweden), or serum free monoclonal antibody hybridoma supernatant (Hybridoma S/F GIBCO BRL, Life Technologies), were added to 25 µl of COS-7 cells transiently transfected with rFcεRI cDNA ($1.5x10^7$/ml) and incubated on ice for 45 min; washed, and incubated on ice for a further 30 min with 25 µl of a 1/100 dilution of anti-mouse Ig F(ab')$_2$-FITC (Silenus, Melbourne, Australia), washed and resuspended in PBS containing 0.5% bovine serum

albumin (BSA), 0.1% glucose, 3 μg/ml propidium iodide and analysed in a FACScalibur (Becton Dickinson). All washes and dilutions were carried out in PBS containing 0.5% BSA, 0.1% Glucose. Analysis was conducted on viable cells determined by propidium iodide exclusion.

Monoclonal antibodies— Anti-FcεRI-α monoclonal antibody from hybridoma cell line X52-47-5.4 (mAb 47), of IgG1 isotype, was used to determine FcεRI expression. This antibody recognises an epitope in the G strand of FcεRI-α domain two. Murine anti-human FcγRI (IgG1) monoclonal antibody from the hybridoma cell line X54-5/7.1 was kindly provided by Peck Szee Tan (A.R.I., Melbourne, Australia) for use as an isotype control antibody. Chimeric human Fab / mouse Fc anti-NP IgE or IgG3 was supplied by Serotec (Oxford, England).

Surface Plasmon Resonance Determination of Receptor Binding— The synthetic hapten 3-nitro-4-hydroxyphenylacetic caproic acid, succinimide ester (NP-Cap-OSu) (Genosys Biotechnologies, Cambridgeshire, England) was coupled to a CM5 sensor chip. The chip was activated in the manner described by the manufacturer with 1:1 EDC:NHS (*N*-ethyl-*N'*-(dimethylaminopropyl) carbodiimide : *N*-hydroxy succinimide)(10 μl/min), then 12 mM 1,3 Diamino propane (Sigma) (10 μl/min) was passed over the chip surface to create an amino surface, followed by 10 mM NP-Cap-OSu (1 μl/min) dissolved in dry dimethylformamide and diluted in 0.2 M $NaHCO_3$ pH 8.3 immediately before use. The sensor chip was regenerated by washing with 0.5% SDS, followed by water.

Figure 4.3 EA Rosetting of COS cells transfected with ϵϵγ or ϵϵRIII.

A. ϵϵγ (FcϵRI with peptide membrane anchor derived from FcγRIIa) transfected COS cells treated (rosetted) with sheep erythrocytes that have been coated with moIgE anti-TNP (EA's). EA coated COS cells (rosettes) are present, indicating the presence of ϵϵγ on the cell surface.

B. ϵϵRIII (FcϵRI with GPI membrane anchor) transfected COS cells rosetted with moIgE anti-TNP EA's. Rosettes are present, indicating the presence of ϵϵRIII on the cell surface. Rosetting cells transfected with both receptors show characteristic cellular forms, and an apparently similar receptor occupancy.

No aggregation is seen around mock-transfected cells.

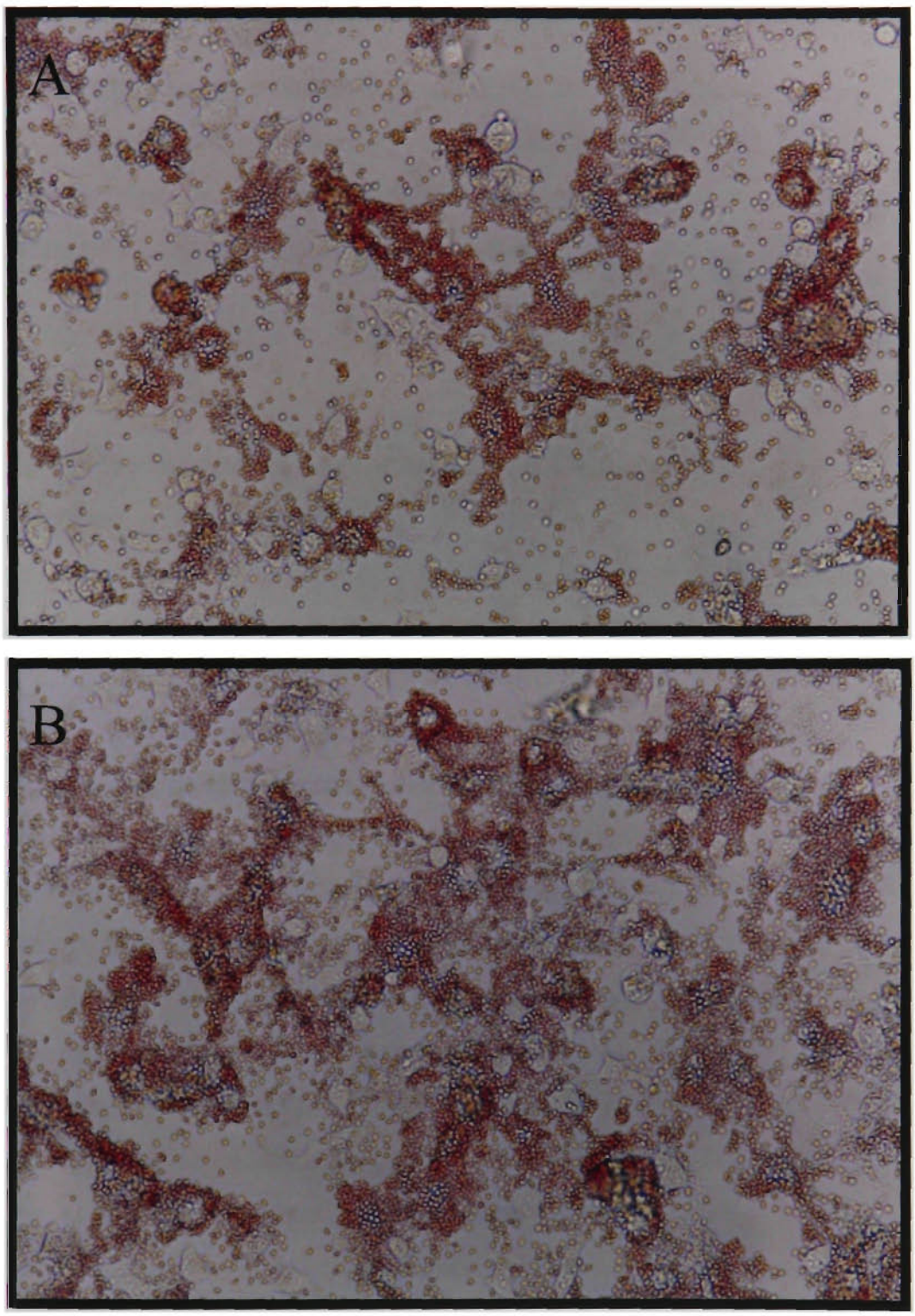
A
B

RESULTS

The Results and Discussion sections of this chapter are separated into two parts: Part A examines the effect of the FcεR chimera membrane anchor on IgE binding, and Part B, the development of an IgE orientation - dependent assay and the rapid expression and recovery of recombinant FcεR for SPR analysis.

PART A.

The Effect of the Membrane Anchor of FcεRI-α Chimeras on IgE Binding

4.A.I. Expression of Chimeric FcεRI

In order to determine whether the membrane anchor of FcεRI-α influences the capacity of the receptor to bind IgE, cDNA for two chimeric IgE binding receptors was constructed; both contained the extracellular domains of FcεRI-α, one with the membrane proximal region and transmembrane anchor of FcγRIIA (εεγ) and one with the GPI anchor of FcγRIIIb (εεRIII). The cDNA was transiently transfected into COS-7 cells. The chimeras were tested for cell surface expression by IgE-EA-rosetting and flow cytometry. EA rosetting indicated that both constructs were expressed on the cell surface (Figure 4.3), and were capable of binding the mouse IgE ligand with similar avidity (Table 4.II). The transiently expressed receptors were then analysed for cell surface expression by flow cytometry using the anti-FcεRI-α monoclonal antibody 47 (Table 4.II). These data indicated that in all cases examined, anchoring by GPI resulted in increased receptor expression. Thus, the εεRIII GPI anchored receptor (mean fluorescence (m.fl.)115.9 units) was expressed in at least two times greater numbers on the cell surface (Figure 4.4) than the peptide anchored receptor (m.fl. 52.8).

The level of the increased apparent cell surface expression was confirmed by additional analyses of other GPI anchored receptors. A chimera of domain one from FcγRIIa, domain two from FcεRI, and the peptide membrane anchor of the FcγRIIa template receptor had previously been constructed. The cDNA for this receptor was used as a template for the construction of γεRIII receptor cDNA (see Experimental

Table 4.II.

Binding and expression of chimeric receptors

	moIgE EA-rosetting[a] (Avidity)	Relative expression detected by IgE[b]	Relative expression detected by mAb[c]	K_D (M)[d]	Relative Affinity[e]
ϵϵγ	3+	1	1	$2.1x10^{-9} \pm 7.2x10^{-10}$	1
ϵϵRIII	3+	3.2	1.9	$5.0x10^{-9} \pm 2.4x10^{-9}$	0.4
ϵϵDAF	3+	3.8	ND[f]	$9.0x10^{-9} \pm 3.6x10^{-9}$	0.2
γϵγ	3+	0.5	1	$4.0x10^{-9} \pm 8.0x10^{-10}$	0.5
γϵRIII	3+	3.1	1.6	$6.9x10^{-9} \pm 1.6x10^{-9}$	0.3
RIIIϵRIII	3+	4.8	2.2	$1.1x10^{-8} \pm 4.9x10^{-9}$	0.2
γ(Gϵ)ϵγ	3+	0.4	0.3[g]	$3.3x10^{-9} \pm 9.5x10^{-10}$	0.6
γ(Gϵ)ϵRIII	3+	1.3	ND	$5.2x10^{-9} \pm 1.8x10^{-9}$	0.4

a. Binding of immune complexes. MoIgE-EA rosetted cells were scored on a scale of + to 3+, with 3+ indicating the highest number of EA associated with a cell.

b. The average expression of a receptor determined by the maximum binding of IgE in equilibrium binding assays, and compared to that of ϵϵγ where ϵϵγ=1.

c. Average cell surface expression of the chimera as detected by anti-FcϵRI mAb 47 in flow cytometry, and compared with expression of ϵϵγ where ϵϵγ=1.

d. The equilibrium binding dissociation constant (average taken from three experiments) with the standard deviation indicated.

e. Relative affinity of chimeric receptors determined by K_D (ϵϵγ=1), all other chimeras had a lower apparent affinity.

f. Not Determined

g. Determined by iodinated antibody.

Figure 4.4 FACS profiles from a representative assay of FcR incubated with mAb47 and fluorescenated anti-mouse IgG.

The ordinate indicates the number of cells counted and the abcissa the level of fluorescence. The 'Mean' indicates the mean value of fluorescence of the cells in the sample tested (mean fluorescence - m. fl.).

A. The FACS profile of $\epsilon\epsilon\gamma$ and $\epsilon\epsilon$RIII clearly indicates the increase in expression of the $\epsilon\epsilon$RIII receptor over that of $\epsilon\epsilon\gamma$, by a mean fluorescence of 115.9 units to 52.8.

B. The FACS profiles of $\gamma\epsilon\gamma$ compared with $\gamma\epsilon$RIII again indicates the increase in expression of the GPI anchored receptor $\gamma\epsilon$RIII which has a mean fluorescence of 86.1 units compared with 50.3, the mean fluorescence of $\gamma\epsilon\gamma$.

C. The mean fluorescence of the FACS profile of the GPI anchored receptor RIIIϵRIII is seen to be greater (145.1) that either that of $\gamma\epsilon\gamma$(50.3) or $\epsilon\epsilon\gamma$ (52.8).
The IgE profile of mock transfected cells is included as a negative control.

A

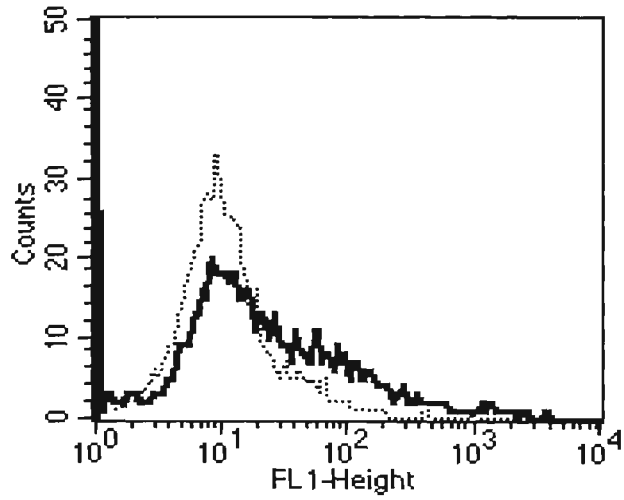

Key	Name	Parameter	Gate	Mean
.....	εεγ	FL1-H	No Gate	52.8
———	εεRIII	FL1-H	No Gate	115.9

B

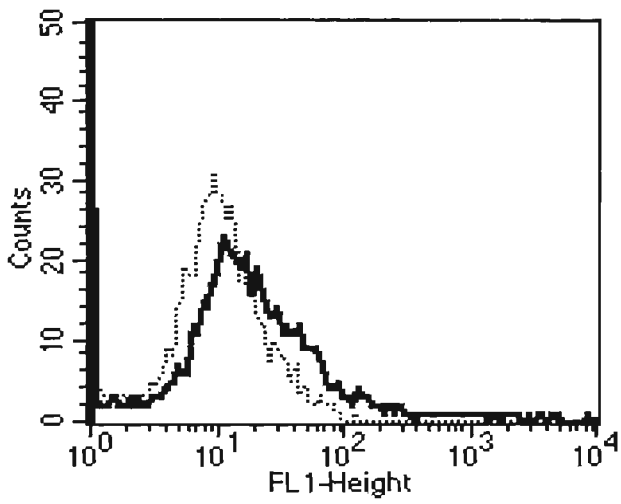

Key	Name	Parameter	Gate	Mean
.....	γεγ	FL1-H	No Gate	50.3
———	γεRIII	FL1-H	No Gate	86.1

C

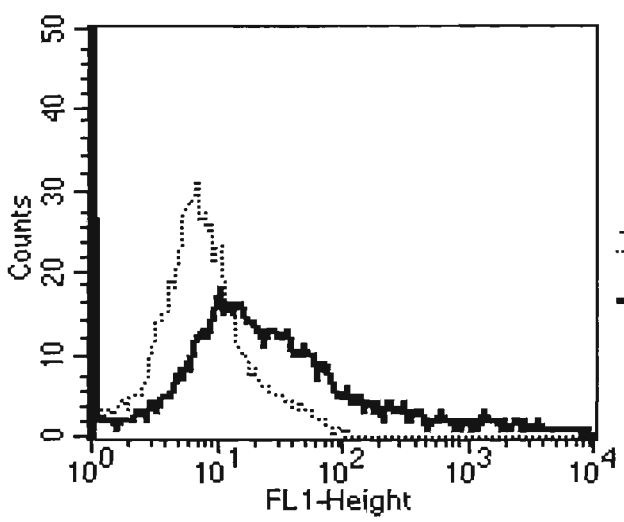

Key	Name	Parameter	Gate	Mean
.....	mock	FL1-H	No Gate	6.3
———	RIIIεRIII	FL1-H	No Gate	145.1

Procedures). The γϵγ and γϵRIII receptors were transiently tranfected into COS-7 cells, then tested by EA-rosetting. The two receptors bound complexed moIgE with a similar avidity to that of the ϵϵγ and ϵϵRIII receptors (Table 4.II).

The γϵγ and γϵRIII receptors were then analysed by flow cytometry with anti-FcϵRI-α antibodies to determine comparative expression (Figure 4.4; Table 4.II). The receptors with similar extracellular regions but different membrane anchors again showed a distinct disparity in their surface expression. The γϵRIII chimera displayed 58% increase in receptor expression of (γϵRIII m.fl. 86.1 versus γϵγ 50.3) over that of the transmembrane anchored receptor γϵγ, that is a relative binding of the mAb 47 of 1.7 : 1 FcγRIIIb : FcγRIIa (see Figure 4.4; and Table 4.II).

4.A.II. Binding affinity.

The ϵϵγ and ϵϵRIII receptors expressed at the cell surface were then assayed for ligand affinity by their ability to bind monomeric human IgE in an equilibrium binding assay (Figures 4.5, 4.6 and Table 4.II). It was determined that the ϵϵRIII receptor (constructed with the GPI anchor of FcγRIIIb) bound monomeric IgE with a lower affinity than the ϵϵγ receptor with the peptide membrane anchor ($5.9x10^{-9}$ ϵϵRIII to $2.1x10^{-9}$ ϵϵγ). Determination of the maximum binding of IgE in the equilibrium binding assays enabled an estimation of the number of receptors expressed on the COS-7 cells to be made. This is given as a number relative to the receptor number for ϵϵγ (see Table 4.II). The GPI anchored ϵϵRIII chimera appeared to express approximately three times more receptors on the cell surface than ϵϵγ, the peptide anchored receptor, when measured by IgE binding (see Table 4.II). This was surprising since the expression of the receptors when determined by mAb binding was only twice as great for the ϵϵRIII chimera as for ϵϵγ; and even more surprising was that the GPI anchored receptor ϵϵRIII displayed less than half the affinity for IgE than did ϵϵγ.

The cause of the increase in surface expression and decrease in ligand affinity of ϵϵRIII could have been either unique to the FcγRIII membrane anchor, or a generic effect

Figure 4.5 IgE equilibrium binding data of the $\epsilon\epsilon\gamma$ chimeric receptor from a single representative assay.

The top graph is an equilibrium binding curve of $\epsilon\epsilon\gamma$, a peptide anchored receptor. The abcissa represents the concentration of ^{125}I IgE added to an aliquot of 2.5×10^4 cells. The ordinate indicates the concentration of ^{125}I IgE that remains bound to the cells after incubation and washing.

The lower graphs are regression analyses of the equilibrium binding data. The more accurate non linear regression is shown on the left, and the linear Scatchard plot is shown on the right. The equilibrium binding dissociation constant (K_D) was obtained from three experiments with a correlation coefficient of >0.99 and is shown in Table 4.II.

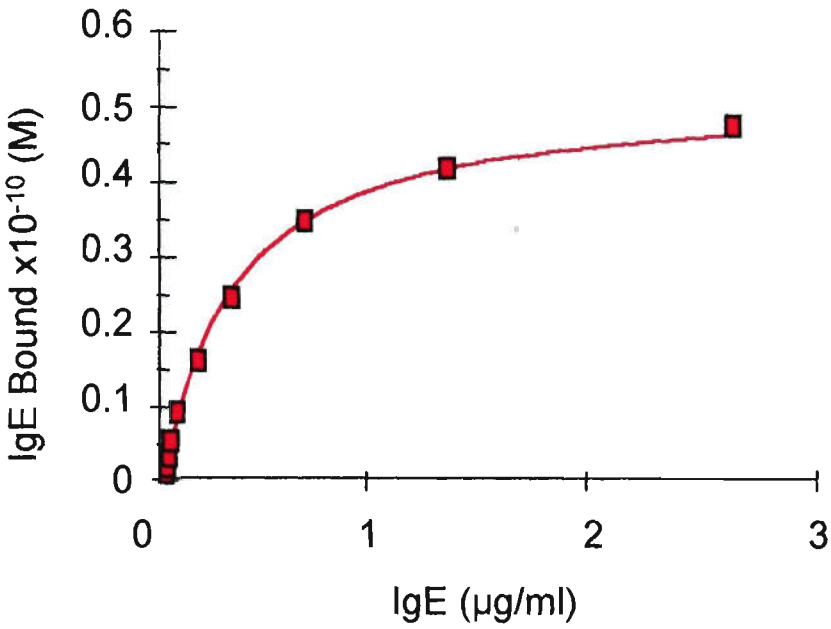

Non linear regression

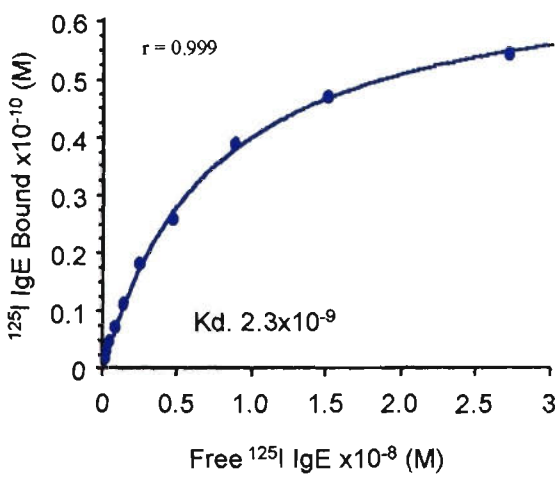

Linear regression

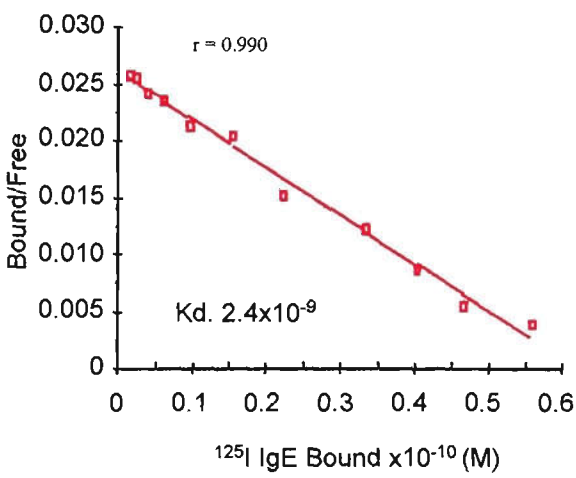

Figure 4.6 IgE equilibrium binding data of the ϵϵRIII chimeric receptor from a single representative assay.

The top graph is an equilibrium binding curve of ϵϵRIII, a GPI anchored receptor. The abcissa represents the concentration of ^{125}I IgE added to an aliquot of $2.5x10^4$ cells. The ordinate indicates the concentration of ^{125}I IgE that remains bound to the cells after incubation and washing.

The lower graphs are regression analyses of the equilibrium binding data. The more accurate non linear regression is shown on the left, and the linear Scatchard plot is shown on the right. The equilibrium binding dissociation constant (K_D) was obtained from three experiments with a correlation coefficient of >0.99 and is shown in Table 4.II.

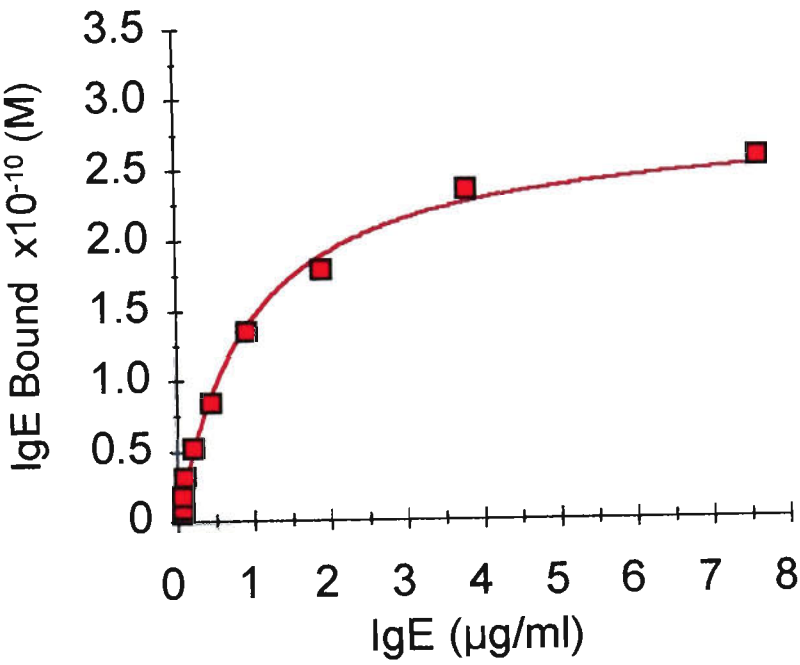
IgE Bound x10-10 (M)
3.5
3.0
2.5
2.0
1.5
1.0
0.5
0
0 1 2 3 4 5 6 7 8
IgE (µg/ml)

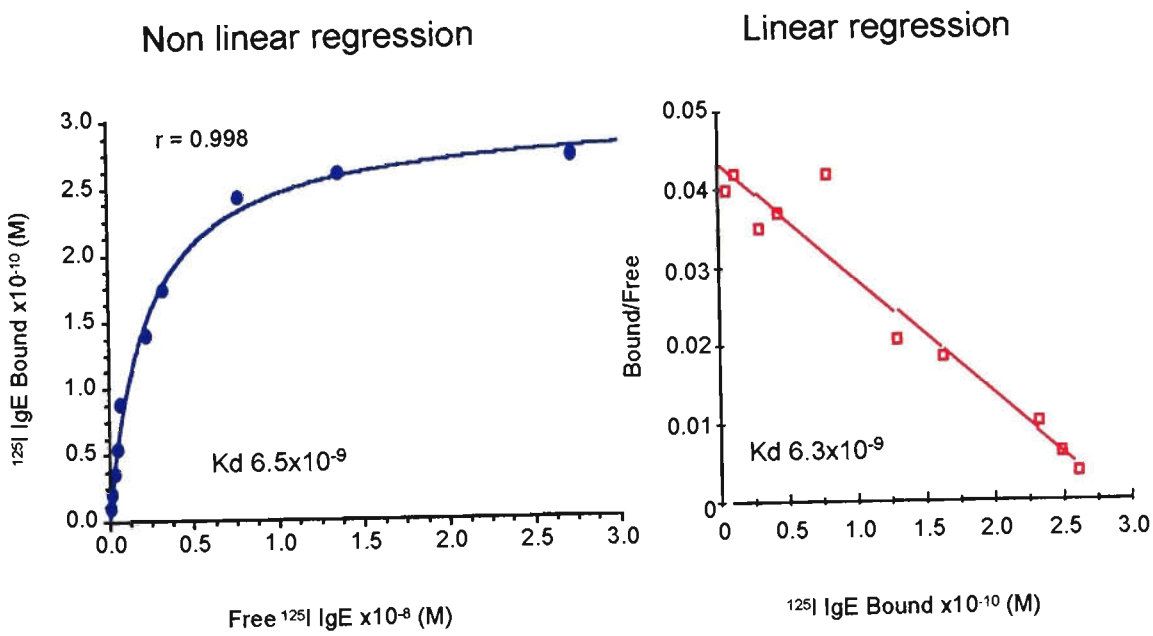
Non linear regression
r = 0.998
Kd 6.5x10-9
125I IgE Bound x10-10 (M)
Free 125I IgE x10-8 (M)
Linear regression
Kd 6.3x10-9
Bound/Free
125I IgE Bound x10-10 (M)

Figure 4.7 IgE equilibrium binding data of the ϵϵDAF chimeric receptor from a single representative assay.

The top graph is an equilibrium binding curve of ϵϵDAF, a GPI anchored receptor. The abcissa represents the concentration of ^{125}I IgE added to an aliquot of $2.5x10^4$ cells. The ordinate indicates the concentration of ^{125}I IgE that remains bound to the cells after incubation and washing.

The lower graphs are regression analyses of the equilibrium binding data. The more accurate non linear regression is shown on the left, and the linear Scatchard plot is shown on the right. The equilibrium binding dissociation constant (K_D) was obtained from three experiments with a correlation coefficient of >0.99 and is shown in Table 4.II.

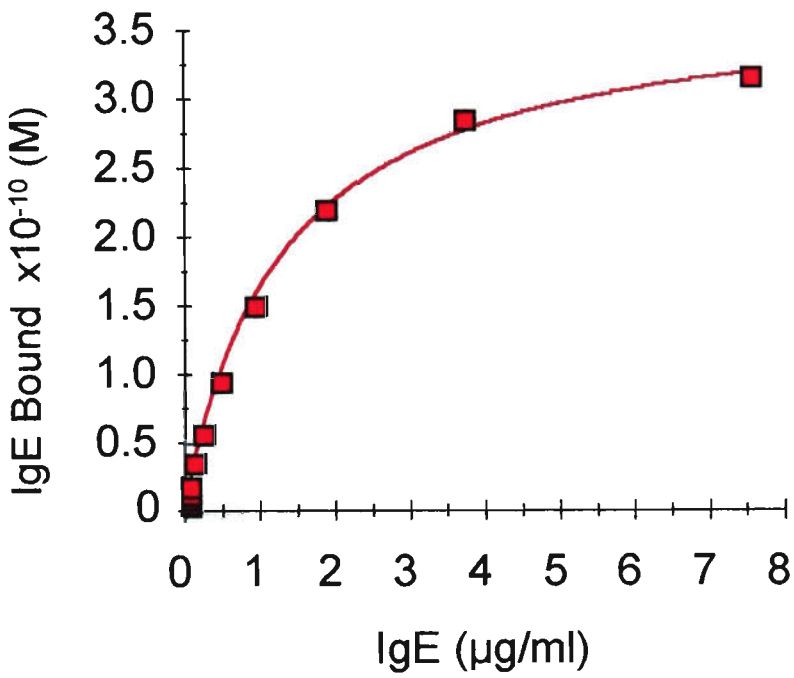
IgE Bound x10-10 (M)
3.5
3.0
2.5
2.0
1.5
1.0
0.5
0
0 1 2 3 4 5 6 7 8
IgE (µg/ml)

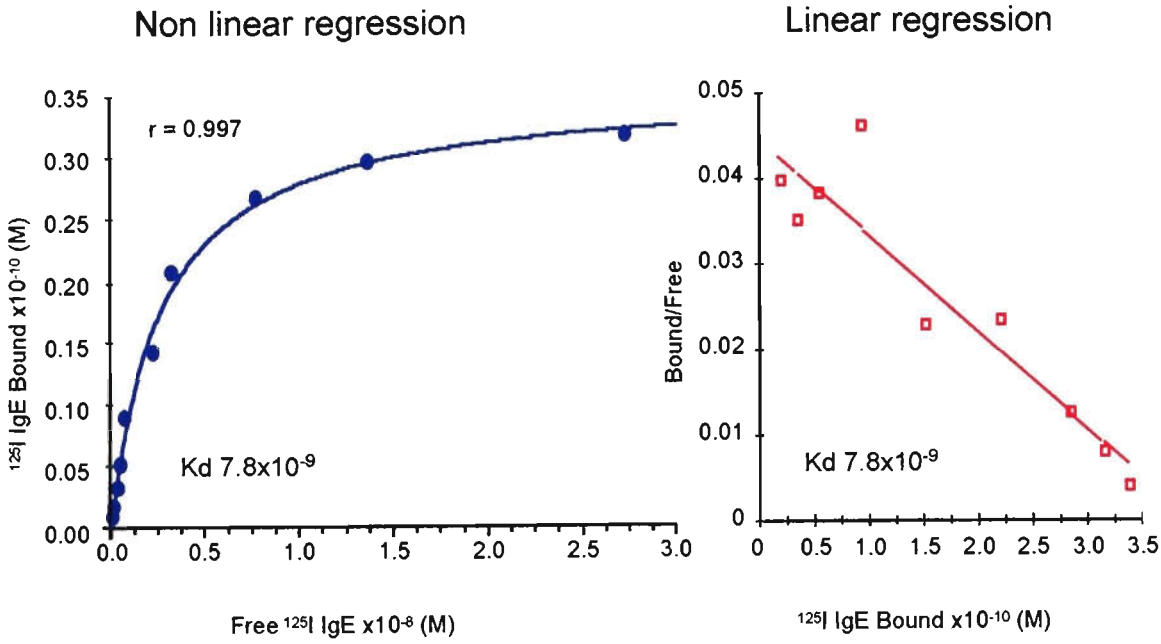
Non linear regression
Linear regression
r = 0.997
Kd 7.8x10-9
125I IgE Bound x10-10 (M)
Free 125I IgE x10-8 (M)
Bound/Free
Kd 7.8x10-9
125I IgE Bound x10-10 (M)

of the GPI anchor. To elucidate this issue an additional receptor was constructed with the extracellular domains of FcεRI, but utilising the cDNA encoding the GPI anchor of decay-accelerating factor (DAF). The membrane proximal and membrane anchor signal region of the decay-accelerating factor (DAF), was spliced to the extracellular domains of FcεRI-α, producing the εεDAF chimera. The εεDAF GPI anchored receptor showed similar avidity for moIgE by EA-rosetting as εεRIII (Table 4.II), and again, like εεRIII, the expression of the εεDAF GPI anchored receptor on the surface was over 300% greater than that of εεγ as determined by IgE binding (see Figures 4.6, 4.7). The affinity of εεDAF for IgE was found to be 80% lower than the affinity for εεγ, again similar to εεRIII that had a 60% lower affinity (see Table 4.II). Clearly the general nature of the attachment to the membrane, rather than the molecular origin of the anchor is the major factor in determining the difference in binding characteristics.

The chimeric γεγ and γεRIII receptors were also used in an equilibrium binding assay to determine their affinity for human monomeric IgE. Once again it was apparent that the apparent cell surface expression - as determined by IgE binding - was greater for the GPI anchored γεRIII than the peptide anchored γεγ. Indeed, the cell surface expression was six times greater for γεRIII (see Table 4.II), but with almost half the affinity of γεγ for IgE (Figures 4.8, 4.9). Again, the expression of the GPI chimera, γεRIII, as determined by IgE binding was greater than the expression determined by mAb, in this case approximately double.

Whilst the receptor pair γεγ and γεRIII differed in their affinities for IgE (see Chapter 3), not surprisingly, both had lower affinities for IgE than the εεγ and εεRIII counterparts, which contained the entire FcεRI-α extracellular binding domains. As both γεγ and γεRIII had a FcγRIIa-derived first domain, a third chimeric receptor was produced, using both the first domain and GPI anchor of FcγRIII , termed RIIIεRIII (see Table 4.I). This construct was used to determine whether differences in binding affinity could be ascribed to the alteration of receptor function by the first domain. Expression of RIIIεRIII was more than four times that of εεγ, and 25% greater than either εεRIII or γεRIII. Associated with the greater increase of expression of the RIIIεRIII chimera was

Figure 4.8 IgE equilibrium binding data of the γϵγ chimeric receptor from a single representative assay.

The top graph is an equilibrium binding curve of γϵγ, a peptide anchored receptor. The abcissa represents the concentration of ^{125}I IgE added to an aliquot of $2.5x10^4$ cells. The ordinate indicates the concentration of ^{125}I IgE that remains bound to the cells after incubation and washing.

The lower graphs are regression analyses of the equilibrium binding data. The more accurate non linear regression is shown on the left, and the linear Scatchard plot is shown on the right. The equilibrium binding dissociation constant (K_D) was obtained from three experiments with a correlation coefficient of >0.99 and is shown in Table 4.II.

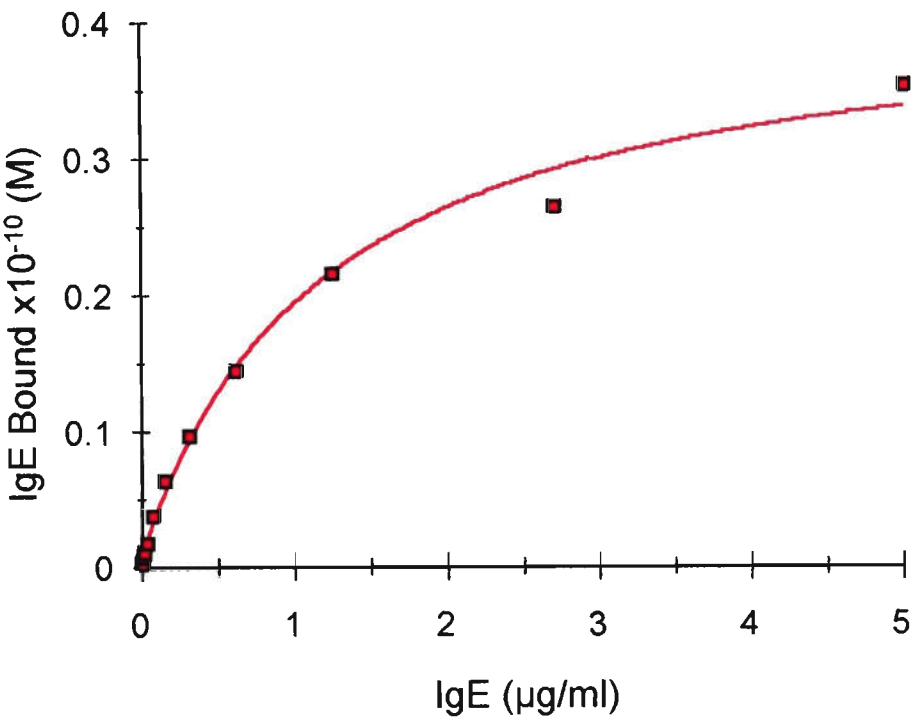

Non linear regression

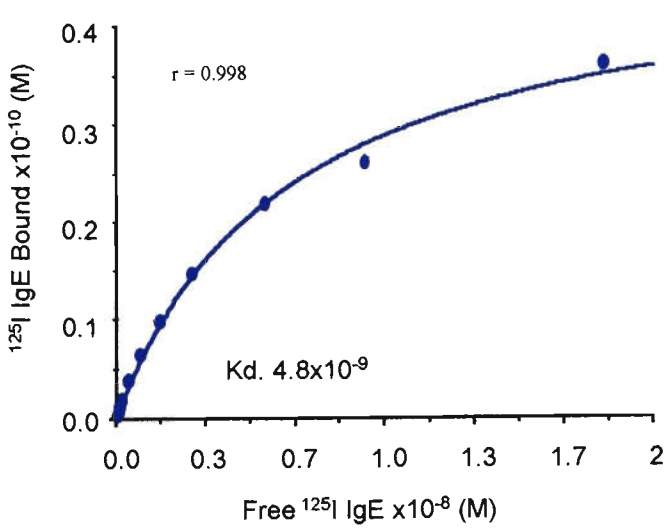

Linear regression

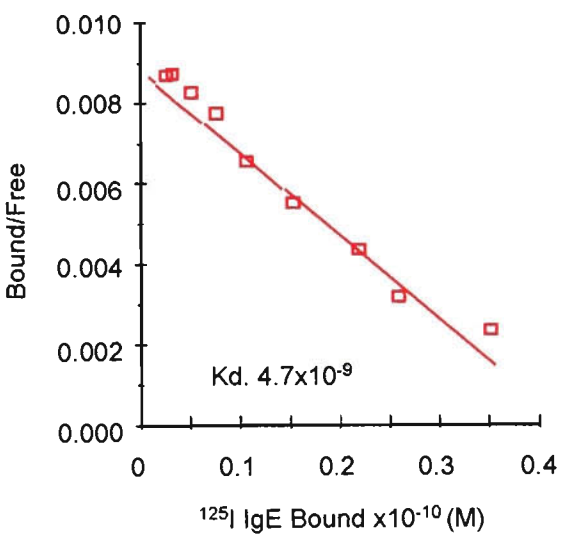

Figure 4.9 IgE equilibrium binding data of the γεRIII chimeric receptor from a single representative assay.

The top graph is an equilibrium binding curve of γεRIII, a GPI anchored receptor. The abcissa represents the concentration of ^{125}I IgE added to an aliquot of $2.5x10^4$ cells. The ordinate indicates the concentration of ^{125}I IgE that remains bound to the cells after incubation and washing.

The lower graphs are regression analyses of the equilibrium binding data. The more accurate non linear regression is shown on the left, and the linear Scatchard plot is shown on the right. The equilibrium binding dissociation constant (K_D) was obtained from three experiments with a correlation coefficient of >0.99 and is shown in Table 4.II.

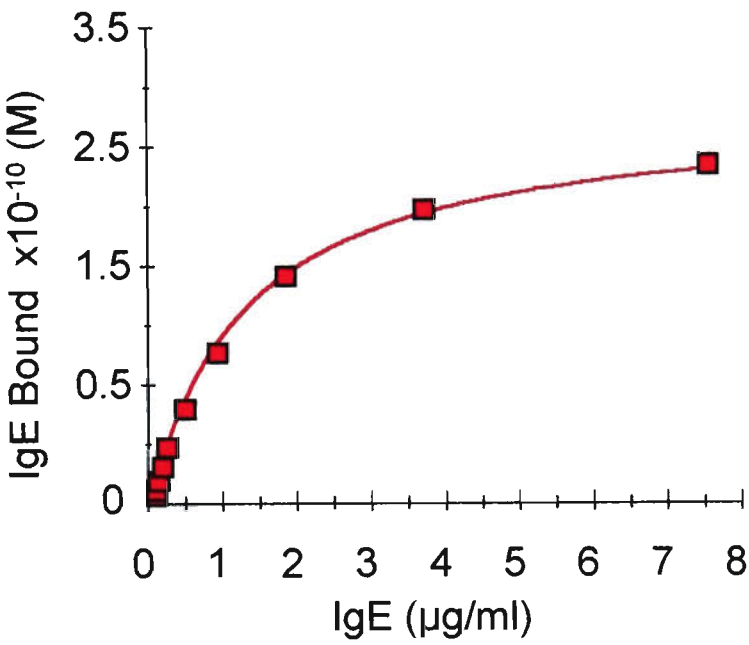

Non linear regression

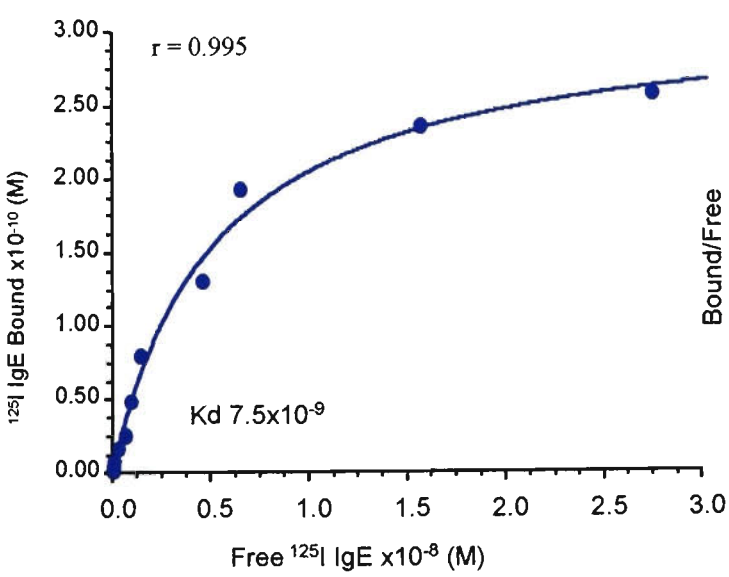

Linear regression

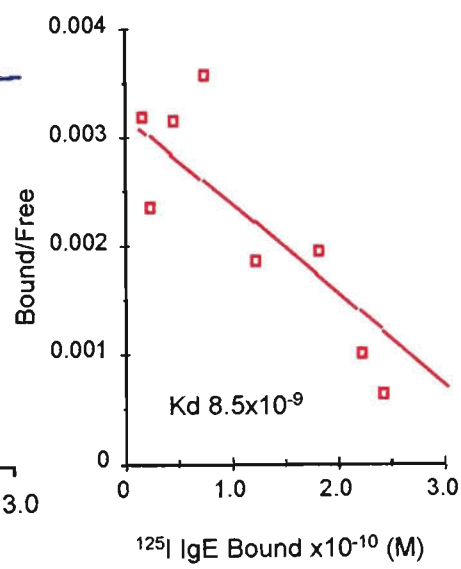

Figure 4.10 IgE equilibrium binding data of the RIIIϵRIII chimeric receptor from a single representative assay.

The top graph is an equilibrium binding curve of RIIIϵRIII, a GPI anchored receptor. The abcissa represents the concentration of ^{125}I IgE added to an aliquot of $2.5x10^4$ cells. The ordinate indicates the concentration of ^{125}I IgE that remains bound to the cells after incubation and washing.

The lower graphs are regression analyses of the equilibrium binding data. The more accurate non linear regression is shown on the left, and the linear Scatchard plot is shown on the right. The equilibrium binding dissociation constant (K_D) was obtained from three experiments with a correlation coefficient of >0.99 and is shown in Table 4.II.

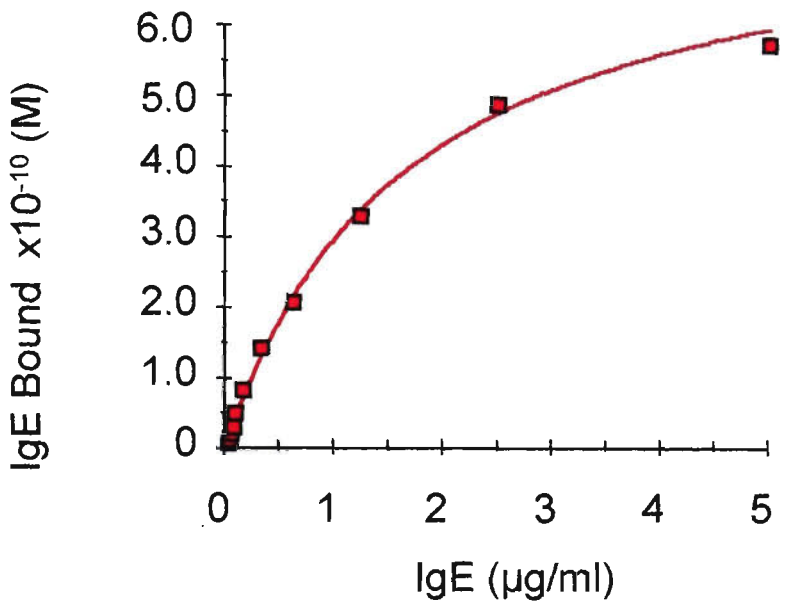

Non linear regression

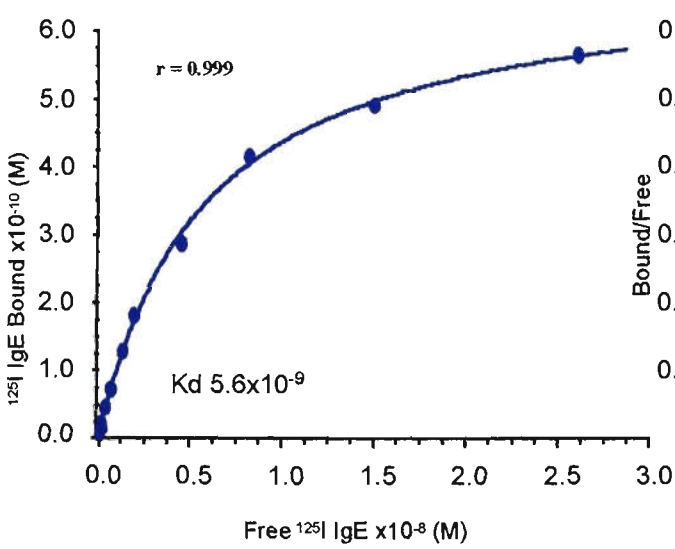

Linear regression

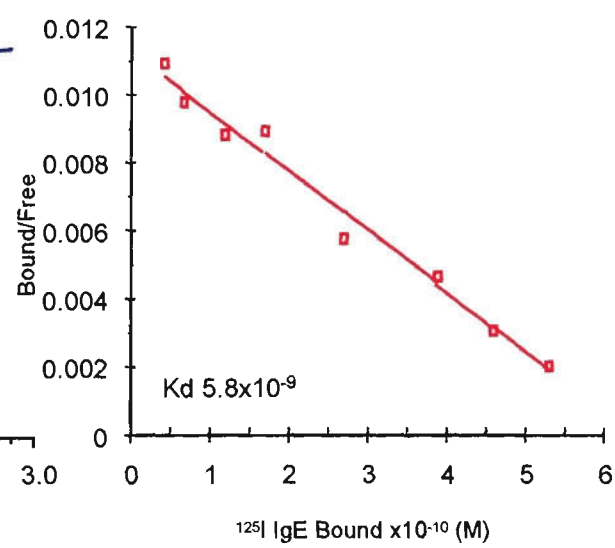

a decrease in the affinity of the receptor for IgE (Figure 4.10). The RIIIϵRIII receptor displayed the lowest affinity for monomeric IgE of any receptor tested (see Table 4.II).

The increase in apparent cell surface expression and decrease in affinity in receptors that differ only in their membrane anchor was confirmed in a third instance where paired receptors were available γ(Gϵ)ϵγ and γ(Gϵ)ϵRIII). These receptors comprised domain one of FcγRIIA as in the γϵγ and γϵRIII receptors, except that the G strand of domain one was FcϵRI-α derived, and maintained the epsilon sequence up to the membrane proximal region, as in the previous receptors (see Table 4.I). These γ(Gϵ)ϵγ and GϵRIII receptors also displayed avidity for moIgE (see Table 4.II), but the γ(Gϵ)ϵRIII receptor was not analysed by flow cytometry. When the γ(Gϵ)ϵγ and γ(Gϵ)ϵRIII receptors were tested in an equilibrium binding assay the expression of γ(Gϵ)ϵRIII was determined to be three to four times greater than that of γ(Gϵ)ϵγ and the affinity for IgE was almost half that of γ(Gϵ)ϵγ, the receptor with the cytoplasmic membrane anchor (Figures 4.11, 4.12).

For each pair of receptors the apparent cell surface expression of receptors with a GPI anchor was greater than for those with a membrane spanning, peptide anchor (see Table 4.II). These results were unexpected and surprisingly consistent. To determine whether the reduction in binding affinity was a result of the GPI membrane anchor itself, or a result of the change in surface presentation of the receptor with the less rigid membrane proximal region of the GPI anchor, it would be necessary to test the extracellular domains of the receptors.

It was theoretically possible to determine the IgE binding profiles of the ectodomains of the GPI anchored proteins without the GPI anchor, by the use of phosphoinositol phospholipase C, an enzyme capable of causing the release of the GPI anchored receptor from the membrane surface (Figure 4.1). However, it would be necessary to create an assay capable of determining FcR:IgE binding characteristics with the IgE in the immobile phase.

Figure 4.11 IgE equilibrium binding data of the γ(Gϵ)ϵγ chimeric receptor from a single representative assay.

The top graph is an equilibrium binding curve of γ(Gϵ)ϵγ, a peptide anchored receptor. The abcissa represents the concentration of ^{125}I IgE added to an aliquot of 2.5×10^4 cells. The ordinate indicates the concentration of ^{125}I IgE that remains bound to the cells after incubation and washing.

The lower graphs are regression analyses of the equilibrium binding data. The more accurate non linear regression is shown on the left, and the linear Scatchard plot is shown on the right. The equilibrium binding dissociation constant (K_D) was obtained from three experiments with a correlation coefficient of >0.99 and is shown in Table 4.II.

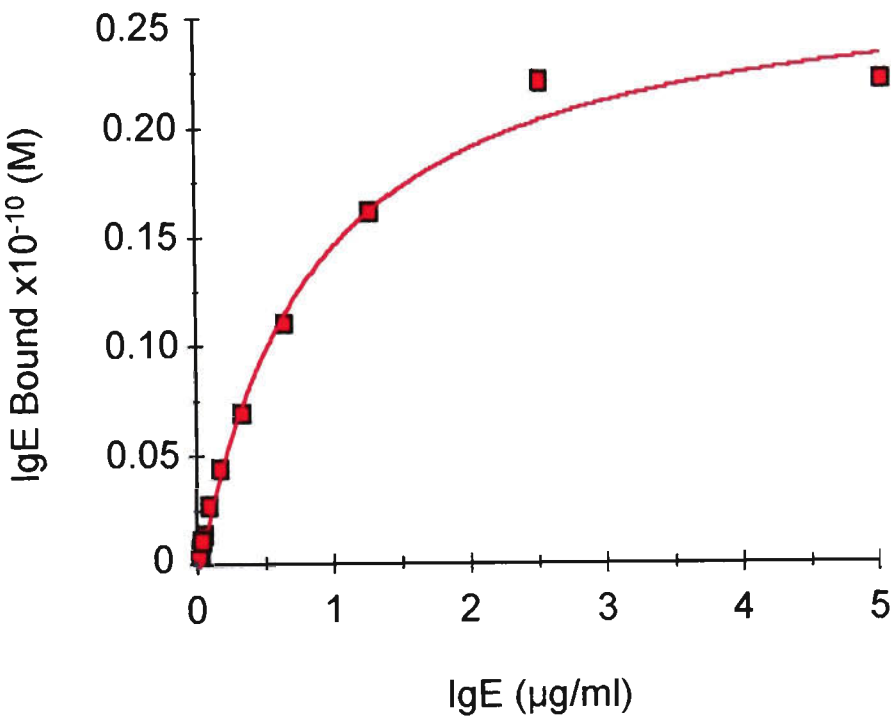

Non linear regression

Linear regression

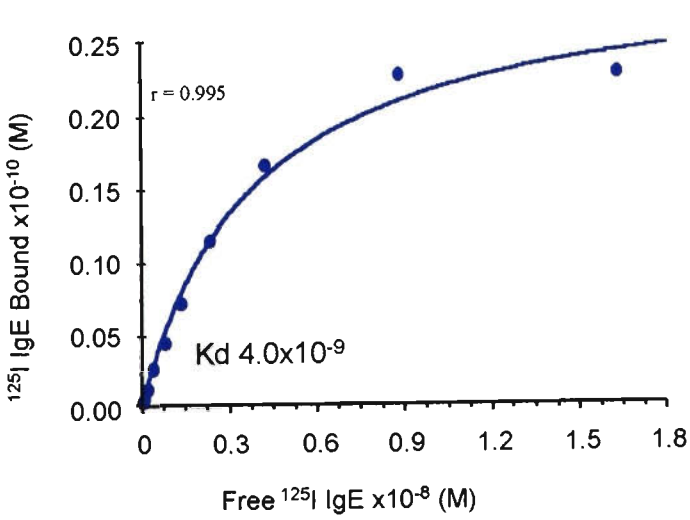

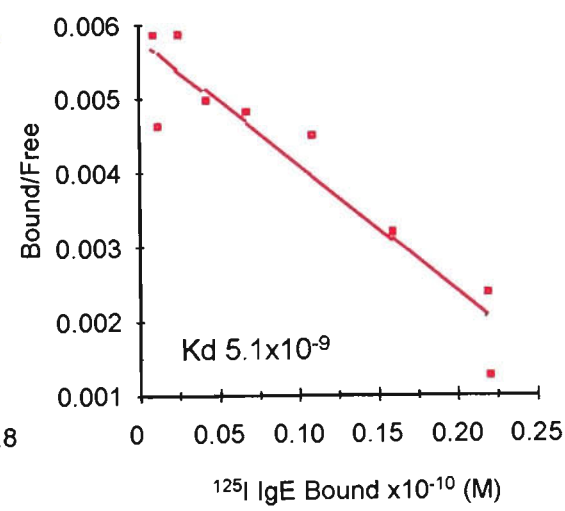

Figure 4.12 IgE equilibrium binding data of the γ(Gϵ)ϵRIII chimeric receptor from a single representative assay.

The top graph is an equilibrium binding curve of γ(Gϵ)ϵRIII, a GPI anchored receptor. The abcissa represents the concentration of ^{125}I IgE added to an aliquot of $2.5x10^4$ cells. The ordinate indicates the concentration of ^{125}I IgE that remains bound to the cells after incubation and washing.

The lower graphs are regression analyses of the equilibrium binding data. The more accurate non linear regression is shown on the left, and the linear Scatchard plot is shown on the right. The equilibrium binding dissociation constant (K_D) was obtained from three experiments with a correlation coefficient of >0.99 and is shown in Table 4.II.

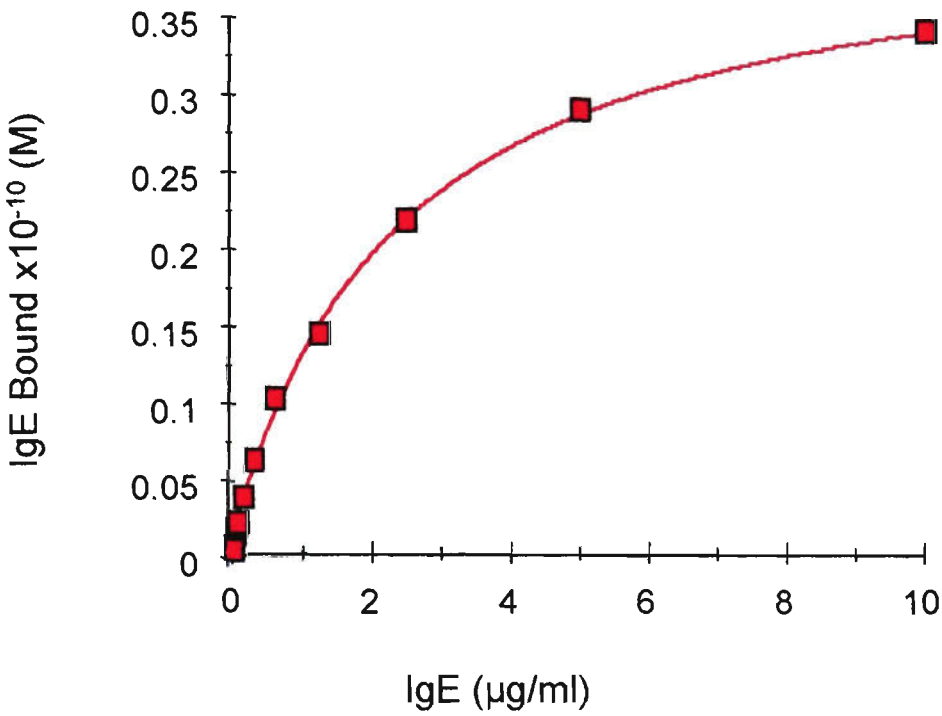

Non linear regression

Linear regression

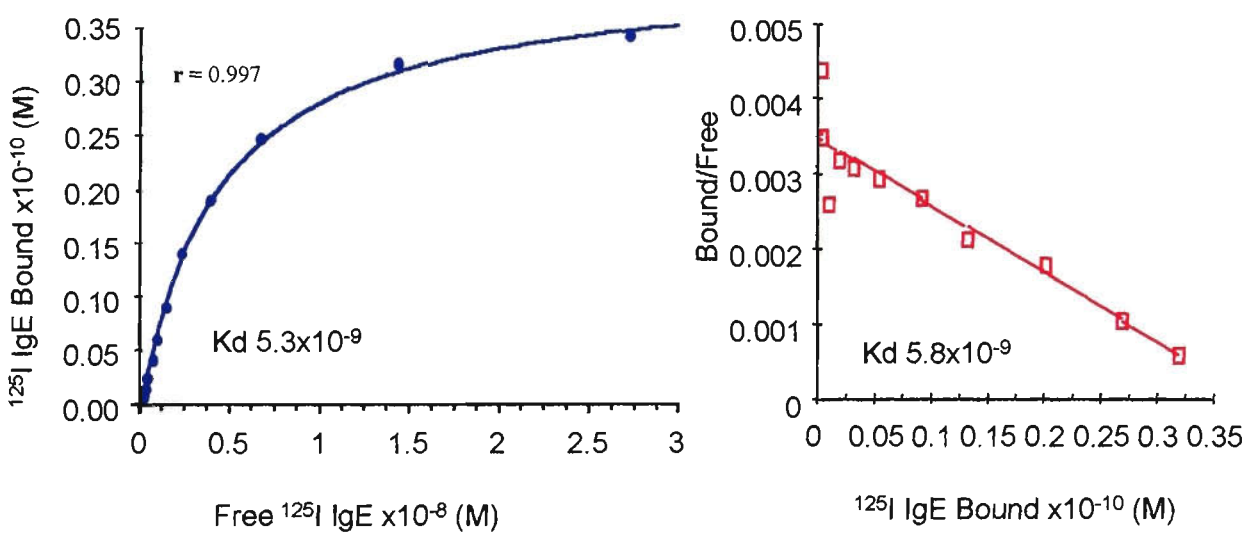

DISCUSSION

The intention of the experiments described in the first part of this chapter was to determine whether there was a change in ligand binding characteristics with an alteration in the membrane anchor. This work led to three findings:

(i) the level of cell surface expression for the GPI anchored protein was apparently greater than for the peptide anchored protein;

(ii) maximum binding of ligand and monoclonal antibody gave different values for the cell surface expression of receptors; and

(iii) the affinity of GPI anchored receptors for IgE was different to the peptide anchored forms of receptor for the same ligand.

The difference in expression between GPI anchored proteins and peptide anchored proteins with the same extracellular domains— The cell surface expression for pairs of receptors was consistently higher for the GPI anchored protein. The pairs of receptors comprised the same extracellular domains with either a peptide membrane anchor (FcγRIIa) or a GPI anchor (FcγRIIIb). When measured by IgE binding, receptors with a GPI anchor were expressed on the cell surface with a density three times greater than a similar protein with a peptide membrane anchor. When measured by mAb binding receptors with a GPI anchor were expressed on the cell surface with a density one and a half to two times greater than a similar protein with a peptide membrane anchor. The consistent elevation of cell surface expression of the GPI anchored protein over the peptide anchored protein was unexpected, as truncation of FcεRI-α has been shown to have no effect on the expression of the receptor as determined by rosetting (21), although receptor numbers by IgE binding or mAb had not previously been determined. However, a receptor using the GPI anchor of DAF with the same extracellular domains (FcεRI) as the FcγRIIIb anchored receptor, confirmed the greater expression of GPI anchored receptors in this system.

This increase in cell surface expression of the GPI anchored protein over the peptide anchored protein has also been seen in FcγRIII, where the peptide anchored

FcγRIIIa associated with γ chain was shown to have almost half the cell surface expression of the GPI anchored FcγRIIIb or a GPI anchored mutant of FcγRIIIa (1), and in FcγRI (7) where there is evidence of an increase in expression of a GPI anchored mutant over 'wild-type' FcγRI. As this increase in expression of GPI relative to peptide anchored proteins is seen in different independent laboratories, it is improbable that technical factors are responsible; thus, it is probably a cell based effect.

There are several possible reasons for the higher level of cell surface expression of the GPI anchored proteins, including:

(i) An increase in receptor synthesis.

An increase in the rate of receptor synthesis would be likely to result in an increase in apparent cell surface expression of the receptor. However, the upregulation of cell surface expression of FcεRI in the presence of monomeric IgE (22) is independent of protein synthesis (23); receptor synthesis and cell surface expression of the receptor are not directly correlated.

(ii) More efficient transport of the receptor to the cell surface.

GPI anchored proteins are more densely packed in membranes than peptide anchored proteins (24). Thus, packaging of GPI anchored receptor into the membranes of transport vesicles and transportation to the cell surface may be more efficient.

(iii) Reduced rate of internalisation.

The upregulation of FcεRI in the presence of monomeric IgE (22) has been attributed to resistance to endocytosis by FcεRI bound to monomeric IgE (25, 26). Protection of the receptor from endocytosis would not be GPI specific, but a lack of receptor clearance rather than an increase in receptor synthesis may be occurring through a separate mechanism. GPI anchors can confer low turnover rates to proteins (27), and this may be a factor here.

(iv) Orientation of the receptor in the membrane.

Orientation of the receptor in the membrane may impact on the numbers of receptors detected. For example, GPI anchored receptors are less rigid than peptide anchored receptors (28) and thus may 'present' the receptor binding site to its ligand less effectively than the peptide anchored receptor. Results presented in this chapter however gave higher levels of ligand binding for the GPI anchored receptor than for the peptide

anchored protein. Thus the higher number of GPI-linked receptors detected is unlikely to be due to differences in orientation. It might reasonably be expected that orientation of peptide anchored proteins would be more favourable than GPI-linked proteins.

Of these options, it is not possible at this stage to determine which factor is responsible for the detection of the greater number of GPI anchored receptors on the cell surface relative to peptide anchored receptors. Future studies comparing the peptide and GPI anchors, such as those following, would be needed to resolve the issue of receptor expression and ligand binding.

(i) Receptor synthesis / turnover could be examined by pulse chase biosynthetic labelling and gel analysis over time.

(ii) Receptor trafficking could be examined using either subcellular fractionation or by fluorescent double labelling with anti-receptor mAb and compartment specific markers e.g. lamp1 or lamp2 for endosomes or lysosomes respectively.

(iii) Mutagenesis of the external domains of the receptor incorporating a 'tag' may also be useful in the surface detection of the orientation of the receptors in the membrane. A drawback of this method is that the 'tag' itself may affect the behaviour of the receptor.

Apparent differences in receptor numbers when determined by a) maximum binding of ligand, and b) by anti-FcεRI monoclonal antibody— The apparent difference in detectable cell surface expression of the chimeric receptors as determined by IgE binding compared to monoclonal anti-FcεRI-α must, of necessity, be an artifact due to differences between antibody and ligand for receptor recognition.

It is likely that these variations are due to differences in receptor configurations either as a result of organisation of the receptor/ligand complex or the conformation of one receptor molecule passing through a series of minor conformational/orientation changes. This ectodomain movement is likely to be the same for both the GPI and peptide anchored form of a receptor; and where FcεRI has some rotational movement in the transmembrane region, the GPI anchor is less rigid (28). Evidence for these

conformational changes and forced orientation comes from work on rat RBL 2H3 cells, where FcεRI-α was determined to undergo 'high' and 'lower' affinity states (29) that are related to the ability to bind ligand; and work that shows that the secretory response of mAb/ FcεRI-α dimers is dependent on orientation restraints and conformational transitions (30). A GPI anchor may change or exaggerate these configurations.

It is possible that there are two main configurations (the term encompassing configuration/orientation and membrane organisation) of the receptor, and there is equilibrium between the two states. The equilibrium between the states could alter on binding ligand or antibody. Put simply, receptor state one (R1) binds IgE well (++), and binds mAb 47 well (++) i.e. the epitope is exposed. Receptor state two (R2) binds IgE very well (++++), and binds mAb 47 poorly, or not at all (+/-). This can be written as follows:

R1	⇌	R2
(IgE ++)(mAb 47 ++)		(IgE++++)(mAb 47 +/-)

It can be seen that IgE binds in either the R1 or R2 'state' of the receptor, but mAb 47 binds better in one state than the other. It is possible that the measurement of receptor expression by mAb 47 or by IgE could produce a different result (mAb : IgE, 1:2) , and this would occur regardless of the membrane anchor. It is also possible that on binding ligand the equilibrium alters to favour one state over the other (e.g. the R2 state over the R1 state) by affinity differences or masking the mAb 47 epitope.

It is also possible that it is not a conformational change within the receptor that conceals the mAb 47 epitope, but organisation of two or more receptors on the membrane. GPI anchored proteins associate in rafts on the cell surface (31), and cluster in clathrin coated pits on ligand binding. The IgE binding site is on the exposed surface of domain 2, but the epitope for mAb 47 is on the G strand of domain 2 and is proximal to the membrane. The close packing of GPI receptors may not affect IgE binding, but may prevent access of mAb 47 to its epitope. Therefore a molecule of IgE would bind each receptor with a stoichiometry of1:1 (32, 33), but one molecule of mAb 47 would be

able to bind to fewer receptors (0.3-0.5:1) and show an apparently lower level of increase.

In the case of peptide anchored FcR, native FcεRI or FcγRIII are organised in the membrane by association with γ chains. Interaction of the γ chain is mediated by the transmembrane domains (34) and, like GPI, they associate with membrane lipids (31). Similarly FcγRIIa although *not* associated with γ chain, has recently been shown to form dimers (35; M. Powell, A.R.I., Melbourne, Australia, personal communication), that are apparently driven by the transmembrane domains. Thus, as the experiments here use the FcγRIIa peptide anchor, and substitute the GPI anchor, it appears that alteration to receptor organisation is likely, and that mAb 47 is only able to access one epitope of the two receptors in the dimer state.

Although it is almost certain that FcεR form dimers (29), whether they are formed only on exposure to IgE, or whether the dimer is the preferred state on the cell surface remains to be determined; it is known 'wild-type' FcεRI-α receptors are normally evenly spaced over the cell surface (25) and not clustered. Parallel or non-symmetric dimerisation of FcR with D2ε could cause masking of the mAb 47 epitope on one of the receptors, leading to a lower estimation of receptor expression than determination by the B_{max} of IgE binding. Pecht and associates (36, 37) have indicated that the minimal requirement for FcεRI-α signalling is two FcεRI-α with two molecules of IgE. The formation of this dimer may be driven by the γ chain of the receptor, the extracellular domains of FcεRI or both. If the extracellular domains are involved in active dimer formation, it may be possible for the chimeric FcεR to form dimers as well. The conformation of these dimers might cause masking of the mAb 47 epitope on one of the receptors. This however is purely conjecture for chimeric receptors, as the intricacies of dimer formation and interaction have not been established.

Other possible explanations for the apparent differences in cell surface expression are:

(i) affinity - Since the affinity of IgE for FcεRI is very strong (K_D $1x10^{-9}$ -10^{-10} M) (38), compared to that of the mAb 47 (K_D $6x10^{-8}$ M), the apparent reduction in the

number of FcεR chimeras detected by mAb 47, relative to IgE, is a product of weaker affinity.

(ii) valency - Antibodies are bivalent and potentially can bind two epitopes whereas IgE (Fc) binds only one receptor. It could be expected that receptor numbers determined by mAb binding could be up to half that determined by IgE binding.

These two points are obvious, but there are two arguments against them; one, expression determined by antibody has been standardised to be relative to the binding of εεγ, and this negates the affect of affinity and stoichiometric differences; and two, there is one chimera that does not fit the overall pattern, mAb 47 detects twice as many surface expressed chimeras of γεγ as does IgE binding.

It is possible that the reduction in IgE binding of the γεγ chimera is an effect of the chimeric FcγRIIa first domain (which is less similar to FcεRI than are FcγRIIIa or FcγRIIIb). Inclusion of the G strand of D1 into the γεγ chimera appears to increase IgE binding relative to mAb binding. However, mAb binding in the γεγ chimera was determined using flow cytometry whilst γ(Gε)εγ was determined by an iodinated monoclonal antibody, therefore the two are not directly comparable (Table 4.II). The crystal structure of the IgE Fc:FcεRI-α interaction indicates that the D1 G strand, D2 A strand linker region comprises part of the IgE binding site, thus inclusion of this region may well increase IgE binding (38). The interdomain interface of FcεRI-α has been shown to be important in supporting the IgE binding site (see Chapter 3). This would infer that mAb 47 binds the epitope on the γεγ chimera readily, but only half these receptors are capable of binding IgE. This difference could be caused by a shift in the proposed equilibrium between two receptor forms, but is more probably caused by a conformational change due to disruption of the interdomain interface. The disruption appears to be exacerbated by the inclusion of the relatively rigid FcγRIIa peptide anchor, as γεRIII does not display the same level of distortion regarding IgE binding.

Thus, it can be concluded that there is greater access of IgE to the binding site than access of mAb 47 for its epitope, and that disruption of the binding site and receptor presentation and configuration are probably the most important facets of these interactions.

The GPI and peptide anchored forms of a receptor display a difference in affinity for IgE— Binding affinity as well as apparent cell surface expression, is seen here to vary with the form of membrane anchor; but whereas cell surface expression is seen to increase where a peptide membrane anchor is replaced with a GPI anchor, affinity for ligand decreases. This difference may simply be due to the presence of the membrane anchor itself. However, this is unlikely to be the case as the anchor does not interact with the IgE ligand. It is more likely that decrease in affinity is the product of presentation of the receptor in the membrane. The lipid nature of the GPI anchor makes it more flexible than a peptide membrane anchor, and it has greater mobility within the membrane (39). This mobility may afford greater access to ligand, but at the same time concedes a reduction in rigidity that may be necessary for high affinity binding.

FcγRI and FcγRIIIa both need the presence of the γ chain to achieve maximum affinity (1), and others have postulated that the reduced affinity of FcεRI-α when expressed using the peptide anchor of FcγRIIa may be due to the lack of the γ chain that is integral to the naturally expressed FcεRI-α (5). Miller *et al.* suggested that the lower affinity of the GPI membrane anchor form of FcγRIII (FcγRIIIb) compared to that of the peptide anchored FcγRIIIa (2) could also be due to the lack of the γ chain, which is also necessary for the expression of the peptide anchored receptor. We find here that εεγ - with the FcγRIIa peptide anchor- displays lower affinity for ligand (K_D:$2x10^{-9}$ M) than the 'wild-type' rat receptor (RBL FcεRI $1x10^{-10}$M (40) although within the general range for human FcεRI (~$1x10^{-9}$ -$1x10^{-10}$ M (38), and that εεRIII displays a lower affinity again (K_D $7.9x10^{-9}$ M). The low affinity of the GPI receptor profile could be exacerbated by the tendency of FcγRIII to shed from the cell surface when bound to ligand (41), and the naturally weak insertion of GPI proteins into the cell membrane (42).

From the above, is it possible that receptors that display low affinities are capable of higher receptor occupancy? Does the organisation of receptors on the surface of cells affect affinity? For example, does clustering of large numbers of receptors impede their interaction with ligand? Conversely, when receptors are present in low numbers or with low occupancy, does this improve the chance of ligand binding? High affinity, with low copy numbers of a receptor may be of physiological advantage, and the development of

high affinity when receptors are plentiful would not be a critical driving force for evolution. The expression/affinity phenomenon has been observed for mouse FcγRI in BALB/c and NOD mice where the NOD mice have low expression of a mutated receptor that has much higher affinity than the 'wild-type' receptor (3), and also in FcγRIIIa and FcγRIIIb where FcγRIIIa has lower expression than FcγRIIIb but a higher affinity for ligand (1, 2).

In summary, we can conclude that replacement of a peptide anchor with a GPI anchor causes a reduction in affinity for ligand, along with an increase in the cell surface expression of the receptor. These changes in receptor properties are probably the result of an alteration in the display of the extracellular protein due to the more flexible nature of the GPI anchor, the loose insertion of the GPI anchor in the membrane, and the slower endocytosis of the GPI linked receptor.

RESULTS

PART B.

The Rapid Expression and Recovery of Recombinant FcεR for Surface Plasmon Resonance Analysis.

4.B.I. The Development of an Orientation Dependent IgE:FcR Binding Assay

In order to ensure that the reduction in affinity and the apparent increase in expression seen in the GPI anchored chimeras was due to the cell surface presentation of the receptor caused by the nature of the anchorage and not a structural alteration it was necessary to develop an alternative method of measuring the binding of receptor to IgE without the physical constraints of cell surface presentation. Previous methods to determine the dynamic interactions between IgE and FcεRI when the receptor is soluble have used fluorescence (32), isothermal titration calorimetry (43) and circular dichroism spectroscopy (43). Despite attempts in this and other laboratories, there has been no information published to date describing a viable SPR assay with IgE immobilised directly on the chip. This is probably because IgE has been found to be unable to bind receptor when immobilised on SPR chips (and indeed ELISA plates). In one report mouse anti-IgE antibody was immobilised onto an SPR chip and this was used to immobilise mouse IgE, before interaction with receptor in the fluid phase (44). This approach enjoyed some success, although the authors found computational problems in the analysis of the dissociation of the mouse IgE from the anti-IgE on the chip during the procedure. In a second report immobilised IgE was used (45) with no methodology detailed in the publication and no confirmatory publication.

Several problems needed to be addressed in the development of a useful SPR based assay for the work described in this thesis:

i. Human IgE was ideally required for the assay, but was found to be difficult to access with both a known antigen and in financially viable quantities.

ii. Mouse IgE was available with a known antigen (NP), but binds human FcεRI with a lower affinity than human IgE.

iii. Active chimeric (human Fc -Cϵ2, Cϵ3, Cϵ4- mouse Fab) IgE recognising a known antigen (NP) and was commercially available (Serotec).

iv. IgE anti-NP was unable to bind NP when the NP was coated directly onto an ELISA plate or a SPR chip. This suggested that appropriate spacing of NP from the SPR chip surface was necessary to allow IgE to bind.

v. Whilst NP is commonly conjugated to BSA for use in other assay systems (e.g. ELISA), it was found that this produced a surface with variable levels of NP.

A novel method to 'space' the NP from the SPR surface was devised using NP-Cap-OSu (Genosys). It was envisaged that the caproic succinate would act as a spacer between the NP hapten and the chip surface, couple firmly to the chip, and permit IgE anti-NP binding. It would also provide a surface that could withstand harsh regeneration conditions.

The dextran surface of the SPR chip was activated using 1:1 EDC:NHS (70 µl, 10 µl/min) according to the manufacturer's instructions. The carboxyl surface (activated ester sites) was transformed to an amino surface using 1,3 diamino propane (Sigma, 100 µl 12 mM, 10 µl/min). The amino groups were then available to react with the succinate ester/ carboxyl groups (100 µl, 10 mM NP-Cap-OSu, 1 µl/min, RU~600) on the chip surface (Figure 4.13). The chip was washed overnight to remove all traces of unbound NP-Cap-OSu. IgE anti-NP bound the immobilised NP with high affinity ($\sim K_A > 10^{10}$ M^{-1} from the SPR trace). Purified soluble FcϵRI bound the IgE Fc (Figure 4.14), and binding specificity was confirmed using an anti-FcϵRI mAb (Figure 4.15).

A variety of procedures were tested to regenerate the SPR chip, it was not possible to effect release or removal of the receptor without losing the IgE however, the inorganic (non-proteinaceous) nature of the surface enabled the use of sodium dodecylsulphate (SDS) desorb solution (0.5% SDS, 150 µl, 10 µl/min) to remove both the receptor and the IgE without affecting the NP surface. Two washes with water (50 µl, 10 µl/min) were used to remove residual SDS (Figure 4.16). Repeated infusions of anti-NP produced consistent levels of binding recorded in response units (RU). It is worthwhile mentioning that thorough cleaning of the biosensor with SDS and rinsing with water using a cleaning chip was necessary, after application of the NP-Cap-OSu in preparation of the chip, and before

Figure 4.13 Diagram depicting the preparation of the nitrophenol BIAcore surface plasmon resonance chip.

(A) Depicts the BIAcore SPR chip with its carboxyl surface. This was activated by (1) EDC/NHS.

(B) The activated carboxyl surface was transformed to an amino surface by the addition of (2) diamino propane (DAP).

(C) Depicts the final NP surface of the chip generated by the passage of (3) NP-Cap-OSu over the amino surface of the SPR chip. The succinate ester of the NP-Cap-OSu reacted with the amino surface, producing an oriented NP surface spaced away from the BIAcore SPR chip.

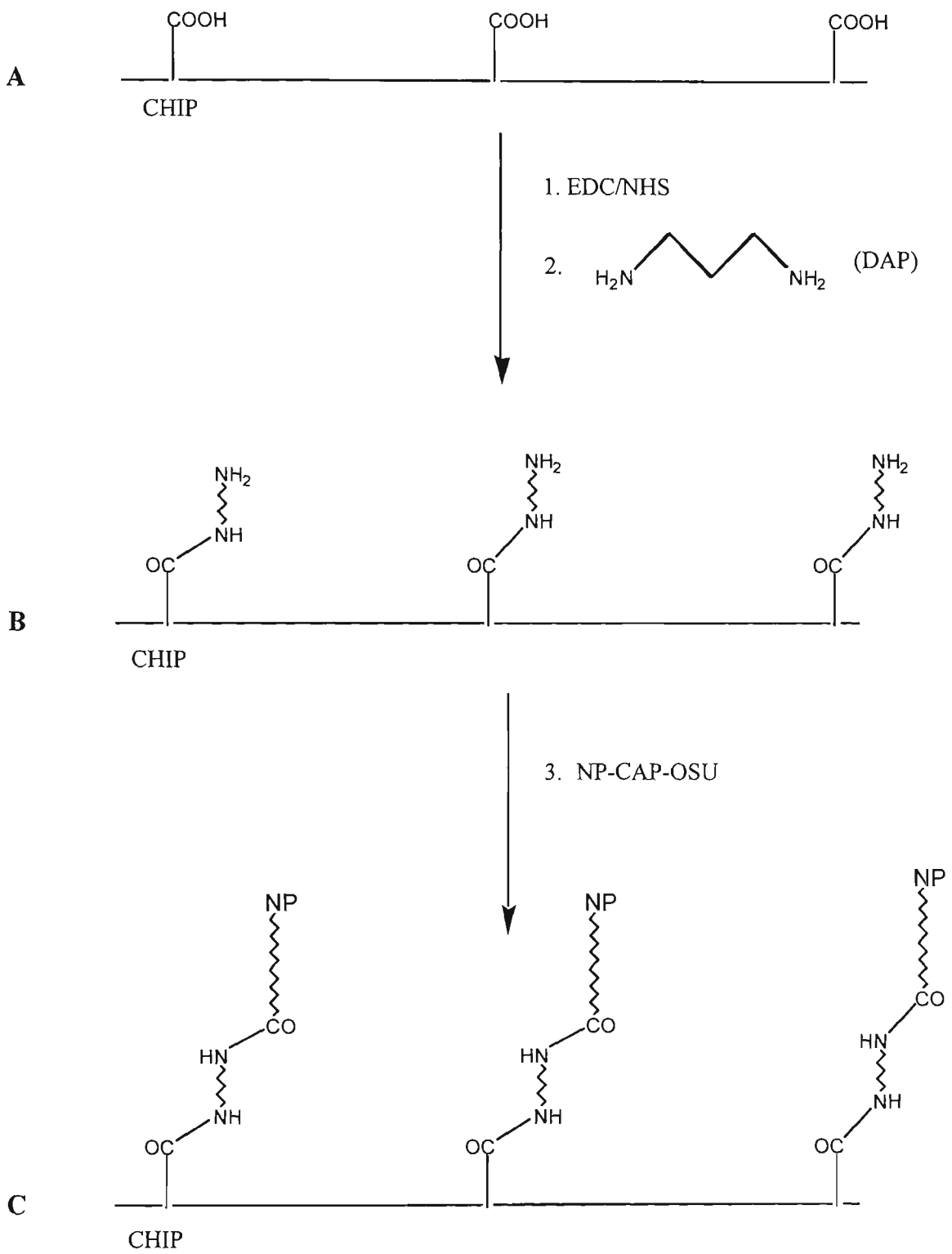
A
COOH
COOH
COOH
CHIP
1. EDC/NHS
2.
H2N
NH2
(DAP)
B
NH2
NH
OC
CHIP
3. NP-CAP-OSU
C
NP
CO
HN
NH
OC
CHIP

Figure 4.14 Diagram depicting the binding of IgE and FcεRI to the NP coupled SPR chip.

1. Depicts the NP coupled BIAcore SPR chip.
2. Shows the IgE anti-NP binding the NP through the Fab binding region in Cε1.
3. The two domain soluble FcεRI (shaded) is shown binding the exposed Cε3 domain of IgE.

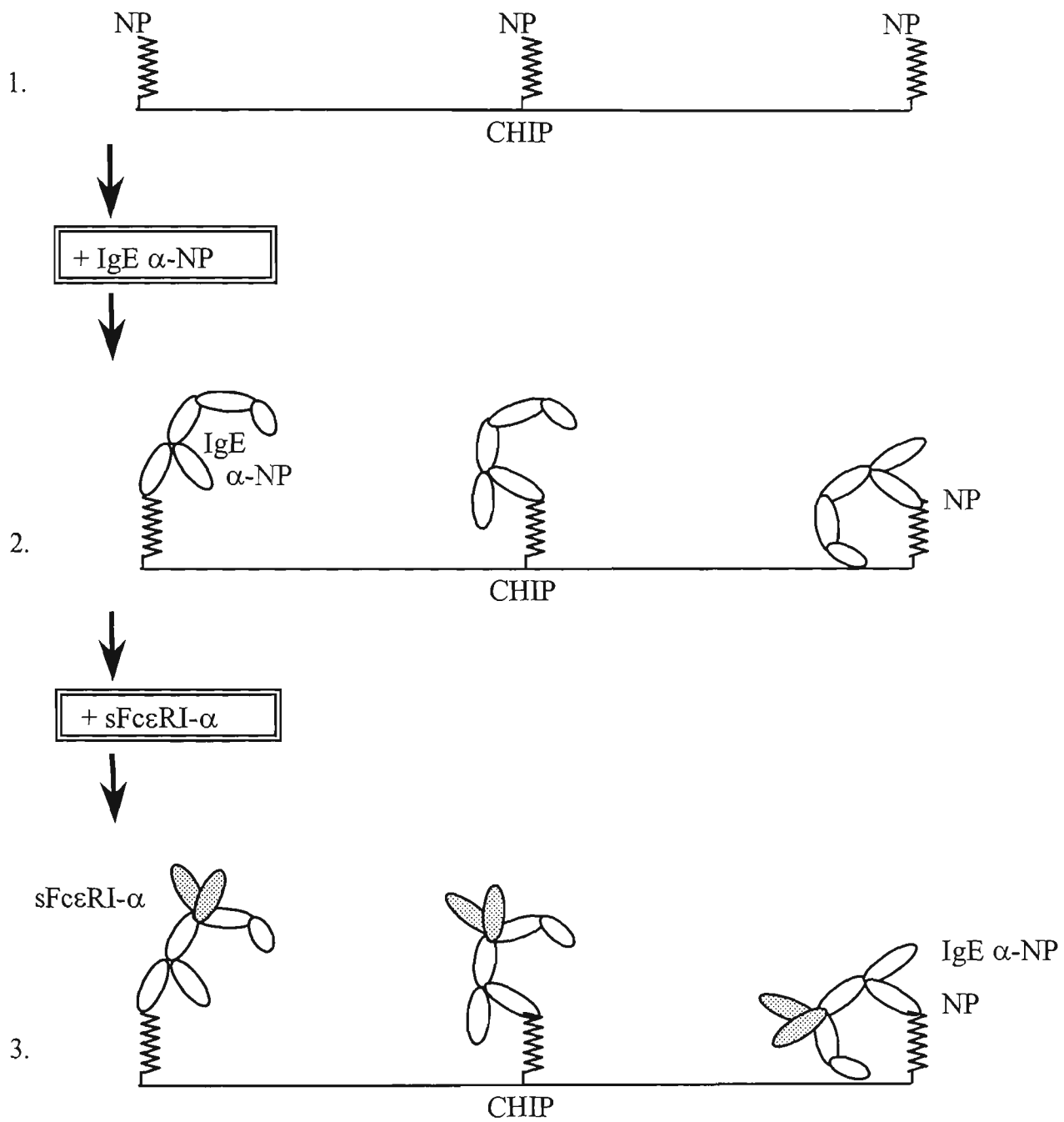
1.
NP
NP
NP
CHIP
+ IgE α-NP
2.
IgE
α-NP
NP
CHIP
+ sFcεRI-α
3.
sFcεRI-α
IgE α-NP
NP
CHIP

Figure 4.15 Sensorgram[1] showing the binding of IgE anti-NP and FcεRI to the NP- Cap- OSu SPR chip.

Numbers in brackets in the trace correspond to:

1. The baseline for the NP-Cap-OSu coupled chip.

2. IgE anti-NP binds the NP surface with high affinity. The horizontal trace following the completion of the IgE anti-NP injection indicates little or no dissociation of the IgE for its NP ligand. This suggests an apparent dissociation constant (K_D) of $>1x10^{-10}$ M.

3. FcεRI binds the IgE anti-NP. After maximum binding an initial rapid dissociation of the receptor from the ligand can be observed. This is commonly observed in the highly sensitive SPR assays, although not detected in conventional assay systems.

4. The presence of bound FcεRI-α is indicated by the binding of an anti-FcεRI-α monoclonal antibody (3B4).

[1] Interpretation of a sensorgram is described in Appendix III.

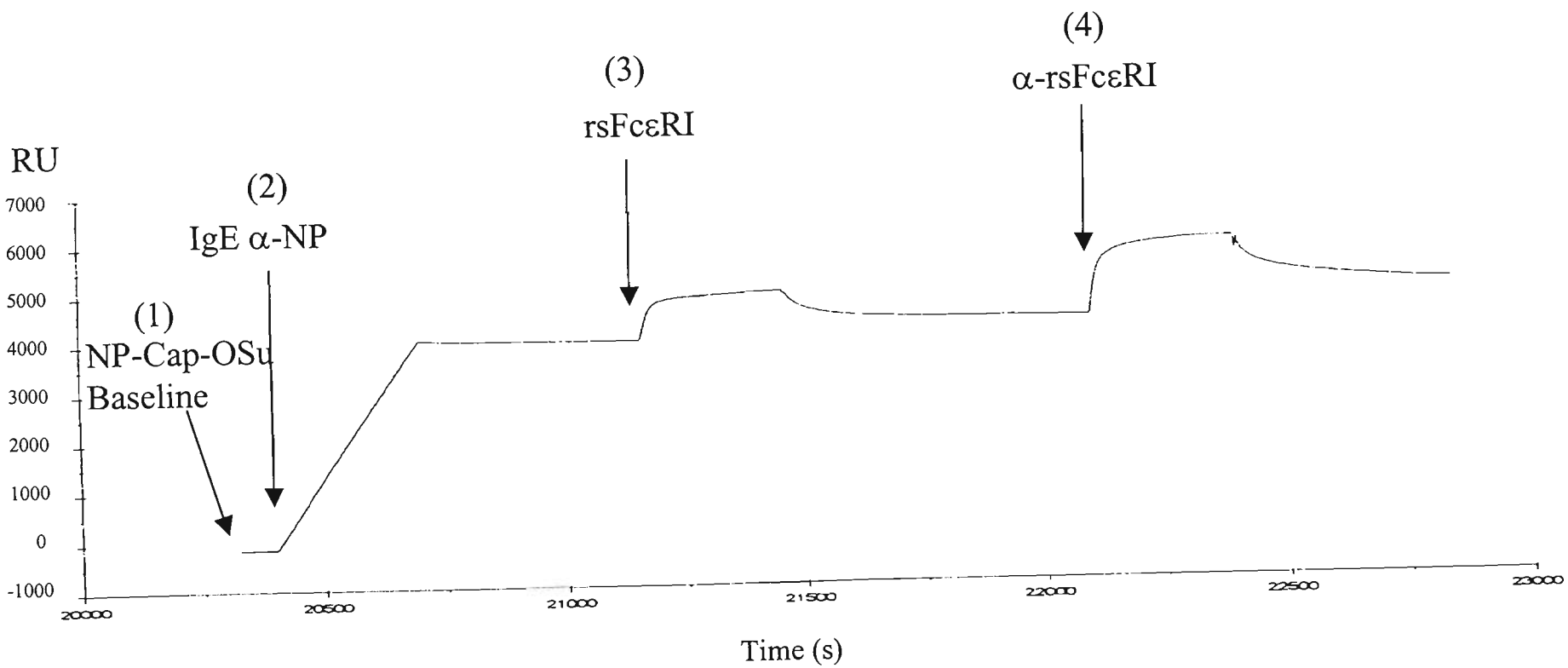
RU
7000
6000
5000
4000
3000
2000
1000
0
-1000
(1)
NP-Cap-OSu
Baseline
(2)
IgE α-NP
(3)
rsFcεRI
(4)
α-rsFcεRI
20000
20500
21000
21500
22000
22500
23000
Time (s)

Figure 4.16 Sensorgram showing the ability of 10% sodium dodecylsulphate (SDS) to regenerate the NP-Cap-OSu SPR chip surface.

Numbers in brackets in the trace correspond to:

1. Baseline of NP-Cap-OSu surface.
2. IgE anti-NP binds the NP surface with high affinity.
3. SDS regeneration causes dissociation of the anti-NP IgE from the NP surface and the chip regains the original baseline.

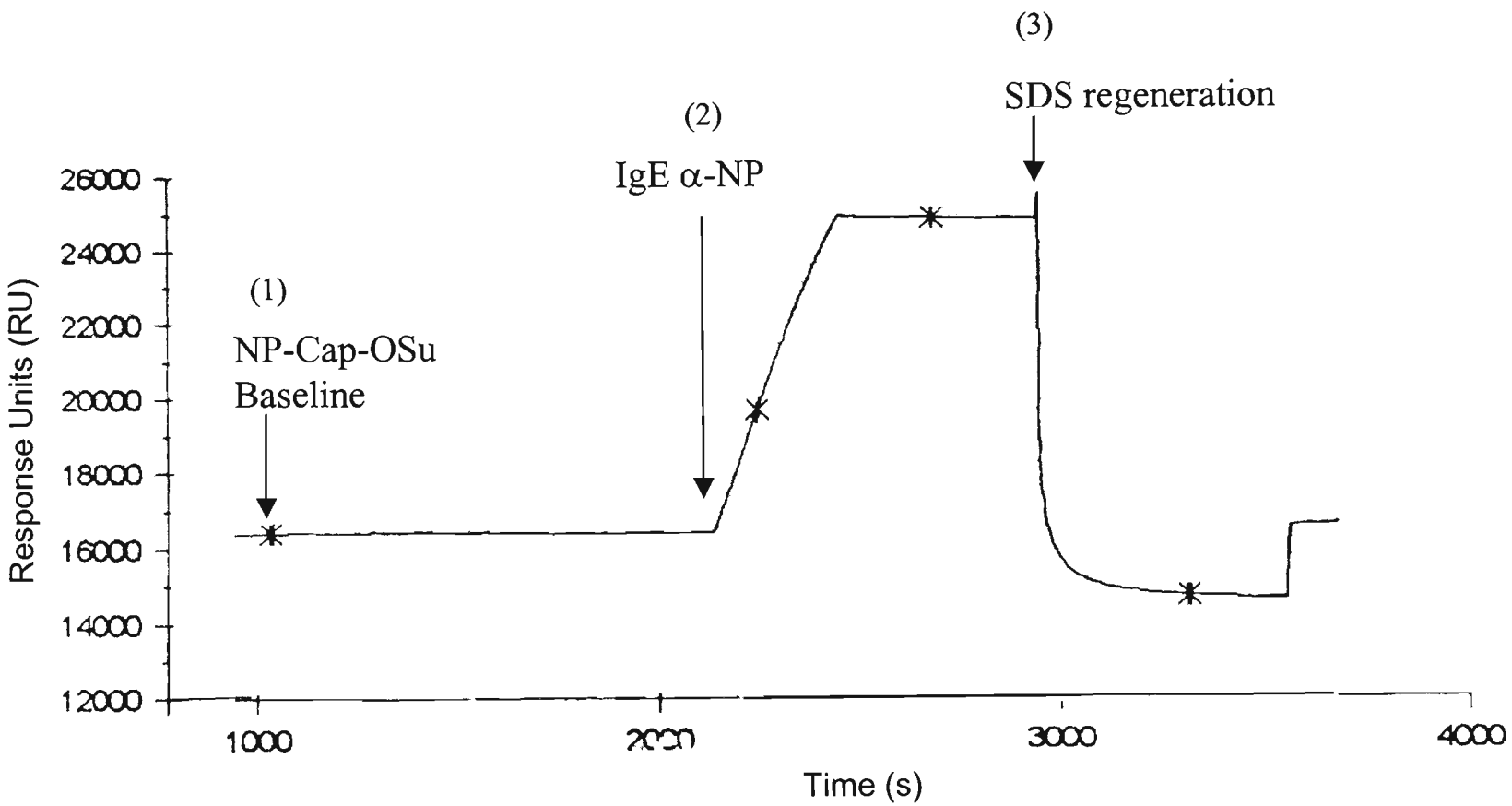
(3)
SDS regeneration
(2)
IgE α-NP
(1)
NP-Cap-OSu
Baseline
Response Units (RU)
26000
24000
22000
20000
18000
16000
14000
12000
1000
2000
3000
4000
Time (s)

each use of the NP chip; in the latter case to prevent extraneous protein being deposited on the chip.

To determine the apparent equilibrium dissociation constant of FcεRI-α with IgE anti-NP, a series of increasing concentrations of rsFcεRI-α were passed over a consistent concentration of IgE anti-NP bound to a NP-Cap-OSu coupled chip surface. The IgE was bound in excess so that binding of the receptor was not limited by a lack of availability of Fc sites. Equilibrium data from the experiments was fed into the 'BIAevaluation' program produced for the BIAcore BIAsensor, and the curve fitting program 'Curve Expert'[2] resulting in an affinity of purified soluble FcεRI-α of K_D $2.3x10^{-8}$ M; by global analysis of the kinetic data using the 'Clamp' program (46) the affinity was found to be K_D $9.1x10^{-9}$ M. This is not consistent with cell binding data (K_D $2.1x10^{-9}$ M see Table II Chapter 3 page 90), and could be the result of a minor conformational change in the structure of IgE caused by Fab binding prior to the binding of Fc - the reverse of the customary order of events. It has also been observed that soluble recombinant FcεRI-α produced in *P. pastoris* binds to IgE with a lower affinity than the same receptor produced in CHO cells, or baculovirus (H. Trist, A.R.I., Melbourne, Australia, personal communication). These variations may be due to differences in post translational modification.

[2] The Curve Expert program (written by Daniel Hyams) is found at web-site http://www2.msstate.edu/~dgh2/cvxpt.htm

The Evaluation of a Rapid Expression and Recovery of Chimeric FcεR for SPR Analysis.

4.B II. Development and Evaluation of a Method for Rapid Analysis of IgE Binding to FcεRI and Chimeric Receptors

Attempts were made to develop a rapid method for analysis of binding IgE to FcεRI and chimeric receptors using the assay developed above and exploiting the GPI membrane anchor for production of soluble receptors. The assay utilised transient transfection of the receptor cDNA, and the ability of phosphoinositol phospholipase C (PIPLC) to cleave the GPI anchor at the membrane surface thus releasing the receptor in soluble form. To determine the feasibility of testing cleaved receptor, COS-7 cells were transiently transfected with cDNA of : a) εεγ - FcεRI with the FcγRIIa peptide membrane anchor, or b) εεRIII - FcεRI with the FcγRIIIb GPI membrane anchor, or c) plasmid alone (mock). After 36 hrs, the cells expressing the chimeric FcεRI or mock transfected cells, were incubated in 1 ml Hepes buffered saline (HBS) with 0.1 U/ml of PIPLC a) with 0.5% BSA, b) without BSA, or c) HBS without PIPLC. The cells were incubated for 1 hour at 37^{0}C, the supernatant then harvested and tested for the presence of FcεRI by ELISA (Material and Methods, Chapter 2). The treated cells were also tested for the presence of residual FcεRI by EA rosetting (Table 4.III, Figure 4.17).

To determine the feasibility of using GPI released FcεRI in this assay system, flasks of 3x10^6 COS-7 cells were then transiently transfected with cDNA of : a) εεγ - FcεRI with the FcγRIIa peptide membrane anchor, or, b) εεRIII - FcεRI with the FcγRIIIb GPI membrane anchor. After 36 hrs, the cells, expressing FcεRI, were lifted from the flask, washed gently in HBS, resuspended and incubated in 1 ml HBS or HBS with 10^{-1}, 10^{-2}, 10^{-3}, 10^{-4}, or 10^{-5} U/ml of GPI specific Phospholipase C (Boehringer Mannheim). The cells were incubated for 1 hour at 20^{0}C, spun down gently, the supernatants were then harvested and tested for :

(i) the presence of FcεRI by ELISA (Figure 4.18, for Material and Method see Chapter 2),

(ii) binding to IgE by the SPR method above (Figure 4.19).

Table 4.III.

PIPLC cleaves the GPI anchored (ϵϵRIII) but not the peptide anchored (ϵϵγ) form of FcϵRI from the cell membrane.

	ϵϵγ[1]			ϵϵRIII[2]			mock[3]		
PIPLC[4]	+PIPLC	+PIPLC	+HBS	+PIPLC	+PIPLC	+HBS	+PIPLC	+PIPLC	+HBS
0.1U/ml	+BSA	-BSA		+BSA	-BSA		+BSA	-BSA	
EA Rosetting[5]	++	++	++	-	-	++	-	-	-
ELISA[6]	-	-	-	++	++	-	-	-	-

1. FcϵRI with the cytoplasmic anchor of FcγRIIA
2. FcϵRI with the glycosylphosphoinositol (GPI) anchor of FcγRIIIB
3. 'Mock' indicates transfection of plasmid alone without the FcϵRI construct.
4. Phosphoinositol phospholipase C (GPI specific)
5. Visual determination of FcϵRI on the surface of transiently transfected COS cells by avidity (the binding of IgE coupled erythrocytes to the receptors).
6. Determination by ELISA of the presence of soluble FcϵRI in the supernatant of transiently transfected cells incubated with PIPLC (see Experimental Procedures).

This table shows that COS-7 cells transiently transfected with a membrane anchored form of FcϵRI (ϵϵγ) bind IgE coated erythrocytes after incubation with 0.1U/ml PIPLC, and that the supernatant is negative for FcϵRI when tested by ELISA. COS-7 cells transiently transfected with a GPI anchored form of FcϵRI (ϵϵRIII) differ from ϵϵγ transfected cells as they do not bind IgE coated erythrocytes after incubation with 0.1U/ml PIPLC, and the supernatant is positive for FcϵRI when tested by ELISA. This implies that PIPLC is able to cleave the FcϵRI from the GPI anchor, and the receptor is then present in a soluble form in the PIPLC supernatant. BSA has no affect on the ability of the PIPLC to cleave the receptor. Mock transfected cells do not express FcϵRI.

Further analysis of receptor:ligand interactions was performed by cleaving both the $\epsilon\epsilon$RIII and $\gamma\epsilon$RIII receptors from the cell membrane with PIPLC, and assaying IgE binding capacity by the SPR method above.

Figure 4.17 EA Rosetting of ϵϵRIII transfected COS-7 cells.

A. ϵϵRIII (FcϵRI with GPI membrane anchor) transfected COS cells treated (rosetted) with sheep erythrocytes that have been coated with moIgE anti-TNP (EA's). EA coated COS cells (rosettes) are present, indicating the presence of the ϵϵRIII on the cell surface. This transfection can be seen to be of low efficiency as the percentage of rosetted to non-rosetted cells is less than 80% (See Figure 4.3 for comparison).

B. ϵϵRIII transfected COS cells rosetted with moIgE anti-TNP EA's, after treatment with PIPLC to release the GPI anchored proteins. It can be seen that there are no rosetting COS cells present, indicating that the ϵϵRIII receptors have been cleaved by the PIPLC and released into the supernatant.

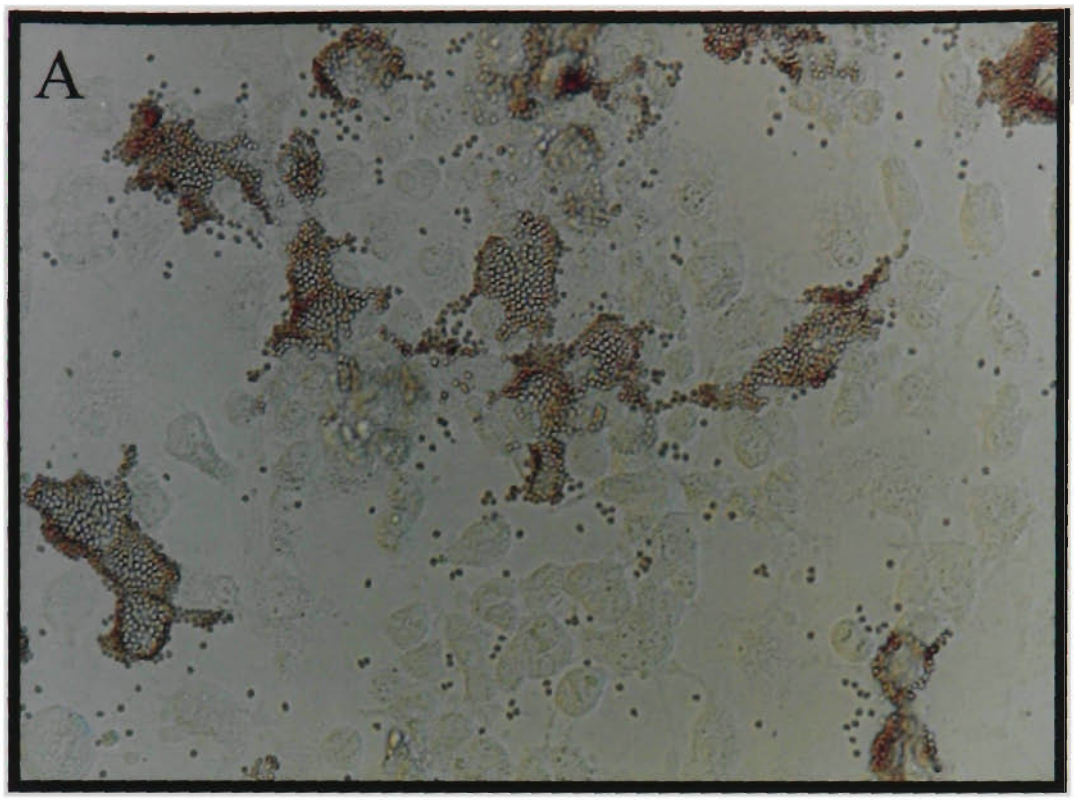
A

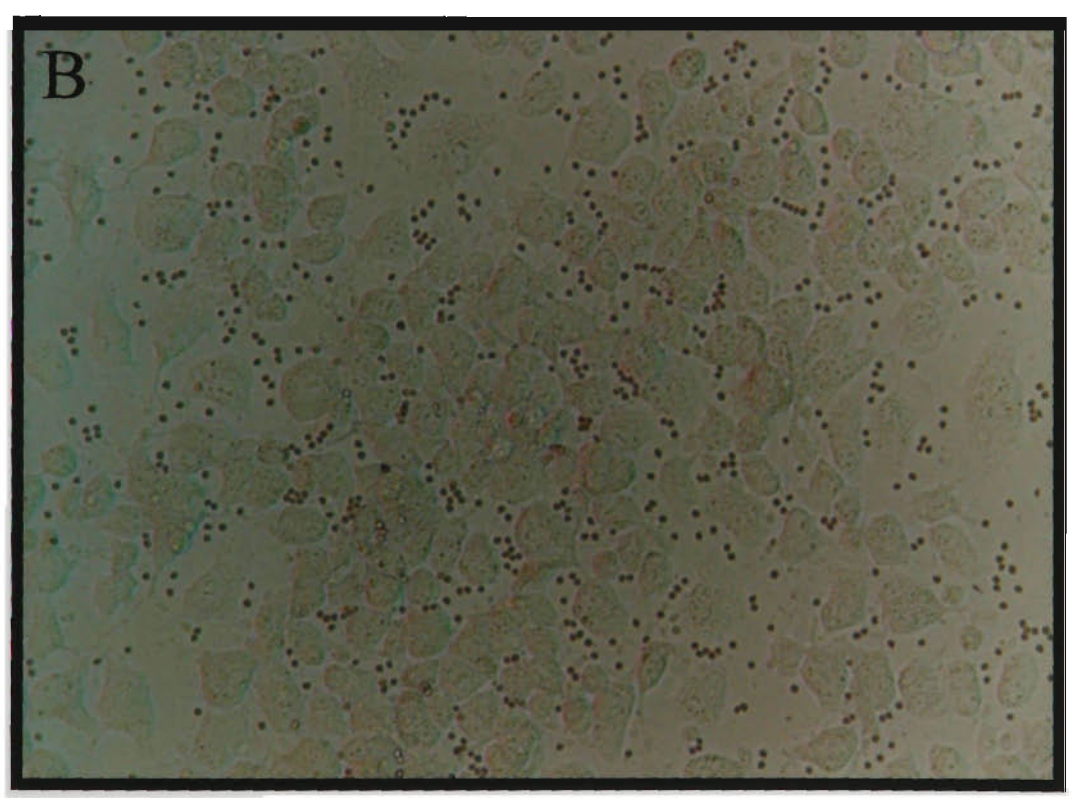
B

Figure 4.18 Graph indicating the presence of FcεRI in the supernatant of COS-7 cells expressing εεRIII and treated with PIPLC.

The abcissa indicates the dilution of the supernatant containing soluble FcεRI-α derived from the treatment of COS cells expressing εεRIII and treated with PIPLC.

The ordinate indicates the optical density (O.D.) of the ELISA colour reaction (λ=490nm). The higher the O.D. reading, the greater the concentration of soluble FcεRI in the supernatant.

Four concentrations of PIPLC (10^{-1}, 10^{-2}, 10^{-3} and 10^{-4} U/ml) were tested for their ability to cleave GPI anchored receptor.

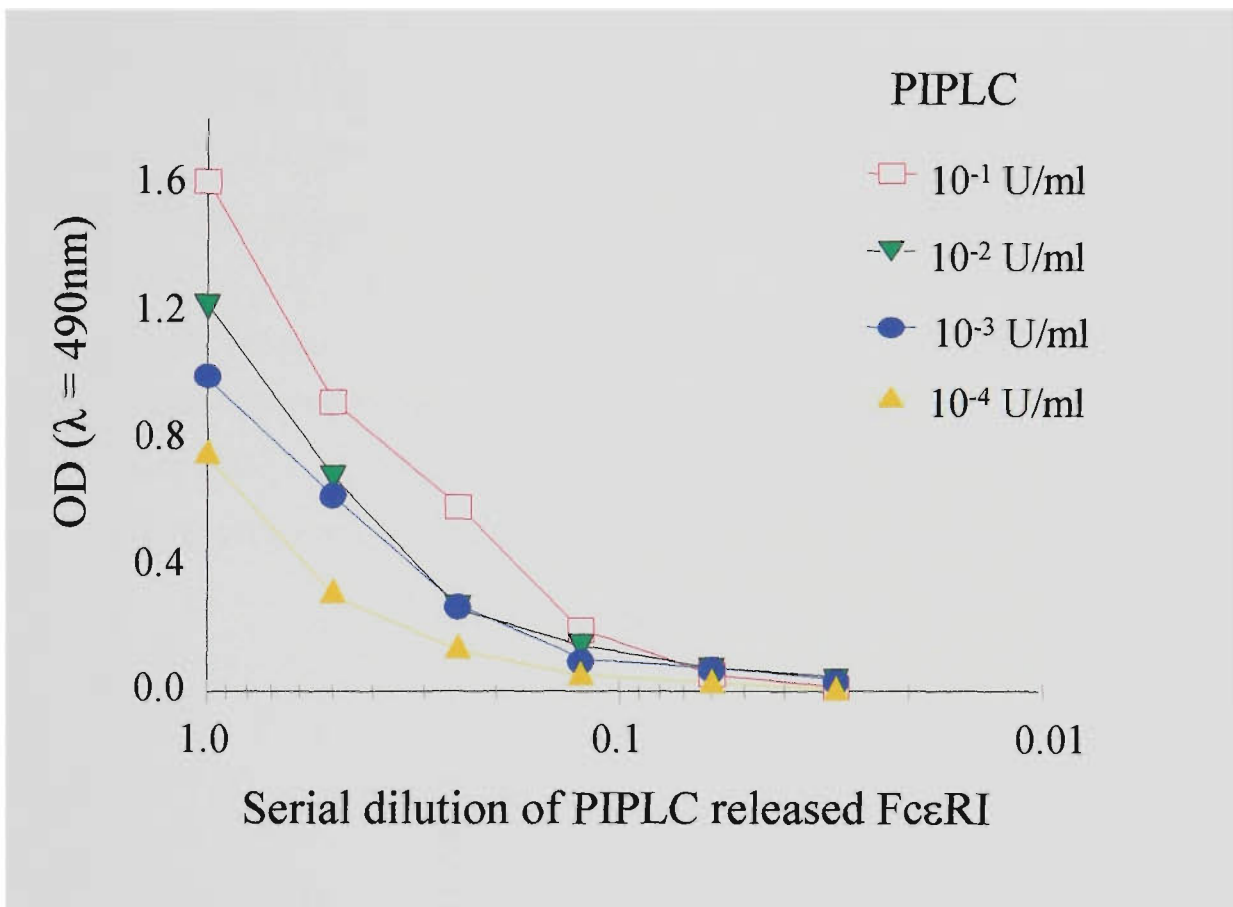
PIPLC
10-1 U/ml
10-2 U/ml
10-3 U/ml
10-4 U/ml
OD (λ = 490nm)
1.6
1.2
0.8
0.4
0.0
1.0
0.1
0.01
Serial dilution of PIPLC released FcεRI

Figure 4.19 Sensorgrams showing the binding of soluble FcεRI to the human IgE (anti-NP) antibody immobilised on the NP SPR chip.

The upper trace depicts the binding of purified recombinant soluble FcεRI to the immobilised human IgE.

The lower trace depicts the binding of PIPLC-released FcεRI from εεRIII transfected COS cells to the same human IgE surface. It is clear that FcεRI bound to ligand, however the concentration of the PIPLC-cleaved receptor was very low in the experiments.

The bar in each of the two traces indicate the association phase of the FcεRI binding to IgE.

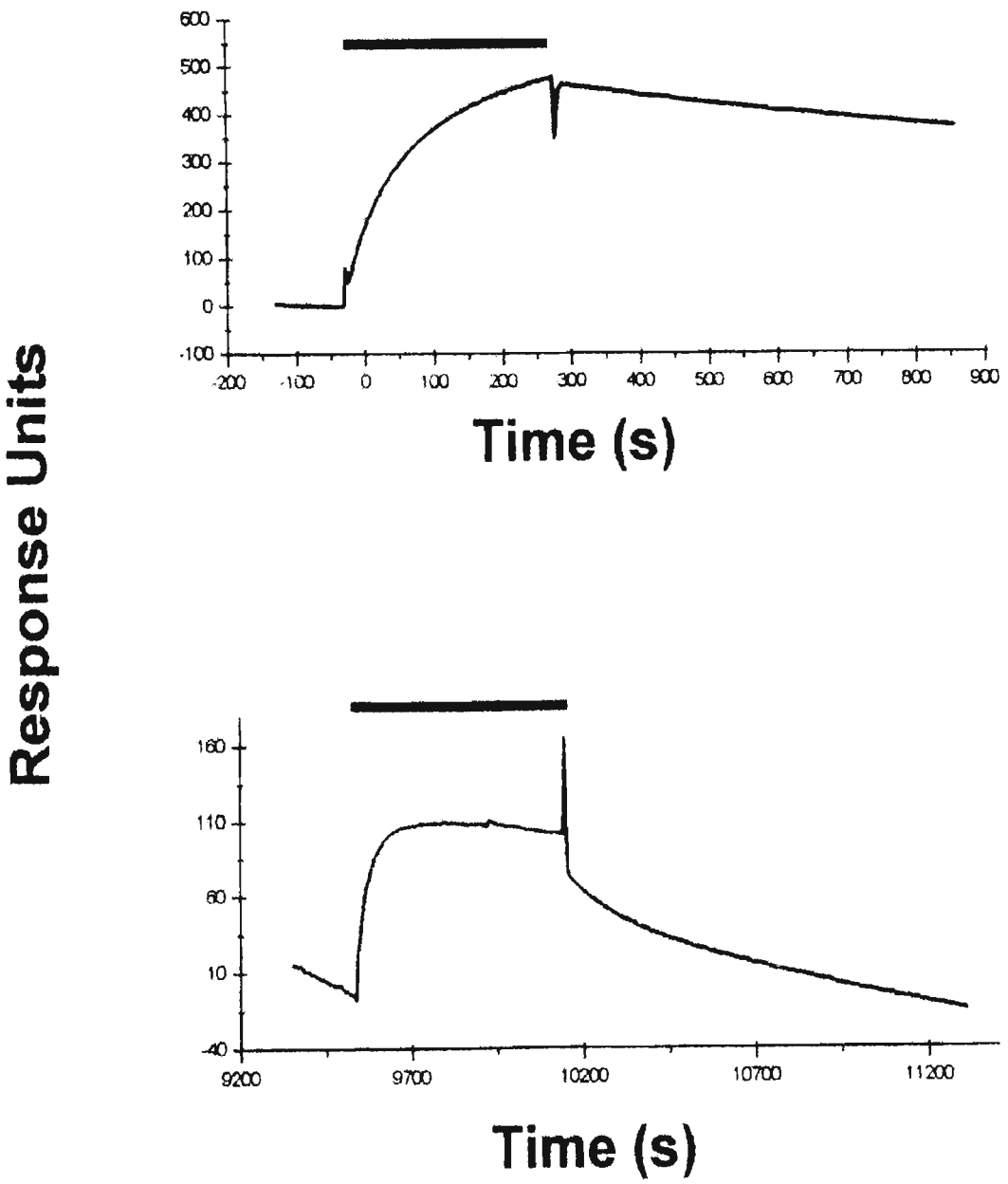
Response Units
600
500
400
300
200
100
0
-100
-200
-100
0
100
200
300
400
500
600
700
800
900
Time (s)
160
110
60
10
-40
9200
9700
10200
10700
11200
Time (s)

DISCUSSION

When IgE is immobilised on an SPR chip (and indeed ELISA plates) it is unable to bind to its receptor when the receptor is in the mobile phase (unpublished observations H.Trist, A.R.I., Melbourne, Australia). Whilst one cannot be certain of the reason for this, it is likely that the IgE immobilised on the chip is oriented so that the Fc region is not presented to the mobile phase. Monoclonal antibodies raised to IgE with an epitope distant from the receptor binding region, such as ATCC clone HB121, are able to detect the presence of IgE on the SPR chip surface (unpublished observations H.Trist, A.R.I., Melbourne, Australia). This implies that the immunoglobulin has not been denatured by the coupling procedure further suggesting that incorrect orientation on the chip is the major cause of the inability of the coupled IgE to bind soluble receptor. Because of the inactivity of immobilised IgE, methods such as analytical centrifugation have been necessary in the past for IgE binding determinations (43).

From rosetting experiments it was clear that initial transfection of receptor cDNA into COS-7 cells in 6 well plates was poor, but sufficient FcϵRI-α was released by PIPLC to be detected in an ELISA, and cells that had been treated with PIPLC were not able to form rosettes (Figure 4.17) indicating that the receptor had been released from the cell surface. Thus, the ability to use PIPLC released receptor in a soluble form was possible. Hepes buffered saline is the recommended running buffer in BIAcore experiments as BSA gives high backgrounds. It was therefore advantageous that PIPLC was active in Hepes buffered saline, and that the presence of BSA was neither required for the activity of the PIPLC, nor necessary for protection of the cell during PIPLC activity. This enabled minimum disruption to BIAcore processes since the same buffer could be used for the release of the cell bound receptors and as the BIAcore running buffer during the assay.

Sufficient receptor was released by PIPLC from $5x10^5$ cells to be detected by both ELISA and SPR (see Figures 4.18 and 4.19). Whilst the quantities of receptor released were low there was nonetheless sufficient for detection. However, the binding characteristics of PIPLC-released chimeric receptors were not significantly different from background supernatant taken from PIPLC treated cells transfected with plasmid alone. There was

insufficient time available to investigate the many possible causes of the failure of the PIPLC-released chimeric receptors to bind the immobilised IgE, but continuing work at the A.R.I. will no doubt clarify this issue and produce a valuable assay.

Although the PIPLC-cleaved chimeric receptors were unable to be detected by this method, it is my view that given more time this approach could be developed to a point where it would be suitable for use in the determination of the active concentration (bindability) of chimeric receptors in comparison with a sFcϵRI-α standard, and with the concentration known, the binding characteristics of the cleaved receptors. This method could also be used to ascertain the activity of each batch of PIPLC enzyme.

REFERENCES

1. Miller KL, Duchemin A-M and CL Anderson. A novel role for the Fc receptor γ subunit: Enhancement of FcgR ligand affinity. J Exp Med 1996; 183:2227-2233.
2. Van de Winkel JGJ, and PJA Capel. Human IgG Fc receptor heterogeneity: molecular aspects and clinical implications. Immunol Today 1993; 14:215-221.
3. Gavin AL, Hamilton JA, Hogarth PM. Extracellular mutations of non-obese diabetic mouse FcgammaRI modify surface expression and ligand binding. J Biol Chem 1996; 271(29):17091-17099.
4. McDonnell JM, Beavil AJ, Mackay GA, Jameson BA, Korngold R, Gould HJ, Sutton BJ. Structure based design and characterisation of peptides that inhibit IgE binding to its high affinity receptor. Nat Struct Biol 1996; 3(5):419-426.
5. Cook JP, Henry AJ, McDonnell JM, Owens RJ, Sutton BJ, and Gould HJ. Identification of contact residues in the IgE binding site of human FcεRIα. Biochemistry 1997; 36(50):15579-15588.
6. Henry AJ, Cook JP, McDonnell JM, Mackay GA, Shi J, Sutton BJ, Gould HJ. Participation of the N-terminal region of Cepsilon3 in the binding of human IgE to its high-affinity receptor FcepsilonRI. Biochemistry 1997; 36(50):15568-78.
7. Powell MS, Barton PA, Emmanouilidis D, Wines BD, Neumann GM, Peitersz GA, Maxwell KF, Garrett TPJ, and Hogarth PM. Biochemical analysis and crystallisation of FcgRIIa, the low affinity receptor for IgG. Immunology Letters 1999; 68:17-23.
8. Harrison PT, Campbell IW and JM Allen. Use of GPI-anchored proteins to study biomolecular interactions by surface plasmon resonance. FEBS letters 1998; 422:301-306.
9. Low MG, Zilversmit DB. Role of phosphatidylinositol in attachment of alkaline phosphatase to membranes. Biochemistry 1980; 19(17):3913-3918.
10. Low MG and Saltiel AR. Structural and functional roles of glycosyl-phosphatidylinositol in membranes. Science 1988; 239:268-275.
11. Selvaraj P, Rosse WF, Silber R, and Springer TA. The major Fc receptor in blood has a phosphatidyl-inositol anchor and is deficient in paroxysmal nocturnal haemoglobulinuria. Nature 1988; 333: 565-567.
12. Simmons D, and Seed B. The Fcγ receptor of natural killer cells is a phospholipid-

linked membrane protein. Nature 1988; 333:568-570.

13. Englund PT. The structure and biosynthesis of glycosyl phosphatidylinositol protein anchors. Annu Rev Biochem 1993; 62:121-138.
14. Hulett MD, McKenzie IFC, Hogarth PM. Chimeric Fc receptors identify immunoglobulin-binding regions in human FcγRII and FcεRI. Eur J Immunol 1993; 23:640-645.
15. Hogarth PM, Ierino FL, Hulett MD. Characterisation of FcR Ig-Binding Sites and Epitope Mapping. Immunomethods 1994;4:17-24.
16. Hibbs ML, Selvaraj P, Carpen O, Springer TA, Kuster H, Jouvin M-H, and Kinet J-P. Mechanisms for regulating expression of membrane isoforms of FcγRIII (CD16). Science 1989; 246:1608-1611.
17. Lanier LL, Cwirla S, Yu G, Testi R and JH Phillips. Membrane anchoring of a human IgG Fc receptor (CD16) determined by a single aminoacid. Science 1989; 246:1611-1613.
18. Sambrook J, Fritsch EF, and Maniatis T. In *Molecular Cloning: A Laboratory Manual*, 1989 2nd Ed., Cold Spring Harbor Laboratory, Cold Spring Harbor, NY.
19. Liu F-T, Bohn JW, Ferry EL, Yamamoto H, Molinaro CA, Sherman LA, Klinman NR, and Katz DH. Monoclonal dinitrophenyl - specific murine IgE antibody: preparation, isolation, and characterization. J Immunol 1980; 124(6):2728-2737.
20. Lopez A.F., Strath M, Sanderson CJ. Mouse immunoglobulin isotypes mediating cytotoxicity of target cells by eosinophils and neutrophils. Immunology 1983; 48:503.
21. Varin-Blank N, Metzger H. Surface expression of mutated subunits of the high affinity mast cell receptor for IgE. J Biol Chem 1990; 265(26):15685-15694.
22.. MacGlashan Djr, McKenzie-White J, Chichester K, Bochner BS, Davis FM, Schroeder JT, Lichtenstein LM. In vitro regulation of FcεRIα expression on human basophils by IgE antibody. Blood 1988; 91(5):1633-1643.
23. Kinet JP. The High Affinity IgE receptor FcεRI: from physiology to pathology. Annu Rev Immunol 1999; 17:931-972.
24. Turner AJ. The diversity of lipid modification of proteins. In '*Lipid modification of proteins*'. Ed Hooper NM and Turner AJ. Oxford University Press, 1992:1-13.
25. Santini F, Keen JH. Endocytosis of activated receptors and clathrin coated pit formation: deciphering the chicken or the egg relationship. J Cell Biol 1996;

132:1025-1036.

26. Isersky C, Rivera J, Segal DM, Triche T. The fate of IgE bound to rat basophilic leukemia cells. II. Endocytosis of IgE oligomers and effect on receptor turnover. J Immunol 1983; 131:388-396.
27. Takeda J, Kinoshita T. GPI anchor biosynthesis. TIBS 1995; 20:367-371.
28. Holowka D, Conrad DH, Baird B. Structural mapping of membrane-bound immunoglobulin E-receptor complexes: Use of monoclonal anti-IgE antibodies to probe the conformation of receptor-bound IgE. Biochemistry 1985; 24:6260-6267.
29. Ortega E., Schweitzer-Stenner R. and I. Pecht. Kinetics of ligand binding to the Type I receptor on mast cells. Biochemistry 1991; 30:3473-3483.
30. Schweitzer-Stenner R., Ortega E and I. Pecht. Kinetics of FcεRI dimer formation by specific monoclonal antibodies on mast cells. Biochemistry 1994; 33:8813-8825.
31. Metzger H. It's spring, and thoughts turn to....allergies. Cell 1999; 97:287-290.
32. Robertson MW. Phage and Escherichia coli expression of the human high affinity immunoglobulin E receptor α-subunit ectodomain. J Biol Chem 1993; 268(17):12736-12743.
33. Schlessinger J., Webb WW., Elson EL and H Metzger. Lateral Motion and Valence of Fc Receptors on Rat Peritoneal Mast Cells. Nature 1976; 264:550-552.
34. Metzger H. The receptor with high affinity for IgE. Immunological reviews 1992; 125:37-48.
35. Maxwell KF, Powell MS, Hulett MD, Barton PA, McKenzie IFC, Garrett TPJ, Hogarth PM. The crystal structure of the human leukocyte Fcreceptor, FcγRIIa. Nat Struct Biol 1999;6(5):437-442.
36. Ortega E., Schweitzer-Stenner R. and Pecht I. Possible orientation constraints determine secretory signals induced by aggregation of IgE receptors on mast cells. EMBO J 1988; 7:4101-4109
37. Schweitzer-Stenner R., Tamir I. and I. Pecht (1997) Analysis of FcεRI-mediated Mast Cell Stimulation by Surface-Carried Antigens. Biophys J 1997; 72:2470-2478
38. Garman SC, Wurzburg BA, Tarchevskaya SS, Kinet J-P, Jardetzky TS. Structure of the Fc fragment of human IgE bound to its high-affinity receptor FcεRIα. Nature 2000;406:259-266.
39. Medof ME, Nagarajan S, Tykocinski ML. Cell-surface engineering with GPI

anchored proteins. FASB J 1996; 10:574-586.

40. Kulczycki Jnr A, Metzger H. The interaction of IgE with rat basophilic leukemia cells. II. Quantitative aspects of the binding reaction. J Exp Med 1974; 140:1676-1695.

41. Huizinga TWJ, de Haas M, Kleijer M, Nuijens JH, Roos D, and von dem Borne AEGKr. Soluble Fcγ Receptor III in human plasma originates from release from neutrophils. J Clin Invest 1990; 86:416-423.

42. Ilangumaran S, Robinson PJ, Hoessli DC. Transfer of exogenous glycosylphosphatidylinositol (GPI)-linked molecules to plasma membranes. Cell Biology 1996; 6:163-167.

43. Keown MB, Henry AJ, Ghirlando R, Sutton BJ, Gould HJ. Thermodynamics of the interaction of human immunoglobulin E with its high-affinity receptor FcεRI. Biochemistry 1998; 37:8863-8869.

44. Sayers I, Cain SA, Swan JRM, Pickett MA, Watt PJ, Holgate ST, Padlan EA, Schuck P, Helm BA. Amino acid residues that influence FcεRI mediated effector functions of human immunoglobulin E. Biochemistry 1998; 37:16152-16164.

45. Nechansky A, Pursch E, Effenberger F, Kricek F. Characterisation of monoclonal antibodies directed against the α-subunit of the human IgE high-affinity receptor. Hybridoma 1997; 16(5):441-446.

46. Morton TA, Myszka DG. Kinetic analysis of macromolecular interactions using surface plasmon resonance biosensors. Methods Enzymol 1998: 295:268-294.

CHAPTER FIVE:

Surface Plasmon Resonance Analysis of FcεRI:IgE Interactions.

SUMMARY

The interaction between IgE and its high affinity receptor FcεRI-α is a basic component of the pathology of asthma, hay fever and other inflammatory disorders. The understanding of this receptor:ligand interaction will aid the development of biochemical antagonists that prevent degranulation and may be less allergenic than structural blocks to binding. In the work described in this chapter surface plasmon resonance was used to investigate interaction between IgE and recombinant soluble FcεRI-α (εε), FcγRIIa (γγ) and the chimeric receptor γε (domain one of FcγRIIa and domain two FcεRI-α). The receptors were immobilised onto the SPR chip by aldehyde coupling and the influence of pH and ionic strength on the receptor:ligand interactions was determined.

FcγRIIa immobilised onto the SPR chip did not bind IgE. FcεRI-α receptor bound the same ligand with a K_D of 2.3×10^{-9} M, which was comparable with cell binding studies, but the K_D of γε under the same conditions (6.5×10^{-8} M) was lower than that found in cell binding studies. The interaction of IgE and FcεRI-α was determined to be pH dependent, with the highest affinity for the interaction at pH 7.0-7.5. Conversely, highest receptor occupancy occurred at ~pH 6.0, a finding that is consistent with a role for histidine in binding. Maximum binding of the ligand took place at low salt concentration (50 mM), binding decreasing with increasing ionic strength, and the affinity of the interaction was greatest at 150 mM (physiological).

Since intracellular signalling following occupancy of the receptor is dependent on receptor dimer formation, crosslinked with ligand, maintained for a minimum amount of time, it is tempting to consider that the affinity of receptor for its ligand has evolved to be maximal at physiological conditions to promote this event.

INTRODUCTION

This chapter follows the format of Chapter 3 and that of the Journal of Biological Chemistry, additional information on materials, recipes and methods will be given in Appendix III.

Surface plasmon resonance (SPR) is a technique that is used to characterise interactions between molecules that bind to each other (1). This technique has been used in the biological sciences to characterise interactions between receptors and ligands (2), as well as DNA and DNA binding proteins (3).

SPR is an optical phenomenon caused by interaction between electrons on the surface of a thin metal (gold) film and photons from a focussed polarised light source. At a specific angle of incidence the light resonates and the light energy is transferred to the electrons of the gold surface, resulting in a dip in the intensity of the reflected light. The specific angle at which this occurs varies with the refractive index of the contents of the flow channel lying against the sensor surface. When an interaction occurs between a molecule immobilised on the chip (incorporating the gold film) and a ligand in the flow channel, the concentration of ligand at the sensor surface alters causing a change in the refractive index of the light, resulting in a change of the angle at which resonance occurs. The angle at which this change occurs is recorded in a sensorgram as a function of time. In this way an interaction can be monitored and recorded in real time using arbitrary resonance units (RU).

A 1^0 shift in resonance is recorded as a 1000 RU change in signal and is equivalent to a surface protein concentration of 1 μg/ml (4) with a linear correlation between 10,000 and 30,000 RU (4). There has been some suggestion that immobilising proteins at a density of greater than 1000 RU may create mass transport effects that distort kinetic measurement (5), and this should be balanced against the resulting decrease in the signal to noise ratio.

The standard CM5 biosensor chip for Pharmacia's BIAcore 2000 biosensor has a carboxymethyl dextran surface attached to a gold film. The carboxymethyl groups are

derivitised with *N*-hydroxy succinimide (NHS) and *N* - ethyl - *N'*- (dimethylaminopropyl) carbodiimide (EDC). The resultant activated NHS-esters react with uncharged amine groups, predominantly lysines, in the protein to be immobilised as it passes through the flow cell and over the surface. Free NHS-esters remaining after protein immobilisation are sealed with ethanolamine hydrochloride. Proteins immobilised by this method are bound in random orientations. In addition, if a lysine is part of the binding site, as it is in FcεRI-α (5, 6), immobilisation through the lysine will reduce or abrogate the activity of the immobilised protein. Under these circumstances other methods of coupling can be used (7).

In this chapter, Fc receptors (εε, γγ and γε) were coupled through periodate oxidised aldehyde groups in the carbohydrates of the receptors. The dextran surface of the biosensor chip was pre-activated by NHS, EDC and hydrazine. The resultant hydrazone bond is unstable at low pH and was reduced by sodium borohydride to increase the stability of the ligand immobilised surface. Purified soluble recombinant FcεRI-α (εε), FcγRIIa (γγ) and a chimeric receptor comprising D1 FcγRIIa and D2 FcεRI-α (γε) were then immobilised to the CM5 biosensor chip, and the interactions of the receptors with IgE were examined under varying conditions of pH and ionic strength. The results suggest that there is pH-dependent binding, and the presence of salt bridges in the IgE:FcεRI-α interaction.

EXPERIMENTAL PROCEDURES

Production and nomenclature of the chimeric γε cDNA receptor construct— A previously produced chimeric cDNA receptor construct (8) was used as template in the construction of the γε FcR. The chimeric template was based on a simple domain exchange, and comprised D1 of FcγRIIa and D2 of FcεRI-α, also with the transmembrane region and cytoplasmic sequence of FcγRIIa, and was designated **γεγ** (see Chapter 3, Table 1).

Production of recombinant soluble human FcεRI-α— Soluble recombinant human FcεRI (hFcεRI) was produced in yeast (*Pichia pastoris*). cDNA encoding the two extracellular domains of FcεRI-α (residues 1-173, Appendix I) was generated by PCR from rFcεRI-α cDNA (9) using the oligonucleotides,

HT11 - 5'-AGCGTG GAATTC GTCCCTCAGAAACC-3' (sense primer)

HT12 - 5'-GTACTT GAATTC CTAAGCTTTTATTACAG-3' (antisense primer).

HT12 adds a termination codon (TAG) after codon 173 and a following *Eco*RI site. The product was digested with *Eco*RI and ligated into the unique *Eco*RI site in pPIC9 (*P. pastoris* expression vector, Invitrogen). The cDNA was transformed into *P. pastoris,* with selection and expression as described by the manufacturer (Invitrogen). The *P. pastoris* expression system used here is under patent to Invitrogen.

Chimeric soluble recombinant γε was produced in the same manner, and srFcγRIIA was the gift of M.Powell and N.Barnes (A.R.I., Melbourne).

Purification of soluble recombinant Fc receptors— A total of 5 L of buffered MGY (Invitrogen) minimal media with glycerol was innoculated with 50 ml of a *P. pastoris* clone producing rsFcεRI-α and incubated with vigorous shaking for 2 days at 30^{0}C. The cells were harvested and resuspended in buffered BMMY (Invitrogen) minimal media and incubated (225-250 rpm, 30^{0}C, 72 hrs) with 1% methanol, for induction of protein expression. The supernatant was filtered, precipitated with 66% saturated ammonium sulphate, resuspended in, and dialysed (x2, overnight) against 10 mM sodium dihydrogen orthophosphate pH 5.8 and loaded onto a Q-Sepharose column (Pharmacia). The column was eluted with 40% then 100% 200 mM sodium dihydrogen orthophosphate

pH 5.8, rsFcεRI fractions were identified by ELISA, pooled, dialysed against 10 mM Tris pH 7.5 and passed over an affinity column consisting of the anti-FcεRI mAb 3B4 immobilised onto CNBr- Sepharose 4B (Pharmacia). No affinity column was available for purification of the γε chimera, so a second purification over Q-Sepharose was carried out as above. FcεRI was then eluted with 0.1 M sodium acetate/0.5 M sodium chloride, and immediately neutralised with saturated Tris pH 10.0. Fractions containing FcεRI were pooled, and the concentration was determined by OD at 280 nm using a molar extinction coefficient of $E^{1mg/ml} = 2.5$ (10).

Activation and attachment of purified receptor to a CM5 biosensor chip— Purified Fc receptors were attached to the sensor chip by aldehyde coupling according to the manufacturer's instructions in the BIA applications handbook. Briefly, FcεRI (εε) and FcγRIIa (γγ) at 1 mg/ml, and the chimeric Fc receptor (γε) at 0.5 mg/ml were oxidised using sodium periodate (Sigma), and buffer exchanged into filtered 10 mM sodium acetate buffer pH 4. The pre and post oxidation receptors were run on a protein gel and silver stained. The oxidised receptors were stored in Eppendorf tubes at 4^0C overnight. The sensor chip was activated using the procedure described by the manufacturer, NHS/EDC 1:1, 15 µl, 5 µl/min; then 5 mM hydrazine hydrate (Sigma) 35 µl, 5 µl/min. Activated receptors at 50 µg/ml were passed over the activated sensor chip (35 µl, 5 µl/min). 0.1 M sodium borohydride (40 µl, 2 µl/min) was used to seal the chip which was then regenerated with three 5 µl injections (5 µl/min) of 0.2 M Glycine/ HCl pH 2.5. The final response units (RU) of each of the four channels of the chip indicated the mass of receptor immobilised, and were as follows: 1. rsFcεRI - 10274.4 RU of a total 25407 RU on the channel; 2. The chimeric rsFcγε R - 10724.7 of 30320 final RU; 3. rsFcγRIIa - 9137 RU of 24177 final RU; 4. Flow path 4 was not activated.

Biosensor automated methods— Methods and programming language required for automated procedures is provided in the BIAcore 2000 Instrument Handbook. MAb 47 (see Chapter 2 of this thesis for details of this antibody) was injected over the chip in BIAcore running buffer (HBS). Chimeric mouse/human anti-NP IgE (Serotec) was diluted in HBS, for equilibrium determinations. IgE was diluted at a nominal 1 µM (not corrected for bindability) in HBS with varying ionic strength or variable pH buffer as described

Figure 5.1 Examples of programs used in biosensor analysis.

METHOD mAb47 is an example of a loop program. A series of concentrations of the monoclonal antibody 47 were assayed to determine their binding to FcεRI-α (εε), γε and γγ immobilised onto separate channels of an SPR chip by aldehyde coupling. Each ligand concentration on each receptor was separately recorded and the resulting sensorgrams overlayed for direct comparison.

METHODIgE is an example of a strip program. A series of concentrations of IgE were assayed to determine their binding to FcεRI-α (εε), γε and γγ immobilised onto separate channels of an SPR chip by aldehyde coupling. IgE was injected over the chip surface for 60 seconds, with a 900 second dissociation phase in HBS before regeneration of the chip surface.

```
METHOD mAb47


DEFINE APROG screen
   PARAM %position %sample
   CAPTION %sample
      ! binding mAb47 to aldehyde coupled FcER1, and mutants
      ! Fc1 EE Fc 2 EG Fc3 GG Fc4 untouched by human hand
      ! 2-200nM, regeneration 10mM HCl

          FLOW            5
          FLOWPATH        1,2,3,4
          KINJECT         %position 50 1200
          INJECT          R1A1 5
          INJECT          R1A1 5
          EXTRACLEAN
          WASH            n
          WASH            i
END

DEFINE LOOP samplelist

LPARAM    %position     %sample
          r1d1          2nM_mAb47
          r1d2          5nM_mAb47
          r1d3          20nM_mAb47
          r1d4          50nM_mAb47
          r1d5          100nM_mAb47
          r1d6          200nM_mAb47
          r1c1          300nM_mAb47
          r1c2          500nM_mAb47
          r1c3          600nM_mAb47

END

MAIN
   FLOWCELL    1,2,3,4
   LOOP samplelist STEP
    APROG         screen %position %sample

   ENDLOOP
   APPEND       continue
END
```



```
METHODIgE


DEFINE APROG strip
       ! CHIP 54
       ! binding huIgE (10-900nM,60ul)
       ! r1d1 is regeneration 0.2M GlycineHCl pH2.5
       ! sample volume is 60ul, 600s dissociation
      FLOW       5
      FLOWPATH   1,2,3,4

   WAIT 5:00
   KINJECT    r1a1     60 900   ! 10nM
   inject     r1d1     5        ! regeneration
   inject     r1d1     5        ! 2nd regen
   KINJECT    r1a1     60 900   ! 50nM
   inject     r1d1     5        ! regeneration
   inject     r1d1     5        ! 2nd regen
   KINJECT    r1a3     60 900   ! 100nM
   inject     r1d1     5        ! regeneration
   inject     r1d1     5        ! 2nd regen
   KINJECT    r1a4     60 900   ! 300nM
   inject     r1d1     5        ! regeneration
   inject     r1d1     5        ! 2nd regen
   KINJECT    r1a5     60 900   ! 500nM
   inject     r1d1     5        ! regeneration
   inject     r1d1     5        ! 2nd regen
   KINJECT    r1a6     60 900   ! 700nM
   inject     r1d1     5        ! regeneration
   inject     r1d1     5        ! 2nd regen
   KINJECT    r1b1     60 900   ! 900nM
   inject     r1d1     5        ! regeneration
   inject     r1d1     5        ! 2nd regen
END
MAIN
   FLOWCELL   1,2,3,4
   APROG      strip
   APPEND     continue
END
```

Figure 5.2 Examples of programs used in biosensor analysis.

MethodpH is an example of a loop program. A single concentration of IgE in a 150 mM salt buffer at a series of pH concentrations was assayed to determine binding to FcεRI-α (εε), γε and γγ immobilised onto separate channels of an SPR chip by aldehyde coupling. Samples were injected using the coinject option that enabled the dissociation phase of the interaction to take place in the same buffer environment as the injection phase.

MethodNaCl is an example of a loop program. A single concentration of IgE at pH 7.4 in a series of salt concentrations was assayed to determine binding to FcεRI-α (εε), γε and γγ immobilised onto separate channels of an SPR chip by aldehyde coupling.

```
METHODpH


DEFINE APROG screen
   PARAM %position %position2 %sample
   CAPTION %sample
      ! binding IgE to aldehyde coupled FceRl, and mutants
      ! Fcl EE Fc 2 EG Fc3 GG Fc4 untouched by human hand
      ! 200nM IgE in mixed buffer 150mM NaCl pH5.5 - 8.5
      ! 110s dissoc in mixed buffer 150mM NaCl pH5.5 - 8.5


         FLOW              5
         FLOWPATH          1,2,3,4
         COINJECT          %position 55 %position2 110
         INJECT            R1A1 5
         EXTRACLEAN
         WASH              n
         WASH              i
  END

DEFINE LOOP samplelist

   LPARAM %position        %position2     %sample
            r1d1           r1c1            pH5.5
            r1d2           r1c2            pH6.0
            r1d3           r1c3            pH6.5
            r1d4           r1c4            pH7.0
            r1d5           r1c5            pH7.5
            r1d6           r1c6            pH8.0
            r1b6           r1a6            pH8.5

  END

MAIN
   FLOWCELL    1,2,3,4
   LOOP samplelist STEP
     APROG       screen %position %position2 %sample

   ENDLOOP
   APPEND      continue
END
```

```
METHODNaCl


DEFINE APROG screen
   PARAM %position %position2 %sample
   CAPTION %sample
      ! binding IgE to aldehyde coupled FcER1, and mutants
      ! Fcl EE Fc 2 EG Fc3 GG Fc4 untouched by human hand
      ! IgE in Hepes 50-300mM NaCl

         FLOW              5
         FLOWPATH          1,2,3,4
         COINJECT           %position 55 %position2 110
         INJECT            R1A1 6
         EXTRACLEAN
         WASH              n
         WASH              i
  END

DEFINE LOOP samplelist

   LPARAM    %position   %position2   %sample
             r1d1        r1c1         50mM_NaCl
             r1d2        r1c2         100mM_NaCl
             r1d3        r1c3         150mM_NaCl
             r1d4        r1c4         200mM_NaCl
             r1d5        r1cs         250mM_NaCl
             r1d6        r1c6         300mM_NaCl

   END

MAIN
   FLOWCELL    1,2,3,4
   LOOP samplelist STEP
      APROG       screen %position %position2 %sample

   ENDLOOP
   APPEND      continue
  END
```

below. Interactions were carried out at 4°C. Examples of automated methods are shown (Figures 5.1 and 5.2). Flow Channel 3 (Fc3) FcγRIIa was subtracted from Fc1 and Fc2 as a background solvent control. Determination of apparent equilibrium and kinetic affinity constants was carried out using BIAevaluation (BIAcore), Clamp (11) and "Curve Expert" (© Daniel Hyams)[1].

Buffers— BIAcore HBS: 10 mM HEPES, 150 mM sodium chloride, 3.4 mM Na EDTA, pH 7.4.

Variable pH buffer was produced according to the method of Wines *et al.* (12): 5 mM sodium acetate (pKa - 4.77), 5 mM PIPES (pKa - 6.8), 5 mM MOPS (pKa - 7.2), 5 mM HEPES (pKa - 7.55), 5 mM Tris base (pKa - 8.3), 150 mM sodium chloride, 3.4 mM Na EDTA, and adjusted to a pH of 5.5, 6.0, 6.5, 7.0, 7.5, 8.0, or 8.5.

Variable ionic strength buffer was based on BIAcore running buffer: 10 mM HEPES, 50-300 mM sodium chloride, 3.4 mM Na EDTA. 50, 100, 150, 200, 250 and 300 mM concentrations of sodium chloride were used.

Monoclonal antibodies— Anti-FcεRI-α monoclonal antibody from hybridoma cell line X52-47-5.4 (mAb 47), of IgG1 isotype, was used to determine the presence of receptor on the CM5 chip. This antibody recognises an epitope in the G strand of FcεRI-α domain two.

[1] The Curve Expert program written by Daniel Hyams is found at the web-site http://www2.msstate.edu/~dgh2/cvxpt.htm

RESULTS

Recombinant soluble purified receptors FcεRI-α (εε)[1], Fcγε R (γε)[2] and FcγRIIa (γγ)[3] were immobilised to the dextran surface of the CM5 chip through carbohydrate groups of the receptor using aldehyde coupling. These immobilised receptors were used to analyse binding characteristics with IgE. FcεRI-α has four possible glycosylation sites in D1 and three in D2 but FcγRIIa has only one site in D1and one in D2. Therefore the γε chimera has three fewer glycosylation sites than the εε receptor, four sites are lost and only one replaced with the exchange of FcεRI-α D1 and FcγRIIa D1. The extent of the coupling of each receptor to the chip was similar for all three receptors (see Experimental Procedures for details of RU). The γγ receptor (low affinity IgG receptor, FcγRIIa) is closely related to the εε (FcεRI) receptor and was utilised as a negative background control.

MAb 47, which recognises the PLN epitope on the G strand of FcεRI domain 2, was injected over the prepared chip to verify the presence of the εε and γε receptors (Figure 5.3). The slightly higher RU of the γε chimera was reflected in the higher Bmax of the mAb, and mAb 47 had a similar affinity ($6.3x10^{-8}$ M) on binding both γε and εε indicating that it was unlikely that the coupling process had induced any global structural abnormality of the receptors. This is important as this epitope to which mAb 47 binds is located in the G strand of the receptor and the F/G loop is part of the IgE binding site.

In a second experiment IgE was passed over the sensor chip (Figure 5.4). Results from this work indicate that there is a considerable difference in the amount of IgE that bound to wild type receptor compared to chimera, i.e. 5,000 RU versus 150 RU at 900 nM IgE. This is in complete contrast to the binding of mAb 47. Determining affinity using kinetic analysis for IgE binding to the receptors gave a K_D of $2.3x10^{-9}$ M for the εε and a K_D of $6.5x10^{-8}$ M for the γε receptor. Affinity analysis for the same ligand

[1] FcεRI-α (εε) has the extracellular domains 1 and 2 from FcεRI-α.

[2] FcγεR (γε) comprises domain 1 from FcγRIIa and domain 2 from FcεRI-α.

[3] FcγRIIa (γγ) comprises domains 1 and 2 from FcγRIIa.

Figure 5.3 mAb 47 binds FcεRI-α (εε - red), and chimeric receptor (γε - blue) immobilised on a biosensor chip.

Mab 47 was injected over the εε and γε receptors at ten different concentrations, and the response units of the interaction versus time were recorded. Responses for each of the injections were overlaid. The concentration of antibody used in each injection is given at the right of the εε receptor trace; the same concentrations were used for the γε receptor trace. The affinity (measured using the dissociation constant) of mAb 47 for both receptors was found to be K_D $6.3x10^{-8}$ M. This value was determined independently for each receptor.

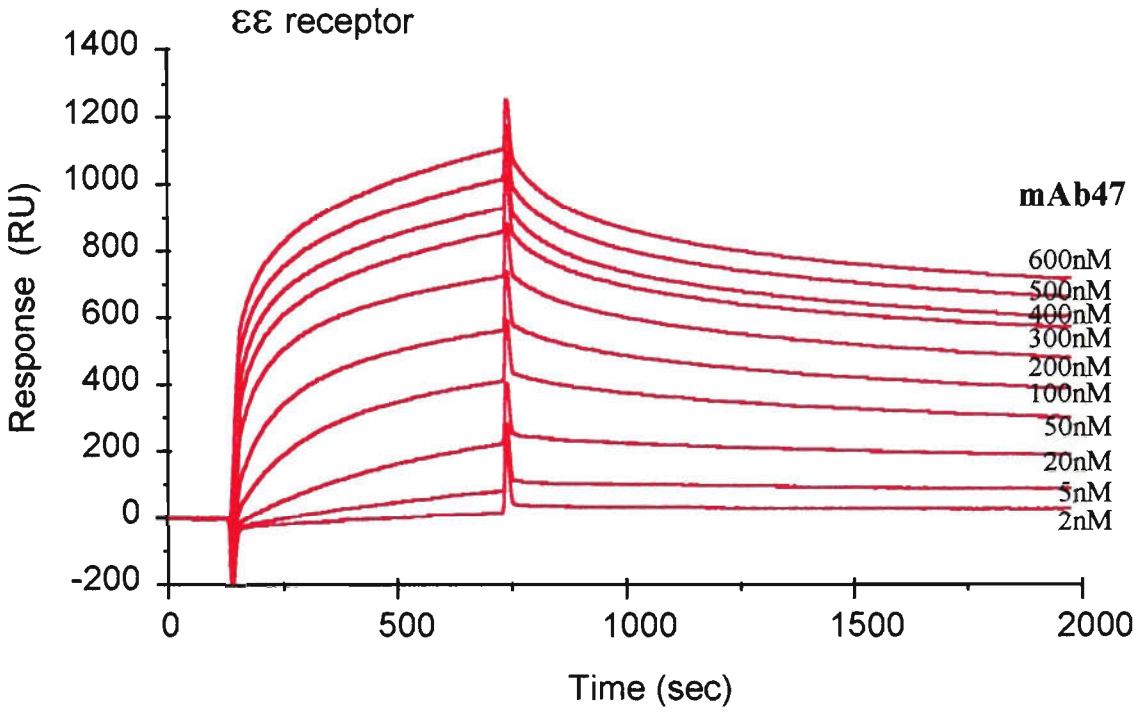
εε receptor
1400
1200
1000
800
600
400
200
0
-200
Response (RU)
0
500
1000
1500
2000
Time (sec)
mAb47
600nM
500nM
400nM
300nM
200nM
100nM
50nM
20nM
5nM
2nM

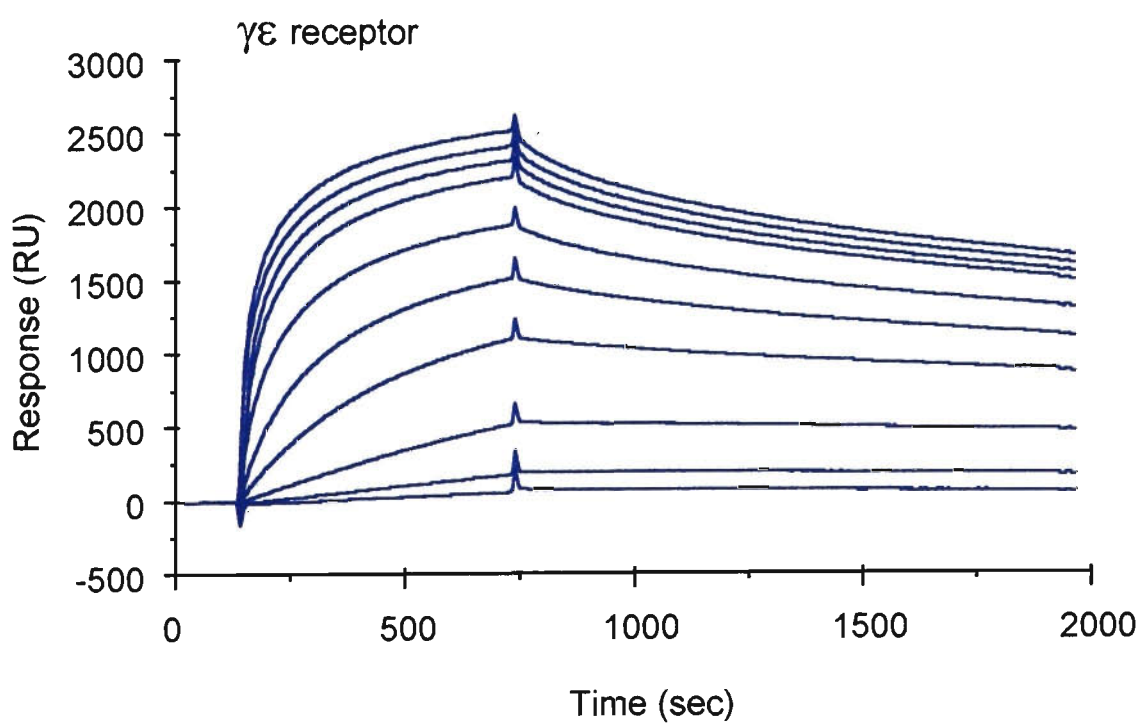
γε receptor
3000
2500
2000
1500
1000
500
0
-500
Response (RU)
0
500
1000
1500
2000
Time (sec)

Figure 5.4 IgE binds the $\epsilon\epsilon$ and $\gamma\epsilon$ receptors.

IgE was injected at increasing concentrations (10-90 nM) over the $\epsilon\epsilon$ (shown in red) and $\gamma\epsilon$ (shown in blue) receptors and the kinetics of the interaction (response units versus time) recorded. Responses for each of the injections were overlaid. The concentration of antibody used in each injection is given at the right of the $\epsilon\epsilon$ trace; the same concentrations were used for the $\gamma\epsilon$ receptor trace. The dissociation constant (K_D) of the interaction was determined from the association and dissociation rates to be 2.3×10^{-9} M for $\epsilon\epsilon$ and 6.5×10^{-8} M for $\gamma\epsilon$. Note that the RU of $\gamma\epsilon$ is approximately 50x lower than that of $\epsilon\epsilon$.

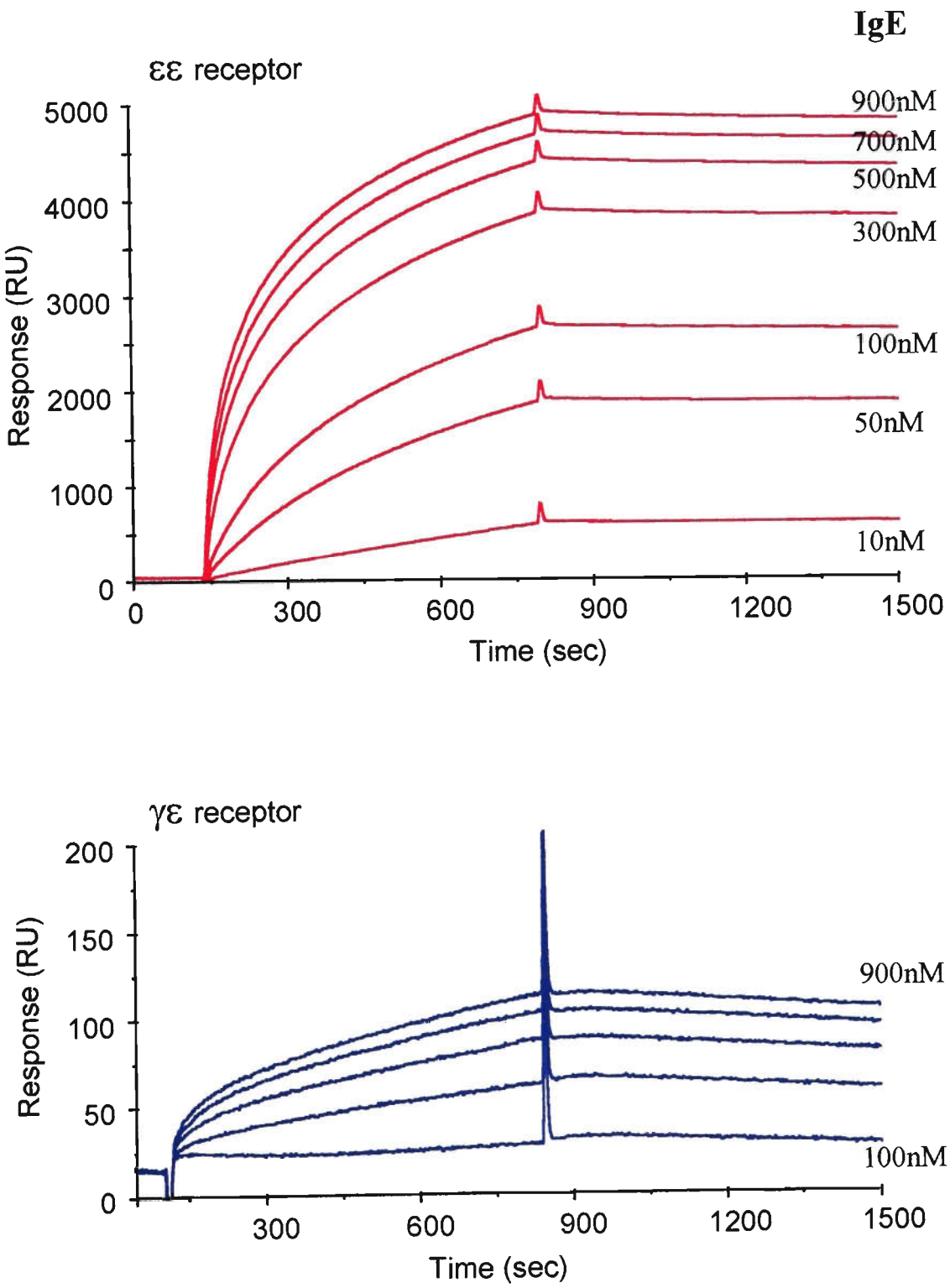
IgE
εε receptor
5000
4000
3000
2000
1000
0
Response (RU)
900nM
700nM
500nM
300nM
100nM
50nM
10nM
0
300
600
900
1200
1500
Time (sec)
γε receptor
200
150
100
50
0
Response (RU)
900nM
100nM
300
600
900
1200
1500
Time (sec)

receptor interactions but using the predicted equilibrium response (Appendix 2) gave K_D values of $2.6x10^{-8}$ for $\epsilon\epsilon$ and $5.2x10^{-7}$ for $\gamma\epsilon$ (Figure 5.5).

The interaction between IgE and receptors was then observed under varying pH and ionic strength. IgE binding to FcϵRI was initially tested over the range pH 5.5 to 8.5 with different pH buffers used in the association phase and pH 7.4 buffer used during the dissociation phase in every sample. This indicated the effect of pH on association and B_{MAX} (Figure 5.6A). The fastest response, indicating the greatest receptor occupancy for IgE, was at pH 6.0, however the optimum affinity was seen to be at pH 7.5 to 8.0 (Figure 5.6B). From the data in Figure 5.6B it appears that $\gamma\epsilon$ is more sensitive to changes above or below the optimum; optimal binding as indicated by affinity is achieved over a narrower pH range than is the case for $\epsilon\epsilon$.

Association and dissociation of IgE with $\epsilon\epsilon$ and the $\gamma\epsilon$ chimera was then analysed with both procedures carried out in the same buffer, thus maintaining the variable pH, and a dramatic effect on binding of IgE to the chimeric receptor was observed. pH had a minor effect on association, but in both the wild type and mutant receptor it had a major effect on dissociation (Figure 5.7). In $\gamma\epsilon$ the dissociation rate decreased with increasing pH from pH 5.5 up to pH 7.0 - 7.5. In contrast there was little change for $\epsilon\epsilon$ up to pH 8.5 (Figure 5.7A) where the dissociation rate increased with increasing pH (Figure 5.7B). This was most dramatically observed with the instantaneous dissociation of IgE at pH 5.5 from the chimera (data too rapid to quantitate), compared to the relatively slow dissociation of IgE from the wild type receptor at this pH. Therefore the affect on binding affinity is most likely to be caused by the effect of the dissociation rate.

Analysis of the relative differences in the half life ($t_{1/2}$) of dissociation of IgE at different pH's for wild type or chimeric receptor, indicates that over the pH range analysed the $t_{1/2}$ of the complex of IgE:FcϵRI or IgE:$\gamma\epsilon$ are distinct. Initially the $t_{1/2}$ for IgE:FcϵRI or IgE:$\gamma\epsilon$ were similar in that they increased (dissociation rate decreased), over the range pH 5.5 to pH 7, 7.5. There after, however, the $t_{1/2}$ for IgE:FcϵRI was largely maintained over pH 7.5, 8 and 8.5. This is in sharp contrast to dissociation of the chimera which was more rapid overall (Figure 5.8).

Figure 5.5 Langmuir isotherm of IgE binding $\epsilon\epsilon$ and $\gamma\epsilon$ receptors.

The Langmuir isotherm (Appendix II) for equilibrium binding was plotted from the predicted equilibrium (Req) of the data in Figure 5.4 . The non-linear regression analysis of these data provided an apparent K_D for the interaction with IgE with $\epsilon\epsilon$ of 2.6×10^{-8} M and with $\gamma\epsilon$ of 5.2×10^{-7} M.

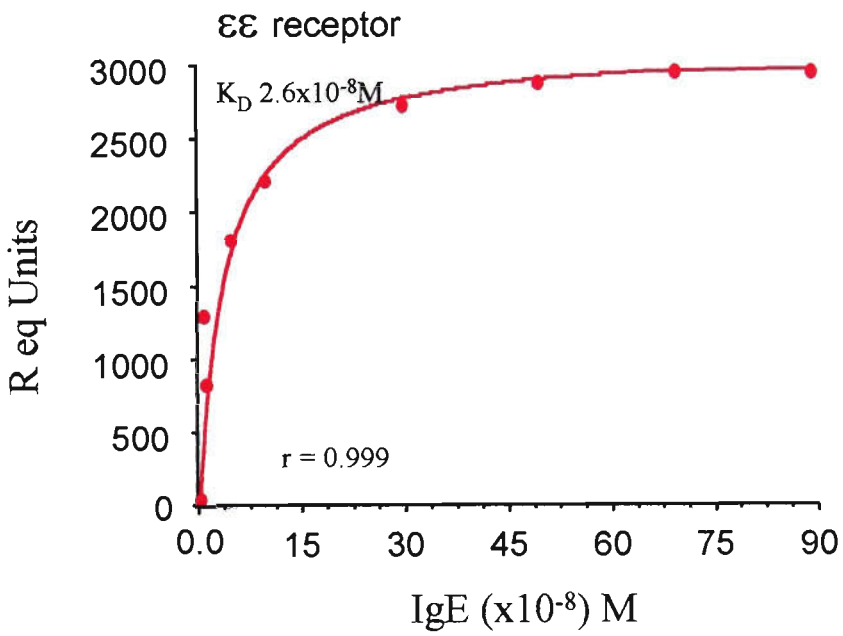
εε receptor
K_D 2.6x10^{-8}M
r = 0.999
R eq Units
3000
2500
2000
1500
1000
500
0
0.0
15
30
45
60
75
90
IgE (x10^{-8}) M

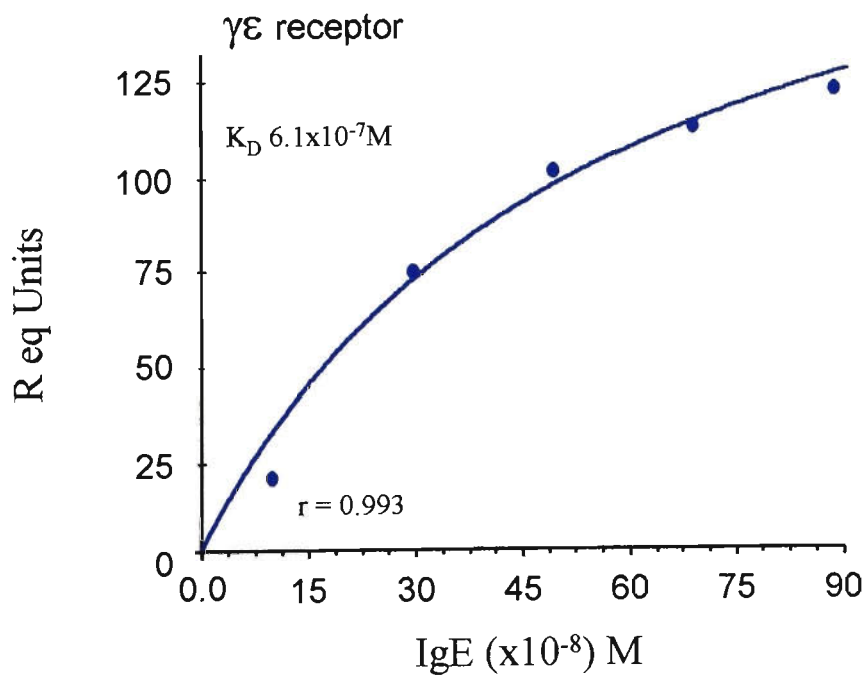
γε receptor
K_D 6.1x10^{-7}M
r = 0.993
R eq Units
125
100
75
50
25
0
0.0
15
30
45
60
75
90
IgE (x10^{-8}) M

Figure 5.6 The association of IgE with ϵϵ and γϵ receptors is pH dependent.
IgE at 1 μM in buffers of pH 5.5-8.5 was injected over immobilised ϵϵ and γϵ receptors. The wash-off or dissociation phase of the interaction took place in BIAcore running buffer (HBS pH 7.4).

A. Association of IgE with the ϵϵ receptor was determined at a range of pH's. The binding of IgE to ϵϵ receptors is shown for each pH as RU versus time. It can be seen that the greatest receptor occupancy occurred at pH 6.0 with a reduction in occupancy at pH 5.5 and from pH 6.0 to approximately 65% of maximum at pH 8.5. A marginal elevation from the trend can be seen at around pH 7.5 indicating a small peak or higher receptor occupancy at physiological pH. The increased occupancy at pH 6.0 with an elevation around pH 7.5 could indicate a role for histidine (pK_a 7.0) in IgE binding.

B. The affinity of the IgE:FcϵRI-α interaction is depicted here as a bar graph, with the response for each pH shown consecutively and independently. Ordinate data for the ϵϵ receptor are shown in red, and that for the γϵ receptor in blue. Note that the scale differs for each receptor. For both receptors the affinity was greatest at pH 7.5-8.0, close to physiological pH.
* Data too low to quantitate.

A

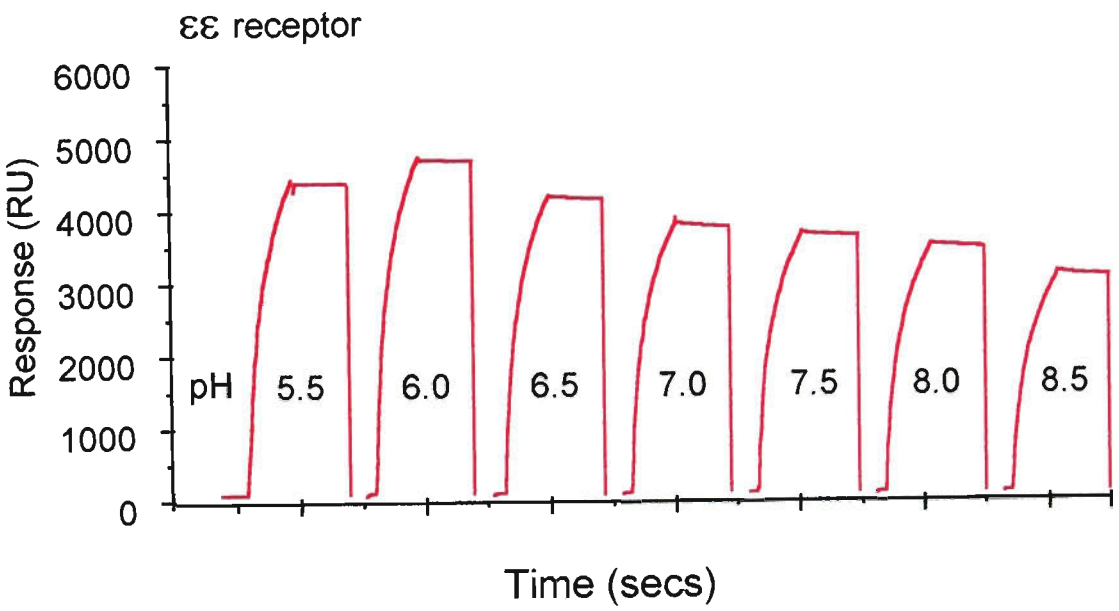
εε receptor
6000
5000
4000
3000
2000
1000
0
Response (RU)
pH
5.5
6.0
6.5
7.0
7.5
8.0
8.5
Time (secs)

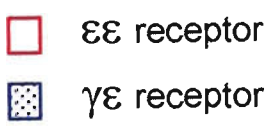
εε receptor
γε receptor

B

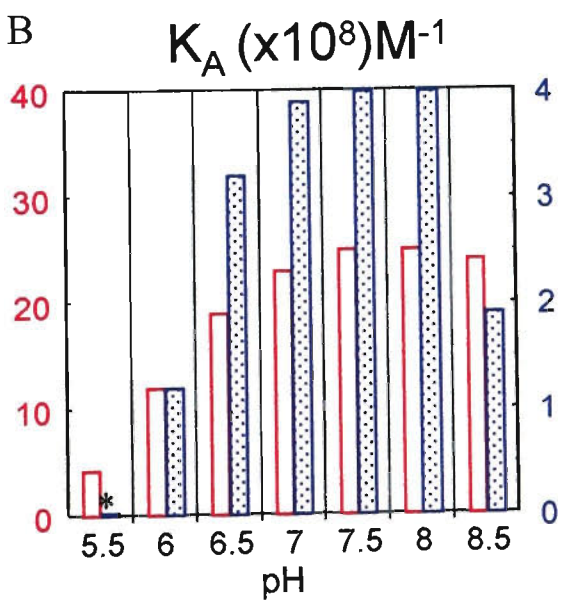
K_A (x10^8)M^{-1}
40
30
20
10
0
4
3
2
1
0
*
5.5
6
6.5
7
7.5
8
8.5
pH

Figure 5.7 Association and dissociation phases of $\epsilon\epsilon$ and $\gamma\epsilon$ receptors for IgE are pH dependent.

The $\epsilon\epsilon$ receptor (A) displayed high receptor occupancy at pH 5.5-6.0, with decreasing occupancy to pH 8.5. The $\gamma\epsilon$ receptor (B) displayed a greater sensitivity to alteration in pH, with receptor occupancy being highest at pH 6.0-6.5, and dissociation slowest at pH 7.0-7.5.

It should be noted that the overall response for $\gamma\epsilon$ was much lower than that for $\epsilon\epsilon$. Similar data was obtained on two separate occasions.

* Unable to analyse data.

A εε receptor

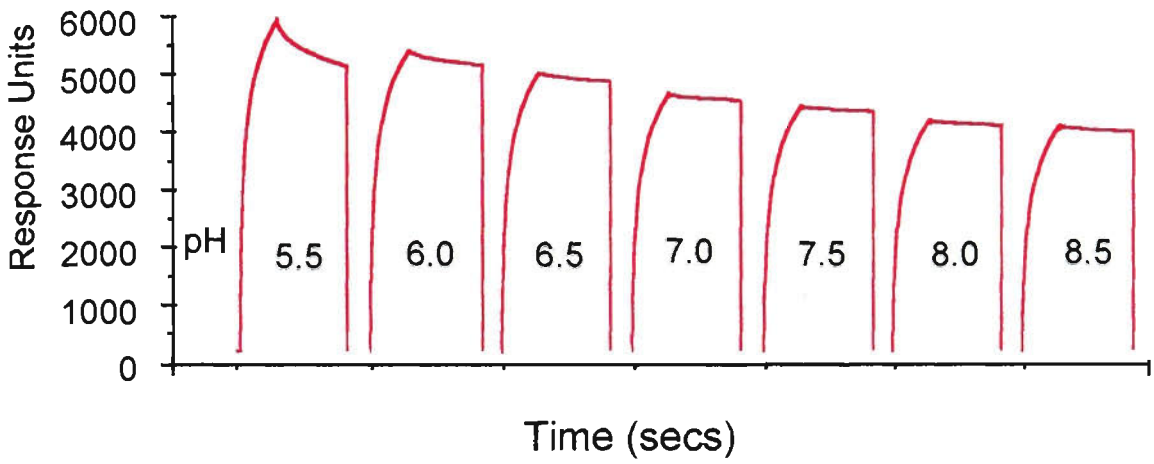

B γε receptor

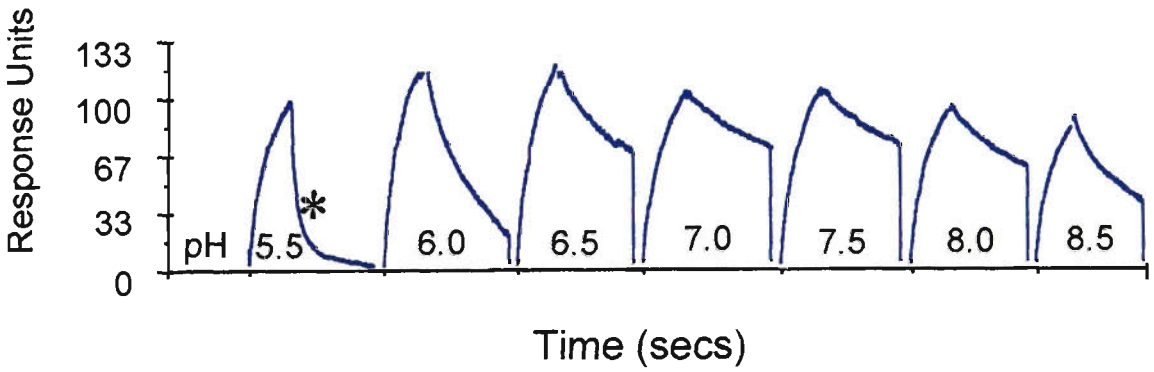

To determine the effect of ionic strength on receptor : ligand interaction, the ligand was buffer exchanged into HBS buffer containing varying concentrations (50, 100, 150, 200, 250 and 300 mM) of sodium chloride, and passed over the SPR chip. Increasing salt concentration decreased Bmax (Figure 5.9A), and at physiological salt (150 mM) the Bmax of the interaction was 50% of the Bmax at 50 mM sodium chloride. The effect was more evident on the chimeric than the wild type receptor where binding was one sixth at physiological compared to that at 50 mM NaCl.

As evident from half life calculations of the IgE: receptor interactions, the interaction of $\epsilon\epsilon$ with IgE was optimal at 150 mM whereas that of the chimeric $\gamma\epsilon$ receptor was optimal at 50 mM in the ranges given and decreased thereafter (Figure 5.9B). The K_D is also seen to be low at 150 mM salt, indicating a high affinity interaction at this concentration (Figure 5.9C). This would imply that salt bridges are necessary to stabilise the interaction between IgE and FcϵRI and are optimal at physiological pH. This is not evident in the chimeric $\gamma\epsilon$ receptor.

Figure 5.8 The half life ($t_{1/2}$) of IgE binding the $\epsilon\epsilon$ and $\gamma\epsilon$ receptors is pH dependent. The $t_{1/2}$ of IgE binding to the $\epsilon\epsilon$ and $\gamma\epsilon$ receptors was greatest at pH 7.5-8.0 for $\epsilon\epsilon$ (shown in red), and at pH 7.0-7.5 for the $\gamma\epsilon$ receptor (shown in blue), indicating a greater sensitivity to pH in the $\gamma\epsilon$ chimera manifested as rapid dissociation at non-physiological pH. Note that the ordinate data for $\epsilon\epsilon$ are on the left in red and at a different scale to the data for $\gamma\epsilon$ at right.

* Unable to analyse data.

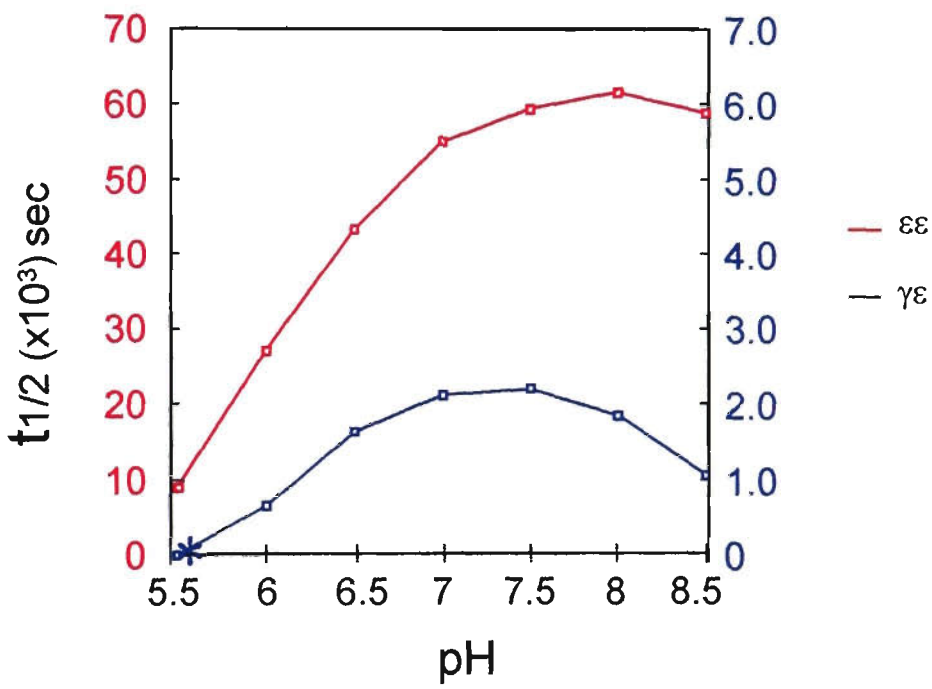
70
60
50
40
30
20
10
0
7.0
6.0
5.0
4.0
3.0
2.0
1.0
0
5.5
6
6.5
7
7.5
8
8.5
pH
t1/2 (x10³) sec
εε
γε

Figure 5.9 IgE binding to $\epsilon\epsilon$ and $\gamma\epsilon$ receptors is sensitive to ionic strength.
Data are displayed as bar graphs with salt concentrations on the abcissa. Note that the ordinate units are different for $\epsilon\epsilon$ (shown in red) than $\gamma\epsilon$ (in blue).

A. Receptor occupancy for $\epsilon\epsilon$ and $\gamma\epsilon$ is shown in relative units, and indicates that receptor occupancy decreases with increasing salt concentration to a minimum at 250 mM.

B. The half life of the IgE:FcϵRI interaction is an indicator of dissociation. The $\epsilon\epsilon$ and $\gamma\epsilon$ receptors show distinct interactions with IgE as a function of NaCl concentration. The $\epsilon\epsilon$ receptor can be seen to display an increase in $t_{1/2}$ at 150 mM salt concentration indicating an increase in the tendency for IgE and FcϵRI to stay together at physiological ionic strength.

C. The affinity of the interaction between IgE and receptor can be seen to follow a trend of increased dissociation with increasing salt concentration.

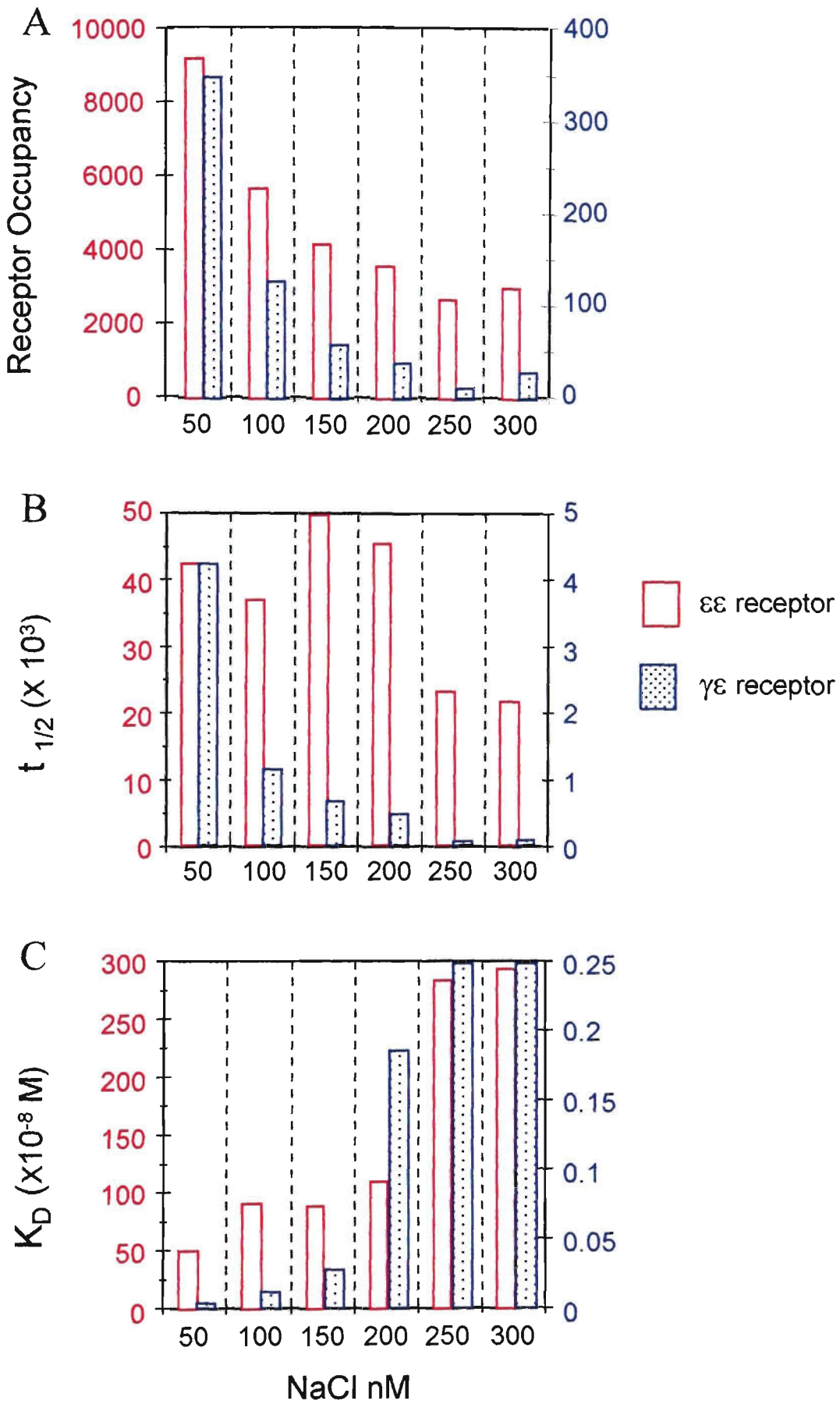
A
Receptor Occupancy
10000
8000
6000
4000
2000
0
400
300
200
100
0
50 100 150 200 250 300
B
t 1/2 (X 10³)
50
40
30
20
10
0
5
4
3
2
1
0
50 100 150 200 250 300
εε receptor
γε receptor
C
K_D (X10⁻⁸ M)
300
250
200
150
100
50
0
0.25
0.2
0.15
0.1
0.05
0
50 100 150 200 250 300
NaCl nM

DISCUSSION

The data described above suggest that the interaction between hIgE and FcεRI-α is pH dependent and involves one or more salt bridges.

In the experiments described in this chapter the εε and γε receptors were immobilised to the CM5 SPR chip by aldehyde coupling. MAb 47 bound to the εε and γε receptors with a similar K_D as determined by Biacore (SPR) analysis. This indicates that the receptors were immobilised to the chip with the domain 2 epitope intact. The greater amount of γε attached to the chip relative to εε, and the recognition of twice the RU of γε relative to εε was consistent with the binding of mAb 47 to cell surface γε. In contrast, εε bound over thirty times more IgE than γε. One possible reason for the considerable difference in IgE binding is differences in the glycosylation patterns of the two receptors; there are four carbohydrates in FcεRI domain 1, and three in domain 2, but there is only one carbohydrate in the domain 1 of FcγRIIa. Thus, the conjugation of the receptors to the chip that occurs through these carbohydrate groups may occur largely through the domain 1 carbohydrate in the wild type receptor, but, in the γε chimera, through the carbohydrates in the FcεRI derived domain 2, resulting in possible occlusion of the binding site. In addition, immobilisation through the carbohydrate may restrict the receptor in such a way as to reduce its capacity to form the IgE binding site correctly. It is likely that a combination of these factors explains the observations of IgE binding to the γε receptor as: (i) there is no global change in chimeric receptor structure as the mAb 47 binds with equal affinity to the chimeric and 'wild-type' receptors. (ii) The IgE binding site is not destroyed as the carbohydrate based coupling method successfully coupled active 'wild-type' receptor to the chip and gave affinities of IgE binding equivalent to that measured in cells, and (iii) there is some alteration to the chimeric receptor as the affinity of IgE binding was lower than that observed for IgE binding to this chimera on the cell surface (see below).

The apparent affinity, using the predicted response at equilibrium (Req) in a Langmuir Isotherm, was ten to twenty times lower than that obtained from cell binding data and kinetic data (K_D - 2.6×10^{-8} M εε, 5.2×10^{-7} M γε - Langmuir isotherm; 2.1×10^{-9} M εε,

$4x10^{-9}$ M γε - cell surface; $2.3x10^{-9}$M εε to $6.5x10^{-8}$ M γε - kinetic); on close scrutiny of the data there are very few points in the region of Bmax/2 and below - the area used to generate the curve. The absence of critical data points is likely to produce an inaccurate curve despite good correlation (Figure 5.5). However, the K_D from the SPR kinetic data for εε ($2.3x10^{-9}$M) was comparable to that from cell binding data. This is consistent with data from other workers (5,13,14) who have found the affinity of the IgE:FcεRI interaction to be similar to cell surface data. The affinity, as determined from kinetic studies, of the γε chimera relative to the εε 'wild-type' receptor determined by SPR is lower than that of cell surface receptors by a factor of sixteen ($2.1x10^{-9}$ M εε to $4x10^{-9}$ M γε - for cell surface measurements, $2.3x10^{-9}$ M εε to $6.5x10^{-8}$ M γε - kinetic data). This could be explained by differences in presentation of the two immobilised receptors, with inactivation of the γε chimera as suggested above. However, despite the inactivation of most of the immobilised γε chimeric receptors, detectable binding is still evident and an interesting comparison to the εε chimera.

Experiments exploring effects of pH on IgE binding produced some interesting data. The initial experiment was designed to determine the effect of pH on association kinetics of IgE binding to receptor. The dissociation phase in this experiment was buffered at pH 7.4 (physiological) in HBS. It was observed that there was definite pH dependent binding of IgE to the wild-type and chimeric receptors, with receptor occupancy greatest at pH 6, and a 'shoulder' peak or levelling of the decrease in occupancy at pH 7 to 7.5. Data from other laboratories using hIgE with human basophils (15), or rat IgE with rat RBL cells (16) found peaks at pH 6.8 and pH 7.4, and pH 6.8 and pH 7.6-8.0 respectively. More recent data using hIgE and human RBL cells (17) showed greatest receptor occupancy at pH 6.3 and a smaller peak at pH 7.3 to 7.5 - physiological pH. Cell surface binding data (16, 17) displayed a drop in binding at pH 5.9 which was not observed in my data, where binding still occurred at pH 5.5. The sudden loss of binding in the work of Kulczycki (16) and Helm (17) was probably due to a cellular effect, or degeneration of the receptor, that does not occur in SPR, where the receptor is isolated from the cell and immobilised; this permits testing of a wider range of conditions, not easily achievable using whole viable cells.

The pH at which optimal occupancy occurred (pH 6.0) is consistent with histidine residues being involved in the receptor ligand interaction; histidine in proteins has a basic 'R' group with a p*Ka* of 6.5-7.4 and thus is likely to be positively charged at pH 6.0, making it a suitable candidate for ionic interactions. A further series of experiments in which both the association and dissociation phases of the FcεRI : IgE interaction were determined in the same buffer at varying pH confirmed a role for histidine.

In studies by Garman *et al.* (6) His 424 was involved in the IgE receptor interaction. The structure of FcεRI bound to IgE, as determined by X-ray diffraction, indicated that His 424 from both chains of Cε3 interacted with FcεRI. The sole interaction of His 424 in binding site 2 was with Trp 113, a residue that has been shown by mutation (18) to be an important residue in IgE binding FcεRI. Other histidine residues that could contribute to pH dependent FcεRI : IgE binding are His 134 (in the C'E loop region of FcεRI D2) and His 108 (in the BC loop region of FcεRI D2). His 134 is part of the C'E loop binding region of the FcεRI binding site proposed by mutagenesis and mAb binding (reviewed in Chapter 1), but has been mutated previously (18) with no effect on IgE binding. His 108 is in a region of FcεRI suggested by Riske et al (19), to be involved in IgE:FcεRI binding. His 108 has been shown by X-ray crystallography not to be part of the FcεRI : IgE binding site, however it does participate in maintaining the FcεRI D1:D2 interface where it appears to have a 'space-filling' role. In the model of FcεRI developed and described in chapters 2 and 3 of this thesis, His 108 contacts Phe 17 and other residues (see Chapter 3), and is also within 3Å contact with Phe 17 in the structure of FcεRI (6). Phe 17 is essential for maintaining the interdomain structure (Chapter 3) and the IgE binding site, interacting with Asp 86 in the linker region of FcεRI (see Figure 3.4 of Chapter 3). In both the model and the structure of the wild type receptor, His 108 is buried and would presumably not be affected by changes in the extramolecular environment. However, in the γε chimera there are clearly alterations in the interdomain interface, since not all FcγRIIa residues are conserved in the interface and such alterations may make His 108 more accessible to changes in solvent. His 108 interacts with Asp 20 in the model of the chimera, and has no interaction with the linker binding site (Figure 5.10). The interdomain interface in FcεRI, suggests greater flexibility than in FcγRIIa where water molecules contribute to stability between the domains (20). In

any event, the presence of a non-homologous first domain profoundly effects the nature of the receptor : ligand interaction at different pH.

Other data from experiments presented in this chapter clearly show that ionic strength is important for receptor:ligand interaction. Increasing salt concentrations decreased receptor occupancy as seen in Bmax values obtained from Biacore experiments (see Figure 5.9). More importantly, the half life of the receptor :ligand interaction is maximum (in $\epsilon\epsilon$) at physiological concentration (150 mM). The affinity is highest at low salt concentration, it stabilises at 100-200 mM, before dropping rapidly at higher salt concentrations. This is suggestive of a role for salt bridge formation in the binding of IgE to its receptor. Such a conclusion is consistent with mutagenesis data of IgE:FcϵRI , where receptor residues Glu 132, Asp 159, (18) and Asp 117 (5) have been shown to be important in IgE binding, and in IgE where Arg 334 (13) and Arg 427 (21) are important in binding to receptor.

Prior to the publication of the structure of IgE (22) and the complex of IgE bound to receptor (6), mutagenesis data implied that acidic and basic side chains were important for interaction, presumably through electrostatic interaction. In the structure of receptor interacting with the Fc portion of IgE, it is suggested that there are two possible sites for salt bridges (FcϵRI-αK117 - Cϵ3 D362 and FcϵRI-αE132 - Cϵ3 R334). Data generated from the Biacore experiments presented in this thesis are consistent with this.

In addition to salt bridge formation between amino acids in the IgE binding site, the interdomain interface has also been shown to be important in IgE binding by supporting and maintaining the configuration of the binding site (Chapter 3). It is also possible that the essential Arg 15 in this interface forms a salt bridge with adjacent residues and alteration of the ionic strength of the surrounding medium may affect the configuration of the interface. An interaction between His 108 and Asp 20 is seen in the model of the chimeric $\gamma\epsilon$ interface (Figure 5.10), which is not present in the interface of the FcϵRI model.

Charges in a region or molecule play a role in complementarity across an interface (23), so electrostatic charges can produce an influence not limited to a single interaction, and although a salt bridge effect may not occur in the εε wild type, such interactions in the interdomain interface may occur in the γε chimera leading to the dramatic effects in the chimera as a consequence of its greater sensitivity to ionic strength.

The demonstration that pH dependent FcεRI:IgE binding has optimum receptor occupancy at pH 6.0 reducing with increased pH but displaying a small shoulder peak at pH 7.5 (coinciding with the highest affinity) (Figure 5.6) concurs with the data of Helm et al. using intact cells (17). The major peak of occupancy at pH 6.0-6.4 has led to the speculation that it may reflect a physiologic response against parasites within the low pH of the intestine (17). This is an interesting point since sites of inflammation are also acidic. When the dissociation phase of the IgE:FcεRI interaction was carried out in buffer at the same pH as the association phase the γε receptor displayed a similar result, but the εε receptor occupancy decreased steadily from a maximum pH 5.5 (Figure 5.6). The affinity of the interaction does not follow the same pattern, and is stronger at ~pH 7.5 (Figure 5.8). The lumen of the intestine is not only acidic, but has a high (bile) salt concentration, and the disintegration of IgE:FcεRI binding at high salt (Figure 5.9), sadly, does not corroborate Helm's suggestion (17). However, high receptor occupancy with a low affinity under acid conditions may be a positive physiologic response at a site of inflammation, as an increased dissociation with pH would assist in increased loss of inappropriate or damaged IgE from the receptor allowing undamaged IgE to occupy the receptor of effector cells.

Use of a BIAcore (SPR) for analysis of protein:protein interaction has many benefits over traditional approaches. The BIAcore enables biomolecular interactions to be studied in cell free systems, providing flexibility to analyse reactions under a wide range of conditions. This permits the collection of data that might be missed in other situations, i.e. the consistent evidence of two site binding for the FcεRI:IgE interaction that was only suspected from other methods of analysis. The biosensor permits rapid analysis of protein:protein interactions, and, with small quantities of material, can provide precise and quantitative information.

Figure 5.10 Two dimensional depiction of the domain 1/domain 2 interface of the γεγ chimera displaying distances of interactions between amino acids[4].

The core amino acids Ile 14, Asn 15, Val 16, Leu 17, Gln 18, Glu 19, Asp 20 and Ser 21 are shown in *brown*, amino acids hydrogen bonded with the core amino acids are shown in *ochre* with the bond length shown in *green*, and other amino acids involved in hydrophobic interactions with the core amino acids are labelled in *black* with a *red* ray. All hydrophobic interactions are displayed in *red* with the atom/s involved in contact/s shown in *black* with a *red* ray.

[4] Figure 5.10 has been scanned from an original print from the computer that generated the image and the colour and clarity of this reproduction was the optimum that could be attained.

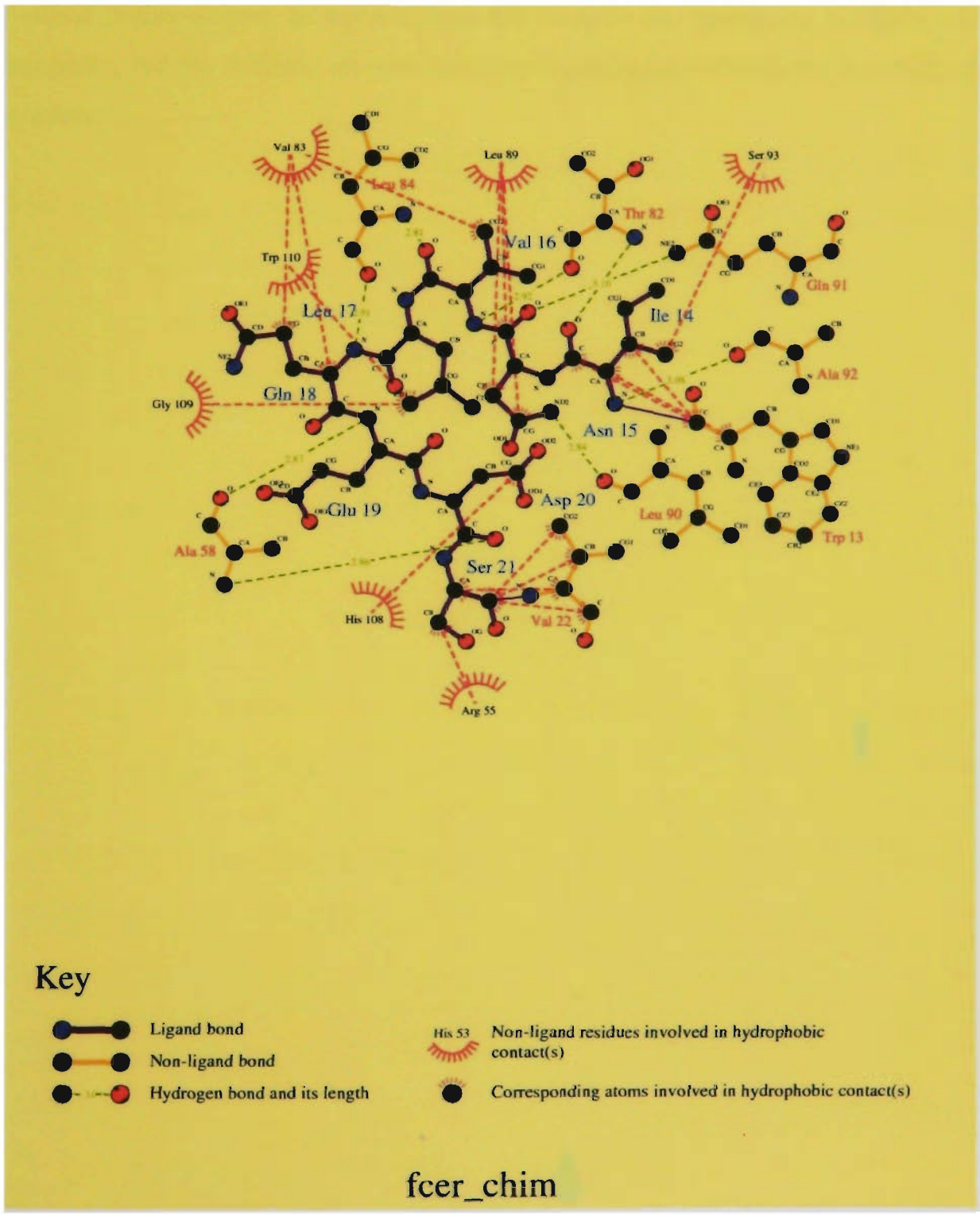
Val 83
Leu 89
Ser 93
Leu 84
Thr 82
Val 16
Trp 110
Gln 91
Leu 17
Ile 14
Ala 92
Gly 109
Gln 18
Asn 15
Asp 20
Glu 19
Leu 90
Trp 13
Ala 58
Ser 21
His 108
Val 22
Arg 55
Key
Ligand bond
Non-ligand bond
Hydrogen bond and its length
His 53
Non-ligand residues involved in hydrophobic contact(s)
Corresponding atoms involved in hydrophobic contact(s)
fcer_chim

However there are limitations in BIAcore analyses, for example, chemistry dependent coupling of proteins to an unnatural surface, as well as forced orientation of the coupled protein (e.g. through coupling via the aldehyde groups) may lead to alteration or inactivation of the protein. This is a particularly important consideration for the work described in this chapter, as the wild type IgE receptor was seemingly unaffected by conjugation, but the chimeric receptor was clearly profoundly affected by the coupling procedure.

REFERENCES

1. Rich RL, Myszka DG. Advances in surface plasmon resonance biosensor analysis. Curr Opin Biotechnol 2000; 11:54-61.
2. Nice E, Layton J, Fabri L, Hellman U, Engstrom A, Persson B, Burgess AW. Mapping of the antibody- and receptor-binding domains of granulocyte colony-stimulating factor using an optical biosensor. Comparison with enzyme-linked immunosorbent assay competition studies. J Chromatog 1993; 646:159-168.
3. Fisher RJ, Fivash M, Casa-Finet J, Erickson JW, Kondoh A, Bladen V, Fisher C, Watson D, Papas T. Real-time DNA binding measurements of the ETS1 recombinant proteins reveal significant kinetic differences between the p42 and p51 isoforms. Protein Sci 1994; 3:257-266.
4. Tunks D, Nice E. A sensor of things to come. Today's Life Sci 1994; 8:54-59.
5. Cook JP, Henry AJ, McDonnell JM, Owens RJ, Sutton BJ and Gould HJ. Identification of contact residues in the IgE binding site of human FcεRIα. Biochemistry 1997; 36:15579-15588.
6. Garman SC, Wurzburg BA, Tarchevskaya SS, Kinet J-P, Jardetzky TS. Structure of the Fc fragment of human IgE bound to its high-affinity receptor FcεRIα. Nature 2000; 406:259-266.
7. O'Shannessy DJ, Brigham BM, Soneson KK, Hensley P, Brooks I. Determination of rate and equilibrium binding constants for macromolecular interactions using surface plasmon resonance: Use of non-linear least squares analysis methods. Anal Biochem 1993; 212:457-468.
8. Hulett MD, McKenzie IFC, PM Hogarth. Chimeric Fc receptors identify immunoglobulin-binding regions in human FcγRII and FcεRI. Eur J Immunol 1993;23:640-645.
9. Hogarth PM, Ierino FL, Hulett MD. Characterisation of FcR Ig-Binding Sites and Epitope Mapping. Immunomethods 1994;4:17-24.
10. Gill SC, von Hippel PH. Calculation of protein extinction coefficients from aminoacid sequence data. Analytical Biochem 1989;182:319-326.
11. Morton TA, Myszka DG. Kinetic analysis of macromolecular interactions using surface plasmon resonance biosensors. Methods Enzymol 1998: 295:268-294.

12. Wines BD, Hulett MD, Jamieson GP, Trist HM, Spratt JM, Hogarth PM. Identification of residues in the first domain of human Fc alpha receptor essential for interaction with IgA. J Immunol. 1999; 162(4):2146-53.

13. Henry AJ, Cook JP, McDonnell JM, Mackay GA, Shi J, Sutton BJ and Gould HJ. Participation of the N-terminal region of Cϵ3 in the binding of human IgG to its high-affinity receptor FcϵRI. Biochemistry 1997; 36:15568-15578.

14. Sayers I, Cain SA, Swan JRM, Pickett MA, Watt PJ, Holgate ST, Padlan EA, Schuck P, Helm BA. Amino acid residues that influence FcϵRI mediated effector functions of human immunoglobulin E. Biochemistry 1998; 37:16152-16164.

15. Levy DA, Osler AG. Studies on the mechanisms of hypersensitivity phenomena. XVII. Passive sensitization *in vitro* of human leukocytes to ragweed pollen antigen. J Immunol 1966; 97:203-211.

16. Kulczycki Jnr A, Metzger H. The interaction of IgE with rat basophilic leukemia cells. II. Quantitative aspects of the binding reaction. J Exp Med 1974; 140:1676-1695.

17. Helm BA, Sayers I, Higginbottom A, Cantarelli M D, Ling Y, Ahmad K, Padlan EA, Wilson APM. Identification of the high-affinity receptor binding region in immunoglobulin E. J Biol Chem 1996; 271:7494-7500.

18. Hulett MD, Brinkworth RI, McKenzie IFC, Hogarth PM. Fine structural analysis of interaction of FcϵRI with IgE. J Biol Chem 1999;274(19):13345-13352.

19. Riske F, Hakimi J, Mallamaci M et al. High affinity human IgE receptor (FcϵRI). Analysis of functional domains of the α-subunit with monoclonal antibodies. J Biol Chem 1991; 266(17):11245-11251.

20. Maxwell KF, Powell MS, Hulett MD, Barton PA, McKenzie IFC, Garrett TPJ, Hogarth PM. The crystal structure of the human leukocyte Fcreceptor, FcγRIIa. Nat Struct Biol 1999;6(5):437-442.

21. Presta L, Shields R, O'Connell L et al. The binding site on human immunoglobulin E for its high affinity receptor. J Biol Chem 1994; 269(42):26368-26373.

22. Garman SC, Kinet J-P, Jardetzky TS. Crystal structure of the human high-affinity IgE receptor. *Cell* 1998;95:951-961.

23. McCoy AJ, Epa VC, Colman PM. Electrostatic complementarity at protein/protein interfaces. J Mol Biol 1997; 268:570-584.

CHAPTER SIX:

Concluding Remarks.

The investigations described in this thesis provide a significant contribution to the understanding of the interactions of FcεRI-α with IgE. In cells this interaction triggers a cascade of events crucial to the development of the allergic diseases asthma and hay fever, and thus provides potential as a target for the design of therapeutic agents that will prevent the pathological sequellae. In western countries (e.g. Australia) approximately 20% of the populations are afflicted with an allergic condition, most commonly allergic rhinitis and also, more seriously, asthma. The incidence of asthma is steadily increasing, and approximately 50% of asthmatics are allergic with mortality rates varying from 1 to 4 per 100,000 of population (1). The economics of FcεRI also testify to its importance in industry with Australians alone spending $150 million annually on allergy related medication.

At the commencement of the work embodied in this thesis, nothing was known of the structure of FcεRI. This is surprising because of the great importance of the structure of this receptor in human disease, not only asthma and seasonal allergy, but also anaphylaxis, eczema and urticaria. Certainly mutagenesis studies (2, 3, 4) have identified residues of FcεRI important in IgE binding, but little was known of the spatial relationships of these residues, or of the two immunoglobulin domains that form the extracellular region.

Solving the structure of the closely related receptor, FcγRIIa, provided the first opportunity to build credible models of FcεRI-α. The model of FcεRI-α based on the crystal structure of FcγRIIa, described and utilised in Chapters 2 and 3, was the most progressive and accurate at that time and has since been shown to be very similar to the crystal structure determined by Garman *et al.* (5). Even after the initial publication in 1998 (5) describing the crystal structure of FcεRI-α, the co-ordinates of the structure were not released, and thus, were not available for use in this thesis. In any event, the model has turned out to be correct; when the model is compared with the crystal structure (accession number: 1F2Q) for the alpha carbon atoms of residues 4-31 and 36-172, the root mean square deviation is 2.5 Angstroms. Residues 32-35 comprise the highly variable C' region of the Ig domain. This clearly indicates the quality of the original modelling, and thus the availability of not only this structure, but other such structures opens up many opportunities for the design and synthesis of new drugs to treat disease.

Work described in this thesis was targeted at resolving the relationships between structure and function of FcεRI-α.

(i) The structure of FcεRI-α, the IgE binding site, and the relationships between regions of the receptor: In Chapters 2 and 3 monoclonal antibodies, synthetic peptides and mutagenesis were used to define functional regions of FcεRI-α. The importance of the cell surface display and function of the receptor cannot be underestimated, and is a crucial adjunct to the crystal based molecular structures in the development of structural antagonists. The importance of structural integrity within the receptor is also crucial, as mutagenesis of specific regions of D1 (e.g. the region containing an intradomain cysteine) can prevent receptor expression, and this may also be an area for intracellular antagonist attack.

(ii) How the regions of the FcR relate to each other, and how they directly influence IgE binding: Studies described in Chapters 2 and 3 showed that domain one played a role in presenting the IgE binding site on the cell surface. Of particular importance was the finding that the integrity of the D1 intradomain disulphide bridges and the D1: D2 interface is crucial for both the ability of the receptor to bind IgE and surface expression of the receptor. The γ(ABCε)εγ and γ(ABCC'ε)εγ chimeras were assumed not to be expressed on the cell surface as they could not be detected by a panel of anti-FcεRI-α antibodies. A γ(EFGε)εγ chimera also failed to express, although a combined γ(ABCε + EFGε)εγ chimera was effectively expressed and bound IgE (data not shown). This intimated that the intradomain cysteines of D1 needed to be 'paired' for cell surface expression, and some confirmation of this was afforded by excellent expression of a γ(C'EFε)εγ chimera (Chapter 2).

(iii) Anchoring of the cell surface influences IgE binding: The means of anchoring the receptor in the membrane has been shown here to alter surface expression and ligand binding of the receptor. The presence of a GPI membrane anchor causes greater surface expression of the receptor than a transmembrane, cytoplasmic anchor, and the affinity for ligand is concomitantly reduced. This would imply that the GPI anchor creates either a unique receptor orientation or a disequilibrium in the production and/or removal

of the receptor at the cell surface which could be driven by the structure of the membrane proximal/ transmembrane/ cell anchor of the receptor, or the interaction of membrane components, but is another previously unrecognised area for the direction of antagonistic activity in the future.

(iv) The structural information derived was used to devise peptides as potential receptor antagonists: For studies in Chapter 2 synthetic peptides were made that mimicked the structure of the IgE binding site of the receptor and acted as antagonists to the binding of IgE. The ϵRI-11 peptide, which comprised amino acids 111-120 of the D2 BC loop region, inhibited IgE binding by 61%. The recent crystal structure indicates the presence of two separate binding sites in FcϵRI-α, both composed of residues from more than one loop or region of the receptor. The studies herein suggest that the IgE binding site that includes the region of the receptor encompassed by the ϵRI-11 peptide is the major binding site, and it is possible that combinations of peptides could increase the inhibition of IgE binding. A series of structurally appropriate smaller peptides would also be less antigenic than a larger molecule, and therefore have greater long-term efficacy.

(v) Knowledge of the IgE binding sites and dynamics of IgE:FcϵRI interaction can aid the development of small chemical entities - chemical drugs - as receptor antagonists: While most structure-based drug design strategies target the obvious i.e. the active site of the protein, the new understanding of the FcϵRI-α interdomain interface revealed in Chapter 2 provides an exciting opportunity to design novel chemical antagonists capable of insertion into the interdomain interface and causing the destruction of the interactions between Arg 15 of D1 with amino acids in D2. Such an antagonist could specifically destroy the ability of FcϵRI-α to bind ligand without affecting the capability of closely related receptors to bind their ligands (e.g. FcγRIIa and IgG), because the nature of the interdomain interface in these receptors is apparently less sensitive to disruption.

For work described in chapter 4 a novel assay was developed in which IgE was immobilised onto a biosensor chip for binding studies. This work enabled the interaction between IgE and FcϵRI-α to be explored in a fluid phase thus facilitating direct measurements of a range of receptor:ligand interactions. Preliminary work with this system

has given indications of a lower binding affinity under these conditions, i.e. with the IgE (bound to antigen) in the immobile phase before Fc binding to FcεRI-α. The increase in understanding of the physiologic response of the FcεRI-α:IgE interaction, and could be utilised in the future - in association with the environmental requirements for ligand binding (Chapter 5) - to reduce the sensitivity of the FcεRI-α:IgE interaction in circumstances where ablation was indicated to be inappropriate. Time did not permit further work on the interactions of chimeric and mutant receptors in this assay system, none-the-less the first and a robust assay system was developed.

Biosensor analysis of the interaction between FcεRI-α and IgE with the receptor immobilised (Chapter 5) has enabled the FcεRI-α:IgE interaction to be studied under varying conditions of pH and ionic strength. When these experiments were performed there was no solved structure of FcεRI-α or of its interaction with IgE. My results indicated the presence of salt bridges in FcεRI-α:IgE binding, and this was subsequently confirmed in the X-ray crystallography data published by Garman *et al.* as suggested by the structure of the interaction (6) and also a K117D mutation (7). The comparison of the responses of FcεRI-α with those of the γε chimera in the receptor : ligand interactions has emphasised responses under the varying conditions, the chimera responding more acutely to controlled variations in the ligand binding environment. This knowledge, in association with the structural knowledge of the IgE binding site, and its activity, can be utilised in the design of small chemical inhibitors to the FcεRI-α:IgE interaction that a) are antagonistic, b) are not antigenic, and c) do not initiate degranulation. This would revolutionise the treatment of FcεRI-α related allergic disease into an area of preventive rather than reactive medicine.

Comparison of data in this thesis with the recently solved structure of FcεRI-α.

The findings presented in this thesis are discussed here in the context of other recent publications on the structure of FcεRI-α (5) and the interaction of FcεRI-α with IgE Fc (6). There are two separate sites in FcεRI-α involved in ligand binding, labelled sites 1 and 2. Initial problems working with FcεRI-α were overcome with the production of monoclonal antibodies to both domain one (mAb 54) and domain two (mAb 47) of FcεRI-α (Chapter 2). The use of these antibodies along with mAb 15-1 (a monoclonal antibody that blocks IgE binding) highlighted a discrepancy between the work of Nechansky *et al.* (8) and the results presented in chapter 2 of this thesis. The epitope of mAb 15-1, was previously thought to be in the region of Val 155 and Trp 156 (8). In this work a W156A mutation was shown to ablate mAb 15-1 binding but not IgE binding, and V155L to reduce binding of both IgE and mAb 15-1. The data presented in Chapter 2 of this thesis indicated that the epitope of mAb 15-1 was in the BC loop region of D2 between the amino acids 111-120. This is confirmed in the crystal structure as the 111-120 sequence includes Trp 113, Lys 117 and Ile 119, all shown to be directly involved in IgE binding (6), as is Trp 156, but not Val 155 (FG loop). Val 155 lies close to the hydrophobic pocket made by Trp 87, Trp 110, Trp 113 and Trp 156 that form part of the IgE binding site 2 (6), and lies almost directly below Trp 156 in an apparently supporting position (Fig 6.1). It is feasible that the mutation V155L could cause displacement of Trp 156 and distort the orientation of the very close Trp 113, in which case the epitope for mAb 15-1 would be placed in the FcεRI-α/IgE binding site 2, probably in the intimate environs of Trp 113. Lys 117 and Ile 119 (C strand) form part of the FcεRI-α / IgE binding site 1, and as such do not present in the same region.

Results presented in Chapter 2 of this thesis showed that the εRI-11 peptide (amino acids 111-120) could block 61% of IgE binding. This is consistent with the x-ray data of Garman *et al.* (6) and is discussed here with reference to the IgE binding sites, previous mutagenesis data (reviewed in Chapter1) and the mAb 15-1 epitope. The mutations V155L (8) and V155A (10) have been shown to considerably reduce the binding of IgE, and, as suggested above, since Val 155 is not part of an IgE binding site, this effect is probably due to distortion of the receptor causing disruption of the binding site. The mutation W156A

Figure 6.1 Diagram of the 'binding site 2' region of FcεRI-α.

FcεRI-α is shown in tubular format, with the β strands shown in blue and the loop regions in grey. The associated regions of IgE are shown in ribbon format in magenta.

Some of the key residues for D1 : D2 interactions and FcεRI-α: IgE interactions are displayed in line style. Interactions between Arg 15 and Leu 90 or Gln 91 are shown in green with the distance between them in Angstroms labelled.

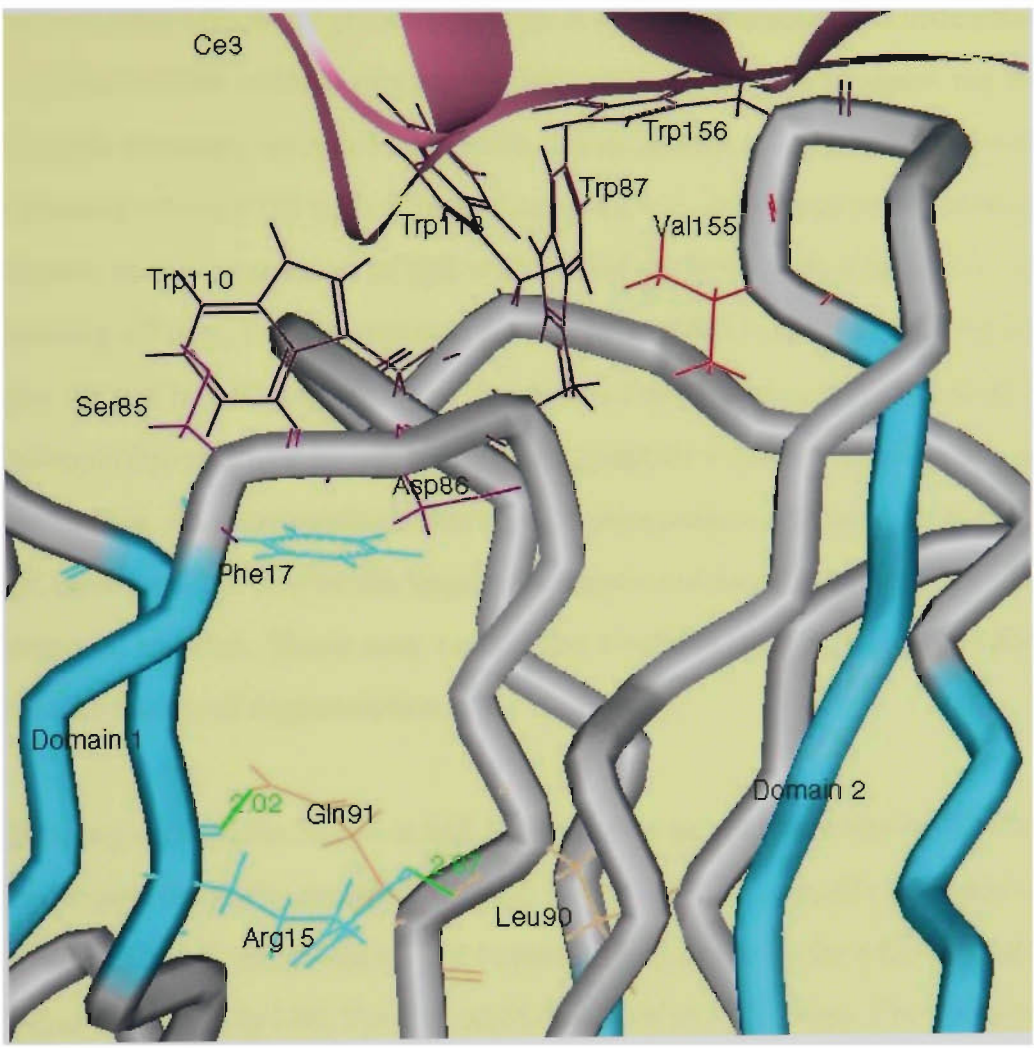
Ce3
Trp156
Trp87
Trp118
Val155
Trp110
Ser85
Asp86
Phe17
Domain 1
Domain 2
202
Gln91
Leu90
Arg15

(8,10), although part of the hydrophobic pocket of binding site 2 does not itself cause reduction of IgE binding, and indeed, has been shown to enhance IgE binding (10). Gln 157 and Leu 158 and Asp 159 are also part of the IgE binding site 2, but Q157A and L158A mutations had little effect on IgE binding (10). A D159K mutation had little effect on IgE binding (7) but D159A reduces binding by 50% (10), there is no apparent reason for this on viewing the structure, as Asp 159 extends out to solvent away from both binding sites with no obvious interactions with other residues. Of the other residues in the hydrophobic pocket shown in the interaction of IgE with FcεRI-α, W87D (7) was shown to slightly reduce binding affinity, Trp 110 was not mutated (6) and W113A (10) was shown to reduce binding by 80%. The εRI-11 peptide encompasses Trp 113, apparently the most dominant of the hydrophobic residues in IgE binding, and peptide blocking data is consistent with mutagenesis data. In constructing a therapeutic antagonist, an alternative to blocking the entire IgE binding site 2 may be the targeted disruption of key residues such as Trp 113 by small chemical entities. These may reduce the FcεRI-α:IgE interaction sufficiently to impede the initiation of degranulation.

Binding site 1 of the FcεRI-α:IgE interaction involves the receptor C'E loop, which is the third region shown by mutation to be involved in IgE binding (2). This site comprises the C strand residues Lys 117 and Ile 119 (also encompassed by the εRI-11 peptide), with Arg 126 and Tyr 129, Trp 130, Tyr 131, and Glu 132 of the C'E loop. The mutation K117D (7) has been shown to overall reduce the affinity of IgE binding, again supporting the peptide data. Of the other residues in binding site 1, mutations of Ile 119 and Arg 126 have not yet been reported, Y129A introduced no change to IgE binding (10), and W130A increased binding (10). The mutations Y131A and E132A (10) both reduced binding, and of these two residues, Tyr 131 interacts with five residues in Cε3, and Glu 132 has been proposed as part of a potential salt bridge with Cε3 R334. Chemical destruction of the Glu 132 salt bridge and thus the interactions of Tyr 131 with Trp 113 may be sufficient to disrupt either or both the FcεRI-α:IgE interaction sites or the initiation of degranulation.

The critical nature of the interdomain interface for receptor presentation and IgE binding were described in Chapter 3. Residues in the A' strand and G strand of D1 were examined, and the mutation of specific residues in the A' strand (R15A and F17A)

suggested their importance in the interdomain interface. The structure of FcεRI-α, based on x-ray crystallography data (5), displays fewer interactions across the D1:D2 interface than the model that is based on the structure of FcγRIIa (9, Chapter 3). The x-ray data confirms the importance of Arg 15 in maintaining the interface, as it is apparently the only residue in the A' strand with interactions across the interface. The point mutation R15A caused ablation of IgE binding. In the structure of the receptor alone (5) the interactions are Arg 15 to Leu 90 - 1.69Å[1], and Arg 15 to Glu 91 - 1.80Å, but in the structure of the IgE bound receptor these distances change to 2.87Å (no bond detected) and 2.02Å respectively. This would imply that interaction with IgE places pressure on the interdomain interface increasing the spatial separation between the domains. There are no water molecules described within the interface to increase interactions between the domains (6), and this is consistent with the relative weakness of this interface, and commends it as a significant potential site for therapeutic disruption. Destruction of the interface would prevent appropriate display of the binding sites and ablate IgE binding; thus preventing signalling and degranulation of the cell. Ablation of IgE binding on mutation of Glu 91 would confirm the importance of Arg 15 in the interface. Phe 17 was the second residue mutated (Chapter 3), and F17A substantially reduced IgE binding. In the crystal structure of FcεRI-α, Phe 17 interacts with no other residue, and as in the model, the affect on binding is probably caused by a spatial effect of the residue filling the upper region of the interface and supporting the linker region above it. Mutation of this amino acid to alanine may create a space in the interface, causing collapse of the linker region and thus IgE binding site 2.

It was shown in Chapter 5 that both pH and electrostatic interactions played a part in the interaction of FcεRI-α with IgE. The high receptor occupancy and rapid dissociation of IgE from the receptor at pH 6.0 is consistent with a histidine being involved in the interaction, and this was more evident in the chimeric γε receptor than in εε. The crystal structure of the interaction between IgE and FcεRI-α (6) verifies this inclusion of a histidine in the binding interaction, as His 424 from both IgE Cε3 domains interact with FcεRI-α. His 424 of one Cε3 interacts with Tyr 131 and Trp 130 in binding site 1. In

[1] Interatomic distances were determined using the molecular modelling program 'WebLab Viewer Pro'.

binding site 2, His 424 of the second Cϵ3 interacts with Trp 113, a residue that has been shown by mutation to be an important residue in IgE binding. Clearly these interactions are likely candidates to explain the pH sensitivity of IgE:FcϵRI interaction.

FcϵRI-α occupancy and ligand dissociation was seen to be affected by alteration in ionic strength. It has been suggested that there are two possible salt bridges Glu 132 - Cϵ Arg 334 (1.77Å, 3.42Å), K 117 - Cϵ D 362 (1.77Å, 2.85Å) in the crystal structure of the interaction (6). This is again consistent with observed sensitivity of binding to changes in ionic strength and these interactions may form the basis of new targets for therapeutic use.

As we look to the future, the impact of rational drug design on modern medicine is just beginning to be felt, e.g. the HIV protease inhibitors or the influenza drug Relenza are recent examples of the potential of such an approach. With the tabling of the 30,000 genes in the Human genome there will be abundant potential targets for the design of New Chemical Entities (NCE). However, it will be essential to derive and use both quality structural and function information for this to become a reality. In this thesis I have attempted to define the structural basis for the function of one of the most important receptors in pathological immunity and hope that this will, in turn, go some way to providing radically new treatments for a widespread human disease.

REFERENCES

1. Wheatley LM and Platts-Mills TAE. Perennial allergens and the asthma epidemic. Science Med 1996; 3:6-13.
2. Hulett MD, McKenzie IFC, Hogarth PM. Chimeric Fc receptors identify immunoglobulin-binding regions in human FcγRII and FcεRI. Eur J Immunol 1993; 23:640-645.
3. Hogarth PM, Hulett MD, Ierino FL et al. Identification of the immunoglobulin binding regions (IBR) of FcγRII and FcεRI. Immunological Reviews 1992; 125:21-35.
4. Mallamaci MA, Chizzonite R, Griffin M et al. Identification of sites on the human FcεRIα subunit which are involved in binding human and rat IgE. J Biol Chem 1993; 268(29):22076-22083.
5. Garman SC, Kinet J-P, Jardetzky TS. Crystal structure of the human high-affinity IgE receptor. Cell 1998;95:951-961.
6. Garman SC, Wurzburg BA, Tarchevskaya SS, Kinet J-P, Jardetzky TS. Structure of the Fc fragment of human IgE bound to its high-affinity receptor FcεRIα. Nature 2000;406:259-266
7. Cook JP, Henry AJ, McDonnell JM, Owens RJ, Sutton BJ and Gould HJ. Identification of contact residues in the IgE binding site of human FcεRIα. Biochemistry 1997; 36:15579-15588.
8. Nechansky A, Aschauer H, and Kricek F. The membrane-proximal part of FcεRIα contributes to human IgE and antibody binding - Implications for a general structural motif in Fc receptors. FEBS 1998;441:225-230.
9. Rigby LJ, Epa VC, Mackay GA, Hulett MD, Sutton BJ, Gould HJ, Hogarth PM. Mutagenesis and homology modelling define the role of domain one in the high affinity Fc epsilon receptor, FcεRI. J Biol Chem 2000; 275:9664-9672.
10. Hulett MD, Brinkworth RI, McKenzie IFC, Hogarth PM. Fine structural analysis of interaction of FcεRI with IgE. J Biol Chem 1999;274(19):13345-13352.
11. Kulczycki Jnr A, Metzger H. The interaction of IgE with rat basophilic leukemia cells. II. Quantitative aspects of the binding reaction. J Exp Med 1974; 140:1676-1695.

12. Helm BA, Sayers I, Higginbottom A, Cantarelli M D, Ling Y, Ahmad K, Padlan EA, Wilson APM. Identification of the high-affinity receptor binding region in immunoglobulin E. J Biol Chem 1996; 271:7494-7500.

APPENDIX ONE

Appendix 1.1. Nucleotide and derived aminoacid sequence of FcεRI-α cDNA, including the leader sequence. Genbank accession # X06948.

The positions of the first and second domains, membrane proximal region, transmembrane region and cytoplasmic tail region are indicated. The interchain disulphide bond Cys residues are marked with a ⊡. The approximate positions of the extracellular domain β strands are underlined and labelled. Numbers above the rows refer to the amino acid position; numbers in italics at the ends of rows refer to the nucleotide position from the start of the leader sequence. The single letter representing the aminoacid residues shown by the crystal structure[1] to be involved in binding are highlighted, blue for binding site one, and yellow for binding site two. Strands are labelled according to the crystal structure of FcεRI-α[2].

D1 = Domain one
D2 = Domain two
MP = Membrane proximal region
TM = Transmembrane region
CT = Cytoplasmic tail region

[1] Garman SC, Wurzburg BA, Tarchevskaya SS, Kinet JP and Jardetzky TS. Structure of the Fc fragment of human IgE bound to its high-affinity IgE receptor FcεRIα. Nature 2000;406:259-266.

[2] Garman SC, Kinet J-P, Jardetzky TS. Crystal structure of the human high-affinity IgE receptor. Cell 1998;95:951-961.

FcεRI-α

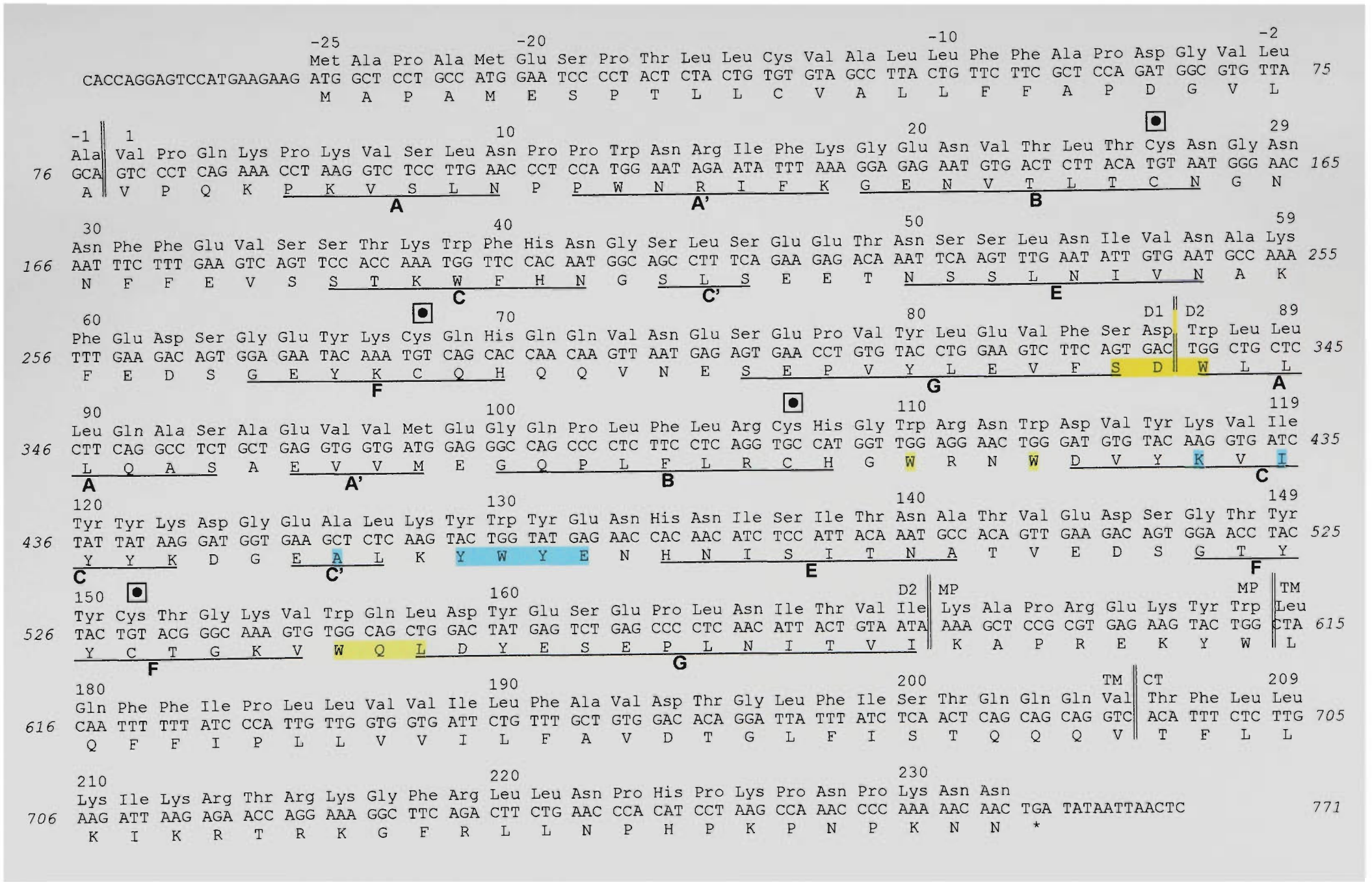
-25 -20 -10 -2
Met Ala Pro Ala Met Glu Ser Pro Thr Leu Leu Cys Val Ala Leu Leu Phe Phe Ala Pro Asp Gly Val Leu
CACCAGGAGTCCATGAAGAAG ATG GCT CCT GCC ATG GAA TCC CCT ACT CTA CTG TGT GTA GCC TTA CTG TTC TTC GCT CCA GAT GGC GTG TTA 75
M A P A M E S P T L L C V A L L F F A P D G V L
-1 1 10 20 29
Ala Val Pro Gln Lys Pro Lys Val Ser Leu Asn Pro Pro Trp Asn Arg Ile Phe Lys Gly Glu Asn Val Thr Leu Thr Cys Asn Gly Asn
76 GCA GTC CCT CAG AAA CCT AAG GTC TCC TTG AAC CCT CCA TGG AAT AGA ATA TTT AAA GGA GAG AAT GTG ACT CTT ACA TGT AAT GGG AAC 165
A V P Q K P K V S L N P P W N R I F K G E N V T L T C N G N
A A' B
30 40 50 59
Asn Phe Phe Glu Val Ser Ser Thr Lys Trp Phe His Asn Gly Ser Leu Ser Glu Glu Thr Asn Ser Ser Leu Asn Ile Val Asn Ala Lys
166 AAT TTC TTT GAA GTC AGT TCC ACC AAA TGG TTC CAC AAT GGC AGC CTT TCA GAA GAG ACA AAT TCA AGT TTG AAT ATT GTG AAT GCC AAA 255
N F F E V S S T K W F H N G S L S E E T N S S L N I V N A K
C C' E
60 70 80 D1 D2 89
Phe Glu Asp Ser Gly Glu Tyr Lys Cys Gln His Gln Gln Val Asn Glu Ser Glu Pro Val Tyr Leu Glu Val Phe Ser Asp Trp Leu Leu
256 TTT GAA GAC AGT GGA GAA TAC AAA TGT CAG CAC CAA CAA GTT AAT GAG AGT GAA CCT GTG TAC CTG GAA GTC TTC AGT GAC TGG CTG CTC 345
F E D S G E Y K C Q H Q Q V N E S E P V Y L E V F S D W L L
F G A
90 100 110 119
Leu Gln Ala Ser Ala Glu Val Val Met Glu Gly Gln Pro Leu Phe Leu Arg Cys His Gly Trp Arg Asn Trp Asp Val Tyr Lys Val Ile
346 CTT CAG GCC TCT GCT GAG GTG GTG ATG GAG GGC CAG CCC CTC TTC CTC AGG TGC CAT GGT TGG AGG AAC TGG GAT GTG TAC AAG GTG ATC 435
L Q A S A E V V M E G Q P L F L R C H G W R N W D V Y K V I
A A' B C
120 130 140 149
Tyr Tyr Lys Asp Gly Glu Ala Leu Lys Tyr Trp Tyr Glu Asn His Asn Ile Ser Ile Thr Asn Ala Thr Val Glu Asp Ser Gly Thr Tyr
436 TAT TAT AAG GAT GGT GAA GCT CTC AAG TAC TGG TAT GAG AAC CAC AAC ATC TCC ATT ACA AAT GCC ACA GTT GAA GAC AGT GGA ACC TAC 525
Y Y K D G E A L K Y W Y E N H N I S I T N A T V E D S G T Y
C C' E F
150 160 D2 MP MP TM
Tyr Cys Thr Gly Lys Val Trp Gln Leu Asp Tyr Glu Ser Glu Pro Leu Asn Ile Thr Val Ile Lys Ala Pro Arg Glu Lys Tyr Trp Leu
526 TAC TGT ACG GGC AAA GTG TGG CAG CTG GAC TAT GAG TCT GAG CCC CTC AAC ATT ACT GTA ATA AAA GCT CCG CGT GAG AAG TAC TGG CTA 615
Y C T G K V W Q L D Y E S E P L N I T V I K A P R E K Y W L
F G
180 190 200 TM CT 209
Gln Phe Phe Ile Pro Leu Leu Val Val Ile Leu Phe Ala Val Asp Thr Gly Leu Phe Ile Ser Thr Gln Gln Gln Val Thr Phe Leu Leu
616 CAA TTT TTT ATC CCA TTG TTG GTG GTG ATT CTG TTT GCT GTG GAC ACA GGA TTA TTT ATC TCA ACT CAG CAG CAG GTC ACA TTT CTC TTG 705
Q F F I P L L V V I L F A V D T G L F I S T Q Q Q V T F L L
210 220 230
Lys Ile Lys Arg Thr Arg Lys Gly Phe Arg Leu Leu Asn Pro His Pro Lys Pro Asn Pro Lys Asn Asn
706 AAG ATT AAG AGA ACC AGG AAA GGC TTC AGA CTT CTG AAC CCA CAT CCT AAG CCA AAC CCC AAA AAC AAC TGA TATAATTAACTC 771
K I K R T R K G F R L L N P H P K P N P K N N *

Appendix 1.2. Aminoacid sequence of the cDNA of the Cϵ2, Cϵ3 and Cϵ4 domains of IgE. Genbank accession #L00022.

The interchain disulphide bond Cys residues are underlined and in bold. Numbers above the rows refer to the amino acid position; numbers in italics at the ends of rows refer to the nucleotide position The single letter code representing the aminoacid residues shown by the crystal structure of Garman et al.[1] to be involved in binding to FcϵRI-α are highlighted in blue for binding site one, and the three letter code is highlighted in yellow for binding site two. The double chain structure of IgE permits the same residue from each chain to be part of the binding site.

[1]Garman SC, Wurzburg BA, Tarchevskaya SS, Kinet J-P, Jardetzky TS.
Structure of the Fc fragment of human IgE bound to its high-affinity receptor FcϵRIα. *Nature* 2000;406:259-266.

IgE

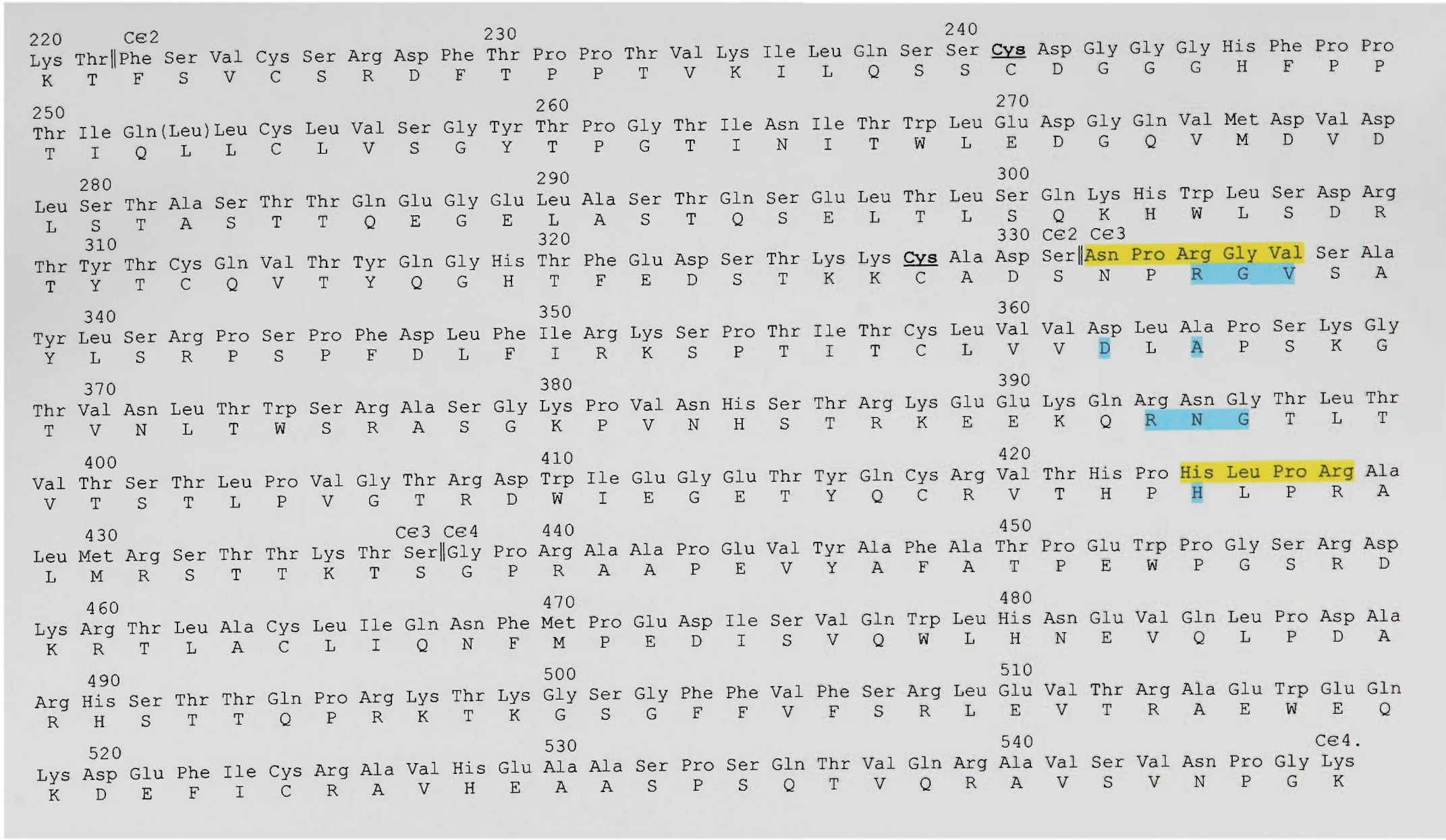
220 Cε2 230 240
Lys Thr‖Phe Ser Val Cys Ser Arg Asp Phe Thr Pro Pro Thr Val Lys Ile Leu Gln Ser Ser Cys Asp Gly Gly Gly His Phe Pro Pro
K T F S V C S R D F T P P T V K I L Q S S C D G G G H F P P
250 260 270
Thr Ile Gln(Leu)Leu Cys Leu Val Ser Gly Tyr Thr Pro Gly Thr Ile Asn Ile Thr Trp Leu Glu Asp Gly Gln Val Met Asp Val Asp
T I Q L L C L V S G Y T P G T I N I T W L E D G Q V M D V D
280 290 300
Leu Ser Thr Ala Ser Thr Thr Gln Glu Gly Glu Leu Ala Ser Thr Gln Ser Glu Leu Thr Leu Ser Gln Lys His Trp Leu Ser Asp Arg
L S T A S T T Q E G E L A S T Q S E L T L S Q K H W L S D R
310 320 330 Cε2 Cε3
Thr Tyr Thr Cys Gln Val Thr Tyr Gln Gly His Thr Phe Glu Asp Ser Thr Lys Lys Cys Ala Asp Ser‖Asn Pro Arg Gly Val Ser Ala
T Y T C Q V T Y Q G H T F E D S T K K C A D S N P R G V S A
340 350 360
Tyr Leu Ser Arg Pro Ser Pro Phe Asp Leu Phe Ile Arg Lys Ser Pro Thr Ile Thr Cys Leu Val Val Asp Leu Ala Pro Ser Lys Gly
Y L S R P S P F D L F I R K S P T I T C L V V D L A P S K G
370 380 390
Thr Val Asn Leu Thr Trp Ser Arg Ala Ser Gly Lys Pro Val Asn His Ser Thr Arg Lys Glu Glu Lys Gln Arg Asn Gly Thr Leu Thr
T V N L T W S R A S G K P V N H S T R K E E K Q R N G T L T
400 410 420
Val Thr Ser Thr Leu Pro Val Gly Thr Arg Asp Trp Ile Glu Gly Glu Thr Tyr Gln Cys Arg Val Thr His Pro His Leu Pro Arg Ala
V T S T L P V G T R D W I E G E T Y Q C R V T H P H L P R A
430 Cε3 Cε4 440 450
Leu Met Arg Ser Thr Thr Lys Thr Ser‖Gly Pro Arg Ala Ala Pro Glu Val Tyr Ala Phe Ala Thr Pro Glu Trp Pro Gly Ser Arg Asp
L M R S T T K T S G P R A A P E V Y A F A T P E W P G S R D
460 470 480
Lys Arg Thr Leu Ala Cys Leu Ile Gln Asn Phe Met Pro Glu Asp Ile Ser Val Gln Trp Leu His Asn Glu Val Gln Leu Pro Asp Ala
K R T L A C L I Q N F M P E D I S V Q W L H N E V Q L P D A
490 500 510
Arg His Ser Thr Thr Gln Pro Arg Lys Thr Lys Gly Ser Gly Phe Phe Val Phe Ser Arg Leu Glu Val Thr Arg Ala Glu Trp Glu Gln
R H S T T Q P R K T K G S G F F V F S R L E V T R A E W E Q
520 530 540 Cε4.
Lys Asp Glu Phe Ile Cys Arg Ala Val His Glu Ala Ala Ser Pro Ser Gln Thr Val Gln Arg Ala Val Ser Val Asn Pro Gly Lys
K D E F I C R A V H E A A S P S Q T V Q R A V S V N P G K

205

Appendix 1.3. Nucleotide and derived aminoacid sequence of FcγRIIA cDNA, including the leader sequence[1].

The positions of the first and second domains, membrane proximal region, transmembrane region and cytoplasmic tail region are indicated. The interchain disulphide bond Cys residues are marked with a ⊡. The approximate positions of the extracellular domain β strands are underlined and labelled. Numbers above the rows refer to the amino acid position; numbers in italics at the ends of rows refer to the nucleotide position. The crystal structure of FcγRIIa indicates Ala -1 (or Ala-2) as the amino terminus of the protein.

D1 = Domain one
D2 = Domain two
MP = Membrane proximal region
TM = Transmembrane region
CT = Cytoplasmic tail region

[1] Hibbs ML, Bonnadonna L, Scott BM, McKenzie IFC, Hogarth PM. Molecular cloning of a human immunoglobulin G receptor. Proc Nat Acad Sci 1988; 85:2240-2244.

FcγRIIa


1/-33 -29 -20 -10 -1
Met Glu Thr Gln Met Ser Gln Asn Val Cys Pro Arg Asn Leu Trp Leu Leu Gln Pro Leu Thr Val Leu Leu Leu Leu Leu Ala Ser Ala Asp Ser Gln Ala
GAATTCCAAC ATG GAG ACC CAA ATG TCT CAG AAT GTA TGT CCC AGA AAC CTG TGG CTG CTT CAA CCA TTG ACA GTT TTG CTG CTG CTG CTG GCT TCT GCA GAC AGT CAA GCT 99
M E T Q M S Q N V C P R N L W L L Q P L T V L L L L L A S A D S Q A
-1 +1 10 20 29
Ala Ala Pro Pro Lys Ala Val Leu Lys Leu Glu Pro Pro Trp Ile Asn Val Leu Gln Glu Asp Ser Val Thr Leu Thr Cys Gln Gly Ala
100 GCA GCT CCC CCA AAG GCT GTG CTG AAA CTT GAG CCC CCG TGG ATC AAC GTG CTC CAG GAG GAC TCT GTG ACT CTG ACA TGC CAG GGG GCT 190
A A P P K A V L K L E P P W I N V L Q E D S V T L T C Q G A
A A' B
30 40 50 69
Arg Ser Pro Glu Ser Asp Ser Ile Gln Trp Phe His Asn Gly Asn Leu Ile Pro Thr His Thr Gln Pro Ser Tyr Arg Phe Lys Ala Asn
191 CGC AGC CCT GAG AGC GAC TCC ATT CAG TGG TTC CAC AAT GGG AAT CTC ATT CCC ACC CAC ACG CAG CCC AGC TAC AGG TTC AAG GCC AAC 280
R S P E S D S I Q W F H N G N L I P T H T Q P S Y R F K A N
C C' E
60 70 80 D1 D2 89
Asn Asn Asp Ser Gly Glu Tyr Thr Cys Gln Thr Gly Gln Thr Ser Leu Ser Asp Pro Val His Leu Thr Val Leu Ser Glu Trp Leu Val
281 AAC AAT GAC AGC GGG GAG TAC ACG TGC CAG ACT GGC CAG ACC AGC CTC AGC GAC CCT GTG CAT CTG ACT GTG CTT TCC GAA TGG CTG GTG 370
N N D S G E Y T C Q T G Q T S L S D P V H L T V L S E W L V
F G A
90 100 110 119
Leu Gln Thr Pro His Leu Glu Phe Gln Glu Gly Glu Thr Ile Met Leu Arg Cys His Ser Trp Lys Asp Lys Pro Leu Val Lys Val Thr
371 CTC CAG ACC CCT CAC CTG GAG TTC CAG GAG GGA GAA ACC ATC ATG CTG AGG TGC CAC AGC TGG AAG GAC AAG CCT CTG GTC AAG GTC ACA 460
L Q T P H L E F Q E G E T I M L R C H S W K D K P L V K V T
A A' B C
120 130 140 149
Phe Phe Gln Asn Gly Lys Ser Gln Lys Phe Ser Arg Leu Asp Pro Thr Phe Ser Ile Pro Gln Ala Asn His Ser His Ser Gly Asp Tyr
461 TTC TTC CAG AAT GGA AAA TCC CAG AAA TTC TCC CGT TTG GAT CCC ACC TTC TCC ATC CCA CAA GCA AAC CAC AGT CAC AGT GGT GAT TAC 550
F F Q N G K S Q K F S R L D P T F S I P Q A N H S H S G D Y
C C' His E F
150 160 170 MP MP 179
His Cys Thr Gly Asn Ile Gly Tyr Thr Leu Phe Ser Ser Lys Pro Val Thr Ile Thr Val Gln Val Pro Ser Met Gly Ser Ser Ser Pro
551 CAC TGC ACA GGA AAC ATA GGC TAC ACG CTG TTC TCA TCC AAG CCT GTG ACC ATC ACT GTC CAA GTG CCC AGC ATG GGC AGC TCT TCA CCA 640
H C T G N I G Y T L F S S K P V T I T V Q V P S M G S S S P
F G G' TM CT
180 190 200 209
Met Gly Ile Ile Val Ala Val Val Ile Ala Thr Ala Val Ala Ala Ile Val Ala Ala Val Val Ala Leu Ile Tyr Cys Arg Lys Lys Arg
641 ATG GGG ATC ATT GTG GCT GTG GTC ATT GCG ACT GCT GTA GCA GCC ATT GTT GCT GCT GTA GTG GCC TTG ATC TAC TGC AGG AAA AAG CGG 730
M G I I V A V V I A T A V A A I V A A V V A L I Y C R K K R
210 220 230 239
Ile Ser Ala Asn Ser Thr Asp Pro Val Lys Ala Ala Gln Phe Glu Pro Pro Gly Arg Gln Met Ile Ala Ile Arg Lys Arg Gln Leu Glu
731 ATT TCA GCC AAT TCC ACT GAT CCT GTG AAG GCT GCC CAA TTT GAG CCA CCT GGA CGT CAA ATG ATT GCC ATC AGA AAG AGA CAA CTT GAA 820
I S A N S T D P V K A A Q F E P P G R Q M I A I R K R Q L E
240 250 260 269
Glu Thr Asn Asn Asp Tyr Glu Thr Ala Asp Gly Gly Tyr Met Thr Leu Asn Pro Arg Ala Pro Thr Asp Asp Asp Lys Asn Ile Tyr Leu
821 GAA ACC AAC AAT GAC TAT GAA ACA GCT GAC GGC GGC TAC ATG ACT CTG AAC CCC AGG GCA CCT ACT GAC GAT GAT AAA AAC ATC TAC CTG 910
E T N N D Y E T A D G G Y M T L N P R A P T D D D K N I Y L
270 280
Thr Leu Pro Pro Asn Asp His Val Asn Ser Asn Asn OCH
911 ACT CTT CCT CCC AAC GAC CAT GTC AAC AGT AAT AAC TAA 949
T L P P N D H V N S N N *

Appendix 1.4. Nucleotide and derived aminoacid sequence of FcγRIIIA and FcγRIIIB cDNA, including the leader sequence. Scallon et al[1].

The full sequence of FcγRIIIA is shown. The nucleotides and aminoacids of FcγRIIIB are shown below the nucleotides and aminoacids of FcγRIIIA where they differ. The GPI attachment aminoacid (Serine 182) of FcγRIIIB is shown in bold and underlined. The positions of the first and second domains, membrane proximal region, transmembrane region and cytoplasmic tail region are indicated. The interchain disulphide bond Cys residues are marked with a ⊡. The approximate positions of the extracellular domain β strands are underlined and labelled. Numbers above the rows refer to the amino acid position; numbers in italics at the ends of rows refer to the nucleotide position

D1 = Domain one
D2 = Domain two
MP = Membrane proximal region
TM = Transmembrane region
CT = Cytoplasmic tail region

[1]Scallon, B. J., E. Scigliano, V. H. Freedman, M. C. Miedel, Y-C. E. Pan, J. C. Unkeless, and J. P. Kochan. A human immunoglobulin G receptor exists in both polypeptide-anchored and phosphoinositol-glycan-anchored forms. *Proc. Natl. Acad. Sci. USA* 1989; 86:5079-5083.

FcγRIII

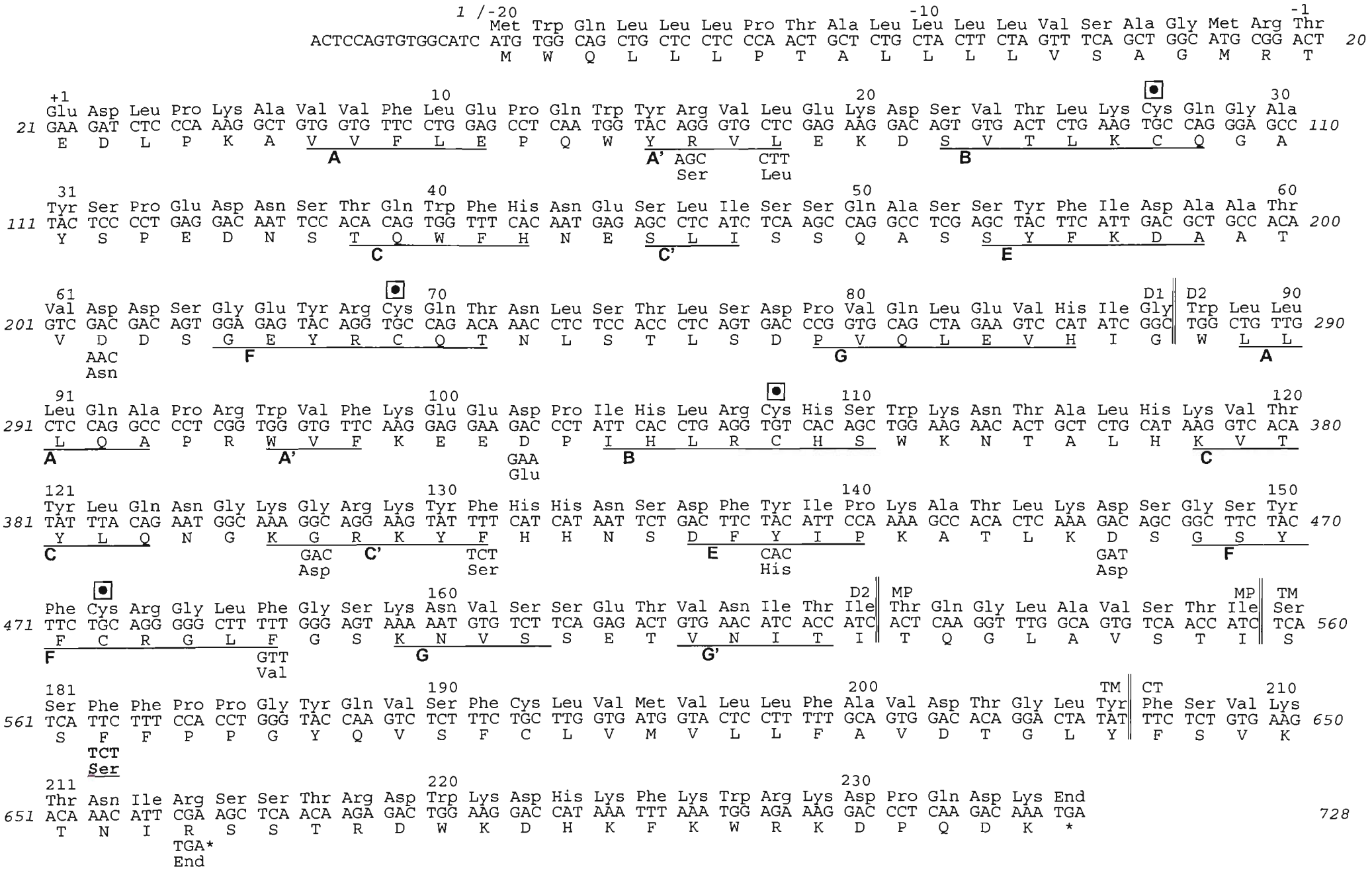
1 /-20 -10 -1
Met Trp Gln Leu Leu Leu Pro Thr Ala Leu Leu Leu Leu Val Ser Ala Gly Met Arg Thr
ACTCCAGTGTGGCATC ATG TGG CAG CTG CTC CTC CCA ACT GCT CTG CTA CTT CTA GTT TCA GCT GGC ATG CGG ACT 20
M W Q L L L P T A L L L L V S A G M R T
+1 10 20 30
Glu Asp Leu Pro Lys Ala Val Val Phe Leu Glu Pro Gln Trp Tyr Arg Val Leu Glu Lys Asp Ser Val Thr Leu Lys Cys Gln Gly Ala
21 GAA GAT CTC CCA AAG GCT GTG GTG TTC CTG GAG CCT CAA TGG TAC AGG GTG CTC GAG AAG GAC AGT GTG ACT CTG AAG TGC CAG GGA GCC 110
E D L P K A V V F L E P Q W Y R V L E K D S V T L K C Q G A
A A' AGC CTT B
Ser Leu
31 40 50 60
Tyr Ser Pro Glu Asp Asn Ser Thr Gln Trp Phe His Asn Glu Ser Leu Ile Ser Ser Gln Ala Ser Ser Tyr Phe Ile Asp Ala Ala Thr
111 TAC TCC CCT GAG GAC AAT TCC ACA CAG TGG TTT CAC AAT GAG AGC CTC ATC TCA AGC CAG GCC TCG AGC TAC TTC ATT GAC GCT GCC ACA 200
Y S P E D N S T Q W F H N E S L I S S Q A S S Y F K D A A T
C C' E
61 70 80 D1 D2 90
Val Asp Asp Ser Gly Glu Tyr Arg Cys Gln Thr Asn Leu Ser Thr Leu Ser Asp Pro Val Gln Leu Glu Val His Ile Gly Trp Leu Leu
201 GTC GAC GAC AGT GGA GAG TAC AGG TGC CAG ACA AAC CTC TCC ACC CTC AGT GAC CCG GTG CAG CTA GAA GTC CAT ATC GGC TGG CTG TTG 290
V D D S G E Y R C Q T N L S T L S D P V Q L E V H I G W L L
AAC
Asn
F G A
91 100 110 120
Leu Gln Ala Pro Arg Trp Val Phe Lys Glu Glu Asp Pro Ile His Leu Arg Cys His Ser Trp Lys Asn Thr Ala Leu His Lys Val Thr
291 CTC CAG GCC CCT CGG TGG GTG TTC AAG GAG GAA GAC CCT ATT CAC CTG AGG TGT CAC AGC TGG AAG AAC ACT GCT CTG CAT AAG GTC ACA 380
L Q A P R W V F K E E D P I H L R C H S W K N T A L H K V T
A A' GAA B C
Glu
121 130 140 150
Tyr Leu Gln Asn Gly Lys Gly Arg Lys Tyr Phe His His Asn Ser Asp Phe Tyr Ile Pro Lys Ala Thr Leu Lys Asp Ser Gly Ser Tyr
381 TAT TTA CAG AAT GGC AAA GGC AGG AAG TAT TTT CAT CAT AAT TCT GAC TTC TAC ATT CCA AAA GCC ACA CTC AAA GAC AGC GGC TTC TAC 470
Y L Q N G K G R K Y F H H N S D F Y I P K A T L K D S G S Y
C GAC C' TCT E CAC GAT F
Asp Ser His Asp
D2 MP MP TM
Phe Cys Arg Gly Leu Phe Gly Ser Lys Asn Val Ser Ser Glu Thr Val Asn Ile Thr Ile Thr Gln Gly Leu Ala Val Ser Thr Ile Ser
471 TTC TGC AGG GGG CTT TTT GGG AGT AAA AAT GTG TCT TCA GAG ACT GTG AAC ATC ACC ATC ACT CAA GGT TTG GCA GTG TCA ACC ATC TCA 560
F C R G L F G S K N V S S E T V N I T I T Q G L A V S T I S
F GTT G G'
Val
181 190 200 TM CT 210
Ser Phe Phe Pro Pro Gly Tyr Gln Val Ser Phe Cys Leu Val Met Val Leu Leu Phe Ala Val Asp Thr Gly Leu Tyr Phe Ser Val Lys
561 TCA TTC TTT CCA CCT GGG TAC CAA GTC TCT TTC TGC TTG GTG ATG GTA CTC CTT TTT GCA GTG GAC ACA GGA CTA TAT TTC TCT GTG AAG 650
S F F P P G Y Q V S F C L V M V L L F A V D T G L Y F S V K
TCT
Ser
211 220 230
Thr Asn Ile Arg Ser Ser Thr Arg Asp Trp Lys Asp His Lys Phe Lys Trp Arg Lys Asp Pro Gln Asp Lys End
651 ACA AAC ATT CGA AGC TCA ACA AGA GAC TGG AAG GAC CAT AAA TTT AAA TGG AGA AAG GAC CCT CAA GAC AAA TGA 728
T N I R S S T R D W K D H K F K W R K D P Q D K *
TGA*
End

Appendix 1.5. Nucleotide and derived aminoacid sequence of Decay Accelerating Factor (DAF) cDNA, supplied by Dr Bruce Loveland.

The positions of the extracellular domain, membrane proximal region, transmembrane region and cytoplasmic region are indicated. The GPI attachment aminoacid (His 341) is indicated in bold and underlined. Numbers above the rows refer to the amino acid position; numbers in italics at the ends of rows refer to the nucleotide position
The nucleotide numbering system of Medof et al[1]. starts at nucleotide 16 on this sequence.

ED = Extracellular Domain
MP = Membrane proximal region
TM = Transmembrane region
CT = Cytoplasmic tail region

[1]Medof ME, Lublin DM, Holers VM, Ayers DJ, Getty RR, Leykam JF, Atkinson JP and Tykocinski ML. Cloning and characterisation of cDNAs encoding the complete sequence of decay-accelerating factor of human complement. *Proc Natl Acad Sci* USA. 1987; 84:2007-2011.

DAF

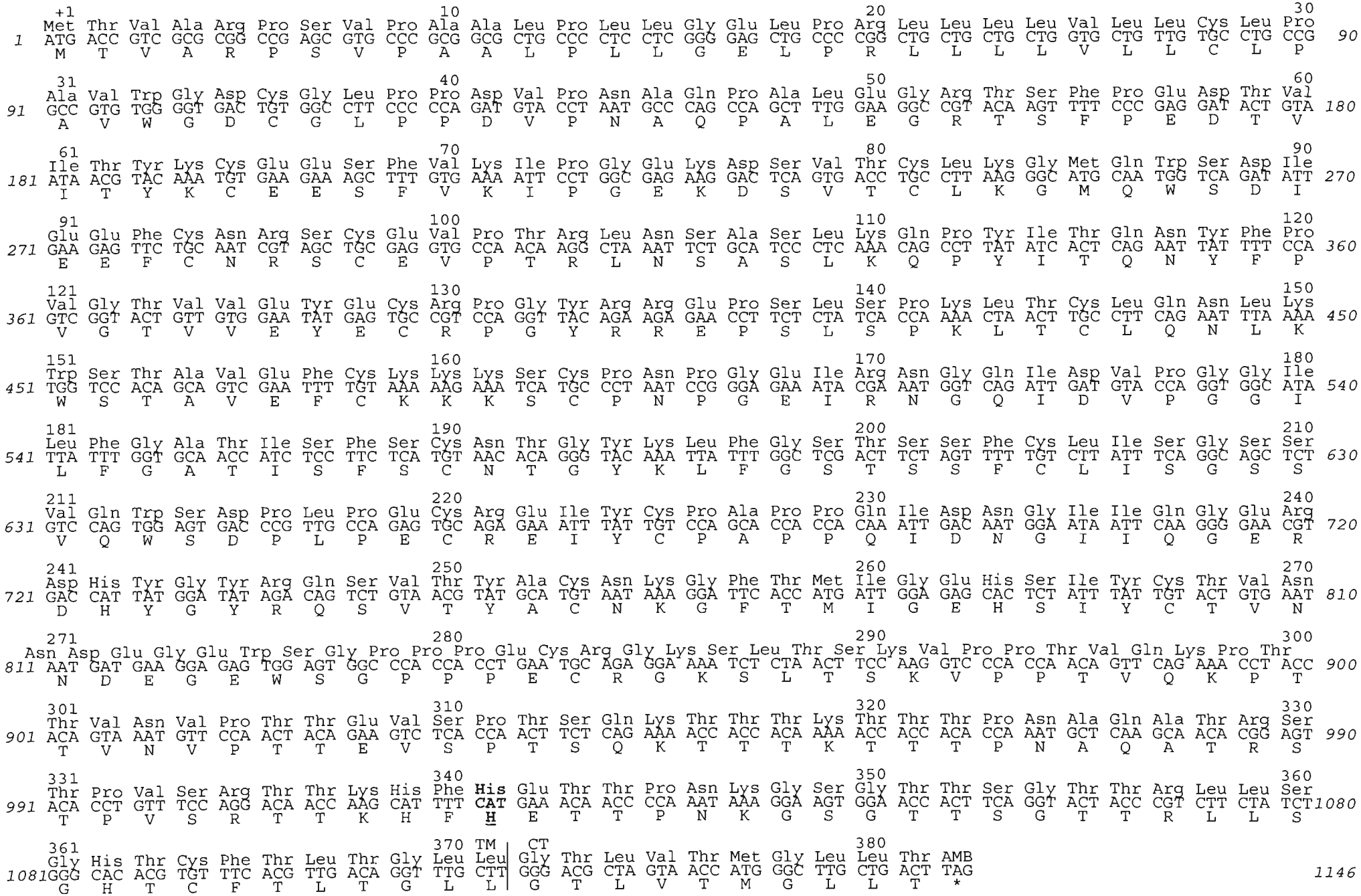
+1 10 20 30
Met Thr Val Ala Arg Pro Ser Val Pro Ala Ala Leu Pro Leu Leu Gly Glu Leu Pro Arg Leu Leu Leu Leu Val Leu Leu Cys Leu Pro
1 ATG ACC GTC GCG CGG CCG AGC GTG CCC GCG GCG CTG CCC CTC CTC GGG GAG CTG CCC CGG CTG CTG CTG CTG GTG CTG TTG TGC CTG CCG 90
M T V A R P S V P A A L P L L G E L P R L L L L V L L C L P
31 40 50 60
Ala Val Trp Gly Asp Cys Gly Leu Pro Pro Asp Val Pro Asn Ala Gln Pro Ala Leu Glu Gly Arg Thr Ser Phe Pro Glu Asp Thr Val
91 GCC GTG TGG GGT GAC TGT GGC CTT CCC CCA GAT GTA CCT AAT GCC CAG CCA GCT TTG GAA GGC CGT ACA AGT TTT CCC GAG GAT ACT GTA 180
A V W G D C G L P P D V P N A Q P A L E G R T S F P E D T V
61 70 80 90
Ile Thr Tyr Lys Cys Glu Glu Ser Phe Val Lys Ile Pro Gly Glu Lys Asp Ser Val Thr Cys Leu Lys Gly Met Gln Trp Ser Asp Ile
181 ATA ACG TAC AAA TGT GAA GAA AGC TTT GTG AAA ATT CCT GGC GAG AAG GAC TCA GTG ACC TGC CTT AAG GGC ATG CAA TGG TCA GAT ATT 270
I T Y K C E E S F V K I P G E K D S V T C L K G M Q W S D I
91 100 110 120
Glu Glu Phe Cys Asn Arg Ser Cys Glu Val Pro Thr Arg Leu Asn Ser Ala Ser Leu Lys Gln Pro Tyr Ile Thr Gln Asn Tyr Phe Pro
271 GAA GAG TTC TGC AAT CGT AGC TGC GAG GTG CCA ACA AGG CTA AAT TCT GCA TCC CTC AAA CAG CCT TAT ATC ACT CAG AAT TAT TTT CCA 360
E E F C N R S C E V P T R L N S A S L K Q P Y I T Q N Y F P
121 130 140 150
Val Gly Thr Val Val Glu Tyr Glu Cys Arg Pro Gly Tyr Arg Arg Glu Pro Ser Leu Ser Pro Lys Leu Thr Cys Leu Gln Asn Leu Lys
361 GTC GGT ACT GTT GTG GAA TAT GAG TGC CGT CCA GGT TAC AGA AGA GAA CCT TCT CTA TCA CCA AAA CTA ACT TGC CTT CAG AAT TTA AAA 450
V G T V V E Y E C R P G Y R R E P S L S P K L T C L Q N L K
151 160 170 180
Trp Ser Thr Ala Val Glu Phe Cys Lys Lys Lys Ser Cys Pro Asn Pro Gly Glu Ile Arg Asn Gly Gln Ile Asp Val Pro Gly Gly Ile
451 TGG TCC ACA GCA GTC GAA TTT TGT AAA AAG AAA TCA TGC CCT AAT CCG GGA GAA ATA CGA AAT GGT CAG ATT GAT GTA CCA GGT GGC ATA 540
W S T A V E F C K K K S C P N P G E I R N G Q I D V P G G I
181 190 200 210
Leu Phe Gly Ala Thr Ile Ser Phe Ser Cys Asn Thr Gly Tyr Lys Leu Phe Gly Ser Thr Ser Ser Phe Cys Leu Ile Ser Gly Ser Ser
541 TTA TTT GGT GCA ACC ATC TCC TTC TCA TGT AAC ACA GGG TAC AAA TTA TTT GGC TCG ACT TCT AGT TTT TGT CTT ATT TCA GGC AGC TCT 630
L F G A T I S F S C N T G Y K L F G S T S S F C L I S G S S
211 220 230 240
Val Gln Trp Ser Asp Pro Leu Pro Glu Cys Arg Glu Ile Tyr Cys Pro Ala Pro Pro Gln Ile Asp Asn Gly Ile Ile Gln Gly Glu Arg
631 GTC CAG TGG AGT GAC CCG TTG CCA GAG TGC AGA GAA ATT TAT TGT CCA GCA CCA CCA CAA ATT GAC AAT GGA ATA ATT CAA GGG GAA CGT 720
V Q W S D P L P E C R E I Y C P A P P Q I D N G I I Q G E R
241 250 260 270
Asp His Tyr Gly Tyr Arg Gln Ser Val Thr Tyr Ala Cys Asn Lys Gly Phe Thr Met Ile Gly Glu His Ser Ile Tyr Cys Thr Val Asn
721 GAC CAT TAT GGA TAT AGA CAG TCT GTA ACG TAT GCA TGT AAT AAA GGA TTC ACC ATG ATT GGA GAG CAC TCT ATT TAT TGT ACT GTG AAT 810
D H Y G Y R Q S V T Y A C N K G F T M I G E H S I Y C T V N
271 280 290 300
Asn Asp Glu Gly Glu Trp Ser Gly Pro Pro Pro Glu Cys Arg Gly Lys Ser Leu Thr Ser Lys Val Pro Pro Thr Val Gln Lys Pro Thr
811 AAT GAT GAA GGA GAG TGG AGT GGC CCA CCA CCT GAA TGC AGA GGA AAA TCT CTA ACT TCC AAG GTC CCA CCA ACA GTT CAG AAA CCT ACC 900
N D E G E W S G P P P E C R G K S L T S K V P P T V Q K P T
301 310 320 330
Thr Val Asn Val Pro Thr Thr Glu Val Ser Pro Thr Ser Gln Lys Thr Thr Thr Lys Thr Thr Thr Pro Asn Ala Gln Ala Thr Arg Ser
901 ACA GTA AAT GTT CCA ACT ACA GAA GTC TCA CCA ACT TCT CAG AAA ACC ACC ACA AAA ACC ACC ACA CCA AAT GCT CAA GCA ACA CGG AGT 990
T V N V P T T E V S P T S Q K T T T K T T T P N A Q A T R S
331 340 350 360
Thr Pro Val Ser Arg Thr Thr Lys His Phe His Glu Thr Thr Pro Asn Lys Gly Ser Gly Thr Thr Ser Gly Thr Thr Arg Leu Leu Ser
991 ACA CCT GTT TCC AGG ACA ACC AAG CAT TTT CAT GAA ACA ACC CCA AAT AAA GGA AGT GGA ACC ACT TCA GGT ACT ACC CGT CTT CTA TCT 1080
T P V S R T T K H F H E T T P N K G S G T T S G T T R L L S
361 370 TM CT 380
Gly His Thr Cys Phe Thr Leu Thr Gly Leu Leu Gly Thr Leu Val Thr Met Gly Leu Leu Thr AMB
1081 GGG CAC ACG TGT TTC ACG TTG ACA GGT TTG CTT GGG ACG CTA GTA ACC ATG GGC TTG CTG ACT TAG 1146
G H T C F T L T G L L G T L V T M G L L T *

APPENDIX TWO

I. DETERMINATION OF THE 'BINDABILITY' OF IODINATED PROTEIN

The following method was taken from Kulczycki and Metzger (3). Adapted by Sutton and Gould (Randall Institute, University College, London)(personal communication).

A minimum of 5 screw-capped microfuge tubes were seeded with varying numbers of FcεRI expressing cells (1 $x10^5$ - 6 $x10^6$ cells per tube) in the appropriate culture medium. To each tube was added 1 μg/ml (5.4 nM) ^{125}I IgE, and the total reaction volume made up to 150 μl with culture medium. The procedure was duplicated using mock transfected cells to determine non-specific binding. All tubes were incubated at room temperature for 60 min, microfuged 1 min, and the supernatant and pellet counted separately.

Cell-bound label was expressed as a percentage of the total counts, and a graph of cells per ml versus percentage of total counts plotted. The data fitted a hyperbolic curve and the extrapolated maximum indicated the percentage bindability. Ligand concentration was corrected for percentage bindability, to give the active ligand concentration.

II. RECEPTOR LIGAND INTERACTIONS

$$R + L \underset{k-1}{\overset{k+1}{\rightleftharpoons}} RL$$

Equation for single site receptor (R) ligand (L) interactions.

Half Life and Rate Constants

The half life of the interaction is defined by simple first order decay process

$$N = N_0 e^{-kt}$$

where:- N_0 = number of complexes at time 0
N = number of complexes remaining at time t
k = rate constant

When N is exactly half of N_0

$$½ = e^{-kt}$$

The natural log of which is:-

$$kt_{1/2} = 0.693 \quad \text{or} \quad k = \frac{0.693}{t_{1/2}}$$

k - the rate constant - is dependent on the temperature being constant,
- has units of reciprocal time (time^{-1}).

If k is large the reaction is fast, and if k is low the reaction slow.

The association rate constant is known as k+1, k_1 or k_f (forward) with units of M^{-1} sec^{-1}.
The dissociation rate constant, as k-1 or k_r (reverse) with units of sec^{-1}.

Therefore,

$$k+1\ [R]\ [L] = k-1\ [RL] \qquad \text{or} \qquad \frac{k+1}{k-1} = \frac{[R]\ [L]}{[RL]}$$

Reaction rates are the concentrations of reactants multiplied by the rate constant.

Equilibrium and Affinity Constants

The equilibrium constant (K) is equal to the ratio of the rate constants as shown below.

1) Equilibrium association constant

$$K_A = \frac{k+1}{k-1} = \frac{[R]\ [L]}{[RL]}$$

2) Equilibrium dissociation constant

$$K_D = \frac{k-1}{k+1} = \frac{[RL]}{[R]\ [L]}$$

Therefore:-

$$K_A = \frac{1}{K_D}$$

K_A describes the tendency of receptor and ligand to come together and stay together and has the units litres/mole (M^{-1}).
K_D describes the tendency to separate and has the units moles/litre (M).

K is the ratio of the association and dissociation constants.

Langmuir isotherm

The Langmuir isotherm is a method to determine K_D from Bmax using a series of concentrations of ligand with a fixed number of receptors as for example with biosensor analysis.

$$\text{Bound RU} = \frac{(B_{max}[L])}{(K_D+[L])}$$

Where Bmax is maximum binding capacity of the receptor (surface)
K_D is equilibrium binding constant
[L] concentration of ligand (mobile phase)
RU response units

A Langmuir isotherm can also be determined by plotting the predicted equilibrium (Req), versus the concentration of ligand, as determined by a data manipulation program such as BIAevaluation. The use of suitable non-linear regression analysis, as indicated below, is then used to determine the K_D .

Linear regression analysis

If the equilibrium association constant is determined mathematically from, for example, Scatchard analysis, it is correctly termed the apparent equilibrium association constant. In Scatchard analysis, linear transformation of equilibrium binding data is achieved by plotting bound ligand/free ligand versus bound ligand. The slope of the line produced by Scatchard analysis, is determined as $-1/K_D$ or $-K_A$, abcissa (x)-intercept (B_L) is equal to Bmax (maximum binding of ligand, equivalent to total receptor number - R_T) and ordinate (y)-intercept ($B_L/[L]$) equal to (B_{max}/K_D).

The formula for linear regression in Scatchard analysis is: $y = a+bx$,
where y = ligand bound,
x = free ligand
a = Bmax (R_T)
b = K_D.

Non-linear regression analysis

Non-linear regression analysis is achieved using a computer based curve fitting program, where free ligand (x) is plotted vs ligand bound (y). The computer determines the 'line/curve of best fit' (by minimising the 'sum of squares' of the residuals) for the data using the formula:-

$y = (a*x)/(b+x)$ single site binding

or

$y = ((a*x)/(b+x))+((c*x)/(d+x))$ two site binding

where $a = B_{max}\ 1$

$b = K_D\ 1$

$c = B_{max}\ 2$

$d = K_D\ 2$

Non-linear regression analysis is considered to be more accurate than linear regression.

Acknowledgements

I would like to thank all those in the Austin Research Institute before me, whose experience has helped me compile these practical calculation notes, especially Mark Hulett, Vivien Sutton, Narin Osman and Gary Jamieson. The Randall Institute, (University College, London.) has also supplied methodologies. Gary Jamieson (Austin Research Institute, Melbourne) has also supplied direction, encouragement, time and outstanding patience. I would like to acknowledge their help whilst accepting that any errors are my own.

Bibliography

1. John C. Matthews 'Fundamentals of Receptor, Enzyme, and Transport Kinetics.' CRC Press

2. Lauffenburger DA, Linderman JL. 'Receptors : models for binding, trafficking and signalling'. 1993. New York. Oxford University Press.

3. Kulczycki A. and Metzger H. The interaction of IgE with rat basophilic leukaemia cells. II. Quantitative aspects of the binding reaction. J Exp Med 1974; 140:1676-1695.

APPENDIX THREE

ALSEVER'S SOLUTION

Alsever's solution should be prepared at least 1 week in advance and allowed to stabilize at 4°C before use.

Dextrose	20.5g
Sodium citrate (dihydrate)	8.0g
Citric acid (monohydrate)	0.55g
Sodium chloride	4.2g

The ingredients were dissolved successively in 800 ml of distilled water, and made up to 1 litre with distilled water. The solution was autoclaved (15 psi, 15 min). The sterilized solution should be pH 6.1. Fresh whole sheep blood was mixed with equal volumes of Alsever's to prevent coagulation. The blood mixture was resuspended before aliquots were removed.

'STICKY' LIGATION

The vector was cut with the required restriction enzyme(s), as was the DNA to be inserted. The products were purified by electroelution from an agarose gel, and samples of the purified vector and insert were run on agarose gel to determine the approximate concentration of each and to verify sizes.

The vector and insert were combined in a 1:2 - 1:10 ratio respectively, *(this was dependent on the relative sizes of each, 1:2 for close sizes, and 1:10 when the insert was small relative to the vector*) generally 1:8 was suitable, with a total volume of 10-50 µl was average.

If 10x ligation buffer was not supplied with the ligase the following recipe was used:

Ligation Buffer 10x

2.5ml	Stock 1M Tris pH7.4
0.5ml	Stock 1M MgCl2
0.5ml	Stock 100mM ATP (Store at -20°C)
0.5ml	Stock 100mM DTT (Store at -20°C)
1.0ml	sterile double distilled water
5.0ml	

Aliquot and store -20°C

NB. ATP and DTT both lose activity with time.

Sample ligation	2 µl	cut Vector	
	10 µl	Insert	
	2 µl	10x Ligation Buffer	
	1 µl	DNA Ligase	
	5 µl	water	
	20 µl		14-16°C 4hrs or O/N

HEPES BUFFERED SALINE (HBS)

10mM HEPES
150mM sodium chloride
3.4mM Na EDTA
pH 7.4

PHOSPHATE BUFFERED SALINE (PBS)

10x Mouse tonicity:

$NaH_2PO_4.2H_2O$	0.624g	
Na_2HPO_4 (anhydrous)	2.271g	(or $Na_2HPO_4.2H_2O$ 2.85g)
NaCl	8.766g	

Dissolve to 1 litre in double distilled water.
pH 7.2

MINIMAL MEDIA (Invitrogen)

MGY (Minimal glycerol media)

800 ml autoclaved water was combined with 100 ml of 10x YNB, 2 ml of 500x B, and 100 ml of 10x GY. The shelf life of the solution when stored at 4°C was approximately two months.

BMMY (Buffered Minimal Methanol-complex Medium):

10 g of yeast extract, 20 g of peptone was combined with 700 ml of water and autoclaved. It was cooled to room temperature and then the following added and mixed well: 100 ml 1 M potassium phosphate buffer, pH 6.0, 100 ml 10x YNB, 2 ml 500x B, 100 ml 10x M. The shelf life of this solution was approximately two months when stored at 4°C.

STOCK SOLUTIONS for Minimal media MGY and BMMY above.

10x YNB (Yeast Nitrogen Base)

134 g of yeast nitrogen base (YNB) without amino acids was dissolved in 1000 ml of water and filter sterilised. It was occasionally necessary to beat in order to dissolve YNB completely in water. The dissolved YNB was stored at 4°C. The solution had a shelf life of approximately one year.

500x B (Biotin)

20 mg biotin was dissolved in 100 ml of water and filter sterilised. The solution had a shelf life of approximately one year.

10x M (Methanol):

Mix 5 ml of methanol with 95 ml of water. Filter sterilise and store at 4°C. The solution had a shelf life of approximately two months.

10x GY (Glycerol):
100 ml of glycerol was mixed with 900 ml of water. The mixture was sterilised either by filtering or autoclaving. Store at room temperature. The solution was stored at room temperature and had a shelf life of greater than one year.

1M Potassium phosphate buffer, pH6.0:
132ml of 1M K_2HPO_4 was combined with of 1M KH_2PO_4 and the pH was confirmed (pH 6.0±0.1 - if the pH needed to be altered phosphoric acid was used). The solution was sterilised by autoclaving and stored at room temperature. The shelf life of the solution was greater than one year.

SILVER STAINING POLYACRYLAMIDE ELECTROPHORESIS GELS (Biorad)
All steps were performed on a horizontal rotating shaker providing gentle movement of the tray contents.

Fixation: After electrophoresis the gel was immediately immersed in the fixing solution for at least 30 minutes (or overnight).

Incubation: The gel was placed in the incubation solution for 30 minutes (or overnight).

Washing: The gel was then washed three times, each time for 10 minutes in double distilled water (DDW).

Silver Reaction: The gel was then placed in silver solution for 20-40 minutes.

Developing: To develop the stain the gel was placed in developing solution and allowed to develop for as long as required. This was usually carried out with consecutive aliquots of the solution, tipping out the first few aliquots before they turned brown.

Stopping: The reaction was stopped by placing the gel in stop solution for 5-10 minutes.

Fixing Solution

80mL	ethanol
20mL	acetic acid

Make up to 200mL with DDW**

Incubation Solution

60mL	ethanol
10.25g	anhydrous sodium acetate
1.04mL	glutardialdehyde (25% w/v) *
0.4g	sodium thiosulphate (Na_2S_2O .$5H_2O$)

Make up to 200mL with DDW

Silver Solution

0.2g	silver nitrate
40mL	formaldehyde *

Make up to 200mL with DDW

Developing Solution

5g	sodium carbonate
20mL	formaldehyde *

Make up to 200mL with DDW.

Stop Solution

2.92g	EDTA

Make up to 200mL with DDW

* Add these components immediately before use.
** DDW = double distilled water

INTERPRETATION OF A BIACORE TRACE.

The readout from a BIAcore indicates interactions over time (e.g. between two proteins) of the mobile phase containing receptor or ligand as it flows over the immobile phase of ligand or receptor. Typically interactions are measured in two phases - association and dissociation.

(i) Association phase: Rate and extent of interaction between the two proteins is seen as an increase in relative Response Units (RU) that approaches an equilibrium at which point a 'plateau' is observed.

(ii) Dissociation phase: This is observed after washing of the chip surface allowing the receptor : ligand complex to fall apart and is observed as a decrease in RU over time. The steeper the gradient the more rapid the dissociation.

The RU will also change with any variation in solvent / buffer. The trace is read from left to right.